The University Of Sheffield.

PATTERNS AND CORRELATES OF ECOMORPHOLOGICAL DIVERSIFICATION IN BIRDS

Angela Maria Chira

A thesis submitted in partial fulfilment of the requirements for the degree of

Doctor of Philosophy

The University of Sheffield

Faculty of Science

Department of Animal and Plant Sciences

September 2018

ABSTRACT

A fundamental theme in macroevolution is understanding the origin and drivers behind the accumulation of phenotypic diversity in deep-time. Specifically, we want to describe and explain the mode (how) and tempo (at what speed) of morphological differentiation between species. Here, I investigate the patterns and correlates of ecomorphological diversification across the most diverse radiation among the tetrapods - birds. First, I investigated how variation in evolutionary rates impacts inferences from models of trait evolution. I show that rate-static models can produce spurious interpretations regarding the process of trait evolution in the presence of rate-heterogeneity, whereas robust conclusions can be drawn by co-utilizing rate-variable approaches and tests for absolute model adequacy. Second, I use a multipredictor approach to investigate correlates for the tempo of beak shape evolution across more than a half of bird species. I find high rates of evolution in morphologically-distinct clades as well as in species-rich groups, showing that ecological opportunity and species-packing impact the tempo of ecomorphological diversification in deep-time. Thirdly, I apply trait evolutionary models with competition alongside ecologically-neutral models to investigate the mode of beak shape, beak size and body mass evolution across birds. I show that models with species-interactions are not uncommonly the best fit for the data in clades, and thus ecological selection pressures can impact the accumulation of morphological diversity at deep-time scales. Lastly, I investigated how competition affects the process of ecomorphological evolution in sympatric avian granivorous assemblages. I find that species-interactions contribute to increased morphological diversity across the globe, however, the strength of competition signal is mediated by the negative association with the tempo of trait evolution. Taken together, these results explore how key ecological processes (the presence and absence of ecological opportunity, niche packing, the strength and resolution of competition) can explain variation in how biodiversity accumulates in deep time.

ACKNOWLEDGEMENTS

I am enormously grateful to my supervisor Gavin Thomas, who is a fantastic thinker and tremendously kind person, and who has been extremely supportive with everything I wanted to do. I also want to thank Rob Freckleton, who provided many useful discussion points and ideas that improved my research outline. Special thanks go to Chris Cooney, who has been a constant source of inspiration and a professional role model, as well as a great friend to me. I thank my amazing office mates Emma, Frane, Jen, Joe, Jon, Joseph, and Yichen, as well as Alison, Anna, Cindy, Dave E, Dom, Elliot, Ileana, Luke, Mike, Paddy, Patrick, Simon, Toni, Yan, and Zoë, for making working at the University an absolute pleasure. Special thanks go to Yichen for being an awesome person and friend, and to Frane for his endless contagious enthusiasm and love for brainstorming! Also thanks Mike for repeatedly encouraging me to be myself, as loud as that meant at times. And I cannot find enough words of praise for Clarissa, Richard, and Zuzanna – thank you beautiful people for your beautiful friendships! I also want to thank my family and my life-time friends for all their loving support. Lastly, this work would not have been possible without funding from the European Research Council.

CONTENTS

LIST OF MAIN TEXT FIGURES

LIST OF MAIN TEXT TABLES

CHAPTER 1

General introduction

GENERAL BACKGROUND

In its broadest sense, biodiversity describes the whole spectrum of life on Earth. In macroevolutionary biology, biodiversity is predominantly measured at or above the species levels, and generally, the two axes of biodiversity considered are species' numbers and species' phenotypes (Simpson, 1953). One of the central themes in macroevolution is to understand why life is so diverse (Benton, 2015; Benton & Emerson, 2007; Darwin, 1859; Futuyma, 2015; Simpson, 1953) and to (1) describe patterns of biodiversity at large scales, (2) understand the mechanisms underlying the patterns we see, and (3) predict future levels of biodiversity. Total species richness and morphological disparity at any given point in time are generally determined by how species originate and die out (Alfaro et al., 2009; Benton, 1995; Rolland et al., 2014), by how species differentiate in their phenotypes (Carroll, 2001; Foote, 1997; Roy & Foote, 1997), and also by universal constraints to total biodiversity (Moen & Morlon, 2014; Oyston et al., 2015). Limits in the accumulation of biodiversity because of internal (e.g. developmental, Gerber, 2014) or external (e.g. ecological, Rabosky, 2009) constraints have been assessed in a wide range of comparative datasets. Therefore, a key component to understanding the diversity of life is to investigate the patterns, correlates and consequences for the tempo and mode of diversification and trait evolution across the tree of life. Here, I address these issues with specific focus on trait evolution.

The fossil record shows that trait evolution can happen at exceptionally rapid rates, or conversely, extremely slowly. The explosive increase in tooth complexity in *Microtus* rodents (late Pliocene and Pleistocene, Hibbard, 1959) and Equidae species (late Miocene, Simpson, 1953) are two well-preserved examples of spectacular, rapid phenotypic diversification. Conversely, some groups such as *Ptilocercus* threeshrews (Li & Ni, 2016), or *Metrarabdotos* bryozoans (Cheetham, 1987) have experienced very little morphological change over extensive deep-time scales. Additionally, studies on extant taxa have also described morphological differentiation over very short evolutionary time scales (e.g. the exceptionally rapid evolution of beak morphology in Darwin's finches, Grant & Grant, 2006, or limb morphology in anoles, Stuart et al., 2014), in striking contrast with observations of "living fossils" (i.e. extant species that experienced little change since their origination), such as *Latimeria* coelacanths (Cavin & Guinot, 2014) or the *Ginkgo* tree (Zhou & Zheng, 2003). In the past decades, the tempo of evolution across a wide range of taxa and time-scales has been inferred with the use of phylogenetic comparative methods, revealing various patterns of rate heterogeneity. Specifically, we have examples of clades in which morphological variation accumulates proportionally with time, but also evidence of dramatic morphological differentiation at the split of two groups (e.g. the change from a broad to a thin and elongated beak shape when swifts split from hummingbirds, Cooney et al., 2017), rapid directional evolution within lineages (e.g. the impressive increase in flower size in Rafflesiaceae, Davis, 2008), and bursts of morphological differentiations across whole clades (e.g. Hawaiian honeycreepers, Lovette et al., 2002, or Madagascan vangas, Reddy et al., 2012). Further, macroevolutionary models have been applied on phylogenetic and phenotypic data for entire taxonomic classes (e.g. Cooney et al., 2017; Igea et al., 2017; Rabosky et al., 2013; Venditti et al., 2011), showing that rate heterogeneity in its various forms is a central part of phenotypic accumulation

across deep-time scales, and understanding its patterns and predictors is essential to understanding the origin and maintenance of present day biodiversity.

There is an abundance of factors that can influence variation in macroevolutionary rates of trait evolution. For example, we see elevated rates of body size evolution in birds and mammals across low-temperature periods in the Cenozoic (Clavel & Morlon, 2017), and in general, biodiversity patterns are intuitively linked with deep-time fluctuations in the abiotic conditions (Brombacher et al., 2018; Ezard et al., 2011; Jaramillo et al., 2006). Moreover, extreme events have drastic impacts on morphological accumulation, particularly when they associate with mass extinctions. Specifically, the extinction of large clades of species creates free ecological niches in which surviving groups can radiate, as shown for example by rapid evolution across eutherians or neognathes after the K-Pg boundary (Brusatte et al., 2015; Halliday et al., 2016). After clades invade new niches, the potential for subsequent evolution is tightly linked with species' packing. Specifically, rates of evolution intuitively decrease as confamilial species accumulate and thus limit the available pool of ecological opportunities (Gavrilets & Losos, 2009; Weir & Mursleen, 2013). Conversely, at more confined geographical and phylogenetic scales, the accumulation of species can increase rates of morphological differentiation. Iconic radiations such as Darwin's finches (Grant & Grant, 2006), or anole lizards (Stuart et al., 2014) are textbook examples of assemblages in which rapid phenotypic evolution occurred to avoid detrimental competitive interactions. We thus have a broad sample of abiotic and biotic drivers for variation in evolutionary rates, however, understanding the relative contribution of these candidate factors in predicting slow and rapid phenotypic evolution across global radiations is still ongoing.

The tempo of evolution acts in concert with the mode i.e. the way or manner of morphological accumulation, to determine global phenotypic diversity (Simpson, 1953). The simplest hypothesis is that morphological variance accumulates gradually in time, and so differences in phenotypic disparity between groups are a product of their relative ages (Cavalli-Sforza & Edwards, 1967). However, this simplistic scenario is not universal, as various constraints and selection pressures act to change the way in which morphological evolution unfolds. For example, the evolution of climatic niches in diprodonts is constrained by the environmental extremes across their distribution (Boucher & Demery, 2016), variation in the speed at which the avian cranial vault evolves seems limited by integration with the evolution of the brain (Felice & Goswami, 2018), and articuliform body plan evolution shows a pattern of diffusion in an ecologically constrained adaptive zone (Wright, 2017). These examples thus show that, rather than being infinite, the possible trait space that species can explore is likely bounded. Further, traits can also be confined to a narrow set of values generally interpreted as adaptive optima, as seen for example in the evolution of pterosaur body size through-out the Triassic and Jurassic (Benson et al., 2014), or chelonian body size evolution across marine and freshwater habitats (Jaffe et al., 2011). In time, such modes of morphological evolution under constraints result in reduced phenotypic diversity within groups (Butler & King, 2004; Martins & Hansen, 1997). Conversely, extensive divergence in traits may be promoted at the onset of adaptive radiations, generally associated with increased ecological opportunities in newly invaded niches (Agrawal et al., 2009; Jønsson et al., 2012; Losos & Ricklefs, 2009; Yoder et al., 2010), but also when selective pressures from antagonistic biotic interactions drive morphological differentiation between species (e.g. MacArthur, 1958). These various modes of phenotypic evolution contribute different amounts to total morphological disparity at any moment in time and space. Understanding how often and why each of these

processes of evolution dominates across a wide range of taxa essentially enables us to explain the accumulation of modern day morphological diversity.

The Darwinian view places a central role of the balance of biotic selection pressures on the evolution of species (Darwin, 1859), and competition in particular has been described as one of the core processes shaping the diversity of life (Mittelbach et al., 2007; Schemske et al., 2009; Thompson, 1999; Van Valen, 1973). The most well-known impact of competition is to increase morphological diversification between sympatric competing species, as famously shown in Darwin's finches (Grant & Grant, 2006), but also across other taxa (Brown & Wilson, 1956; MacArthur, 1958; Schluter, 2000; Stuart et al., 2014). However, interference competition can also lead to phenotypic convergence, for example when signalling traits are associated with recognizing competitors (Grether et al., 2009; Tobias et al., 2014). Further, biotic interactions can act as a barrier to secondary contact (Lovette & Hochachka, 2006; Pigot & Tobias, 2013), resulting in pattern of trait overdispersion in assemblages of species (e.g. Barnagaud et al., 2014). Additionally, competition has also led to a pattern of parallel evolution across multiple geographic transects (e.g. head shape evolution in salamanders, Adams, 2010). In deep-time, biotic interactions are similarly associated with elevated rates of trait evolution and total disparity (Davies et al., 2007; Freeman, 2015). The presence of bounds on the morphospace available to species has been associated with a decrease in rates of evolution with the accumulation of species (Agrawal et al., 2009; Weir & Mursleen, 2013). However, biotic interactions are considered an ever-changing selection force that create dynamic landscapes (Thompson, 1999), and so they can also leave a signal of increased rates of evolution without increased total disparity in clades evolving in a constrained morphospace. Recently, a lot of attention has been directed towards describing and understanding patterns of macroevolution with ecology (Ezard & Purvis, 2016; Jablonski, 2008; Voje et al.,

2015; Weber et al., 2016), but we lack a clear understanding of how prevalent and impactful are modes of evolution with competition compared to other processes in shaping biodiversity accumulation across deep-time scales.

For a long time the general consensus was that stasis (i.e. long periods of time with little morphological change) is the dominant process of trait evolution across the tree of life, an argument supported by the fossil record (Estes & Arnold, 2007; Hunt, 2007). However, extensive meta-analyses that contrast the fit of various models of trait evolution across broad scale comparative datasets showed that other patterns (modes and tempos) of evolution are not only possible, but also frequent (Harmon et al., 2010; Hunt, 2007; Landis & Schraiber, 2017; Uyeda et al., 2011). For example, a recent study using over 8,000 vertebrate species found evidence of pulses of rapid change in body size evolution in a third of the clades included (Landis & Schraiber, 2017). In general, evolution towards adaptive optima and random-walk patterns has also been often preferred across studies, as opposed to directional evolution or models of early acceleration, followed by a deceleration in rates (Harmon et al., 2010; Hunt, 2007). Across the largest family of songbirds, traits involved in resource acquisition were found to evolve predominantly away from each other, as expected under selection pressures from phenotypic-driven interactions (Drury et al., 2018). The accumulation of extensive, high-quality phylogenetic and phenotypic data, alongside the development of more complex trait evolutionary models enabled us to gradually build a broad-scale perspective of the tempo and mode of biodiversity accumulation. However, there are still many gaps in our understanding of trait macroevolution, as highlighted in recent comprehensive reviews of the field (e.g. Benton, 2015; Futuyma, 2015; Oyston et al., 2015). In the next section, I describe the aim and outline of this thesis, in which I address several questions regarding how and at what rate key ecomorphological traits evolve across a global radiation (birds).

OUTLINE OF THESIS

The aim of this thesis is to advance our understanding on patterns, correlates and consequences for the tempo and mode of phenotypic evolution. To do this, I have focused on the evolution of ecomorphological traits across the avian radiation. I used extensive datasets of beak morphology (shape and size), as well as body mass (Wilman et al., 2014), as these represent important ecological traits, often integrative components of adaptive radiations in birds. Furthermore, birds also benefit from high quality phylogenetic datasets (Jetz et al., 2012; Prum et al., 2015), and detailed aspects of their ecology are described for many taxa, making them a good study-system for understanding the processes responsible for generating and maintaining biodiversity at macroevolutionary scales. In the next section, I will briefly outline the main topics I focused on in my thesis.

How accurately do single-process models describe the process of evolution in the face of heterogeneity in rates of trait change?

Despite the knowledge that rate heterogeneity is a major component of phenotypic accumulation across macroevolutionary scales (O'Meara, 2012; Simpson, 1953), many single-process trait evolutionary models rely on the assumption of rate homogeneity (Cavalli-Sforza & Edwards, 1967; Martins & Hansen, 1997) or assume a simplistic scenario of rate variation (e.g. a constant deceleration of rates in time; Blomberg et al., 2003). Such models are by definition bound to underestimate the extent of rate variation in a given dataset, however, we need to understand the extent to which rate heterogeneity causes spurious interpretations regarding the process of phenotypic evolution. For example, using a PGLS approach to test for the correlation between traits of interest has been shown to suffer from type 1 error if the assumption of rate heterogeneity is violated (Mazel et al., 2016). An obvious solution to account for rate variation is to fit available rate-variable models (e.g. Eastman et al., 2011; Rabosky, 2014; Venditti et al., 2011). However, while we

expect such approaches to have improved relative fit, we also need to evaluate whether variable-rates models fit the data well overall. Therefore, a systematic test on how various forms of rate heterogeneity influence the interpretation of trait evolutionary models and the implementation of adequacy tests to correct for potential misinterpretations is needed in order to describe the patterns of phenotypic accumulation robustly and reduce the chances of model misspecification.

In chapter 2, I asked whether heterogeneity in trait evolutionary rates within clades is common, and further, whether and how it affects our interpretation of single-process evolutionary models. To do this, I applied rate-static and rate-variable evolutionary models to body mass data across 88 bird clades, as well as to data simulated under a range of rate heterogeneity scenarios. I furthered assessed the relative and absolute fit of phylogenetic models by using standard model selection criteria, as well as various parametric tests of absolute model adequacy.

What predicts rates of phenotypic macroevolution?

While there are multiple candidate factors that might explain variation in the rate of morphological differentiation, we still lack a comprehensive understanding of predictors for rapid and slow evolution across global radiations. The eco-space model proposed by Simpson (Simpson, 1953) puts a central role on the dynamics of ecological opportunity as a driver of variation in evolutionary rates. Under this hypothesis, the accumulation of phenotypic diversity is linked with the invasion of new eco-morphological spaces and the processes of species packing into these spaces. However, trait evolution has also been linked more generally with episodes of revolution in species' genetic make-up (Futuyma, 2015), as well as with the levels of genetic variability within populations (Simpson, 1953). These theories thus emphasize the role of mutagenic agents (e.g. increased UVB exposure, Rhode, 1992) and drivers of errors in the DNA (e.g. faster turn-over of generations, Thomas

et al., 2010) in predicting evolutionary rates. These factors likely act interdependently, and also their relative contribution will depend on the scale of analyses. Thus, a comprehensive test of multiple hypotheses that explain variation in the rate of evolution across both recent and deep time scale is needed in order to understand which and to what extent candidate factors shaped the accumulation of present-day morphological diversity.

In chapter 3, I tested for predictors of trait evolutionary rates across global radiations, focusing on factors generally associated with variation in the rate of molecular evolution (e.g. life-history and climatic variables), and also on aspects of species' ecologies (island residency, range size, and proxies of ecological opportunity and competition strength). I estimated species-level and clade-level evolutionary rates by using an extensive 3D dataset of bird beaks for over 5,000 species and multivariate variable-rates evolutionary models. I then correlated evolutionary rates with candidate factors using phylogenetic regressions.

How frequent do we find patterns of trait divergence consistent with the presence of ecological selection pressures at macroevolutionary scales?

Despite the pervasive view that competition for shared resources is a powerful selection force (Schluter, 2000; Thompson, 1999; Voje et al., 2015), its impact on morphological differentiation has mostly been associated with recent-scale radiations (Benton, 2009). Therefore, whether and how species interactions affect trait evolution at macroevolutionay scales is less clear. Competitive interactions have been considered as drivers of clade displacement episodes (Sepkoski et al., 2000; Silvestro et al., 2015), and further the extinction of competitors is thought to drive radiations in surviving lineages (e.g. Benson et al., 2014; Halliday et al., 2016). Diversity-dependent models have also been applied to show that the accumulation of species into niches can result in declining evolutionary rates (Weir & Mursleen,

2013). Additionally, methods of trait-driven interactions between lineages have also found evidence of competition signature in some radiations, as well as showing an effect of increased morphological diversification as species likely specialize to avoid foraging on the same resources (Clarke et al., 2017; Drury et al., 2016). However, it is unclear whether such examples are common across broad comparative datasets. We therefore need an extensive survey of patterns of trait divergence consistent with the presence of biotic interactions to understand to what extent ecological selection pressures can contribute to macroevolutionary morphological diversity.

In chapter 4, I focused on the potential importance of ecological selection pressures in driving the mode of phenotypic evolution. Specifically, I test for evidence that trait evolution within clades is influenced by competitive selection forces, or conversely, whether trait evolution is mostly ecologically-neutral at macroevolutionary scales. To do this, I used a more complete set of 3D beak scans to quantify changes in beak shape and size, alongside body mass data for over 7,500 bird species. I then contrasted the fit of ecologically-neutral and novel models that incorporate the effect of competition within well-recognized clades of species to provide a survey for the prevalence of trait evolution patterns that are consistent with an effect of species interactions on trait evolution across the bird tree.

What is the geographical distribution of competition signature across the globe, and how does it associate with the process of trait evolution in assemblages of species?

A long-standing hypothesis in macroecology is that biotic interactions are more prevalent at lower latitudes (Dobzhansky, 1950), and could thus potentially contribute to variation in diversity levels across a latitudinal gradient (Mittelbach et al., 2007; Schemske et al., 2009). However, we lack empirical support for the distribution of species-interactions signal across the world, as well as for whether

and how interactions link with hotspots of biodiversity. Competition in particular has received much attention as a potential selective force for phenotypic evolution within assemblages of species. Specifically, the resolution of competition has been associated with extensive character differentiation (Grant & Grant, 2006; MacArthur, 1958), or phylogenetic overdispersion (Barnagaud et al., 2014), if antagonistic interactions prevent the invasion of closely related species in local communities (Pigot & Tobias, 2013). These patterns have been observed in several communities, but we lack an implementation of eco-evolutionary models in assemblages globally. Such an approach would allow mapping the signal of competition, testing for factors that facilitate intensive species interactions, obtain a global perspective on how competition relates to the process of evolution, and lastly, determine whether and how much competitive interactions contribute to variation in morphological diversity between assemblages of species.

In chapter 5, I tested the correlates and consequences of competition signal in species assemblages across the globe. To do this, I used beak shape, beak size and body mass data for almost 90% of avian granivorous species. I then applied ecologically-neutral trait evolutionary models alongside methods that look for a mode of evolution consistent with species interactions in over 10,000 equal-area grid cell assemblages across the globe. This way, I described the geographical variation in the signature competition across the globe. I further used spatial autoregression models to (1) correlate the strength and signal for competition with environmental variables, as well as with the tempo of trait evolution within assemblages, and (2) estimate the relative contribution of competition to morphological disparity within assemblages.

REFERENCES

Adams, D. C. (2010). Parallel evolution of character displacement driven by competitive selection in terrestrial salamanders. *BMC Evolutionary Biology, 10*(1), 72.

Agrawal, A. A., Fishbein, M., Halitschke, R., Hastings, A. P., Rabosky, D. L., & Rasmann, S. (2009). Evidence for adaptive radiation from a phylogenetic study of plant defenses. *Proc Natl Acad Sci U S A, 106*(43), 18067-18072.

Alfaro, M. E., Santini, F., Brock, C., Alamillo, H., Dornburg, A., Rabosky, D. L., . . . Harmon, L. J. (2009). Nine exceptional radiations plus high turnover explain species diversity in jawed vertebrates. *Proc Natl Acad Sci U S A, 106*(32), 13410-13414.

Barnagaud, J. Y., Daniel Kissling, W., Sandel, B., Eiserhardt, W. L., Sekercioglu, C. H., Enquist, B. J., . . . Svenning, J. C. (2014). Ecological traits influence the phylogenetic structure of bird species co-occurrences worldwide. *Ecol Lett, 17*(7), 811-820.

Benson, R. B., Frigot, R. A., Goswami, A., Andres, B., & Butler, R. J. (2014). Competition and constraint drove Cope's rule in the evolution of giant flying reptiles. *Nat Commun, 5*, 3567.

Benton, M. J. (1995). Diversification and extinction in the history of life. *Science, 268*(5207), 52-58.

Benton, M. J. (2009). The Red Queen and the Court Jester: species diversity and the role of biotic and abiotic factors through time. *Science, 323*(5915), 728-732.

Benton, M. J. (2015). Exploring macroevolution using modern and fossil data. *Proc Biol Sci, 282*(1810), 20150569.

Benton, M. J., & Emerson, B. C. (2007). How did life become so diverse? The dynamics of diversification according to the fossil record and molecular phylogenetics. *Palaeontology, 50*(1), 23-40.

Blomberg, S. P., Garland, T., & Ives, A. R. (2003). Testing for phylogenetic signal in comparative data: behavioral traits are more labile. *Evolution, 57*(4), 717-745.

Boucher, F. C., & Demery, V. (2016). Inferring Bounded Evolution in Phenotypic Characters from Phylogenetic Comparative Data. *Syst Biol, 65*(4), 651-661.

Brombacher, A., Wilson, P. A., Bailey, I., & Ezard, T. H. G. (2018). Temperature is a poor proxy for synergistic climate forcing of plankton evolution. *Proc Biol Sci, 285*(1883), 20180665.

Brown, W. L., & Wilson, E. O. (1956). Character Displacement. *Systematic Biology, 5*(2), 49-64.

Brusatte, S. L., O'Connor, J. K., & Jarvis, E. D. (2015). The Origin and Diversification of Birds. *Curr Biol, 25*(19), R888-898.

Butler, M. A., & King, A. A. (2004). Phylogenetic Comparative Analysis: A Modeling Approach for Adaptive Evolution. *American Naturalist, 164*(6), 683-695.

Carroll, S. B. (2001). Chance and necessity: the evolution of morphological complexity and diversity. *Nature, 409*(6823), 1102–1109.

Cavalli-Sforza, L. L., & Edwards, A. W. F. (1967). Phylogenetic analysis. Models and estimation procedures. *American Journal of Human Genetics, 19*(3), 233-257.

Cavin, L., & Guinot, G. (2014). Coelacanths as “almost living fossils”. *Frontiers in Ecology and Evolution, 2*, 49.

Cheetham, A. H. (1987). Tempo of Evolution in a Neogene Bryozoan: Are Trends in Single Morphologic Characters Misleading? *Paleobiology, 13*(3), 286-296.

Clarke, M., Thomas, G. H., & Freckleton, R. P. (2017). Trait Evolution in Adaptive Radiations: Modeling and Measuring Interspecific Competition on Phylogenies. *Am Nat, 189*(2), 121-137.

Clavel, J., & Morlon, H. (2017). Accelerated body size evolution during cold climatic periods in the Cenozoic. *Proc Natl Acad Sci U S A, 114*(16), 4183-4188.

Cooney, C. R., Bright, J. A., Capp, E. J. R., Chira, A. M., Hughes, E. C., Moody, C. J. A., . . . Thomas, G. H. (2017). Mega-evolutionary dynamics of the adaptive radiation of birds. *Nature, 542*(7641), 344-347.

Darwin, C. (1859). *On the origin of species*. London UK: John Murray.

Davies, T. J., Meiri, S., Barraclough, T. G., & Gittleman, J. L. (2007). Species co-existence and character divergence across carnivores. *Ecol Lett, 10*(2), 146-152.

Davis, C. C. (2008). Floral evolution: dramatic size change was recent and rapid in the world's largest flowers. *Current Biology, 18*(23), R1102-R1104.

Dobzhansky, T. (1950). Evolution in the tropics. *Am. Sci., 38*(2), 209-221.

Drury, J., Clavel, J., Manceau, M., & Morlon, H. (2016). Estimating the Effect of Competition on Trait Evolution Using Maximum Likelihood Inference. *Syst Biol, 65*(4), 700-710.

Drury, J. P., Tobias, J. A., Burns, K. J., Mason, N. A., Shultz, A. J., & Morlon, H. (2018). Contrasting impacts of competition on ecological and social trait evolution in songbirds. *PLoS Biol, 16*(1), e2003563.

Eastman, J. M., Alfaro, M. E., Joyce, P., Hipp, A. L., & Harmon, L. J. (2011). A novel comparative method for identifying shifts in the rate of character evolution on trees. *Evolution, 65*(12), 3578-3589.

Estes, S., & Arnold, S. J. (2007). Resolving the Paradox of Stasis: Models with Stabilizing Selection Explain Evolutionary Divergence on All Timescales. *Am Nat, 169*(2), 227-244.

Ezard, T. H., Aze, T., Pearson, P. N., & Purvis, A. (2011). Interplay between changing climate and species' ecology drives macroevolutionary dynamics. *Science, 332*(6027), 349-351.

Ezard, T. H., & Purvis, A. (2016). Environmental changes define ecological limits to species richness and reveal the mode of macroevolutionary competition. *Ecol Lett, 19*(8), 899-906.

Felice, R. N., & Goswami, A. (2018). Developmental origins of mosaic evolution in the avian cranium. *Proc Natl Acad Sci U S A, 115*(3), 555-560.

Foote, M. (1997). The Evolution of Morphological Diversity. *Annu. Rev. Ecol. Syst., 28*(1), 129-152.

Freeman, B. G. (2015). Competitive Interactions upon Secondary Contact Drive Elevational Divergence in Tropical Birds. *Am Nat, 186*(4), 470-479.

Futuyma, D. J. (2015). Can Modern Evolutionary Theory Explain Macroevolution? *, 2*, 29-85.

Gavrilets, S., & Losos, J. B. (2009). Adaptive radiation: contrasting theory with data. *Science, 323*(5915), 732-737.

Gerber, S. (2014). Not all roads can be taken: development induces anisotropic accessibility in morphospace. *Evol Dev, 16*(6), 373-381.

Grant, B. R., & Grant, P. R. (2006). Evolution of Character Displacement in Darwin's Finches. *Science, 313*(5784), 224-226.

Grether, G. F., Losin, N., Anderson, C. N., & Okamoto, K. (2009). The role of interspecific interference competition in character displacement and the evolution of competitor recognition. *Biol Rev Camb Philos Soc, 84*(4), 617-635.

Halliday, T. J., Upchurch, P., & Goswami, A. (2016). Eutherians experienced elevated evolutionary rates in the immediate aftermath of the Cretaceous-Palaeogene mass extinction. *Proc Biol Sci, 283*(1833).

Harmon, L. J., Losos, J. B., Jonathan Davies, T., Gillespie, R. G., Gittleman, J. L., Bryan Jennings, W., . . . Mooers, A. O. (2010). Early bursts of body size and shape evolution are rare in comparative data. *Evolution, 64*(8), 2385-2396.

Hibbard, C. W. (1959). Late Cenozoic microtine rodents from Wyoming and Idaho. *Papers Michigan Acad. Sci., Arts, and Letters, 44*, 3-40.

Hunt, G. (2007). The relative importance of directional change, random walks, and stasis in the evolution of fossil lineages. *Proc Natl Acad Sci U S A, 104*(47), 18404-18408.

Igea, J., Miller, E. F., Papadopulos, A. S. T., & Tanentzap, A. J. (2017). Seed size and its rate of evolution correlate with species diversification across angiosperms. *PLoS Biol, 15*(7), e2002792.

Jablonski, D. (2008). Biotic interactions and macroevolution: extensions and mismatches across scales and levels. *Evolution, 62*(4), 715-739.

Jaffe, A. L., Slater, G. J., & Alfaro, M. E. (2011). The evolution of island gigantism and body size variation in tortoises and turtles. *Biol Lett, 7*(4), 558-561.

Jaramillo, C., Rueda, M. J., & Mora, G. (2006). Cenozoic plant diversity in the neotropics. *Science, 311*(5769), 1893-1896.

Jetz, W., Thomas, G. H., Joy, J. B., Hartmann, K., & Mooers, A. O. (2012). The global diversity of birds in space and time. *Nature, 491*(7424), 444-448.

Jønsson, K. A., Fabre, P. H., Fritz, S., Etienne, R. S., Ricklefs, R. E., Jørgensen, T. B., . . . Irestedt, M. (2012). Ecological and evolutionary determinants for the adaptive radiation of the Madagascan vangas. *PNAS, 109*(17), 6620–6625.

Landis, M. J., & Schraiber, J. G. (2017). Pulsed evolution shaped modern vertebrate body sizes. *PNAS, 114*(50), 13224-13229.

Li, Q., & Ni, X. (2016). An early Oligocene fossil demonstrates treeshrews are slowly evolving "living fossils". *Sci Rep, 6*, 18627.

Losos, J. B., & Ricklefs, R. E. (2009). Adaptation and diversification on islands. *Nature, 457*(7231), 830-836.

Lovette, I. J., Bermingham, E., & Ricklefs, R. E. (2002). Clade-specific morphological diversification and adaptive radiation in Hawaiian songbirds. *Proc Biol Sci, 269*(1486), 37-42.

Lovette, I. J., & Hochachka, W. M. (2006). Simultaneous effects of phylogenetic niche conservatism and competition on avian community structure. *Ecology, 87*(sp7), S14-S28.

MacArthur, R. H. (1958). Population Ecology of Some Warblers of Northeastern Coniferous Forests. *Ecology, 39*(4), 599-619.

Martins, E. P., & Hansen, T. F. (1997). Phylogenies and the comparative method: a general approach to incorporating phylogenetic information into the analysis of interspecific data. . *Am Nat, 149*(4), 646–667.

Mazel, F., Davies, T. J., Georges, D., Lavergne, S., Thuiller, W., & Peres-Neto, P. R. (2016). Improving phylogenetic regression under complex evolutionary models. *Ecology, 97*(2), 286-293.

Mittelbach, G. G., Schemske, D. W., Cornell, H. V., Allen, A. P., Brown, J. M., Bush, M. B., . . . Turelli, M. (2007). Evolution and the latitudinal diversity gradient: speciation, extinction and biogeography. *Ecol Lett, 10*(4), 315-331.

Moen, D., & Morlon, H. (2014). Why does diversification slow down? *Trends Ecol Evol, 29*(4), 190-197.

O'Meara, B. C. (2012). Evolutionary Inferences from Phylogenies: A Review of Methods. *Annual Review of Ecology, Evolution, and Systematics, 43*(1), 267-285.

Oyston, J. W., Hughes, M., Wagner, P. J., Gerber, S., & Wills, M. A. (2015). What limits the morphological disparity of clades? *Interface Focus, 5*(6), 20150042.

Pigot, A. L., & Tobias, J. A. (2013). Species interactions constrain geographic range expansion over evolutionary time. *Ecol Lett, 16*(3), 330-338.

Prum, R. O., Berv, J. S., Dornburg, A., Field, D. J., Townsend, J. P., Lemmon, E. M., & Lemmon, A. R. (2015). A comprehensive phylogeny of birds (Aves) using targeted next-generation DNA sequencing. *Nature, 526*(7574), 569-573.

Rabosky, D. L. (2009). Ecological limits and diversification rate: alternative paradigms to explain the variation in species richness among clades and regions. *Ecol Lett, 12*(8), 735-743.

Rabosky, D. L. (2014). Automatic detection of key innovations, rate shifts, and diversity-dependence on phylogenetic trees. *PLoS One, 9*(2), e89543.

Rabosky, D. L., Santini, F., Eastman, J., Smith, S. A., Sidlauskas, B., Chang, J., & Alfaro, M. E. (2013). Rates of speciation and morphological evolution are correlated across the largest vertebrate radiation. *Nat Commun, 4*, 1958.

Reddy, S., Driskell, A., Rabosky, D. L., Hackett, S. J., & Schulenberg, T. S. (2012). Diversification and the adaptive radiation of the vangas of Madagascar. *Proc Biol Sci, 279*(1735), 2062-2071.

Rhode, K. (1992). Latitudinal gradients in species diversity: the search for the primary cause. *Oikos, 65*(3), 514–527.

Rolland, J., Condamine, F. L., Jiguet, F., & Morlon, H. (2014). Faster speciation and reduced extinction in the tropics contribute to the Mammalian latitudinal diversity gradient. *PLoS Biol, 12*(1), e1001775.

Roy, K., & Foote, M. (1997). Morphological approaches to measuring biodiversity. *Trends Ecol Evol., 12*(7), 277-281.

Schemske, D. W., Mittelbach, G. G., Cornell, H. V., Sobel, J. M., & Roy, K. (2009). Is There a Latitudinal Gradient in the Importance of Biotic Interactions? *Annual Review of Ecology, Evolution, and Systematics, 40*(1), 245-269.

Schluter, D. (2000). Ecological Character Displacement in Adaptive Radiation. *Am Nat, 156*(S4), S4-S16.

Sepkoski, J. J., McKinney, F. K., & Lidgard, S. (2000). Competitive displacement among post-Paleozoic cyclostome and cheilostome bryozoans. *Paleobiology, 26*(1), 7-18.

Silvestro, D., Antonelli, A., Salamin, N., & Quental, T. B. (2015). The role of clade competition in the diversification of North American canids. *PNAS, 112*(28), 8684-8689.

Simpson, G. G. (1953). *The major features of evolution.*: Columbia University Press.

Stuart, Y. E., Campbell, T. S., Hohenlohe, P. A., Reynolds, R. G., Revell, L. J., & Losos, J. B. (2014). Rapid evolution of a native species following invasion by a congener. *Science, 346*(6206), 463-466.

Thomas, J. A., Welch, J. J., Lanfear, R., & Bromham, L. (2010). A generation time effect on the rate of molecular evolution in invertebrates. *Mol Biol Evol, 27*(5), 1173-1180.

Thompson, J. N. (1999). The Evolution of Species Interactions. *Science, 284*(5423), 2116-2118.

Tobias, J. A., Cornwallis, C. K., Derryberry, E. P., Claramunt, S., Brumfield, R. T., & Seddon, N. (2014). Species coexistence and the dynamics of phenotypic evolution in adaptive radiation. *Nature, 506*(7488), 359-363.

Uyeda, J. C., Hansen, T. F., Arnold, S. J., & Pienaar, J. (2011). The million-year wait for macroevolutionary bursts. *PNAS, 108*(38), 15908-15913.

Van Valen, L. (1973). Van Valen, L. (1973). A new evolutionary law. *Evol Theory, 1*, 1-30.

Venditti, C., Meade, A., & Pagel, M. (2011). Multiple routes to mammalian diversity. *Nature, 479*(7373), 393-396.

Voje, K. L., Holen, O. H., Liow, L. H., & Stenseth, N. C. (2015). The role of biotic forces in driving macroevolution: beyond the Red Queen. *Proc Biol Sci, 282*(1808), 20150186.

Weber, M. G., Mitko, L., Eltz, T., & Ramirez, S. R. (2016). Macroevolution of perfume signalling in orchid bees. *Ecol Lett, 19*(11), 1314-1323.

Weir, J. T., & Mursleen, S. (2013). Diversity-dependent cladogenesis and trait evolution in the adaptive radiation of the auks (aves: alcidae). *Evolution, 67*(2), 403-416.

Wilman, H., Belmaker, J., Simpson, J., de la Rosa, C., Rivadeneira, M. M., & Jetz, W. (2014). EltonTraits 1.0: Species-level foraging attributes of the world's birds and mammals. *Ecological Archives, 95*(7), 2027-2027.

Wright, D. F. (2017). Phenotypic Innovation and Adaptive Constraints in the Evolutionary Radiation of Palaeozoic Crinoids. *Sci Rep, 7*(1), 13745.

Yoder, J. B., Clancey, E., Des Roches, S., Eastman, J. M., Gentry, L., Godsoe, W., . . . Harmon, L. J. (2010). Ecological opportunity and the origin of adaptive radiations. *J Evol Biol, 23*(8), 1581-1596.

Zhou, Z., & Zheng, S. (2003). The missing link in Ginkgo evolution. *Nature, 423*(6942), 821-822.

CHAPTER 2

The impact of rate heterogeneity on inference of phylogenetic models of trait evolution

This chapter was published in the Journal of Evolutionary Biology as:
Chira, A.M. and Thomas, G.H. The impact of rate heterogeneity on inference of phylogenetic models of trait evolution. Journal of Evolutionary Biology, 29: 2502-2518. doi:10.1111/jeb.12979.

Author contributions: AC and GT developed the conceptual framework, devised the analytical protocols, and wrote the manuscript. AC performed the analyses.

Data accessibility: Additional supporting information may be found online in the supporting information tab for this article (doi: 10.1111/jeb.12979). A summary of available material is given at the end of the chapter. Data is deposited at Dryad: doi: 10.5061/dryad.qj367.

ABSTRACT

Rates of trait evolution are known to vary across phylogenies; however, standard evolutionary models assume a homogeneous process of trait change. These simple methods are widely applied in small-scale phylogenetic studies, whereas models of rate heterogeneity are not, so the preva- lence and patterns of potential rate variation in groups up to hundreds of species remain unclear. The extent to which trait evolution is modelled accurately on a given phylogeny is also largely unknown because studies typically lack absolute model fit tests. We investigated these issues by applying both rate-static and variable-rates methods on (i) body mass data for 88 avian clades of 10–318 species, and (ii) data simulated under a range of rate-heterogeneity scenarios. Our results show that rate heterogeneity is present across small-scaled avian clades, and consequently applying only standard single-process models prompts inaccurate inferences about the generating evolutionary process. Specifically, these approaches underestimate rate variation, and systematically mislabel temporal trends in trait evolution. Conversely, variable-rates approaches have superior relative fit (they are the best model) and absolute fit (they describe the data well). We show that rate changes such as single internal branch variations, rate decreases and early bursts are hard to detect, even by variable-rates models. We also use recently developed absolute adequacy tests to highlight misleading conclusions based on relative fit alone (e.g. a consistent preference for constrained evolution when isolated terminal branch rate increases are present). This work highlights the potential for robust inferences about trait evolution when fitting flexible models in conjunction with tests for absolute model fit.

INTRODUCTION

Phenotypic diversity represents a fundamental axis of biodiversity, alongside variation in species richness. Species diversify into a multitude of forms, and significant differences in the magnitude and disparity of phenotypic traits occur across the tree of life. The speed at which traits change (i.e. the rate of evolution) may vary in numerous ways, including between groups of species (e.g. Hawaiian honeycreepers versus Hawaiian thrushes, Lovette et al., 2002), across habitats (e.g. reef versus nonreef, Price et al., 2011), and between distinct speciation regimes (Hipsley et al., 2014; Rabosky & Adams, 2012). Evolutionary rate heterogeneity has been attributed to a multitude of factors that are often taxon and/ or trait specific; for example, piscivorus sunfishes experience higher rates of evolution in jaw morphology than nonpiscivorous relatives (*Centrarchidae*, Collar et al., 2009), forests promote faster rates of avian song divergence compared to open grassland areas (Weir et al., 2012), and among shorebirds, offspring developmental mode is associated with increased rates of evolution for parental care and mating systems (Thomas et al., 2006). At broader scales, geographic distributions (e.g. islands versus mainland, Thomas et al., 2009; temperate versus tropical areas, Martin et al., 2010) and geologic events (impacts of the K-Pg mass extinction, Slater, 2013) have also been shown to influence evolutionary rates.

Although it is clear that rates of trait evolution vary across phylogenetic, temporal and spatial contexts, the prevalence of different forms of heterogeneity, especially within small clades, is not known. The most commonly used models on clades up to hundreds of species assume that trait evolution can be described by a single process across the whole group of interest. The earliest and most straightforward such approach is the Brownian motion or random walk model (BM) of trait evolution. Under the BM process, evolutionary rates are constant, the mean expected trait change is 0, and variance accumulates linearly in time (Figure 2.1a, Cavalli-Sforza

& Edwards, 1967; Felsenstein, 1985). The BM model can describe processes including both genetic drift and adaptation (Hansen & Martins, 1996). Several other approaches build on the BM model, with added parameters aimed to capture the complexities of trait evolution (i.e. deviations from a simple BM process). The Ornstein–Uhlenbeck (OU) model accounts for constrained trait evolution and non-independence between trait changes at each node in the phylogeny of interest (e.g. when species share similar selection regimes, Butler & King, 2004). Under the simplest version of the OU model (the single stationary peak model), evolutionary rates are constant, but traits are always pulled towards a single optimum value, so that, in time, the phenotype is constrained (Figure 2.1b). Other models relax the assumption of a constant rate of evolution, for example by allowing trait change to accelerate or decelerate through time across the whole phylogeny (e.g. ACDC method, Blomberg et al., 2003 and δ, Pagel, 1999). The most frequently used ACDC approach is the early burst (EB) model, which is a derivation of the BM approach with an extra parameter that models a constant rate-decrease through time. Under an early burst model, evolution peaks early in the phylogenetic history of the group of interest, after which the mean trait change exponentially decreases (e.g. expected across adaptive radiations, Harmon et al., 2010, Figure 2.1c).

If evolutionary rate heterogeneity is prevalent, and potentially unpredictable across phylogenies, can we still use single-process approaches to make inferences about the underlying tempo of evolutionary processes for a specific trait? The interpretation of single-process models of evolution is apparently appealing and straightforward, but fitting only these models may mask complexity and may not adequately describe variation in the data. The prevailing current approach when studying trait evolution is to fit several models to the data, and then choose the best

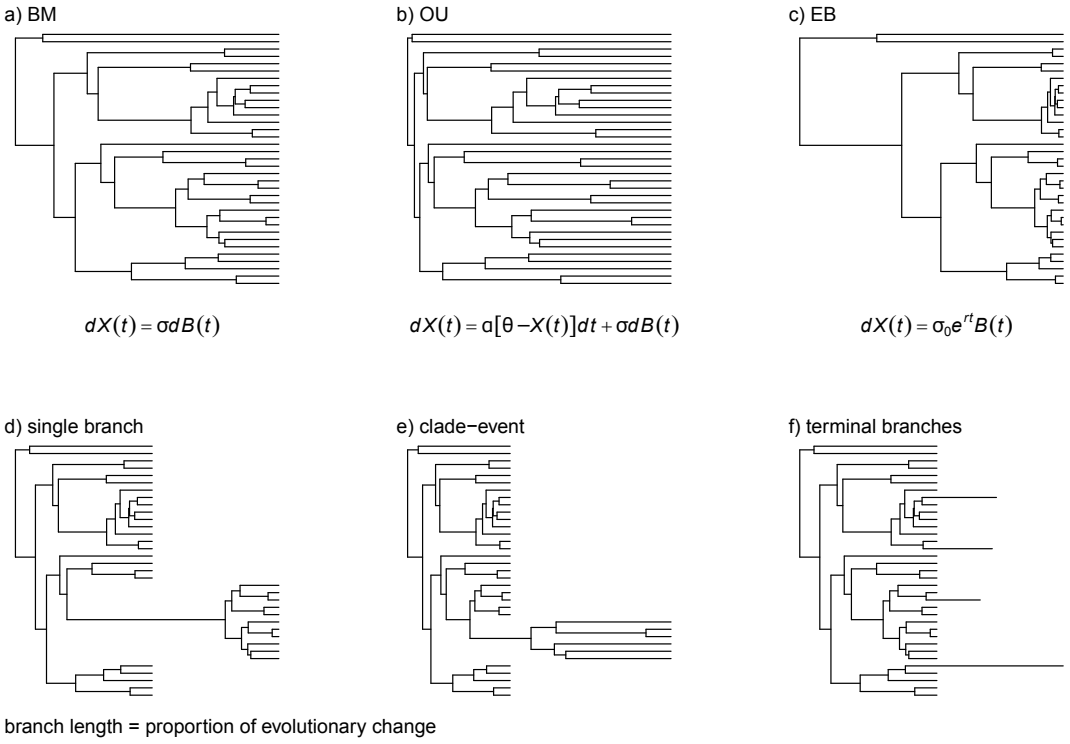

Figure 2.1. Tree transformations showing how trait evolution is modelled by single-process approaches: the (a) Brownian Motion (BM), (b) Ornstein–Uhlenbeck (OU), and (c) Early Burst (EB; exemplified by a constant rate-deceleration process from root to tips) models. The equations describe the process of trait change inferred by models, where $dX(t)$ represents the change in the trait of interest, σ is the rate of change, $dB(t)$ quantifies random noise by time t, α represents the "rubber-band" parameter acting to pull back the trait values to an optimum phenotype θ (OU-specific), σ_0 is the initial rate of trait change, and *r* is the constant rate of rate decrease (EB-specific). Hypothetical rate-heterogeneity scenarios captured by variable-rates models: rate changes (d) on a single, internal branch, (e) across a whole clade, and (f) on isolated tip branches.

relative fit based on maximum likelihood or Akaike information criterion (AIC, Burnham & Anderson, 2004). As the absolute adequacy of models is not accounted for, one cannot detect whether all alternative models are deficient. Further, models cannot always differentiate between alternative processes leading to the same trait distribution at the end of the phylogeny (Boettiger et al., 2012, Kaliontzopoulou & Adams, 2016). Therefore, the pattern of trait evolution can easily be misidentified.

This problem has been recognised (e.g. Freckleton and Harvey 2006, Pennell et al. 2015), and more recently, models have been developed that account for heterogeneity in the tempo of evolution in flexible ways. Several approaches, including Eastman et al. (2011) and Venditti et al. (2011), use reversible-jump MCMC to search rate shifts across the phylogeny of interest, assuming a BM mode of evolution between potential transitions (Huelsenbeck et al., 2001), whereas others use parametric methods to model distributions of rates (e.g. Elliot & Mooers, 2014). Such methods reveal that rate changes can occur on isolated branches (Figure 2.1d), throughout the phylogeny or across whole clades (e.g. Figure 2.1e-f; also Baker et al., 2016). Changes in the rate of trait evolution can also be modelled as heterogeneity in rate-regimes that are temporally variable, as implemented in the Bayesian Analysis of Macroevolutionary Mixture model (BAMM, Grundler & Rabosky, 2014; Rabosky, 2014; Rabosky et al., 2014a; Rabosky et al., 2013; Shi & Rabosky, 2015).

Although the use of single process models has tended to focus on smaller scales (e.g. clade size in Harmon et al., 2010 ranges from 6 to 179 species), to date most applications of rate variable models have been at relatively large scales on phylogenies including thousands of species (e.g. Venditti et al., 2011, Baker et al., 2015; Rabosky et al., 2013). Consequently, the prevalence of rate heterogeneity and its potential role in misleading single-process models inferences on trees of the order of hundreds of species is unknown. The aim of this study was to address this knowledge gap by resolving the following issues: (i) how prevalent is rate heterogeneity at relatively small phylogenetic scales, (ii) does the form of rate heterogeneity lead to predictable biases in favour of particular single-process evolutionary models, and (iii) does accounting for rate heterogeneity improve model fit and provide an ade- quate description for the data?

To address the first question, we use single-process and variable-rates approaches to examine body mass evolution within 88 bird groups, summing up to a total of over 6,500 species. Heterogeneity in the rate of evolution for several traits has been previously recorded between avian clades (e.g. Lovette et al., 2002) and sister-species (Martin et al., 2010; Weir & Wheatcroft, 2011). Early bursts of rapid evolution have also been identified in some groups such as ovenbirds (Derryberry et al., 2011), vangas (Reddy et al., 2012), and Hawaiian honeycreepers (Lovette et al., 2002). Avian phylogeny is resolved at the species level (Jetz et al., 2012; recent discussions also in Jarvis et al., 2014, Prum et al., 2015); moreover, body mass data are readily available for most species (Dunning, 2008; Wilman et al., 2014), making this system appealing when investigating the prevalence of rate heterogeneity. We further investigate in more detail when and how different forms of rate heterogeneity incapacitate evolutionary models, using simulated rate-variation scenarios informed by empirical observations. We anticipate that the extent and form of evolutionary rate variability will mislead the patterns of trait evolution quantified by single-process methods and model choice, leading to spurious inferences of macroevolutionary processes. Conversely, variable-rates approaches should perform better both in relative fit and in absolute adequacy.

MATERIALS AND METHODS

Models of trait evolution

We used the BM (Cavalli-Sforza & Edwards, 1967), OU (Butler & King, 2004) and EB (Harmon et al., 2010) models as representatives of popular single-process approaches. The models were fitted using fitContinous() in the R package GEIGER (Pennell et al., 2014), using 100 iterations. For some clades (the accentors, olive warbler, and woodpeckers in the empirical analyses), the likelihood surface for the OU alpha parameter consisted of a flat ridge (similar to Harmon et al., 2010) and could not be estimated reliably; therefore we excluded the OU-analyses on these

clades. The relative fit of models was determined using the AICw selection criteria (Burnham & Anderson, 2004). We are aware that AIC can be biased towards models with increasing number of parameters and provide a flawed relative hierarchy between nested methods (e.g. Kaliontzopoulou & Adams, 2016); however, our objective was to replicate and assess the common approach when studying trait evolution, and for the BM, OU and EB models, the number of parameters differs by a maximum of 1.

The Variable Rates Model for Continuous Traits in BayesTraits V2 (further referred to as BayesTraits for simplicity; http://www.evolution.rdg.ac.uk/BayesTraits.html) was used as a first representative of variable-rates models. BayesTraits implements changes in the rate of evolution using two scaling mechanisms that can be added at any location in the tree: a singlebranch modification (modifies the rate on a target branch) and a clade modification (adjusts a target branch and all its descendants; Venditti et al., 2011). The model outputs posterior configurations of rate shifts that best predict the tip trait data on the phylogeny of interest. Uniform (default) priors with no restrictions were used for alpha (phylogenetic mean) and sigma (Brownian variance) parameters. Four chains were run to ensure convergence between independent runs. Within- and between-chains convergence was assessed using trace and auto-correlation plots, effective sample size and the Gelman–Rubin diagnostic, all tested in the R package CODA (details in the supporting information; Plummer et al., 2006). We further used BAMM version 2.3.0 (http://bamm-project.org/) as a second example of methods allowing for variation in the rate of trait evolution. Under BAMM, the process of rate change is dependent on time, following:

$$\sigma(t) = \sigma_0 \exp(zt),$$

where $\sigma(t)$ represents the rate of gradual trait change in time t, t is the elapsed time from the start of the regime, σ_0 is the initial regime-rate, and z is a rate

parameter that controls for the magnitude of trait change in time. BAMM thus models multiple time-dependent, gradual rate changes, giving an approximation of continuous rate-variation processes with occasional jumps. For each tree and associated tip data, the priors for the Poisson rate (in BAMM 2.5.0, this is equivalent with the inverse of the expected number of shifts), initial evolutionary rate and rate-change parameter in each regime were calculated in R, using the function setBAMMpriors (Rabosky et al., 2014b). Throughout, the function set the poissonRatePrior = 1, whereas values for the betaInitPrior and betaShiftPrior varied between trees. The model also put a uniform prior density on the distribution of ancestral states, with bounds depending on the range of the observed data (useObservedMinMaxAsTraitPriors = 1). BAMM offers the possibility to switch between time-constant and time-varying processes of trait evolution when modelling rate variation via the time-flip proposal. We performed BAMM analyses: (i) with the time-flip proposal to allow both time-varying and time-constant processes (betaIsTimeVariablePrior = 0.5 and updateRate BetaTimeMode = 1), and (ii) limiting the model to timevarying rate-heterogeneity processes (betaIsTimeVariablePrior = 1 and updateRateBetaTimeMode = 0, the default in BAMM 2.3.0). Four chains were run and convergence between and within chains was assessed in CODA (details in the supporting information).

Empirical data

We used maximum clade credibility trees for 88 avian clades from the Jetz et al., 2012 stage 1 distribution (trees include genetic data only; accessed via Birdtree.org). Tree size ranged from 10 to 318 species, covering a total of 6,656 extant bird species. Bird body mass data was taken from EltonTraits 1.0 (Wilman et al., 2014). EltonTraits comprises specific body estimates based on (i) the geometric mean of average values for both sexes from Dunning (2008), and (ii) genus average from other sources. Body mass estimates (in grams) for each species were log-

transformed. We calculated the median scaled trees from the outputs of BayesTraits and BAMM, in which each branch length is stretched and shortened proportional to the median rate of evolution across the posterior scaled tree distribution for that particular branch. Posterior scaled trees are readily available in the output of BayesTraits. For BAMM, we modified the function getMeanBranchLengthTree() in R (package BAMMtools, Rabosky et al., 2014b), so that it computed the per-branch median rates across the posterior tree distribution (instead of the mean; code deposited at doi: 10.5061/dryad.qj367). Median scaled trees were used to visualize and describe patterns of trait evolution, and further as input for absolute model fit analyses (across both the empirical and simulated data). For the avian data sets, we also compared the fit of alternative models with various number of supported shifts given by BAMMflip using BayesFactors (calculated with computeBayesFactors() in BAMMtools, Rabosky et al., 2014b).

Simulations

We simulated trees with 100 tips under a pure birth model using TreeSim (Stadler, 2011), with a speciation rate set to 1. We chose this specific tree size because standard trait evolutionary models are typically applied on relatively small phylogenies with 50–200 tips. The root-to-tip distance was standardized to 1 in all trees. Rate-heterogeneity scenarios were simulated by changing the length for specific branches of interest (discrete shifts), or by generating gradual processes using the function rescale() in GEIGER. Brownian motion trait evolution with a variance rate of 1 was further simulated on these transformed trees. The original tree and the simulated trait data were used as input data for alternative models of trait evolution. We simulated rate variation as (i) a single, internal branch shift not passed to descendants (Figure 2.1d), (ii) a clade event, in which all members of a particular group record a change in the rate of evolution (Figure 2.1e), (iii) rate shifts on nonclustered terminal branches (Figure 2.1f), (iv) a constant ratedeceleration

process from the root to tips (Figure 2.1c) and (v) a case when a single clade goes through an initial increase in the rate of evolution (95) followed by a constant-rate decay (same process as Figure 2.1c, but constrained to a clade). The number of terminal branches and the size of clades that recorded rate shifts were set to 15–30 species. Combinations of the first three scenarios were also added. All code used for the simulations is deposited at doi: 10.5061/dryad.qj367. Parameter choices for the simulations were informed by the rate-heterogeneity patterns observed on the empirical data, and also by inference to the literature (discrete branch shifts: Revell et al., 2012; Venditti et al., 2011, Puttick et al., 2014; Thomas & Freckleton, 2012, Baker et al., 2016; gradual rate-decreases: Harmon et al., 2010, Rabosky et al., 2014a; Slater & Pennell, 2014). Discrete shifts were given magnitudes of 90.05, 90.1, 90.2, 90.5, 92, 95, 910 and 920. Gradual rate decreases were set under a rate-deceleration parameter (a) of ln (0.5), ln(0.2), ln(0.1) and ln(0.05). Each heterogeneity scenario with its respective magnitude was simulated on 100 trees, resulting in a total of 6,400 trees and trait data. We used an additional 1000 constant-rate trees, that is trees with a simulated BM process of trait evolution, and associated tip data, to assess model fit in the absence of rate heterogeneity. We also investigated whether the size of trees influences the ability of variable-rates models (BayesTraits and BAMM-flip) to detect heterogeneity. To do this, we simulated additional 400 trees with 25, 50, 100 and 200 tips (100 trees for each size), and we repeated the discrete ratevariation scenarios. The size of clades and number of terminal branches that recorded rate changes were set to 10–15, in order to accommodate for trees of only 25 tips.

The probability of internal branch shifts, clade events and terminal branch shifts to be detected by models was also quantified using the simulated data. We fitted the BM model: (i) on the simulated trees, that is trees with incorporated rate heterogeneity, alongside the simulated trait data, and (ii) on trees before applying

rate changes, alongside the simulated trait data. The differences in log-likelihood between (ii) and (i) were calculated; small differences in log-likelihood indicate that a particular heterogeneity scenario does not leave much signal in the tip data.

Absolute model fit

Freckleton and Harvey (2006) proposed bootstrapping approaches to assess the adequacy of the Brownian model as a descriptor of the data. More recently, Pennell et al. (2015) extended this approach with a series of parametric tests of the absolute adequacy of models of trait evolution implemented in the R package ARBUTUS (Pennell et al., 2015). Briefly, the algorithm works as follows: (i) an evolutionary model is fitted to the data, (ii) a unit tree is built by transforming the original tree according to the model parameters, (iii) Felsenstein's independent contrasts (Felsenstein, 1985) are calculated on this unit tree, making up the 'observed data', (iv) trait evolution is simulated on the unit tree, following a BM process with variance = 1, and the contrasts are calculated again (i.e. the 'simulated data'), and (iv) the observed and simulated distribution of contrasts are compared. ARBUTUS takes a phylogeny and the associated tip-trait distribution as input; therefore, for the variable-rates models, a BM model was run on the median scaled tree at step (i), and the unit tree was built according to the BM parameters on the scaled tree.

ARBUTUS provides six diagnostics that test model fit: (1) the coefficient of variation of the absolute value of contrasts (C.VAR) tests whether the candidate model underestimates ($C.VAR_{obs} > C.VAR_{sim}$) or overestimates ($C.VAR_{obs} < C.VAR_{sim}$) total rate-heterogeneity, (2) the mean of the squared contrasts (M.SIG) assesses model ability to quantify the overall rate of evolution, (3) the D statistic (Kolmolgorov-Smirnov test) compares the distribution of the contrasts with the expected $X \sim N(0, \sigma^2)$; D.CDF tests for deviations from the expected normal distribution of contrasts. The last three diagnostics represent the slopes of several linear models

fitted to the absolute value of contrasts (iv) against node heights (S.HGT), which assesses model ability to account for temporal variation (positive slopes show rate overestimations late in the phylogeny and underestimations early on), (v) against the variances of contrasts (S.VAR), signalling if models account for variation related to branch lengths (positive slopes show rate underestimation on long branches and overestimation on short ones), and (vi) against the weighted average values at each node (S.ASR), which tests whether the model accounts for variation related to ancestral states (positive slopes show overestimates at smaller nodes and underestimates at larger nodes). A candidate model is considered inadequate for a particular test when the observed and simulated test statistics are significantly different ($P < 0.05$). We used the P-values to calculate the frequency of inadequate trees and associated trait data (referred as inadequacy levels) given by each candidate model across our simulated scenarios. The ability of variable-rates models to detect rate shifts on simulated trees of different sizes was assessed by calculating (i) the posterior probability for the simulated branch and clade rate shifts (for BayesTraits), and (ii) the relative odds of a clade shift (i.e. marginal odds ratio) for BAMM-flip; currently, a protocol for assessing the probability of individual branch shifts is not formally described for this model.

We used the simulated trees and data under various heterogeneity scenarios to compare the rate estimates from variable-rates models with the true, simulated ones. Specifically, for each branch where a rate change was simulated, we calculated the natural logarithm for the proportion between the estimated and true rate of evolution. Positive values indicated that models overestimated the evolutionary rate on branches. These differences were calculated for the branches without simulated rate changes as well.

We also used constant-rate trees and associated trait data to evaluate potential tendencies of variable-rates models to infer false rate heterogeneity. BayesTraits has revealed a wealth of rate changes in body mass evolution across the mammalian tree (Venditti et al., 2011); therefore we first calculated the prevalence of branch rate-changes inferred in constant-rate trees by BayesTraits that could potentially be interpreted as shifts in the rate of evolution. Secondly, BAMM has been used to identify time-varying evolution within clades (Grundler & Rabosky, 2014; Rabosky et al., 2014a). We thus tested whether the default BAMM model (where all rate regimes are modelled as time-varying) infers false gradual rate-changes processes, particularly early in the phylogeny. We further tested whether any such biases are alleviated by using BAMM's time-flip proposal that allows both time varying and time constant rates to be modelled. We used the function getEventData() in BAMMtools to extract the rate-change parameter (β) for the root process. These β parameters should distribute normally around 0 if no rate change regime characterizes the root. We also plotted the β distribution for the simulations involving rate-discrete shifts, to test for a potential link between specific rate heterogeneity scenarios and falsely inferred gradual processes at the root.

RESULTS

Avian groups

Heterogeneity in the rate of body mass evolution was prevalent across bird phylogenies (Figure 2.2, considering per-branch rate-changes more substantial than x2 or x0.5 as evidence for rate-variation), and the intensity and patterns of rate changes varied across clades. Several recurrent forms of rate-heterogeneity stood out (Figure 2.2): rate changes affecting whole clades (e.g. *Paradoxornis* genus, Figure S71; *Geospiza* and *Camarhynchus* genera, Figure S78; *Cinclodes* genus, Figure S84), rate increases on isolated terminal branches (e.g. Figure S76, S81, S83), and evolutionary rate increases on an internal branch not passed to

descendants (referred to as ‘single-lineage ancestral bursts’ in Venditti et al., 2011 and Baker et al., 2016; e.g. Figure S99a). There was also evidence of time-dependent declining rates of evolution within groups, and BAMM revealed fast rates early in the phylogeny followed by declining rates in few cases (e.g. *Pachycephalidae* Figure S36b; *Procellariidae,* Figure S99b). Further, BAMM detected 35 groups that had strong evidence for at least one regime shift (Bayes factors for one or more shifts relative to the null model > 20), and in 43 groups there was at least some effect for one or more rate regime changes (Bayes factors > 12; Table S5). Highest extents of rate-variation were typically inferred in the large clades, but there was no clear relationship between the prevalence of heterogeneity and clade size (Figure 2.2). Rate-shifts were found across small groups (e.g. pheasants, quail, guineafowl, 11 species, Figure S91; orioles, allies, 32 species, Figure S67), and also some larger clades had little to no rate-variation throughout (e.g. cuckoos, 128 species, Figure S53; buntings, American sparrows, brush−finches, 127 species, Figure S57). Typically rate shifts did not exceed a 30 fold increase or a 5 fold decrease, but there were a limited number of exceptions (e.g. the *Platysteiridae* family undergoes a 14 fold decrease in the amount of body mass change relative to the length of the identical branch in the input phylogeny, Figure S100).

Variable-rates models generally represented an adequate approach to model body mass evolution across avian clades (Figure 2.3). Conversely, single-process models underestimated the total amount of rate variation in almost 50% of the groups included in the analyses. Further, the inadequacy of single-process approaches was predominant across phylogenies that showed high rate heterogeneity (as described by rate-variable models, Figure S15). Most important, variable-rates models were not just better at capturing the evolutionary process relative to single-process approaches (expected, since absolute fit does not penalize complexity), but

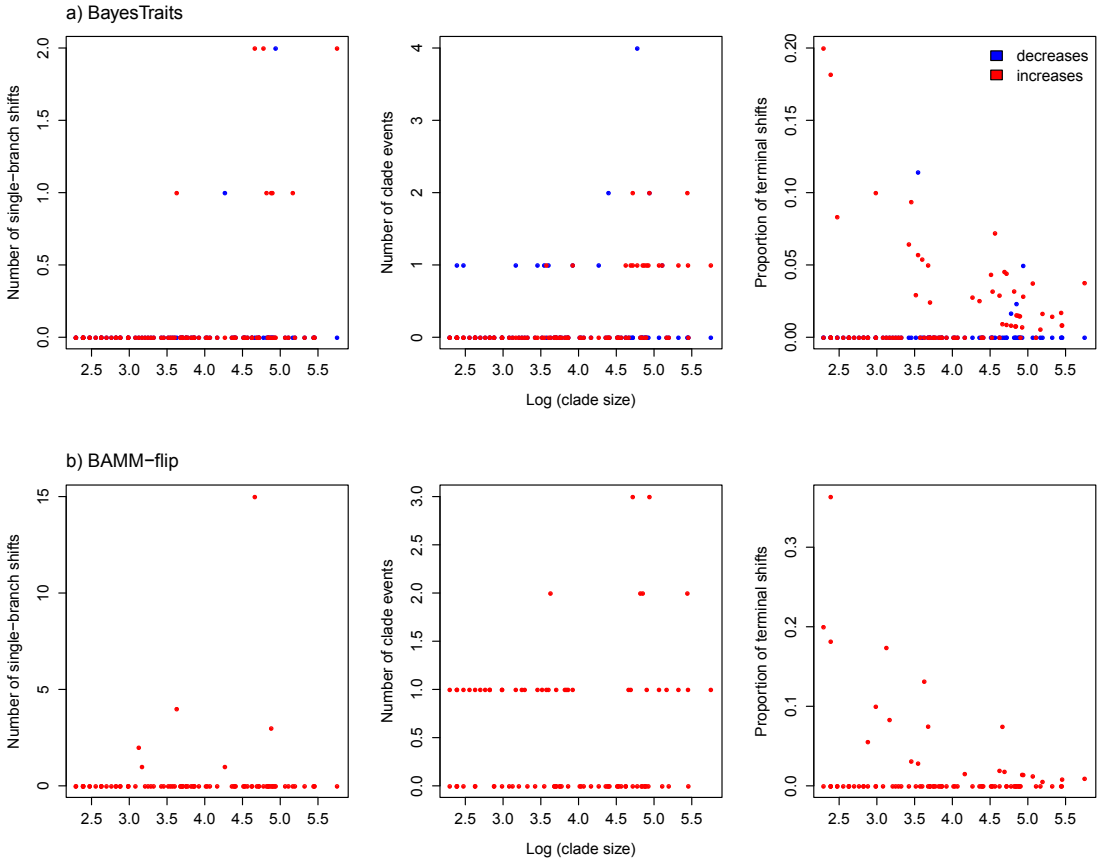

Figure 2.2. Patterns of rate-heterogeneity in avian body mass evolution given by (a) BayesTraits, and (b) BAMM-flip, plotted against clade size. Rate-variation is measured as: number of single-branch rate changes, number of clade events, and proportion of isolated changes at the tips. Rate decreases and increases are represented in blue and red, respectively.

they also recorded high levels of absolute adequacy. Therefore, such methods provide robust descriptions of the statistical patterns in the data, whereas single-process models frequently do not. BAMM and the EB model described the temporal aspect of evolution best (best adequacy in the S.HGT diagnostic), as the rest of the models tended to underestimate the rate of evolution early in the phylogeny, and/or overestimate it towards the tips (positive S.HGT, Table S3). The BAMM version constrained to time-varying processes typically produced stronger rate-deceleration processes at the root compared to the BAMM-flip alternative (Figure S14), mostly in small clades (less than 50 tips).

The BM model had highest AICw in 54% of trees (Figure S17-S63), followed by the OU (24%; Figure S64-S86), and EB models (22%; Figure S87-S104). The relative and absolute adequacies of single-process models were not tightly related. Rather the prevalence of highest AICw for the OU model increased as models missed more and more sources of variation (Figure 2.4). Thus often a superior relative fit of the OU model was not a result of best absolute fit, but of alternative evolutionary processes that were not accounted for by any of the single-process models included. We found 11 clades in which the OU model had over 90% support from the AICw over the BM and EB, but all three models had poor absolute adequacy (select *Pellorneidae* and *Sylviidae*, Figure 71c; *Alaudidae*, Figure S72c; select *Anatidae*, Figure S74c; *Pycnonotidae*, Figure S76c; *Lari*, Figure S77c; select *Thraupidae*, Figure S78c and Figure S81c; *Psittacidae*, Figure S79c; *Fringillidae*, Figure S80c; *Muscicapidae*, Figure S83c; *Furnariidae*, Figure S84c); within these groups, variable rates models typically identified rate increases late in the phylogeny, in the form of clade events and/or increases on isolated terminal branches. Absolute adequacy levels also helped distinguishing between the relative fit of models with similar AICw. We found 12 clades in which the BM and EB models were not clearly separated by their AICw, but were assigned different adequacy levels by ARBUTUS (*Trogonidae*, Figure S35c; select *Acanthizinae*, Figure S42c; *Conopophagidae*, Figure S87c; *Melanocharitidae* and *Cnemophilidae*, Figure S88c; *Maluridae*, Figure S90c; *Petroicidae*, Figure S92c; *Cardinalidae*, Figure S94c; *Vireonidae*, Figure S95; *Procellaridae*, Figure S99c; select *Psittacidae*, Figure S101c; *Numididae*, Figure S102c; *Meliphagidae*, Figure S103c). Within these groups, the BM (and BayesTraits) failed to account for temporal variation, and underestimated rates late in the phylogeny; conversely, the EB (and BAMM) was adequate across all diagnostics.

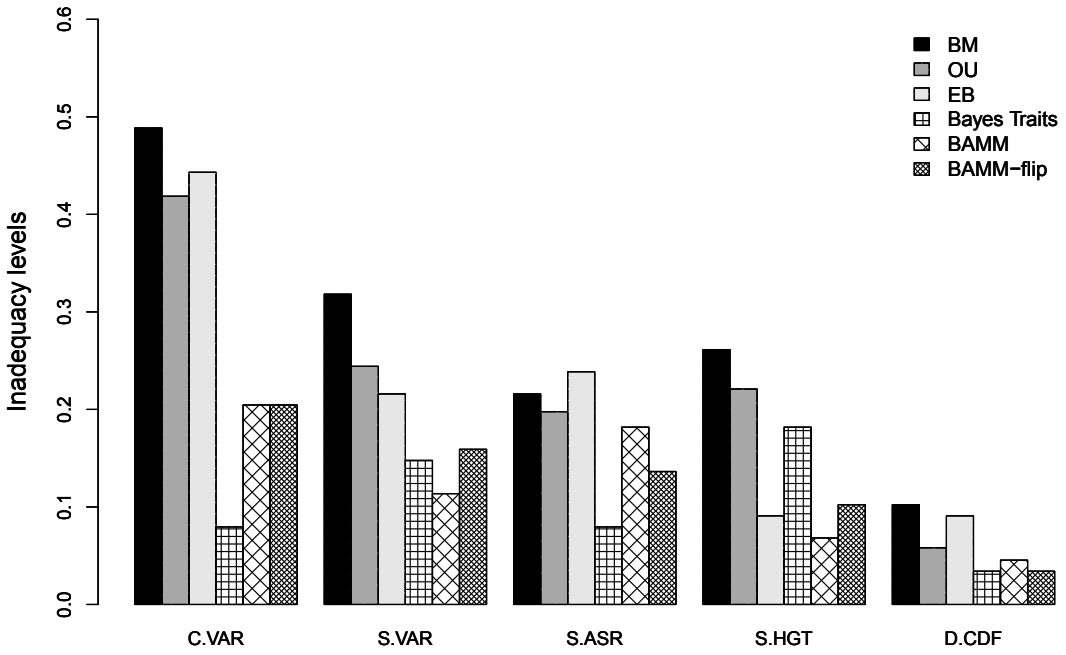

Figure 2.3. Inadequacy levels (quantified as the frequency of trees and associated trait data where the focal model was inadequate) for evolutionary models across avian clades, showing model inability to account for total variation in the rate of evolution (C.VAR), variation related to branch lengths (S.VAR), ancestral states (S.ASR), and node heights (S.HGT). D.CDF inadequacy refers to deviations in the distribution of independent contrasts from the expected normality under a BM. Single-process (BM, OU and EB) and variable-rates models (BayesTraits and BAMM with time-flip proposal) are considered.

Model fit in the presence of simulated rate-heterogeneity

In the absence of rate-heterogeneity (constant-rate trees) all models perform adequately. However, the single process models vary in their ability to capture evolution on heterogeneous trees (Figure 2.5). Similar to results on the empirical data, variable-rates models generally performed better than single process models, and also recorded low levels of inadequacy overall. The magnitude of rate changes affected the absolute fit of models consistently across all simulated rate heterogeneity scenarios. Specifically, the fit of single-process models was better on simulations involving decreases in the rate of evolution compared to rate-increases.

On branches with simulated rate-changes, variable-rates models typically underestimated the magnitude of rate-changes (Figure 2.6; also Figure S3b). This effect was stronger with increasing magnitudes of rate-shifts, and ARBUTUS diagnostics also detected a poorer model fit as the magnitude of rate-shifts became bigger for both rate-increases and decreases (Figure 2.5). The mean of the squared contrasts (M.SIG) was very rarely inadequate across our analyses, and this particular diagnostic has been previously identified as having low power to detect model inadequacy (Pennell et al., 2015). We therefore do not report or discuss M.SIG further. Also, we did not specifically model directional trends of rate variation in relation to ancestral states or branch lengths. Accordingly, these ARBUTUS diagnostics do not reveal any specific problems related to the models fitted; rather, inadequacy levels follow the trends predicted by the tests related to temporal and total rate variation (Figure S1).

Model ability to account for overall rate heterogeneity

Single-process models recorded particularly high levels of inadequacy when heterogeneity is simulated as rate-increases on isolated terminal branches or on several branches forming a clade (Figure 2.5a). In addition, and as expected, the BM and OU models frequently fail to account for rate-deceleration processes across the whole tree. Although designed to model rate heterogeneity, BAMM also tended to underestimate total rate variation (mostly positive C.VAR differences, Figure S5a), and especially missed the rate-increases on isolated terminal branches. However, the inadequacy levels for BAMM were typically lower than the single process models. Further, the time-flip proposal improved absolute adequacy relative to the fixed time-varying prior in BAMM (Figure S4a). Overall, model adequacy in terms of capturing rate heterogeneity was highest for BayesTraits; however, it was also the only model that regularly overinflated estimates of the total rate variation

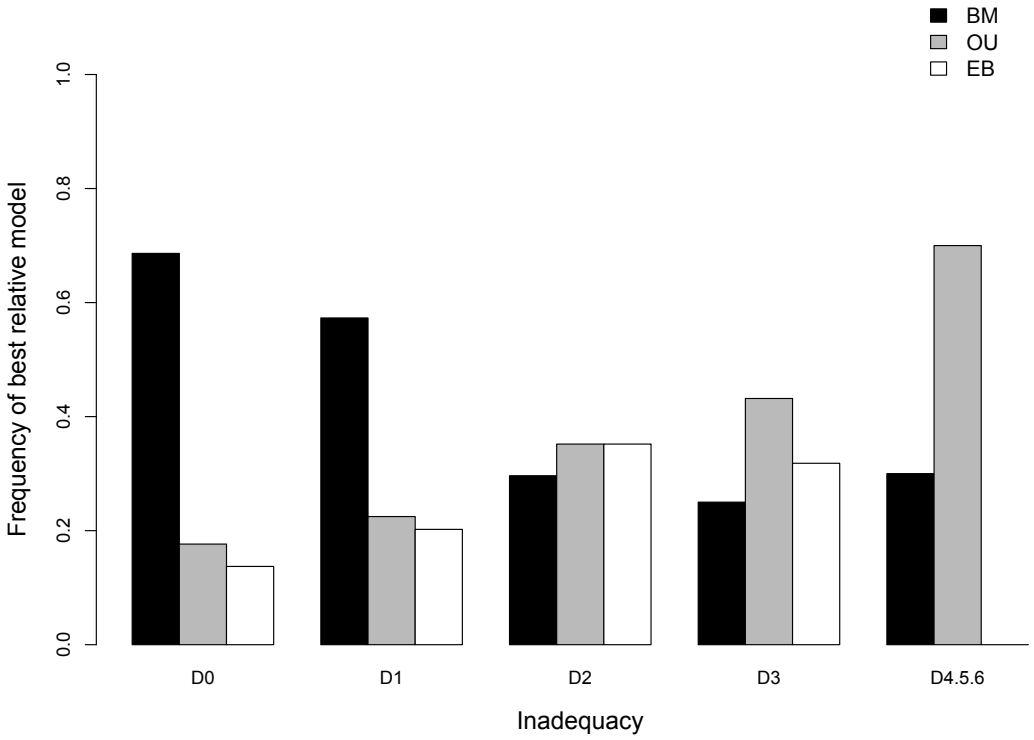

Figure 2.4. Frequency of the best relative single-process model (highest AICw) for increasing levels of inadequacy across avian clades. Inadequacy levels are quantified as the number of model fit diagnostics failed across all three models (from D0 – no adequacy tests failed, to D4.5.6 – four or more failed tests).

(negative C.VAR differences, Figure S5a; also slightly higher differences between true and estimated rates of evolution compared to BAMM; Figure 2.6).

Model ability to account for temporal rate-variation

Not surprisingly, the BM and EB models described the temporal aspect of rate-variation poorly when rate increases were simulated on terminal isolated branches (Figure 2.5b), as they underestimated these late shifts (negative S.HGT, Figure S5b). BAMM also showed a ubiquitous tendency to overestimate rates early on and underestimate the late increases (all negative S.HGT; Figure S5). All models except BAMM were unable to accurately account for rate-deceleration processes across the whole phylogeny (Figure 2.5b), as they underestimate high initial rates and

overestimate terminal rates (all positive S.HGT, Table S1). The EB model performed better than the BM, OU models (as expected), and BayesTraits, but still tended to miss fast decelerating processes. Early bursts also led to the highest inadequacy levels for BayesTraits compared to all other heterogeneity scenarios (Figure 2.5, Figure 2.6).

The influence of tree size on model ability to detect rate shifts; Tendency of variable-rates models to overfit; Likelihood Tests

The ability of BayesTraits to detect a rate-shift on individual branches or across a whole-clade was not influenced by the size of the simulated trees (Figure S6, S7, S8). The ability of BAMM-flip to detect a clade rate shift did not differ between trees of different sizes although on average the model recovered rate increases better in bigger trees (Figure S9). Further, the ability of BayesTraits to detect a clade-shift in trees of 100 tips was little influenced by the size of the heterogeneous clade (Figure S10). Similarly, BAMM-flip recovered clade rate-changes similarly well across different clade-sizes (Figure S11). Universally, the main factor affecting model ability to detect rate shifts was the shift magnitude, and models recovered big shifts better than smaller ones, both in respect of increases and decreases in the rate of evolution.

BayesTraits commonly inferred rate increases up to two-fold when fitted on constant-rate trees and associated data (26–33% frequency of trees with rate shifts); however, the frequencies of trees with shifts dropped considerably when considering rate changes bigger than x5 (8.5%), x10 (0.5%) and x20 (0%, Table S2). Further, the vast majority of rate increases occurred on terminal branches. There was no clear tendency for BAMM to infer false early rate-decelerating processes when fitted on constant-rate trees and trait data, either using a time-flip proposal (β distributions average around a mean = - 0.14 ± 0.18 SD, and a median

= -0.08) or not (β mean = - 0.12 ± 0.43 SD, and a median = - 0.07, Figure S12). Per-branch comparisons between the estimated and true rates of evolution across constant rate-trees also show no worrying amount of overfit from variable-rates models; however, rates inferred by BAMM-flip show more noise around the true values compared to BayesTraits (Figure S2).

When considering the simulated data with single-branch, clade and terminal shifts, β values also distributed normally, but the central points and deviations differed across heterogeneity scenarios (Figure S13). When evolution was constrained to time-varying processes (Figure S13b), β distributions were slightly shifted right towards positive values for simulated rate-increases; that is BAMM infers processes of slight gradual rate increases at the root when some late rate-increases are present. This trend was, however, corrected by BAMM-flip (Figure S13a). Using the time-varying constrained BAMM alternative also resulted in many weak deceleration processes at the root, rectified by BAMM-flip (β much narrowly distributed along the 0 line). Both BAMM versions approximated slightly steeper rate-deceleration processes as a response to discrete rate-decreases late in the clade (wider ranged β distributions). Per-branch differences between estimated and simulated rates of evolution also showed a small tendency for BAMM-flip to overestimate rates of evolution on non-changed branches as a response to big rate increases at the tips (Figure S2b). Conversely, BayesTraits underestimated rates on nonchanged branches in these trees (Figure S2a).

As expected, single-branch shifts do not leave much signal in the tip data, whereas clade events and shifts on multiple isolated terminal branches have a high likelihood of being detected by models. Similarly, rate decreases are much less detectable compared with rate increases, and, as the magnitude of a shift increases, so does its signal in the tip data (Figure 2.7).

Absolute vs. relative model fit selection criteria in the presence of rate heterogeneity

Across scenarios simulated under a BM process with discrete shifts (internal branch shift, clade event and terminal rate shifts), the BM model was expectedly most often favoured by model selection criteria, followed by the OU and EB processes (Figure 2.8). Similar to the empirical data, the relative preference for the OU model was not spread randomly across the heterogeneity scenarios considered; rather, the OU model was particularly favoured in scenarios involving big rate increases on branches late in the phylogeny (Figure 2.8b). Further, relative model selection criteria did not reflect the absolute fit of models, and the cases in which the OU model was picked up as best across these simulations were clearly linked with a high inadequacy of all three single-process models fitted (Figure 2.9).

DISCUSSION

Patterns of rate heterogeneity in avian body mass evolution and consequences to model fit

Generally, variable-rates models performed well in capturing the phylogenetic distribution of the data, as highlighted by their low levels of inadequacy across ARBUTUS diagnostics, on both simulated and empirical data sets. Allowing for rate heterogeneity when mod- elling trait evolution can thus provide a robust approach to understanding trait evolution, both in the presence and absence of variability in rates. Conversely, assuming a constant process can misguide the choice of best model and generate poor inferences about the evolutionary process across groups of interest. The intensity of body mass rate variation fluctuated across avian phylogenetic groups, but rate heterogeneity was prevalent. As a consequence, single-process models commonly gave poor estimates on the total amount of rate variation present in these data sets and were highly inadequate compared with the more flexible variable-rates approaches.

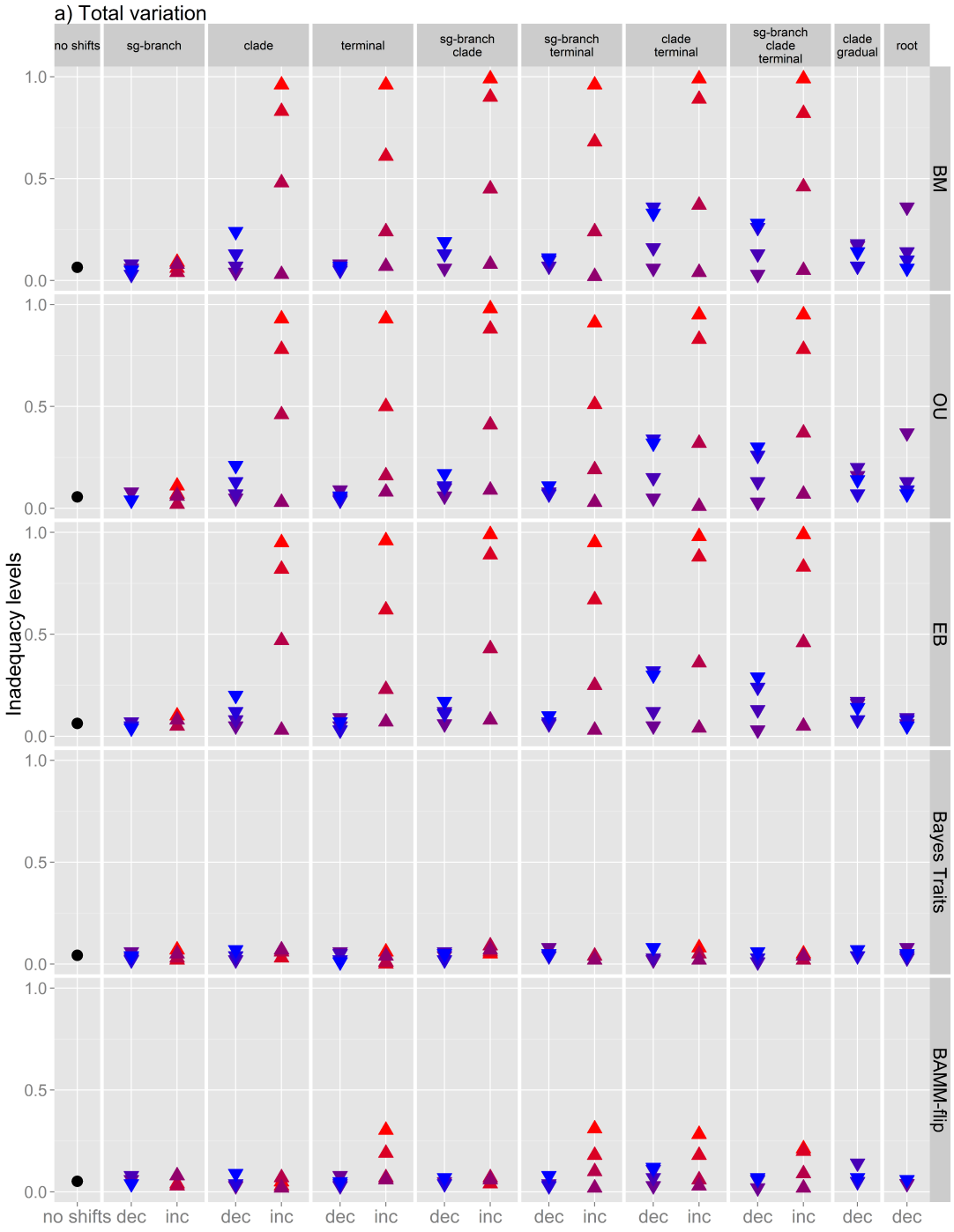

Figure 2.5a. Model inadequacy levels (quantified as the frequency of trees and associated trait data where the focal model was inadequate) across a simulated Brownian Motion process (no shifts i.e. shift magnitude = 1) and rate-heterogeneity scenarios: internal branch shift; clade event; rate-changes on isolated, terminal branches; rate-burst followed by gradual decreases within a clade, and constant rate-deceleration process from root to tips. Single-process (BM, OU and EB) and variable-rates models (BayesTraits and BAMM with time-flip proposal) are considered.

Inadequacy levels measure model ability to account for (a) total rate variation. Inadequacy is quantified separately for rate increases (up-pointing triangles) and decreases (down-pointing triangles), and the exact magnitude of each shift is highlighted by the blue-red colour scheme. For scenarios involving gradual rate-changes, the natural logarithm of the shift magnitude represents the constant rate-change parameter.

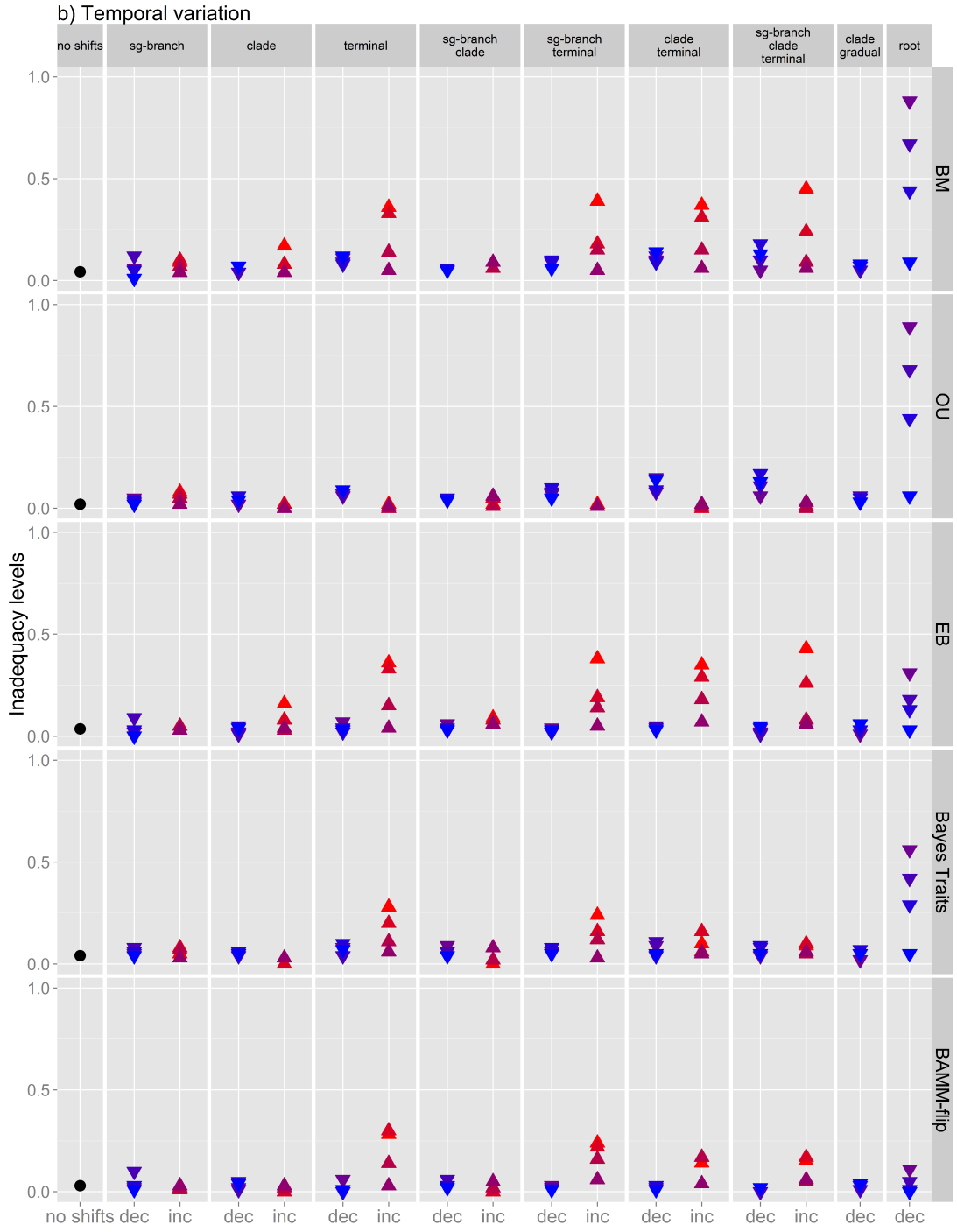

Figure 2.5b. Model inadequacy levels (quantified as the frequency of trees and associated trait data where the focal model was inadequate) across a simulated Brownian Motion process (no shifts i.e. shift magnitude = 1) and rate-heterogeneity scenarios: internal branch shift; clade event; rate-changes on isolated, terminal branches; rate-burst followed by gradual decreases within a clade, and constant rate-deceleration process from root to tips. Single-process (BM, OU and EB) and variable-rates models (BayesTraits and BAMM with time-flip proposal) are considered.

Inadequacy levels measure model ability to account for (b) temporal variation. Inadequacy is quantified separately for rate increases (up-pointing triangles) and decreases (down-pointing triangles), and the exact magnitude of each shift is highlighted by the blue-red colour scheme. For scenarios involving gradual rate-changes, the natural logarithm of the shift magnitude represents the constant rate-change parameter.

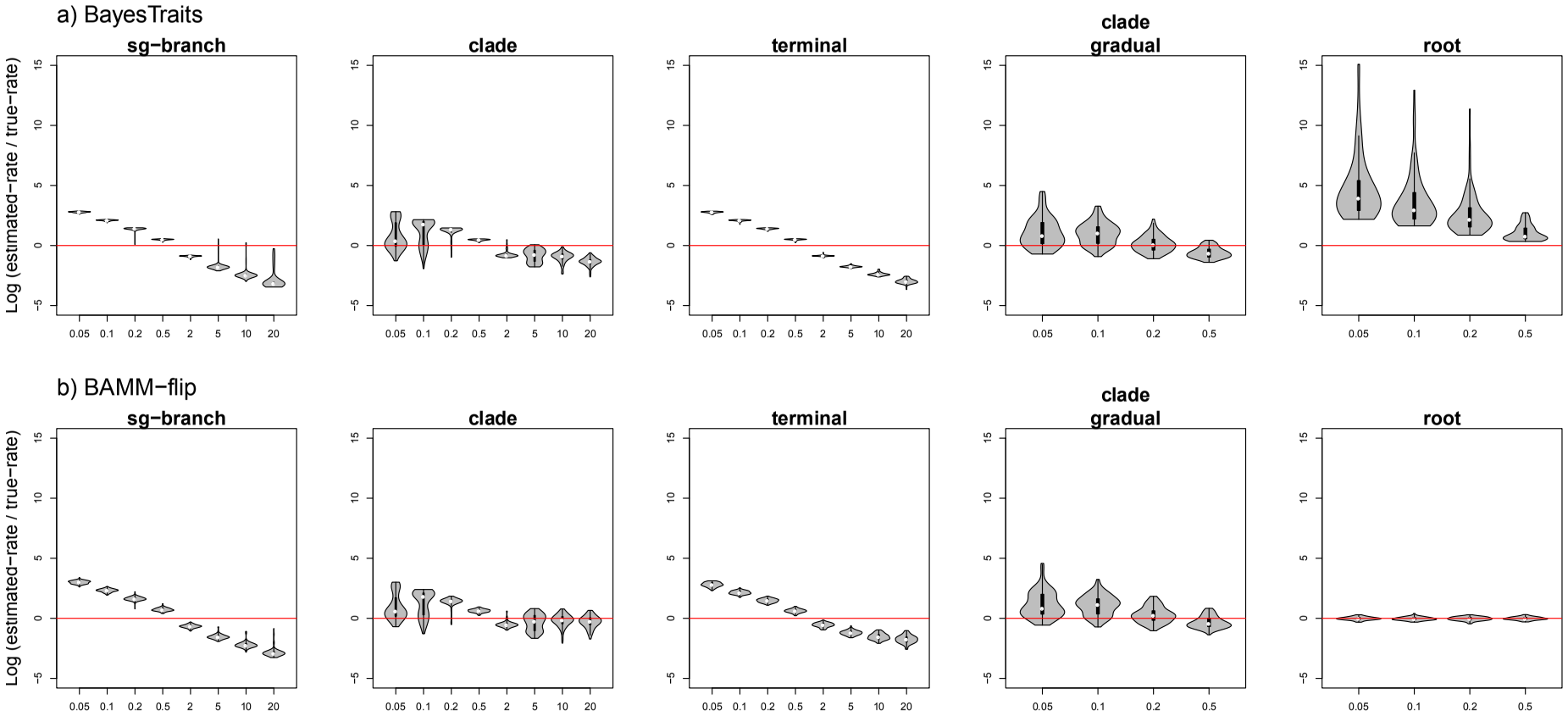

Figure 2.6. Distributions of log-proportions between rates estimated by variable-rates models and the true (simulated) rate-changes on the identical branches. Distributions are shown for various shift magnitudes (x-axis) and heterogeneity scenarios: internal branch shift; clade event; rate-changes on isolated, terminal branches; rate-burst followed by gradual decreases within a clade, and constant rate-deceleration process from root to tips. Results for BayesTraits (a) and BAMM-flip (b).

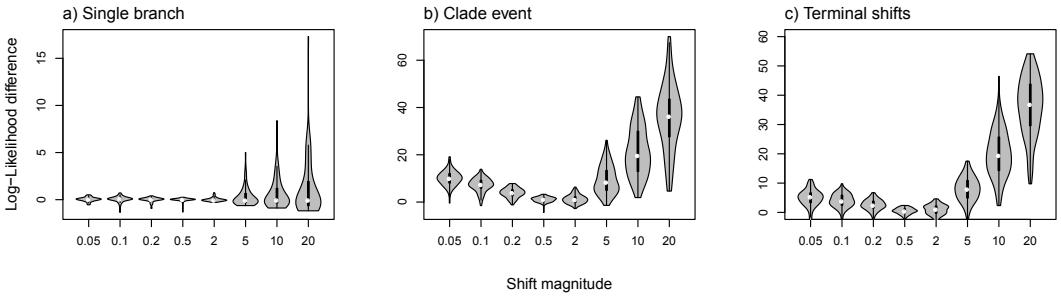

Figure 2.7. Log-likelihood differences between runs on original and transformed trees (with incorporated rate changes) for three rate-heterogeneity scenarios: (a) internal branch shift, (b) clade event, and (c) multiple non-clustered rate-changes at the tip. The magnitudes of shifts in each category are represented on the x-axis.

In general, evolutionary models recorded similar inadequacy tendencies across simulated and empirical data sets, ruling out biases such as phylogenetic or measurement error as determinants of inadequacy differences between models in favour of rate heterogeneity. Observations on model inadequacy specific to the empirical data sets likely signalled attributes of avian body mass evolution. Several clades (e.g. albatrosses, shearwaters, petrels, Figure S99b; whistlers, Figure S36b) showed a characteristic of high rates early in the phylogeny followed by rate decelerating processes, identified by BAMM and the EB model. The simulation step highlighted the tendency of BM, OU and BayesTraits to miss such patterns. Therefore, where inferred, early bursts are likely an accurate description of body mass evolution. Accordingly, the distribution of the BAMM rate-decay parameters at the root (β) across the empirical data was fat-tailed, with the outliers signalling the burst processes (Figure S14). BAMM without the time-flip algorithm recorded more powerful decelerating processes at the root (i.e. smaller β values), alerting on a potential bias for this strict time-varying alternative to infer false extreme early rate-decay processes (especially in clades < 50 species).

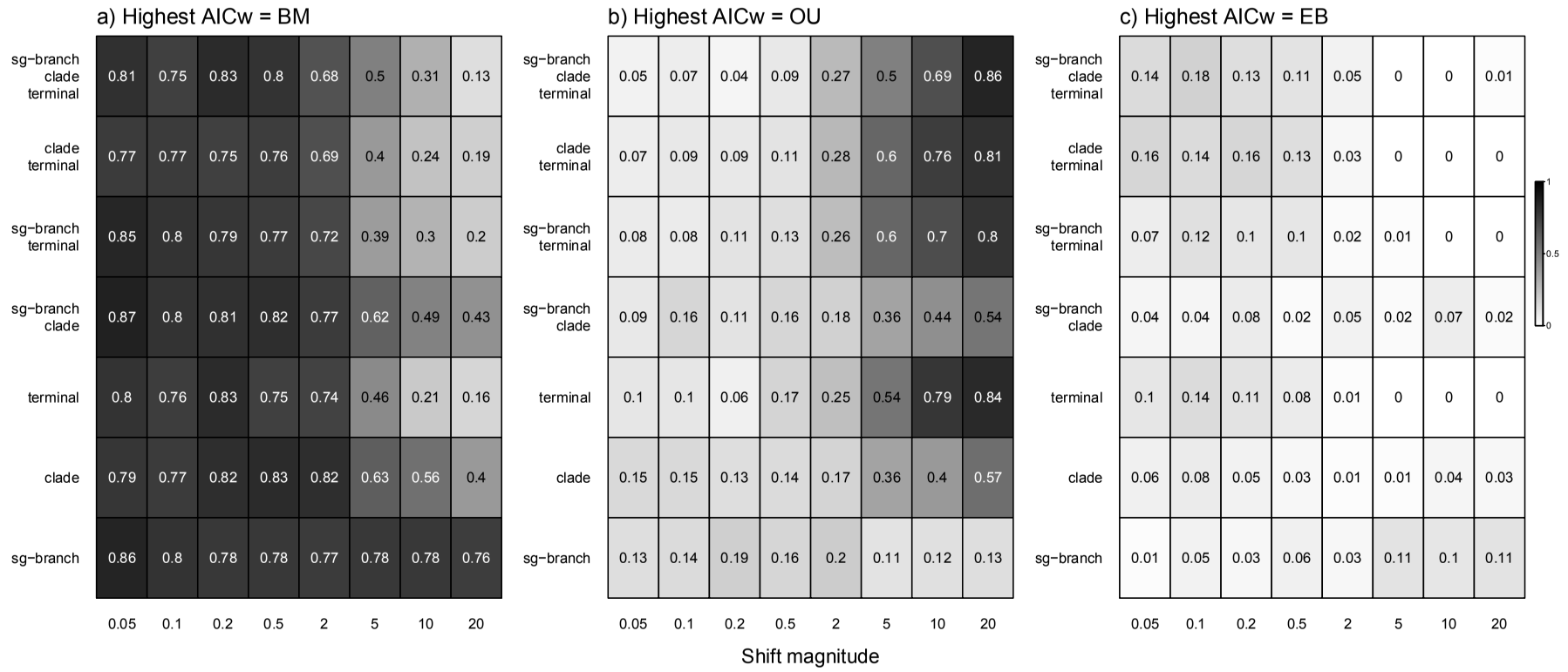

Figure 2.8. Frequency of best relative model (highest AICw) for the BM, OU and EB models across simulated heterogeneity scenarios: internal branch shift, clade events, isolated terminal changes, and combinations. Columns correspond to specific shift magnitudes for each scenario. The colour scheme highlights low (white) to high (black) frequencies of best relative AICw.

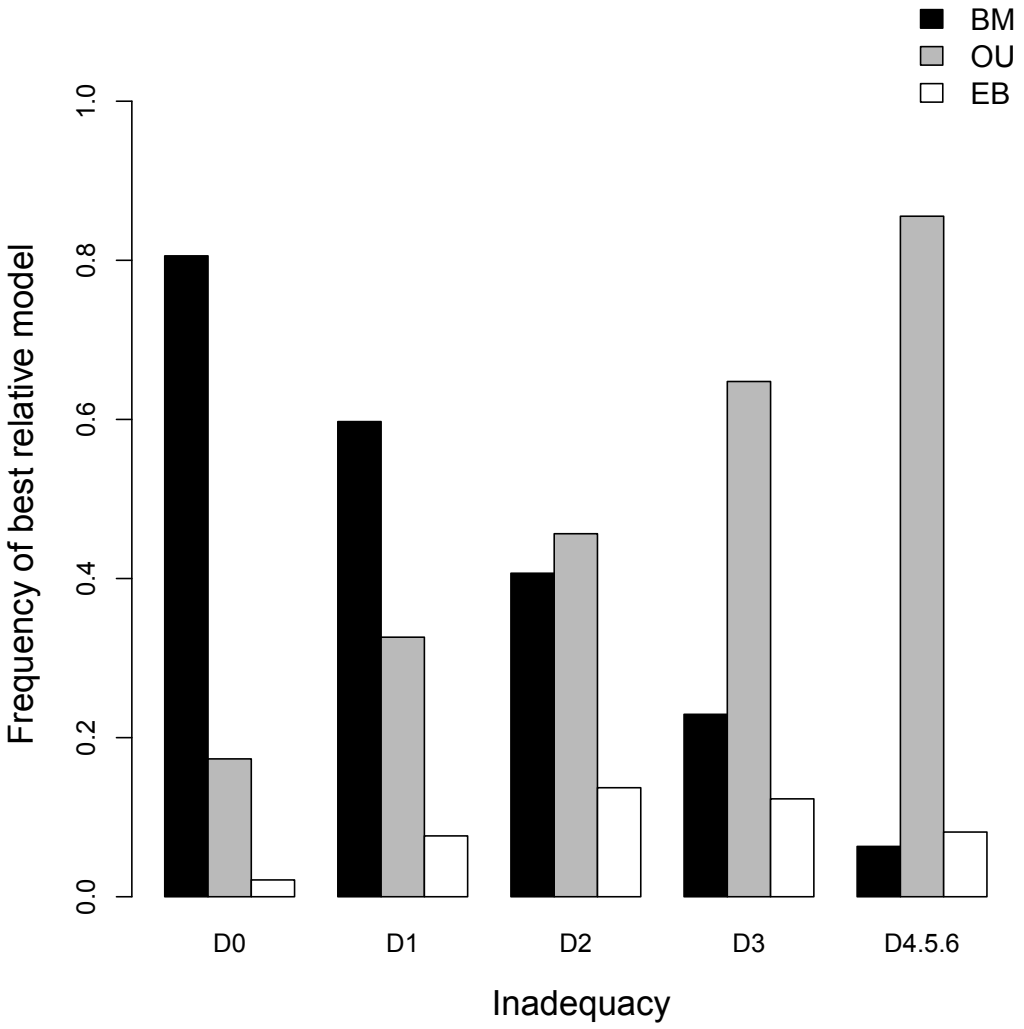

Figure 2.9. Frequency of the best relative single-process model (highest AICw) for increasing levels of inadequacy across all simulated discrete rate-heterogeneity scenarios. Inadequacy levels are quantified as the number of model fit diagnostics failed across all three models (from D0 – no adequacy tests failed, to D4.5.6 – four or more failed tests).

Additionally, variable-rates models identified rate-heterogeneity in the form of branch rate decreases or increases that are not passed to descendants making up a monophyletic group, recurrent whole-clade events, and changes on non-clustered, terminal branches. Both BayesTraits and BAMM reveal a similar prevalence of rate-variation in avian clades (Figure 2.2). We are aware that quantifying the extent of this variation based on per-branch shifts is not particularly suitable for BAMM, as it

can miss or misinterpret gradual processes. However, the algorithm was generally robust, and there was only one extreme case in our analyses: the fast rate-deceleration process in albatrosses, shearwaters, petrels was quantified as a BAMM-flip output of 15 single-branch bursts (Figure 2.2b). Some of the avian clades identified in our analyses with a high degree of rate-heterogeneity in body mass evolution have also been associated with high diversification rates and rapid radiations (e.g. ovenbirds, select gulls, hummingbirds, ant birds and tyrants; Jetz et al., 2012). The forms of rate heterogeneity we report are most likely not a statistical artefact, given the high prevalence of consistent rate-variation patterns and the general low inadequacy levels of variable-rates models. Moreover, similar patterns have also been reported across a variety of phylogenetic groups: clade rate increases (Pacific minnows, Martin & Bonett, 2015) and decreases (*Taphozous* bats, Venditti et al., 2011), similar group events, but involving a basal shift, propagated then through-out the clade of interest (*Ctenotus* lizards, Rabosky et al., 2014a), single-lineage internal bursts restricted to the branches leading to *Hominidae* (great apes), *Chiroptera* (bats, Venditti et al., 2011), or *Mysticeti* (baleen whales, Baker et al., 2016). Such phylogenetic distributions of rates reinforce the importance of allowing for lineage-specific rate changes when modelling trait evolution, in order to avoid inaccurate inferences about the evolutionary process. As presented, even for phylogenetic scales up to hundreds of species one could attribute differences in the rate of evolution between groups to a general clade event rather than to considerable changes on a single or restricted number of lineages.

We used the output of variable-rates models in conjunction with adequacy checks to clarify the conclusions on the tempo of trait evolution in some problematic avian groups. For example, across tanagers and allies, the OU model had a clear superior relative fit. However, all single-process models were inadequate, and variablerates models further showed an exceptional burst of evolution within the clade consisting

of Galapagos finches (Figure S78). Thus based on relative fit only, an interpretation of constrained evolution could have been preferred to a completely different, limited island radiation hypothesis. We identified the same issue even when the number of radiating species was very small (like the case of steamer ducks, a genus of only four flightless ducks, Figure S74). Absolute adequacy checks also guided output interpretation for variable-rates models. For example, in the clade *Procelariidae*, BayesTraits inferred a single-branch shift increase ancestral to albatrosses, evolving towards a big body size (Figure S99a). BAMM however inferred this ancestral increase as part of an early burst process spanning across the whole phylogeny (Figure S99b). ARBUTUS signalled that BayesTraits inadequately described the temporal variation in this group and missed early fast rates, thus favouring the BAMM interpretation of rate variation on this tree. The EB model also modelled temporal heterogeneity accurately but missed the complexities of rate-variation across the whole clade (positive C.VAR, Figure S99c).

We only used trees containing species where sequence data was available, ruling out a potential over inflation of rate heterogeneity (especially towards the tips) or biased model preference towards an OU model due to incorporating species based on taxonomic information only (Rabosky, 2015). We did not, however, incorporate measurement error into our empirical analyses, which could potentially cause an overestimation of rate heterogeneity across the body mass data (Silvestro et al., 2015). From the two variable-rate models included in our analyses, BayesTraits can account for measurement error by modelling many rate-increases on isolated terminal branches, but it cannot be distinguished whether the presence of such increases in the outputted scaled trees is caused by noisy data or real rate-changes at the tips. However, our analyses on simulated datasets showed that the model rarely gives false substantial rate-changes at the tips. Still, we argue that some rate-variation across empirical datasets should be interpreted with caution, if at all, and

the above mentioned considerations led us to not take into account rate-shits smaller than x2 when quantifying patterns of avian trait evolution (Figure 2.2).

Heterogeneity patterns that mislead models

As a general rule, specific forms of heterogeneity and not the general complexity of rate variation caused problems for evolutionary models. That is, when a specific rateheterogeneity pattern caused a model to fit poorly, the effect occurred frequently across all simulations. For example, data simulated with a shift in rate across a whole clade led to poor performance of candidate models, regardless of whether other types of shifts were also simulated. Having simulated under a range of scenarios and magnitudes enabled us to mark how models approximate trait evolution in response to various heterogeneity cases, and also highlight which and to what extent rate-variation scenarios mislead model inference.

There was a clear difference between how models handled increases and decreases in the rate of evolution. Single-process models came out as more adequate in the presence of rate decreases compared with increases. This difference in model fit is probably a consequence of the small likelihood that discrete branch rate decreases leave any signal in the data (Figure 2.7). That is, single-process approaches do not approximate rate decreases better; rather, this form of rate variation is hardly tractable in the data, and many different processes alongside rate shifts can theoretically lead to that particular tip trait distribution. Similar to rate decreases, single internal branch shifts were typically not flagged up as being inadequately described across models, because a single internal branch has little impact on the likelihood of the model (except when the shifts have a large magnitude, Figure 2.7a). Variable rates methods also showed good absolute fit when ran on trees and tip-data simulated under single-branch shifts and rate-

decreases scenarios; however, models estimated these rate-changes with a similar true accuracy as other heterogeneity scenarios (Figure 2.6).

Multiple branch increases had a high negative impact on model adequacy. Isolated terminal increases were particularly troublesome compared with whole-clade events, potentially because single-process models accommodate rate variation by changing estimated r^2 on several branches adjacent to the ones presenting rate shifts. Thus, changes on non-clustered branches can cause a wide spread of falsely inferred rates. Similarly, BAMM shapes rate heterogeneity as a process across multiple branches, and it is less able to capture single-branch shifts (Rabosky & Huang, 2016). In BAMM, detection of single branch shifts requires two events (i.e. nested rate shifts with modelling of an increase at the start of a branch followed by a subsequent decrease). In contrast, BayesTraits explicitly allows changes on single branches with one event. Accordingly, BAMM had poorer ARBUTUS diagnostics in the presence of isolated tip increases (Figure 2.5), and overestimated rates of evolution on the untransformed branches in trees with simulated terminal rate-changes (Figure S2). However, the method accurately described heterogeneity in the form of whole clade rate increases. Also, the accuracy of estimates improved when using the more flexible BAMM-flip version.

The root to tip rate decelerating process caused most spurious results across all models except BAMM. Even the EB model missed these processes in almost 20% of cases, particularly when a steep decrease was involved (a = log(0.05) or log(0.1)). BayesTraits was also largely unable to describe early bursts (Figure 2.5, Figure 2.6). The lack of strength in modelling early bursts by models (expect BAMM) was highlighted in the empirical datasets as well, and the EB was often not separated clearly from the BM in terms of relative fit, despite its superior adequacy in modelling temporal rate variation. These results add to the body of ideas

advocating that early bursts are often not identified across datasets (Harmon et al., 2010, Slater et al., 2010; Venditti et al., 2011, Alhajeri et al., 2015) not necessarily because such scenarios are scarce in nature, but because current models do not have the power to detect them, and early shifts leave little signal in the tip-data (Slater & Pennell, 2014).

The size of simulated trees did not generally affect the ability of variable-rates models to recover rate shifts, and these methods were similarly robust for trees of 25 to 200 species. The detectability of rate shifts was largely influenced by the shift magnitude, and by whether a shift was on isolated branches or as part of a clade (for BayesTraits, grouped events were more easily detected). These results hence mirror the patterns of absolute adequacy seen throughout the main analyses, and variable-rates models prove suitable for detecting heterogeneity even when the group of interest is fairly small. Similarly, we did not find the number of species involved in a clade event to affect the shift detectability; however, we only had data for clades ranging between 10 and 30 species. Conversely, the magnitude of the regime shift had a substantial effect on the model ability to recover the event, and most likely potential effects of a larger variability in clade sizes wane when the shift magnitude is taken into account; that is, small clades with a big magnitude shift will be successfully recovered by models (e.g. body mass evolution in the steamer ducks, Figure S74), but for small magnitudes, a bigger clade might be needed. Out of the two variable-rates models included, BAMM-flip showed some sensitivity to both tree and clade-size, specifically regarding its ability to detect the larger rate shifts.

Other limitations of variable rate models

BayesTraits generally approximated trait evolution with low inadequacy levels; however, the model did tend to overestimate total rate heterogeneity, mostly

because it inferred multiple false terminal rate increases. We repeated the adequacy analyses on the simulated heterogeneity scenarios using the mean (rather than the median) branch lengths to summarise the posterior scaled trees from the variable-rates models. Following this approach, BayesTraits clearly registered higher inadequacy levels (Table S4, Figure S16), mostly determined by cases of extreme terminal increases with a low probability in the posterior that caused additional untrue terminal branch shifts in the averaged scaled trees. Approaches such as BayesTraits have been accused of overinflating rate variation before (Ho et al., 2014), mainly because of the relaxed/permissive nature of (default) priors. Further, our analyses on trees and trait data simulated with no rate-shifts showed that, while considerable rate-shifts (i.e. > five-fold) inferred using BayesTraits are probably supported by the data, more caution is needed when making inferences about smaller (< two-fold) rate changes at the tips.

BAMM was prone to underestimations of total rate variation and an inability to account for isolated tip increases, expected since heterogeneity is modelled in a less flexible framework compared to BayesTraits (Rabosky & Huang, 2016). Allowing the model to flip between time-varying and time-constant processes did, however, improve fit in comparison to the constrained time-varying version (Figure S4a). Further, BAMM showed an inclination towards rate-decelerating processes, as shown by: (i) a negative S.HGT ubiquitously across the analyses, (ii) the distributions of the rate-change parameters governing the root regime (β), and (iii) the comparison between estimated and true rates on branches with no simulated rate-shifts. Therefore, BAMM tends to infer some false early bursts both in the presence and absence of rate heterogeneity, but the intensity and prevalence of these erroneous inferences is low. Using a BAMM-flip alternative also reduces the occurrence of false rate-bursts, however, BayesTraits still showed best true fit under the assumption of homogeneity in rates (Figure S2).

There are several other approaches to rate-heterogeneity in trait evolution, and a notable body of such models use parametric methods to model a distribution of evolutionary rates that allows jumps (e.g. Landis et al., 2013, Elliot & Mooers, 2014). Elliot and Mooers (2014) method is readily available in StableTraits, however, the outputted scaled tree (i.e. a tree with branches scaled by the rate of trait evolution) cannot be equated with a parameterized global transformation of the branch lengths. Hence, we could not use the output of StableTraits to build the unit tree in ARBUTUS. Pennell et al. (2015) also warn that jump methods are not (yet) compatible with the ARBUTUS framework. Further, BayesTraits is a non-parametric approach, and the single-lineage bursts are likely a good approximation of a rate jump. Thus, we believe that jump methods would produce similar patterns in the evolutionary process, and record similar adequacy levels with BayesTraits.

Absolute vs. relative model fit in the presence of rate heterogeneity

A relative preference for the OU model (and derivatives) over other single-process models is widespread in the literature (e.g. Collar et al., 2009, Harmon et al., 2010, Blackburn et al., 2013, Knope & Scales, 2013, Price & Hopkins, 2015), but there are many challenges attributed to estimation and interpretation of this model (Cooper et al., 2016; Ho et al., 2014). Pennell et al. (2015) found the OU method is largely inadequate even though it predominantly scored highest AICw over the BM and EB models on angiosperm datasets. Our adequacy analyses also linked high relative fit for OU methods with cases of high inadequacy for all single-process models included, both across simulated and empirical datasets. Particularly, when species record very high rates of evolution late in the phylogeny (especially nonclustered species), the OU model is favoured by relative selection criteria over other approaches. The link between inadequacy levels and model relative fit was stronger across the simulated compared with the empirical data, likely due to the existence of

other evolutionary processes besides rate shifts that affect relative fit across avian data sets. Nonetheless, often a high relative fit for the OU model was a consequence of rate heterogeneity, and not of body mass evolution under an OU-type process. Not accounting for measurement error could have also caused a biased preference for the OU model across the empirical data sets (Silvestro et al., 2015); however, the link between late rate heterogeneity and a bias for the OU model clearly emerges from the results on the simulated datasets, ruling out the possibility that measurement error is solely responsible for the biased selection criteria across the avian datasets.

Evolutionary models continue to be developed to approximate the macroevolutionary process with a higher degree of realism, by dealing with increasingly complex deviations from a simple process. Here we used a large data set of avian body mass to show that variation in the rate at which traits change can be a common event in relatively small phylogenetic clades (up to hundreds of species). We further used both empirical data and simulated rate-heterogeneity scenarios to show that allowing rates of evolution to vary in the absence of a priori assumptions about the magnitude or location of shifts represents a reliable method to pattern trait evolution. Variable-rates approaches do have limitations; heterogeneity in the form of rate rate-decreases and single-branch changes is hard to detect, and generates poor method fit. Further, rate-increases on terminal branches can be poorly approximated even when allowing for rate-variation, and early bursts in particular are often misquantified by BayesTraits. However, we show that interpretation can be guided by the use of absolute adequacy tests. We also underline the potential for misleading inferences when using relative model selection criteria only e.g. missing early bursts or favouring OU-type processes when late rate-variation is present. This work does not invalidate the concepts behind standard single-process methods, rather we advise using the more flexible

applications of these approaches (e.g. implementation of EB and OU models in a Bayesian framework, Pennell et al., 2014, Uyeda & Harmon, 2014).

ACKNOWLEDGMENTS

We thank R. Freckleton, C. Cooney, J. Bright, E. Hughes, A. Krystalli, M. Clarke, E. Barnett and M. Pennell for useful feedback on alternative versions of the manuscript. This work was funded by the European Research Council (ERC-2013-CoG-615709-ToLERates) and a Royal Society University Research Fellowship to GHT.

REFERENCES

Alhajeri, B. H., Schenk, J. J., & Steppan, S. J. (2015). Ecomorphological diversification following continental colonization in muroid rodents (*Rodentia*: *Muroidea*). *Biol. J. Linn. Soc., 117*(3), 463-481.

Baker, J., Meade, A., Pagel, M., & Venditti, C. (2015). Adaptive evolution toward larger size in mammals. *Proc Natl Acad Sci U S A, 112*(16), 5093-5098.

Baker, J., Meade, A., Pagel, M., & Venditti, C. (2016). Positive phenotypic selection inferred from phylogenies. *Biol J Linn Soc, 118*(1), 95-115.

Blackburn, D. C., Siler, C. D., Diesmos, A. C., McGuire, J. A., Cannatella, D. C., & Brown, R. M. (2013). An adaptive radiation of frogs in a southeast Asian island archipelago. *Evolution, 67*(9), 2631-2646.

Blomberg, S. P., Garland, T., & Ives, A. R. (2003). Testing for phylogenetic signal in comparative data: behavioral traits are more labile. *Evolution, 57*(4), 717-745.

Boettiger, C., Coop, G., & Ralph, P. (2012). Is your phylogeny informative? Measuring the power of comparative methods. *Evolution, 66*(7), 2240-2251.

Burnham, K. P., & Anderson, D. R. (2004). Multimodel Inference: Understanding AIC and BIC in Model Selection. *Sociol. Method. Res., 33*(2), 261-304.

Butler, M. A., & King, A. A. (2004). Phylogenetic comparative analysis: a modeling approach for adaptive evolution. *Am Nat, 164*(6), 683-695.

Cavalli-Sforza, L. L., & Edwards, A. W. F. (1967). Phylogenetic analysis. Models and estimation procedures. *American journal of human genetics, 19*(3 Pt 1), 233-257.

Collar, D. C., O'Meara, B. C., Wainwright, P. C., & Near, T. J. (2009). Piscivory limits diversification of feeding morphology in centrarchid fishes. *Evolution, 63*(6), 1557-1573.

Cooper, N., Thomas, G. H., Venditti, C., Meade, A., & Freckleton, R. P. (2016). A cautionary note on the use of Ornstein Uhlenbeck models in macroevolutionary studies. *Biol J Linn Soc, 118*(1), 64-77.

Derryberry, E. P., Claramunt, S., Derryberry, G., Chesser, R. T., Cracraft, J., Aleixo, A., . . . Brumfield, R. T. (2011). Lineage diversification and morphological evolution in a large-scale continental radiation: the neotropical ovenbirds and woodcreepers (aves: Furnariidae). *Evolution, 65*(10), 2973-2986.

Dunning, J. B. e. (2008). Handbook of Avian Body Masses. *2nd ed. CRC press., CRC, Boca Raton, FL.*

Eastman, J. M., Alfaro, M. E., Joyce, P., Hipp, A. L., & Harmon, L. J. (2011). A novel comparative method for identifying shifts in the rate of character evolution on trees. *Evolution, 65*(12), 3578-3589.

Elliot, M. G., & Mooers, A. Ø. (2014). Inferring ancestral states without assuming neutrality or gradualism using a stable model of continuous character evolution. *BMC evolutionary biology, 14*(1), 226-241.

Felsenstein, J. (1985). Phylogenies and the comparative method. *Am. Nat., 125*(1), 1-15.

Freckleton, R. P., & Harvey, P. H. (2006). Detecting non-Brownian trait evolution in adaptive radiations. *PLoS Biol, 4*(11), e373.

Grundler, M. C., & Rabosky, D. L. (2014). Trophic divergence despite morphological convergence in a continental radiation of snakes. *Proc Biol Sci, 281*(1787), 20140413.

Hansen, T. F., & Martins, E. P. (1996). Translating between microevolutionary process and macroevolutionary patterns: the correlation structure of interspecific data. *Evolution, 50*(4), 1404-1417.

Harmon, L. J., Losos, J. B., Jonathan Davies, T., Gillespie, R. G., Gittleman, J. L., Bryan Jennings, W., . . . Mooers, A. O. (2010). Early bursts of body size and shape evolution are rare in comparative data. *Evolution, 64*(8), 2385-2396.

Hipsley, C. A., Miles, D. B., & Muller, J. (2014). Morphological disparity opposes latitudinal diversity gradient in lacertid lizards. *Biol Lett, 10*(5), 20140101.

Ho, L. S. T., Ané, C., & Paradis, E. (2014). Intrinsic inference difficulties for trait evolution with Ornstein-Uhlenbeck models. *Methods Ecol. Evol., 5*(11), 1133-1146.

Huelsenbeck, J. P., Ronquist, F., Nielsen, R., & Bollback, J. P. (2001). Bayesian inference of phylogeny and its impact on evolutionary biology. *Science, 294*(5550), 2310-2314.

Jarvis, E. D., Mirarab, S., Aberer, A. J., Li, B., Houde, P., Li, C., . . . Zhang, G. (2014). Whole-genome analyses resolve early branches in the tree of life of modern birds. *Science, 346*(6215), 1320-1331.

Jetz, W., Thomas, G. H., Joy, J. B., Hartmann, K., & Mooers, A. O. (2012). The global diversity of birds in space and time. *Nature, 491*(7424), 444-448.

Kaliontzopoulou, A., & Adams, D. C. (2016). Phylogenies, the Comparative Method, and the Conflation of Tempo and Mode. *Syst Biol, 65*(1), 1-15.

Knope, M. L., & Scales, J. A. (2013). Adaptive morphological shifts to novel habitats in marine sculpin fishes. *J Evol Biol, 26*(3), 472-482.

Landis, M. J., Schraiber, J. G., & Liang, M. (2013). Phylogenetic analysis using Levy processes: finding jumps in the evolution of continuous traits. *Syst Biol, 62*(2), 193-204.

Lovette, I. J., Bermingham, E., & Ricklefs, R. E. (2002). Clade-specific morphological diversification and adaptive radiation in Hawaiian songbirds. *Proc Biol Sci, 269*(1486), 37-42.

Martin, P. R., Montgomerie, R., & Lougheed, S. C. (2010). Rapid sympatry explains greater color pattern divergence in high latitude birds. *Evolution, 64*(2), 336-347.

Martin, S. D., & Bonett, R. M. (2015). Biogeography and divergent patterns of body size disparification in North American minnows. *Mol Phylogenet Evol, 93*, 17-28.

Pagel, M. (1999). Inferring the historical patterns of biological evolution. *Nature, 401*(6756), 877-884.

Pennell, M. W., Eastman, J. M., Slater, G. J., Brown, J. W., Uyeda, J. C., FitzJohn, R. G., . . . Harmon, L. J. (2014). geiger v2.0: an expanded suite of methods for fitting macroevolutionary models to phylogenetic trees. *Bioinformatics, 30*(15), 2216-2218.

Pennell, M. W., FitzJohn, R. G., Cornwell, W. K., & Harmon, L. J. (2015). Model Adequacy and the Macroevolution of Angiosperm Functional Traits. *Am Nat, 186*(2), E33-50.

Plummer, M., Best, N., Cowles, K., & vines, K. (2006). CODA: Convergence Diagnosis and Output Analysis for MCMC. *R News, 6*(1), 7-11.

Price, S. A., Holzman, R., Near, T. J., & Wainwright, P. C. (2011). Coral reefs promote the evolution of morphological diversity and ecological novelty in labrid fishes. *Ecol Lett, 14*(5), 462-469.

Price, S. A., & Hopkins, S. S. (2015). The macroevolutionary relationship between diet and body mass across mammals. *Biol. J. Linn. Soc., 155*(1), 173-184.

Prum, R. O., Berv, J. S., Dornburg, A., Field, D. J., Townsend, J. P., Lemmon, E. M., & Lemmon, A. R. (2015). A comprehensive phylogeny of birds (Aves) using targeted next-generation DNA sequencing. *Nature, 526*(7574), 569-573.

Puttick, M. N., Thomas, G. H., & Benton, M. J. (2014). High rates of evolution preceded the origin of birds. *Evolution, 68*(5), 1497-1510.

Rabosky, D. L. (2014). Automatic detection of key innovations, rate shifts, and diversity-dependence on phylogenetic trees. *PLoS One, 9*(2), e89543.

Rabosky, D. L. (2015). No substitute for real data: A cautionary note on the use of phylogenies from birth-death polytomy resolvers for downstream comparative analyses. *Evolution, 69*(12), 3207-3216.

Rabosky, D. L., & Adams, D. C. (2012). Rates of morphological evolution are correlated with species richness in salamanders. *Evolution, 66*(6), 1807-1818.

Rabosky, D. L., Donnellan, S. C., Grundler, M. C., & Lovette, I. J. (2014a). Analysis and visualization of complex macroevolutionary dynamics: an example from Australian scincid lizards. *Syst. Biol., 63*(4), 610-627.

Rabosky, D. L., Grundler, M., Anderson, C., Title, P., Shi, J. J., Brown, J. W., . . . Kembel, S. (2014b). BAMMtools: an R package for the analysis of evolutionary dynamics on phylogenetic trees. *Methods Ecol. Evol., 5*(7), 701-707.

Rabosky, D. L., & Huang, H. (2016). A Robust Semi-Parametric Test for Detecting Trait-Dependent Diversification. *Syst Biol, 65*(2), 181-193.

Rabosky, D. L., Santini, F., Eastman, J., Smith, S. A., Sidlauskas, B., Chang, J., & Alfaro, M. E. (2013). Rates of speciation and morphological evolution are correlated across the largest vertebrate radiation. *Nat Commun, 4*, 1958.

Reddy, S., Driskell, A., Rabosky, D. L., Hackett, S. J., & Schulenberg, T. S. (2012). Diversification and the adaptive radiation of the vangas of Madagascar. *Proc Biol Sci, 279*(1735), 2062-2071.

Revell, L. J., Mahler, D. L., Peres-Neto, P. R., & Redelings, B. D. (2012). A new phylogenetic method for identifying exceptional phenotypic diversification. *Evolution, 66*(1), 135-146.

Shi, J. J., & Rabosky, D. L. (2015). Speciation dynamics during the global radiation of extant bats. *Evolution, 69*(6), 1528-1545.

Silvestro, D., Kostikova, A., Litsios, G., Pearman, P. B., Salamin, N., & Münkemüller, T. (2015). Measurement errors should always be incorporated in phylogenetic comparative analysis. *Methods Ecol. Evol., 6*(3), 340-346.

Slater, G. J. (2013). Phylogenetic evidence for a shift in the mode of mammalian body size evolution at the Cretaceous-Palaeogene boundary. *Methods Ecol. Evol., 4*(8), 734-744.

Slater, G. J., & Pennell, M. W. (2014). Robust regression and posterior predictive simulation increase power to detect early bursts of trait evolution. *Syst Biol, 63*(3), 293-308.

Slater, G. J., Price, S. A., Santini, F., & Alfaro, M. E. (2010). Diversity versus disparity and the radiation of modern cetaceans. *Proc Biol Sci, 277*(1697), 3097-3104.

Stadler, T. (2011). Simulating trees with a fixed number of extant species. *Syst Biol, 60*(5), 676-684.

Thomas, G. H., & Freckleton, R. P. (2012). MOTMOT: models of trait macroevolution on trees. *Methods in Ecology and Evolution, 3*(1), 145-151.

Thomas, G. H., Freckleton, R. P., & Szekely, T. (2006). Comparative analyses of the influence of developmental mode on phenotypic diversification rates in shorebirds. *Proc Biol Sci, 273*(1594), 1619-1624.

Thomas, G. H., Meiri, S., & Phillimore, A. B. (2009). Body size diversification in anolis: novel environment and island effects. *Evolution, 63*(8), 2017-2030.

Uyeda, J. C., & Harmon, L. J. (2014). A Novel Bayesian Method for Inferring and Interpreting the Dynamics of Adaptive Landscapes from Phylogenetic Comparative Data. *Syst Biol, 63*(6), 902-918.

Venditti, C., Meade, A., & Pagel, M. (2011). Multiple routes to mammalian diversity. *Nature, 479*(7373), 393-396.

Weir, J. T., & Wheatcroft, D. (2011). A latitudinal gradient in rates of evolution of avian syllable diversity and song length. *Proc Biol Sci, 278*(1712), 1713-1720.

Weir, J. T., Wheatcroft, D. J., & Price, T. D. (2012). The role of ecological constraint in driving the evolution of avian song frequency across a latitudinal gradient. *Evolution, 66*(9), 2773-2783.

Wilman, H., Belmaker, J., Simpson, J., de la Rosa, C., Rivadeneira, M. M., & Jetz, W. (2014). EltonTraits 1.0: Species-level foraging attributes of the world's birds and mammals. *Ecological Archives, 95*(7), 2027-2027.

SUPPLEMENTARY MATERIAL

Additional supporting information may be found online in the supporting information tab for this article (doi: 10.1111/jeb.12979). Supplementary material (jeb12979-sup-0001-SupInfo.pdf) comprises of:

Appendix S1: Implementation of BayesTraits and BAMM models (also reproduced in text below).

Table S1: Model inadequacy levels across a simulated constant rate-deceleration process from root to tips, and a simulated rate-burst followed by a gradual decrease within a clade.

Table S2: Frequency at which BayesTraits infers rate shifts in the absence of rate-heterogeneity (i.e. on trees and associated tip-data simulated under a BM mode of evolution).

Table S3: Frequency of positive significant differences ($P < 0.05$) between test statistics across key ARBUTUS diagnostics; results on the empirical data.

Table S4: Model inadequacy levels across a simulated constant rate-deceleration process from root to tips, and a simulated rate-burst followed by a gradual decrease within a clade. Results when models are fitted using mean scaled trees.

Table S5: BayesFactor (BF) evidence for alternative models with various numbers of rate-shifts given by BAMM-flip across the empirical datasets.

Figures S1-S5: Model fit in the presence of simulated rate-heterogeneity. Figure S2 reproduced below.

Figures S6-S11: The influence of tree size on model ability to detect rate shifts.

Figures S12-S14: Tendency of variable-rates models to overfit. Reproduced below.

Figure S15: Rate heterogeneity and general absolute adequacy on empirical data.

Figure S16: Absolute Adequacy on Simulated datasets – results on mean scaled trees.

Figures S17-S104: Avian trees scaled by the rate of body mass evolution as described by BayesTraits and BAMM.

Appendix S1: Implementaiton of BayesTraits and BAMM models

The Variable Rates model in BayesTraits was used with 25 million iterations, sampling every 20000 generations and discarding the 20% iterations as burn in. This left a sample of 1000 scaledtrees. MCMC chains were re-run if the effective sample size (ESS) for the likelihood, alpha, sigma or number of variable rates was smaller than 200. Further, trace and autocorrelation plots were visualised to ensure convergence. Lastly, we checked the multivariate and individual potential scale reduction factor for each variable, and values of psrf > 1.1 were taken as evidence that the runs had not mixed. Four independent chains were used for each tree, and, if converged, estimates from all four were put together. For BAMM, the MCMC chain was run with 30 million iterations, sampling every 15000 generations, so that 2000 samples remained recorded. The burn in period was set for 25%. MCMC chains were re-run if the ESS for the number of shifts, logPrior, log likelihood, event or acceptance rates was under 200. In a limited number of simulated trees, within chain convergence was not successful even after four repeated runs; these trees were further discarded from the analyses (2 cases in the discrete simulations, 2 cases for the gradual deceleration within a clade, and 1 case for the constant-rate deceleration process from root to tips). Similar to BayesTraits, between chain convergence was checked using the potential scale reduction factor, and, if the runs had successfully mixed, estimates for four independent chains were combined.

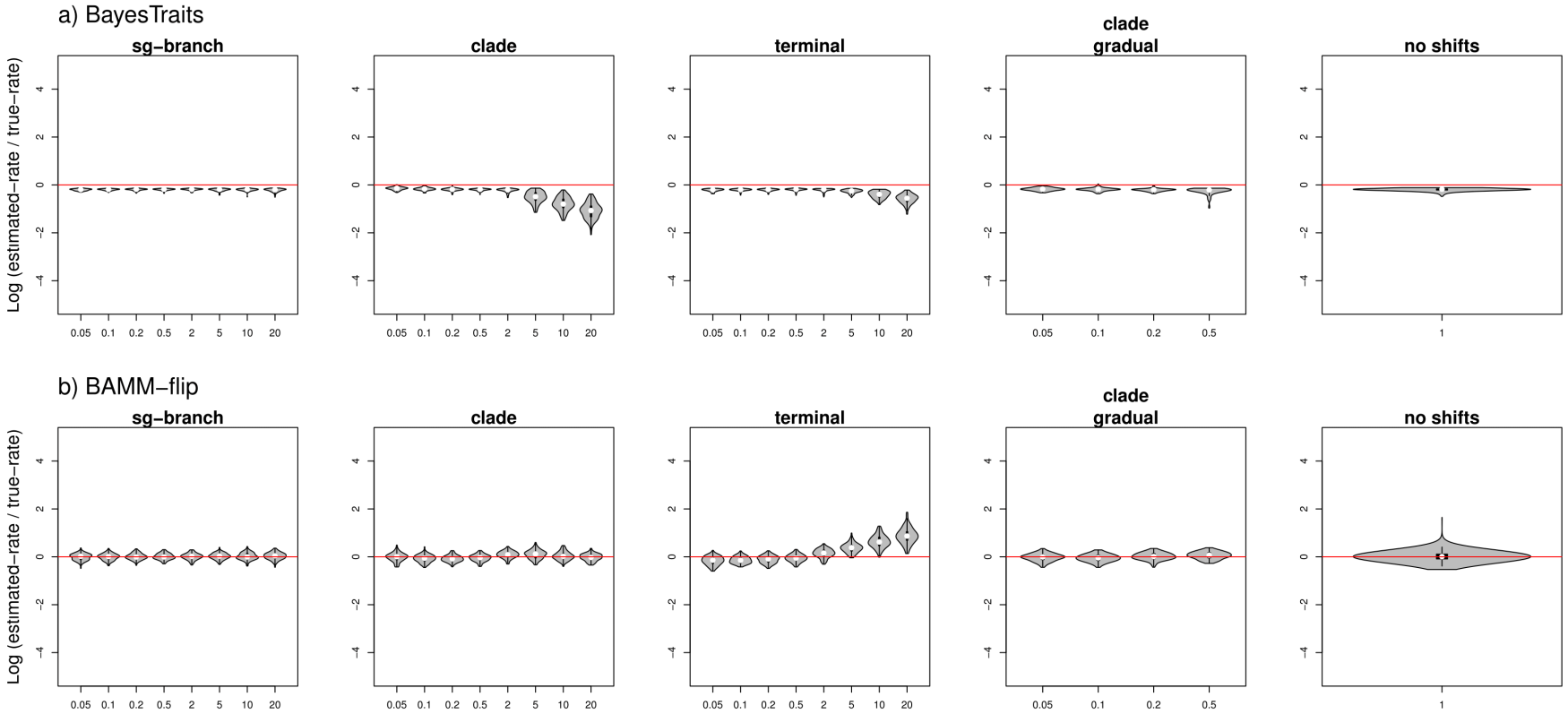

Figure S2. Distributions of log-proportions between rates estimated by variable-rates models and the true (simulated) rates of evolution. Only branches with no simulated rate-changes are considered (i.e. true $\sigma^2 = 1$). Distributions are shown for various shift magnitudes (x-axis) and heterogeneity scenarios: internal branch shift; clade event; rate-changes on isolated, terminal branches; rate-burst followed by gradual decreases within a clade. Per-branch comparisons within trees with no simulated rate-shifts are also shown. Results for BayesTraits (a) and BAMM-flip (b).

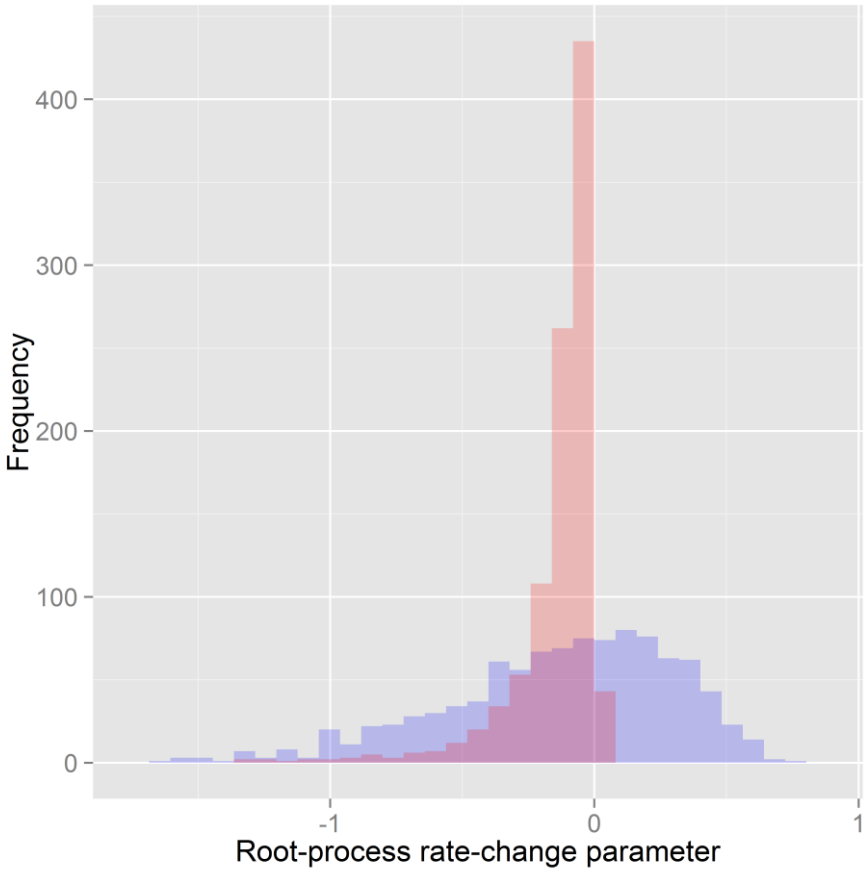

Figure S12. Frequency of rate-change parameters for the root process across constant-rate trees, estimated using BAMM with (red) and without (blue) a time-flip proposal. The expected mean for no rate-changes at the root is at x = 0.

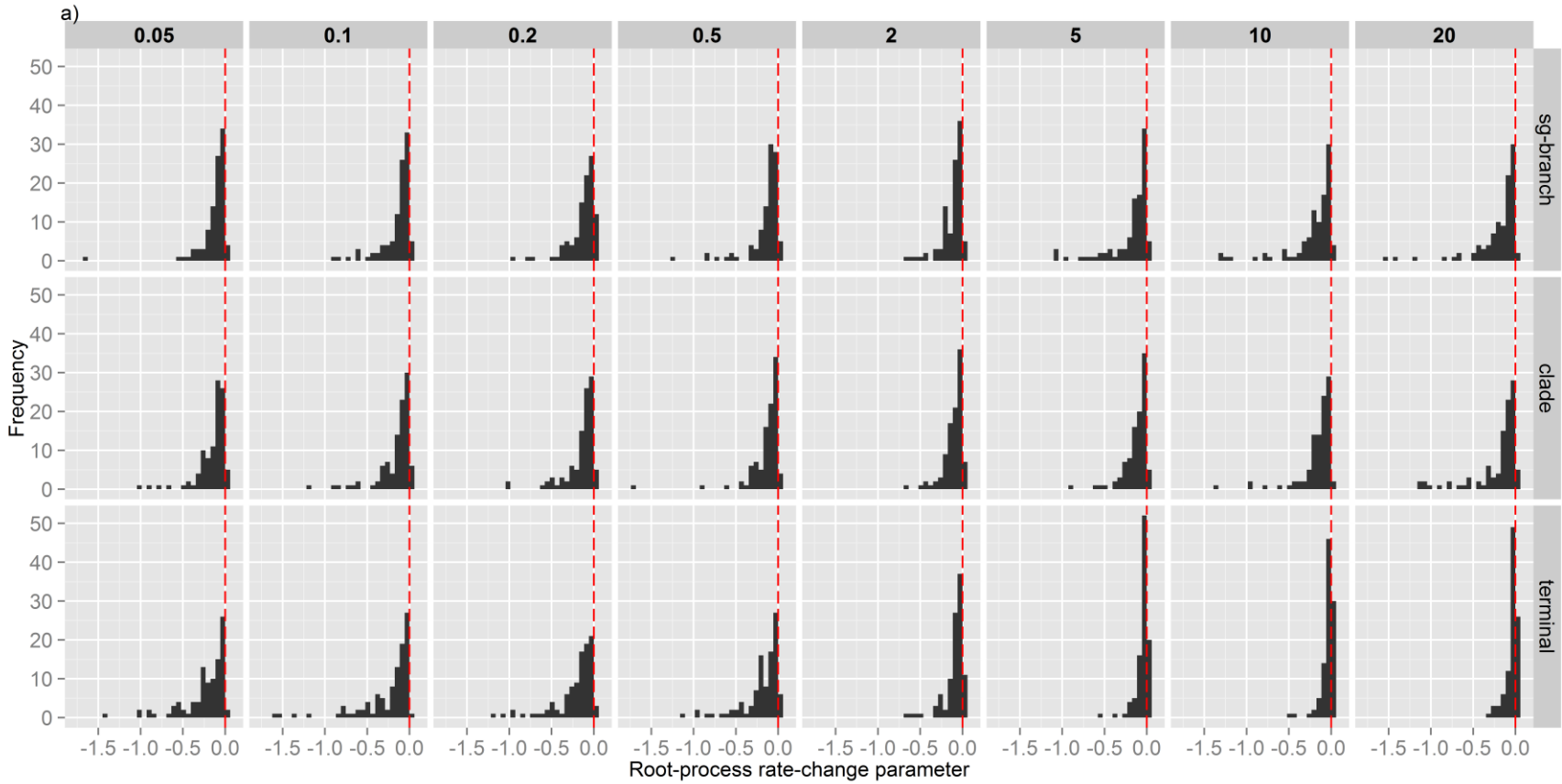

Figure S13a. Frequency of rate-change parameters for the root process across simulated heterogeneity scenarios: single branch shift, clade event, and changes on isolated terminal branches. The magnitudes of shifts in each scenario are recorded on the vertical panel. The expected mean for no rate-changes at the root is the 0 line (dashed red). Rate change parameters are estimated by a BAMM model with a time-flip proposal.

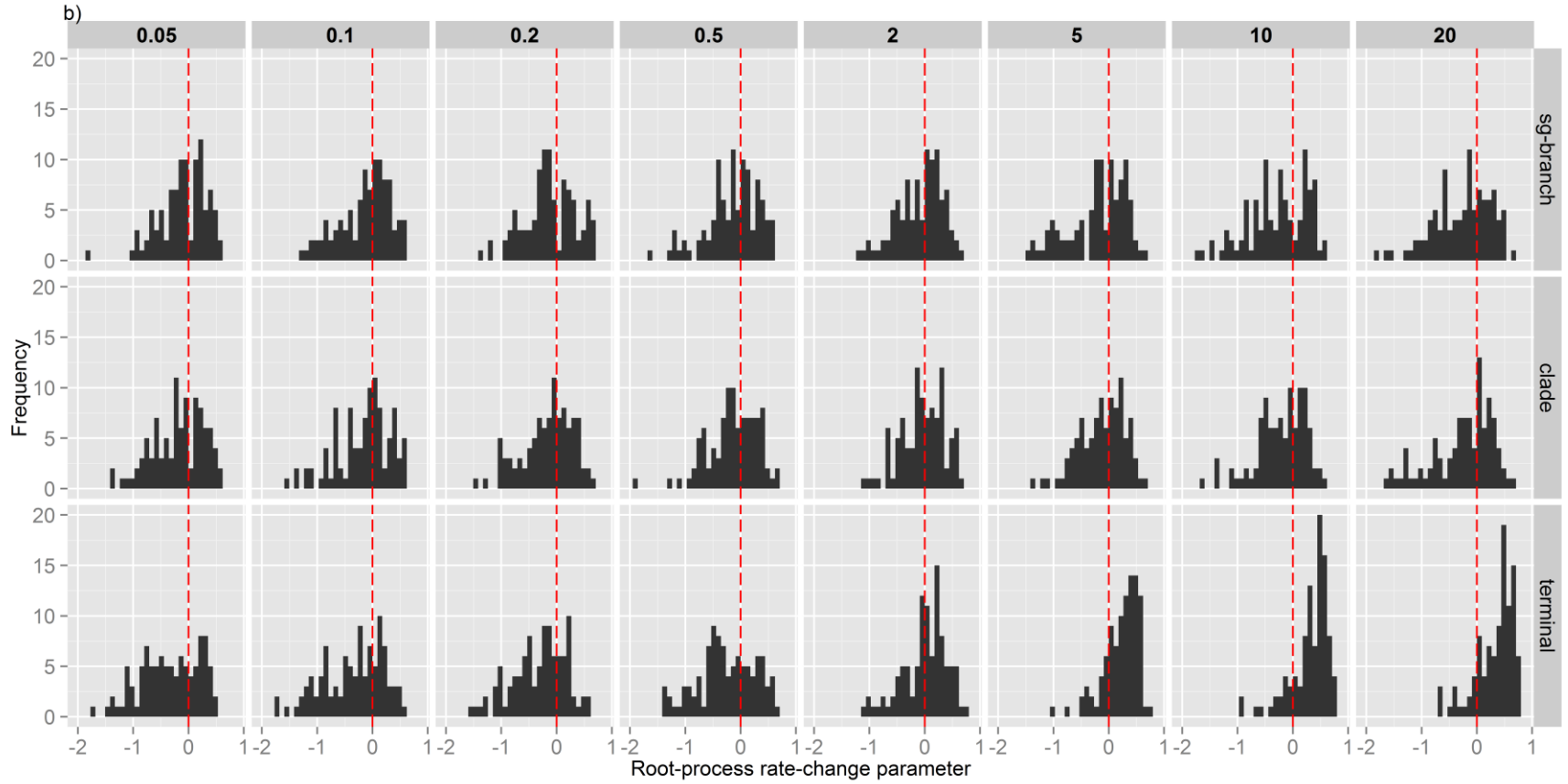

Figure S13b. Frequency of rate-change parameters for the root process across simulated heterogeneity scenarios: single branch shift, clade event, and changes on isolated terminal branches. The magnitudes of shifts in each scenario are recorded on the vertical panel. The expected mean for no rate-changes at the root is the 0 line (dashed red). Rate change parameters are estimated by a BAMM model constrained to time-varying processes only.

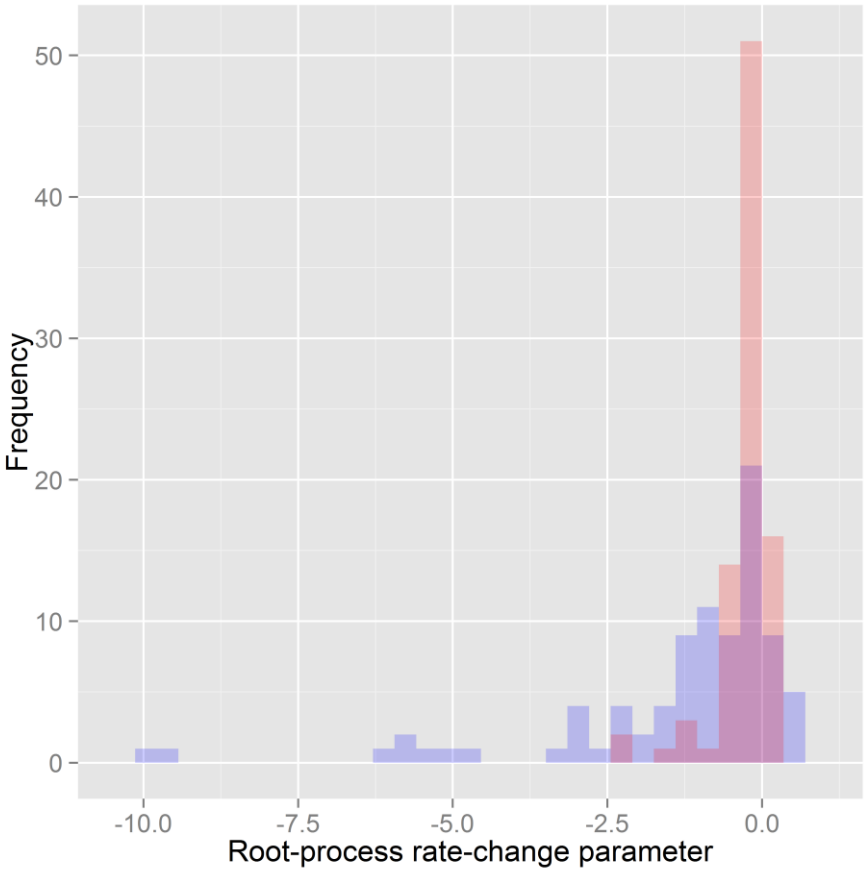

Figure S14. Frequency of rate-change parameters for the root process across empirical datasets, estimated using BAMM with (red) and without (blue) a time-flip proposal. The expected mean for no rate-changes is at x = 0.

CHAPTER 3

Correlates of rate heterogeneity in avian ecomorphological traits

This chapter was published in Ecology Letters as:

Chira, A.M., Cooney, C.R., Bright, J.A., Capp, E.J.R., Hughes, E.C., Moody, C.J.A., Nouri, L.O., Varley, Z.K. and Thomas, G.H., 2018. Correlates of rate heterogeneity in avian ecomorphological traits. Ecology letters. 21: 1505-1514. doi:10.1111/ele.13131.

Author contributions: AC, CC and GT developed the conceptual framework, devised the analytical protocols, and wrote the manuscript. AC performed the analyses. All the authors were involved in data collection and processing, and provided valuable input in writing the manuscript.

Data accessibility: Additional supporting information may be found online in the supporting information tab for this article (doi:10.1111/ele.13131). The data supporting the results (species' landmark configurations, (p)PC scores, rates of evolution, predictor variables and alternative trees) are available at Dryad repository (provisional DOI: https://doi.org/10.5061/dryad.4006fm8). The raw data (3D scans of beaks) can be accessed via NHM data portal (http://data.nhm.ac.uk/dataset/markmybird).

ABSTRACT

Heterogeneity in rates of trait evolution is widespread, but it is unclear which processes drive fast and slow character divergence across global radiations. Here, we test multiple hypotheses for explaining rate variation in an ecomorphological trait (beak shape) across a globally-distributed group (birds). We find low support that variation in evolutionary rates of species is correlated with life history, environmental mutagenic factors, range size, number of competitors, or living on islands. Indeed, after controlling for the negative effect of species' age, 80% of variation in species-specific evolutionary rates remains unexplained. At the clade level, high evolutionary rates are associated with unusual phenotypes or high species richness. Taken together, these results imply that macroevolutionary rates of ecomorphological traits are governed by both ecological opportunity in distinct adaptive zones and niche differentiation among closely related species.

INTRODUCTION

Phenotypic diversity accumulates via different mechanisms and at different speeds, and understanding which factors predict the tempo of phenotypic diversification represents a longstanding question in evolutionary biology (Pagel, 1999; Simpson, 1953). Candidate drivers include predictors related to a general increase in the potential for genetic variability and fixation rates (mostly associated with rates of molecular evolution), but also predictors relevant only for specific types of traits e.g. diet links with the rate of jaw morphology evolution in *Centrachidae* (Collar et al., 2009). Rates of ecomorphological trait evolution in particular have received considerable interest. The classic research on Darwin's finches in the Galapagos has shown that fluctuations in resource availability, colonisation of islands, and interspecific competition can cause exceptionally rapid differentiation in beak size (Grant & Grant, 2003, 2006). Recently, studies addressed patterns of trait evolution for entire global radiations, involving thousands of species (Cooney et al., 2017;

Rabosky et al., 2013; Venditti et al., 2011), but whether it is possible to identify the factors that accelerate or constrain phenotypic evolution in ecological traits at broad taxonomic scales is unclear.

The pace of evolution depends in part on factors that increase the potential for genetic variability in populations (Simpson, 1953). Aspects of species life history, such as faster turnover of generations and increased levels of fecundity increase the potential for copy error (Bromham, 2009, 2011; Bromham et al., 2015; Lanfear et al., 2010b). Similarly, species with shorter-life spans, smaller body sizes, and higher metabolic rates suffer from a less efficient DNA repair process (Galtier et al., 2009). An increase in the total number of gene changes can be an important source of variation for selection to act on, and also a rapid turnover of generations should speed up the process of fixation under selection. However, the evidence that species life histories are linked with the rate of molecular evolution is mixed (Lanfear et al., 2010a; Mooers & Harvey, 1994; Smith & Donoghue, 2008; Thomas et al., 2010; Thomson et al., 2014). The potential for genetic variability has also been linked to factors extrinsic to species. Specifically, it has been hypothesised that abiotic mutagenic factors such as increased temperatures and high UVB exposure can drive rapid evolution (Davies et al., 2004; Dowle et al., 2013; Gillman et al., 2014; Rhode, 1992, but see Bromham & Cardillo, 2003). Drivers of molecular evolution can impact trait evolution (Davies & Savolainen, 2006), although it is not clear whether nor how rates of molecular and phenotypic change are related (Bromham et al., 2002). Indeed, few studies test the impacts of factors associated with increased genetic variability and fixation rates on trait macroevolutionary rates (but see Cooper & Purvis, 2009).

In contrast, biotic interactions have received much attention, particularly as drivers of rate variation in ecomorphological traits (e.g. Drury et al., 2018). Antagonistic

interactions between species can accelerate trait evolution if lineages rapidly differentiate in key traits to avoid competition (Grant & Grant, 2006). Accordingly, secondary sympatry has been linked with high evolutionary rates via character displacement (Dayan & Simberloff, 2005; Pfennig & Pfennig, 2009; Voje et al., 2015, but see Tobias et al., 2014). The absence of competitors is also thought to drive rapid evolution, as species diverge to exploit free resources. Indeed, isolated environments, especially islands, have long been hypothesised as drivers of rapid diversification and phenotypic evolution (Losos & Ricklefs, 2009).

At deep-time scales, patterns of phenotypic accumulation have mostly been linked to the potential to explore novel ecological resources, and also to the feedbacks of species packing on morphological diversification (Hunter, 1998; Mahler et al., 2010; Rabosky & Adams, 2012; Weir & Mursleen, 2013). Heterogeneity in evolutionary rates has been described as a mixture of rapid evolutionary episodes generating large morphological differences between sister-clades, and phases of gradual, cumulative change as species diverge and adapt to the niche invaded by their common ancestor (Cooney et al., 2017; Landis & Schraiber, 2017; Simpson, 1953; Uyeda et al., 2011). It is debated how episodes of rapid evolution should affect subsequent evolution of descendants (recently reviewed in Rabosky, 2017). Bursts of evolution that mark clade-wide shifts towards unique morphologies are thought to associate with access to novel ecological resources and rapid evolution of descendants (Hunter, 1998; Losos, 2010; Losos & Mahler, 2010). Alternatively, evolution of morphologically distinct lineages might inhibit subsequent divergence when there are adaptive (Wright, 2017) or developmental (Felice & Goswami, 2018) constraints on phenotypic change, and also if distinctiveness links to specialisation to a narrow set of resources (Collar et al., 2009). The number of species accumulating within clades is also linked to phenotypic evolution and to the distinctiveness of ancestral phenotypes (Ricklefs, 2004; Schoener, 1965), and

morphological distinctiveness has been associated with species-poor clades (Ricklefs, 2005). Clade species richness impacts the rate of trait change because with more species, the potential for biotic interactions among closely related (and ecologically similar) species increases. Also, as the niche occupied by the ancestral phenotype fills with species and the potential for ecological opportunity declines, the rate of trait evolution is expected to slow down (Gavrilets & Losos, 2009). Alternatively, fast trait divergence is expected to expand clade morphological and ecological space (Hulsey et al., 2013; Weir & Mursleen, 2013), and thus enable high species richness (Jonsson et al., 2012; Rundle & Nosil, 2005; Schluter, 2001).

Here, we test multiple hypotheses for explaining variation in rates of trait evolution at both deep and more recent taxonomic levels. We focus on avian beak shape, an ecologically relevant trait for which there is already evidence of high variability in rates of evolution (Cooney et al., 2017; Lovette et al., 2002; Reddy et al., 2012). We use an extensive dataset of 3D scans of beaks from 5,551 species and multivariate models to estimate rates of trait evolution. We predict that rapid beak shape evolution should be associated with aspects of species ecology (e.g. increased strength of resource competition and ecological opportunity), and with factors generally associated with rapid molecular evolution (fast life history cycles and living in highly mutagenic environments).

MATERIALS AND METHODS

Beak shape data

We collected beak shape data for 5,551 species across 193 (out of 194) bird families, sampling at least 25% of species in each bird family (except *Caprimulgidae* and *Rhipiduridae*, where data was available for only 19% of the species in the family; the full list of species and proportion of species covered in each family can be found in Appendices S1 and S2). Our 3D scanning, landmarking, and geometric

morphometrics analyses follow protocols in Cooney et al. (2017). Briefly, we used study skins from the Natural History Museum (Tring) and from the Manchester Museum collections to measure one mature individual (preferentially male, reflecting sex biases in ornithological collections) for each species. For groups where the beak is obscured by feathers (obstructing the scanning of the beak, see below), and for species with no suitable specimens in the collections, skeletal material was used instead.

We took 3D scans of bird beaks using white and blue structured light scanning (*FlexScan3D*). For each beak, we obtained 5-25 scans and used FlexScan3D (LMI Technologies, Vancouver, Canada) software to align and combine them. We used Geomagic Studio (3dSystems) to reduce each combined scan to 500,000 faces, and to remove any flaws (holes, feather excess, reversed normals, high aspect ratio spikes). The clean meshes were processed using landmark based geometric morphometrics analysis, which analyses geometric shape variation by placing homologous key points (landmarks) on Procrustes-aligned study surfaces (Adams et al., 2013). We define a total of four landmarks and 75 semilandmarks, which were slid to reduce bending energy (see Cooney et al., 2017 Extended Data Figure 3.1). The four landmarks were: (1) the tip of the upper beak, and the posterior margin of the upper beak on the (2) dorsal midline profile, (3) left, and (4) right tomial edges. The 75 sliding semi-landmarks constitute the dorsal profile (joining points 1 and 2), and the left and right tomial edges (curves joining point 1 to points 3 and 4 respectively). Landmarking was performed by the authors (63% of total markups) and by members of the public on the MarkMyBird crowdsourcing website (http://www.markmybird.org). Each beak was marked by at least three independent users (over 20,000 markups in total). We used R scripts to quality control the data. A landmarking effort was considered unsuitable if: (i) the left and right tomial edges were inversed or placed asymmetrically, (2) the semi-landmarks along the left and

right tomial edges were placed in the incorrect order or did not correctly follow the curve of the beaks, and (3) there was a large discrepancy in the position of equivalent landmarks between different users (between-users Procrustes distance >=0.2). Using this crowd-sourcing approach for landmarking avian beaks produces reliable results, as landmarks show a high repeatability between users (Cooney et al., 2017). We used the R package Geomorph (Adams et al., 2017) to process the user-averaged beaks shape of each species via geometric morphometrics analysis. Here we focus on beak shape, as it represents a key axis of ecomorphological differentiation between major avian groups (Cooney et al., 2017). While size is also a major axis of ecomorphological differentiation, shape is more indicative of how a structure functions biomechanically and functionally, with size simply scaling that function. Furthermore, differences in size tend to overwhelm differences in shape, which is particularly problematic when shapes are highly disparate (as here) because dramatically different shapes may have the same centroid size (Zelditch et al., 2012). We therefore first removed the effects of size, translational, and rotational position on landmark configurations by performing a Generalized Procrustes Analysis. We then extracted the main axes of shape variation via a PCA and phylogenetic PCA analysis (pPCA, Revell, 2009). The latter is designed to account for potential biases in the PCA analysis resulting from the non-independence in phenotypes between species caused by shared ancestry (Polly et al., 2013; Revell, 2009; Uyeda et al., 2015).

Phylogenetic data

To assess the impacts of phylogenetic uncertainty we used phylogenetic tree distributions from http://www.birdtree.org (Jetz et al., 2012) to generate consensus trees. We sampled 10,000 Hackett backbone (Hackett et al., 2008) ‘stage 1’ trees (i.e. trees including only species for which genetic data is available), and ‘stage 2’ trees (i.e. trees with all 9,993 species). We then pruned the sampled trees to

generate distributions for species in our dataset (5,551 species out of which 4,108 species had genetic data). We used Tree-Annotator (Drummond et al., 2012) to generate maximum clade credibility trees and used two alternative methods to infer branch lengths by setting node heights (i) equal to "common ancestor" node heights, and (ii) equal to the heights of the target tree. Additionally, we used the recently published avian phylogeny from Prum et al. (2015) to build alternative consensus trees for our list of species. We followed Cooney et al. (2017) to merge the species level resolution of Jetz et al. (2012) to the backbone phylogeny derived from Prum et al. (2015) and build maximum clade credibility trees. A list of all alternative trees and datasets used to perform the multivariate rate analyses is given in Table S1.

Rates of beak evolution

We estimated rates of beak shape evolution using the variable rates model (VarRates command) in the software BayesTraits, version 2 (available from http://www.evolution.rdg.ac.uk/), which uses a single tree and allows for the analysis of multivariate traits. The model was run setting uniform (default) priors, with no restrictions for the phylogenetic mean (alpha) and Brownian variance (sigma), and allowing correlation between variables. While in principal PCs are orthogonal, hence uncorrelated multivariate runs would be justified (Cooney et al., 2017), we used a more flexible approach and allowed for correlation between variables as it could account for potentially weak correlations between the PCs that emerge due to phylogenetic history. Allowing for non-independence between variables, alongside the large ratio of species to target traits minimises potential biases in multivariate trait analyses (Adams & Collyer, 2018). Each run was set for least 2 billion iterations (running for ~ six months on a 2.30 GHz Linux machine), sampling every 100,000 iterations, with a 50% post burn-in. For each tree, we ran the models with the PC and pPC axes (i.e. traits) that explained 99% variation in beak shape. Runs were

set up at least once (Table S1), and a potential scale reduction factor smaller than 1.1 was considered as an indicator of between-chains convergence (i.e. the Gelman-R diagnostic; R package CODA, Plummer et al., 2006). Within chain convergence was assessed using trace and auto-correlation plots, alongside effective sample size (values ≥ 200 were taken as indicators of chain convergence; Plummer et al., 2006).

The multivariate variable rates model allows for heterogeneity in rates of evolution by scaling both single branches and a target branch plus its descendants at any location in the tree (Venditti et al., 2011). We summarise alternative configurations of rate scaled trees by calculating the median rate of evolution for each branch across the posterior. We used tip rates (i.e. rate values on the tip branches) as a measure of species-specific rates of beak shape evolution. We calculate rates of evolution using the number of PC and pPC axes that explained 99% of beak shape variation.

In order to predict patterns of phenotypic accumulation across deep-time scales, we also calculated rates of evolution for well-defined, monophyletic groups of species (Jetz et al., 2012). We split the non-passerines into orders, and passerines into well-supported families and superfamilies (Jetz et al., 2012). We pruned the consensus trees to include only species belonging to clades with at least five representatives and used transformPhylo.ML in the R package MOTMOT (Thomas & Freckleton, 2012) to calculate multivariate relative clade rates of evolution. We report results from fitting multivariate models of trait evolution on the PC scores in the main text, and the results from the rate-analysis using pPC scores in the supplement (Table S5, Table S6).

Correlates for rates of beak shape evolution

We used species body mass (g) from Elton Traits (Wilman et al., 2014). We used the average age of parents as an estimate of the turnover of generations, or generation length (BirdLife International (2018) IUCN Red List for birds. Downloaded from http://www.birdlife.org on 05/05/2017). We used species' distribution maps from BirdLife International (BirdLife International and Handbook of the Birds of the World (2016) bird species distribution maps of the world. Version 6.0. Available at http://datazone.birdlife.org/species/requestdis), considering only native species and also subsetting ranges to breeding areas where species are highly probable or known to occur. We used these maps to calculate: (i) species' range sizes, (ii) the proportion of species' ranges that occurs on islands, (iii) mean annual temperature (Hijmans et al., 2005), (iv) mean annual UVB levels (Beckmann et al., 2014), and (v) an index of potential competition. The index of potential competitors was calculated by dividing species' distribution ranges into equal area grid cells (resolution of ~ 110 km), and counting the number of confamilial species that share diet and foraging strategy with the focal species in each grid cell (based on EltonTraits, Wilman et al., 2014). We then averaged these values across grid cells. The spatial data handling was done using the R packages letsR (Vilela et al., 2015) and raster (Hijmans & von Etten, 2012). We controlled for species' age by including the length of the branch leading to each species in the consensus tree. Lastly, we included the mean Procrustes distances between users marking each beak to account for user error (referred to as measurement error).

Species level analyses

We used PGLS analysis (Grafen, 1989; Martins & Hansen, 1997) in the R package caper (Orme et al., 2013) to correlate species-specific rates of evolution with the potential drivers for rate variation described above. We also ran the analyses with species' clade included as an interaction term, in order to estimate whether and how

the relationship between rates and potential explanatory variables changes in specific clades. Furthermore, migratory birds will likely spend most of the annual cycle in their non-breeding ranges. To account for potential biases of using breeding ranges only, we also performed the analyses including migratory status as an interaction term (i.e. full migrant versus resident as described in BirdLife International (2018) IUCN Red List for birds. Downloaded from http://www.birdlife.org on 05/05/2017).

Clade level analyses

We measured the distinctiveness of each clade in beak shape morphospace by calculating the Euclidean distance between the centre of the clade and the overall centre of the morphospace using the PCs that explained up to 99% of beak shape variation (Figure S1). Longer distances imply more peripheral clades with greater potential ecological opportunity. We correlate this measure with clade rates of evolution, also considering species richness (the total number of species in each clade), an index of the potential strength of competition in the clade (by averaging the species-specific competition index estimated above), clade age (age of its most recent common ancestor), and controlling for the proportion of island species in each clade, and the average range size for species in the clade. We logged body mass, generation length, range size, number of competitors, beak distinctiveness, and age to ensure normal distribution of predictors. We used variance inflation factors to test the independency of predictors.

RESULTS

Patterns of beak shape evolutionary rates

The first eight PC axes from the PCA analysis explained 99% of variation in beak shape, with almost half of this variation being explained by PC1 (variation from a long, narrow beak to a short, wide beak; Figure S2, Table S2). Some species and

clades of species show extreme PC values on one or two axes (e.g. *Anseriformes*, *Bucerotiformes*), while others consistently show extreme PC scores on multiple axes, marking major deviations from the general cone-like beak shape (e.g. *Phoenicopteriformes*, *Apodiformes*; Figure S2).

We find evidence of extensive variation in evolutionary rates, both among tip and internal branches (Figure 3.1). Tip rates in particular show a high degree of skewness, and examples of exceptionally high species-specific rates are mostly associated with the evolution of very unusual beaks e.g. we see extreme PC and rate values for the laterally curved beaks of *Anarhynchus frontalis* (wrybill) and the *Loxia* genus (crossbills). We find several internal single-lineage high rates of evolution including several major shifts that were not detected by Cooney et al. (2017). These mark the evolution of lineages towards the periphery of the beak shape morphospace (e.g. *Strigiformes*, *Bucerotiformes*, *Accipitriformes*, *Phoenicopteriformes*, *Psittaciformes*), and can coincide with major differences in morphology between descendant sister-clades. Similar to species-specific evolutionary rates, we find great variation in evolutionary rates between broadly recognized clades of species (Figure 3.1). We see high rates of evolution in some large passerine groups with generally average beak types (e.g. *Passeroidea*, *Sylvioidea, Corvoidea*). Many non-passerines groups also have high rates of evolution, but most of these are clades with unique beak shapes, several of which are also species poor (e.g. *Phoenicopteriformes*; Figure S8b).

Correlates of species-specific rates of evolution

We find a strong negative effect of species' age on species-specific rates of evolution, with age alone explaining 20% of variation in tip evolutionary rates (Figure 3.2a). In addition to age, the full model identifies significant positive effects of proportion of range occurring on islands (Figure S3a), UVB levels (Figure S3b), and

measurement error (Figure S3c). However, the effect sizes and variation explained by these variables are small (Table 3.1). We find no effect of life history traits, range size, or number of competitors on tip rates of evolution (Table 3.1, Figure S4), and overall almost 80% of variation in species-specific evolutionary rates remained unexplained (Figure 3.2b). In resident species, both temperature and UVB levels have a weak, negative effect on evolutionary rates (Figure S6). There is no significant effect of climatic variables on rates of evolution for migratory species. When including clade as an interaction term in the model, we largely recover the same trends observed in the main model (Table S4, Figure S5).

Correlates of clade rates of evolution

Clade evolutionary rates were positively correlated with clade beak distinctiveness and species richness (Figure 3.3a, b, Table 3.2). We also find a weak negative effect of potential competition strength on evolutionary rates (Figure S7a). The number of species in clades relates negatively with the distinctiveness of their phenotype, and clades with distinct beaks are typically species poor (Figure S8). Together, these factors explain just above half of the variation in clade rates of evolution (Figure 3.3c). Clade age does not have a significant impact on rates. However, using a finer split of species in clades with more variability in clade age, we recover a negative impact of clade age, alongside the effects of beak distinctiveness and richness on clade rates (Figure S9, Figure S10, Table S7). The results we find at species and clade levels are generally robust to alternative avian phylogenies, methods for building a consensus tree, and the inclusion of species without genetic data (Table S3, Table S5, Table S6, Figure S11).

Table 3.1. Correlates of species-specific rates of evolution; λ = 0.626, d.f. = 9,3734, adjusted R-squared = 0.21.

Predictor	Slope ± SE	*t*	*P*
Log species' age	-0.478 ± 0.010	-30.186	**<0.001*** **
Log body mass	0.040 ± 0.022	1.794	0.073
Log generation length	0.103 ± 0.080	1.294	0.196
Mean annual temperature	-0.002 ± 0.002	-0.669	0.504
Mean annual UVB levels	0.000 ± 0.000	-2.195	**0.028***
Log range size	-0.009 ± 0.006	-1.379	0.168
Proportion of island range	0.115 ± 0.046	2.488	**0.013***
Log number of competitors	0.004 ± 0.013	0.271	0.786
Measurement error	0.917 ± 0.420	2.184	**0.029***

DISCUSSION

Here, we describe heterogeneity in rates of avian beak shape evolution and find considerable variation in the rate of phenotypic change among both species and clades (Figure 3.1). We see several instances of rapid major morphological differentiation between sister-clades, consistent with Cooney et al. (2017). When such events place clades at the periphery of the eco-morphospace, we see subsequent high rates of evolution of descendants. Rapidly evolving groups are not necessarily distinct however, and several clades with average (i.e. non-peripheral) beak types also show high rates of evolution. We find that variation in species-specific rates of ecomorphological traits evolution is difficult to predict, and after controlling for species age, the factors we considered associate weakly with evolutionary rates. Species' age correlates negatively with rates of phenotypic change, as expected under speciational trait evolution followed by stasis. We note, however, that phylogenetic and/or measurement error can also cause an over-inflation of trait evolutionary rates that is particularly prevalent for young species (Rabosky, 2015).

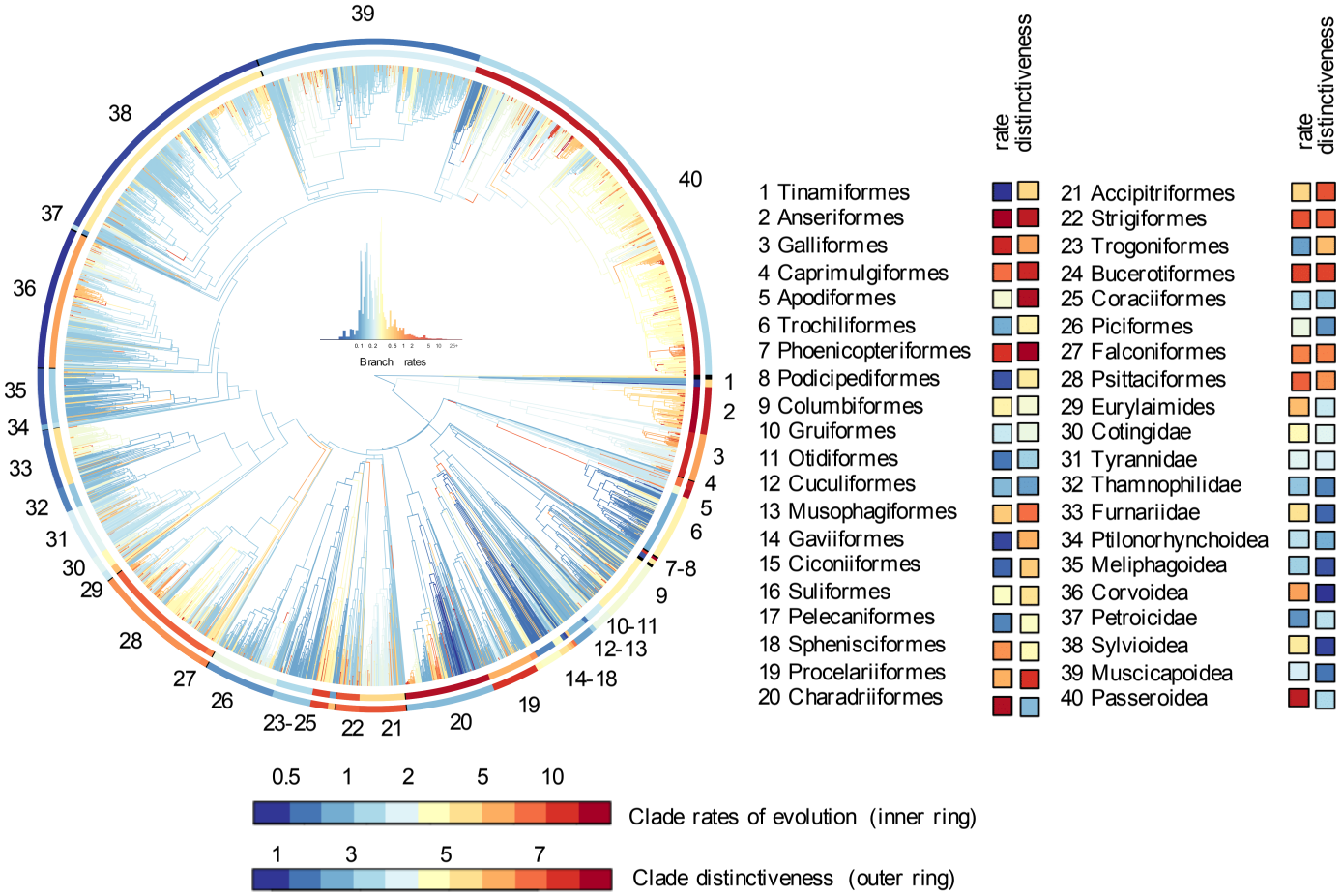

Figure 3.1. Multivariate rates of beak shape evolution. Branches are coloured by the median multivariate rate of evolution. Rings are coloured by clade rates of evolution (inner ring) and clade morphological distinctiveness i.e. the Euclidean distance between the centre of the clade and the overall centre of the morphospace (outer ring). Black indicates clades smaller than 5 species, which were not included in the clade-level analyses.

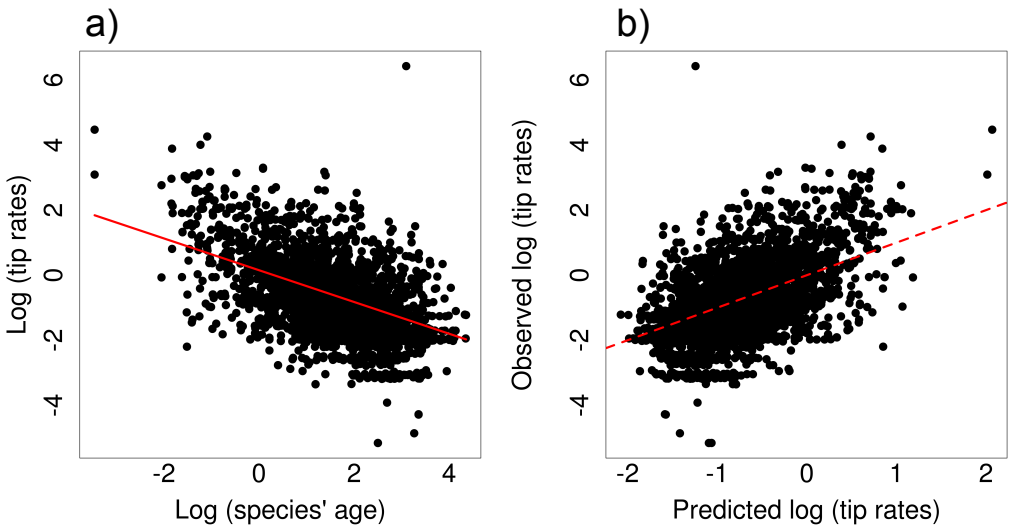

Figure 3.2. (a) The relationship between species-specific rates of evolution and species' age, $p < 0.001$, R-sq = 0.20. (b) The relationship between the observed and predicted rate of evolution by the full PGLS model: adj. R-sq = 0.21. The dashed line indicates the 1:1 line of predicted versus observed values.

Table 3.2. Correlates for clade rates of evolution; λ = 1.000, d.f. = 6,33, adjusted R-squared = 0.52.

Predictor	Slope ± SE	*t*	*P*
Log clade age	-0.077 ± 0.348	-0.221	0.827
Log clade beak distinctiveness	0.881 ± 0.227	3.882	**<0.001*** **
Log clade species richness	0.501 ± 0.119	4.218	**<0.001*** **
Log average range size	-0.157 ± 0.081	-1.933	0.062
Proportion of island species	-0.322 ± 0.841	-0.383	0.704
Log average number of competitors	-0.376 ± 0.179	-2.097	**0.044***

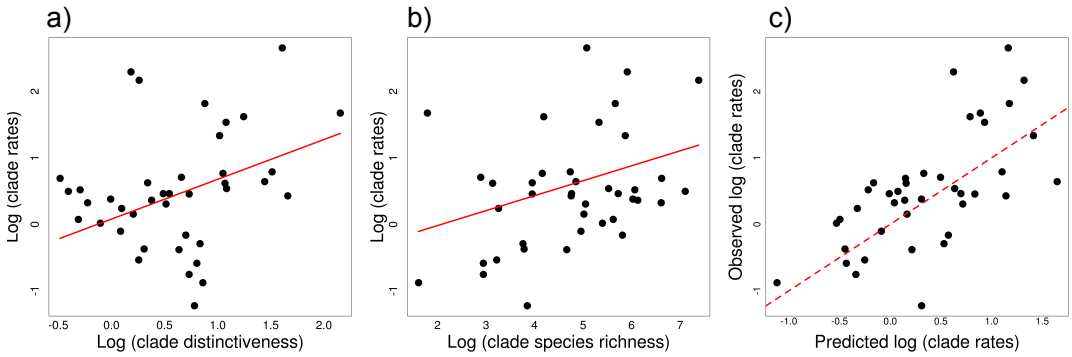

Figure 3.3. The relationship between clade rates of evolution and (a) clade beak distinctiveness, $p < 0.001$, (b) clade species richness, $p < 0.001$. (c) The relationship between the observed and predicted clade rates of evolution by the full PGLS model: adj. R-sq = 0.52. The dashed line indicates the 1:1 line of predicted versus observed values.

We found little to no effect of life history, environmental mutagenic factors, or range sizes on species-specific trait evolutionary rates (Table 3.1). UVB levels (and temperature values for resident species only, Figure S6) weakly associate with evolutionary rates (Figure S3b). However, the trend we note is negative i.e. opposite to predictions based on the mutagenic effect of high temperatures and UVB levels (Rhode, 1992). If anything, such a relationship might reflect the effect of environmental instability on rates. That is, colder and UVB-poor environments (e.g. at higher altitude or latitude) may be associated with high prevalence of fragmented and unstable range sizes, further thought to inflate evolutionary rates (Flenley, 2011; Lawson & Weir, 2014; Liu et al., 2006; Martin et al., 2010). Thus overall, our candidate factors associated with an increase in the potential for genetic variability or speed of mutation fixation show little to no impact on ecomorphological rates of evolution (but see Cooper & Purvis, 2009).

We also tested whether rates of evolution link to potential for competition. We find that most species do not overlap geographically with close relatives that also share foraging strategies and diet, and accordingly, we find no link between number of

potential competitors and evolutionary rates (Figure S4). Further, we recover high evolutionary rates in many famous insular radiations in beak shapes, including Galapagos finches, Hawaiian honeycreepers, birds of paradise, flowerpeckers, and also select parrots, white-eyes and starlings (Figure 3.1). In general, however, island species exhibit both slow and fast evolutionary rates, and within the same clade, mainland species can have similar rates to those on islands. Consequently, we find that the effect of islands on evolutionary rates is limited to several small-scale exceptional radiations, and has a relatively small impact on the accumulation of phenotypic diversity across a global radiation such as Aves. Overall, our results imply that species-specific ecomorphological rates of evolution are likely contingent on chance events, and hence difficult to predict across global radiations.

Rates of evolution were more predictable at the clade level. We found that the distinctiveness of clade phenotype and its species richness act additively to explain half of the variation in clade evolutionary rates. Specifically, we find that clades that occupy the periphery of the morphospace have high rates of evolution (Figure 3.3a), in agreement with the idea that adaptation to a novel set of ecological resources can drive rapid phenotypic differentiation (Martin & Wainwright, 2011; Price et al., 2010, but see Wright, 2017). The effect of evolution towards the periphery of the morphospace is analogous to Simpsonian jumps to new adaptive zones, also hypothesised to drive subsequent rapid evolution via increased ecological opportunity (Simpson, 1953). We also see a negative relationship between clade species richness and the distinctiveness of their beak shapes (Figure S8b), supporting the hypothesis that lineages that evolved to exploit specialised (and thus potentially limited) resources are not expected to proliferate (Ricklefs, 2005). These results imply that ecological opportunity in the form of evolution towards unique phenotypes is an important driver of rapid evolution, but the peculiarity of the

ancestral phenotype constrains the prospective number of, and disparity among, descendants.

Species richness and trait evolutionary rates are, however, also positively linked (Figure 3.3b), and passerines in particular represent fast evolving, species-rich clades with generally average beak types. There is mixed evidence that trait evolutionary rates correlate with diversification and species richness (Adams et al., 2009; Burbrink et al., 2012; Igea et al., 2017; Rabosky & Adams, 2012; Rabosky et al., 2013), and moreover the causality of these relationships is unclear. Species-rich clades are prone to intense competition for shared resources if clade members are sympatric, and could thus show fast phenotypic evolution via character displacement (Davies et al., 2007; Freeman, 2015; Grant & Grant, 2006; Martin et al., 2010). However, in our analyses, the vast majority of bird species show little range overlap with potential competitors (Figure S4), and species with similar ecologies seem to be geographically isolated (consistent with a species-sorting mechanism; Lovette & Hochachka, 2006; Pigot & Tobias, 2013). In clades where we do find a high proportion of species sharing ranges with ecologically similar relatives (e.g. *Trochiliformes, Tyrannidae, Thamnophilidae, Sylvioidea*), we find slower evolutionary rates (Figure S7a); this might reflect limitations to phenotypic evolution with more species sharing the same niche (Simpson, 1953). However, we interpret these results with caution, as when using a finer division of clades, the relationship is not statistically significant (Table 3.1, Table S7). Moreover, the negative effect between competitor numbers and evolutionary rates might be driven by multicollinearity with species richness (Table S8). We also note that our analyses focus on beak shape, but beak size (and associated allometry) is also an important axis of ecomorphological differentiation in birds, particularly within clades (Bright et al., 2016; Grant & Grant, 2006). Removing size from the analyses thus likely reduced our power to detect an effect of biotic interactions on evolutionary rates, as

in some clades competition would have been resolved by differentiation in beak size rather than shape. Overall, while species interactions can be a powerful driver of fast differentiation in (small) select radiations, our results suggest that they are unlikely to have a pervasive influence on the accumulation of beak shape variation across the global bird radiation. Recently developed methods that incorporate the effect of species interactions when modelling trait evolution will likely reveal more subtle effects of competition (Clarke et al., 2015; Drury et al., 2016), and give further insight into if and how biotic interactions link species richness with phenotypic evolution. Additionally, high rates of phenotypic evolution can expand the ecological space available for species, and thus rapidly evolving clades are expected to proliferate (Jonsson et al., 2012; Rundle & Nosil, 2005; Schluter, 2001, but see Claramunt et al., 2012; Dornburg et al., 2011). Our results cannot differentiate the causality and underlying mechanism for the relationship between species richness and trait evolutionary rates.

Similar to our analyses at the species level, we account for age in our clade-level analyses. We consider very broad taxonomic groups with little variation in age, and unsurprisingly, we find no correlation between clade age and rates of evolution. However, age correlates negatively with evolutionary rates when using a finer division of species into clades (Table S7). These results could indicate a deceleration of evolutionary rates with the packing of species in time (Agrawal et al., 2009; Harmon et al., 2010; Hughes et al., 2013; Lloyd et al., 2012; Mahler et al., 2010), but could also reflect the effect of measurement and/or phylogenetic error to inflate evolutionary rates for younger clades. Similar to species-specific rates of evolution, we do not differentiate between these alternative hypotheses.

In this study, we take a comprehensive approach to explain the accumulation of ecological diversity in a major global radiation. We find little to no evidence that

heterogeneity in recent evolutionary rates links to life history, environmental mutagenic factors, or the presence or absence of competitors. In fact, almost 80% of variation in evolutionary rates between species remains unexplained. However, half of the variation in clade evolutionary rates is predicted by the interplay between adaptation to novel ecological resources and the number of species packing within clades. Overall, our results show that increased ecological opportunity in distinct adaptive zones is an important driver of rapid evolution, although it constraints the number of species able to pack into clades. Furthermore, we find support for the hypothesized link between rates of trait evolution and species richness, implying that rapid trait diversification is also linked with high levels of niche differentiation between related species.

ACKNOWLEDGEMENTS

We thank Joseph Brown, Yichen He, Joseph Llanos, Alexandra Pryke, Louie Rombaut, and two anonymous referees for valuable comments and discussion points. We thank M. Adams, H. van Grouw and R. Prys-Jones at the Natural History Museum, and H. McGhie at the Manchester Museum for providing access to and expertize in the collections. We thank all the volunteer citizen scientists at http://www.markmybird.org for helping us build the detailed beak shape dataset. This work was funded by the European Research Council (grant number 615709 Project 'ToLERates') and by a Royal Society University Research Fellowship to G.H.T. (UF120016).

REFERENCES

Adams, D. C., Berns, C. M., Kozak, K. H., & Wiens, J. J. (2009). Are rates of species diversification correlated with rates of morphological evolution? *Proc Biol Sci, 276*(1668), 2729-2738.

Adams, D. C., & Collyer, M. L. (2018). Multivariate Phylogenetic Comparative Methods: Evaluations, Comparisons, and Recommendations. *Syst Biol, 67*(1), 14-31.

Adams, D. C., Collyer, M. L., Kaliontzopoulou, A., & Sherratt, E. (2017). Geomorph: Software for geometric morphometric analyses. R package version 3.0.5. https://cran.r-project.org/package=geomorph.

Adams, D. C., Rohlf, F. J., & Slice, D. E. (2013). A field comes of age: geometric morphometrics in the 21st century. *Hystrix, the Italiam Journal of Mammalogy, 24*(1), 7-14.

Agrawal, A. A., Fishbein, M., Halitschke, R., Hastings, A. P., Rabosky, D. L., & Rasmann, S. (2009). Evidence for adaptive radiation from a phylogenetic study of plant defenses. *Proc Natl Acad Sci U S A, 106*(43), 18067-18072.

Beckmann, M., Václavík, T., Manceur, A. M., Šprtová, L., von Wehrden, H., Welk, E., . . . Tatem, A. (2014). glUV: a global UV-B radiation data set for macroecological studies. *Methods in Ecology and Evolution, 5*(4), 372-383.

Bright, J. A., Marugán-Lobón, J., Cobb, S. N., & Rayfield, E. J. (2016). The shapes of bird beaks are highly controlled by nondietary factors. *Proceedings of the National Academy of Sciences, 113*(19), 5352-5357.

Bromham, L. (2009). Why do species vary in their rate of molecular evolution? *Biol Lett, 5*(3), 401-404.

Bromham, L. (2011). The genome as a life-history character: why rate of molecular evolution varies between mammal species. *Philos Trans R Soc Lond B Biol Sci, 366*(1577), 2503-2513.

Bromham, L., & Cardillo, M. (2003). Testing the link between the latitudinal gradient in species richness and rates of molecular evolution. *Journal of Evolutionary Biology, 16*(2), 200-207.

Bromham, L., Hua, X., Lanfear, R., & Cowman, P. F. (2015). Exploring the Relationships between Mutation Rates, Life History, Genome Size, Environment, and Species Richness in Flowering Plants. *Am Nat, 185*(4), 507-524.

Bromham, L., Woolfit, M., Lee, M. S., & Rambaut, A. (2002). Testing the relationship between morphological and molecular rates of change along phylogenies. *Evolution, 56*(10), 1921-1930.

Burbrink, F. T., Chen, X., Myers, E. A., Brandley, M. C., & Pyron, R. A. (2012). Evidence for determinism in species diversification and contingency in phenotypic evolution during adaptive radiation. *Proc Biol Sci, 279*(1748), 4817-4826.

Claramunt, S., Derryberry, E. P., Brumfield, R. T., & Remsen, J. V., Jr. (2012). Ecological opportunity and diversification in a continental radiation of birds: climbing adaptations and cladogenesis in the Furnariidae. *Am Nat, 179*(5), 649-666.

Clarke, M., Thomas, G. H., & Freckleton, R. P. (2015). Trait Evolution in Adaptive Radiations: Modeling and Measuring Interspecific Competition on Phylogenies. *Am Nat, 189*(2).

Collar, D. C., O'Meara, B. C., Wainwright, P. C., & Near, T. J. (2009). Piscivory limits diversification of feeding morphology in centrarchid fishes. *Evolution, 63*(6), 1557-1573.

Cooney, C. R., Bright, J. A., Capp, E. J. R., Chira, A. M., Hughes, E. C., Moody, C. J. A., . . . Thomas, G. H. (2017). Mega-evolutionary dynamics of the adaptive radiation of birds. *Nature, 542*(7641), 344-347.

Cooper, N., & Purvis, A. (2009). What factors shape rates of phenotypic evolution? A comparative study of cranial morphology of four mammalian clades. *Journal of Evolutionary Biology, 22*(5), 1024-1035.

Davies, T. J., Barraclough, T. G., Savolainen, V., & Chase, M. W. (2004). Environmental causes for plant biodiversity gradients. *Philos Trans R Soc Lond B Biol Sci, 359*(1450), 1645-1656.

Davies, T. J., Meiri, S., Barraclough, T. G., & Gittleman, J. L. (2007). Species co-existence and character divergence across carnivores. *Ecol Lett, 10*(2), 146-152.

Davies, T. J., & Savolainen, V. (2006). Neutral theory, phylogenies, and the relationship between phenotypic change and evolutionary rates. *Evolution, 60*(3), 476-483.

Dayan, T., & Simberloff, D. (2005). Ecological and community-wide character displacement: the next generation. *Ecology Letters, 8*(8), 875-894.

Dornburg, A., Sidlauskas, B., Santini, F., Sorenson, L., Near, T. J., & Alfaro, M. E. (2011). The influence of an innovative locomotor strategy on the phenotypic diversification of triggerfish (family: Balistidae). *Evolution, 65*(7), 1912-1926.

Dowle, E. J., Morgan-Richards, M., & Trewick, S. A. (2013). Molecular evolution and the latitudinal biodiversity gradient. *Heredity (Edinb), 110*(6), 501-510.

Drummond, A. J., Suchard, M. A., Xie, D., & Rambaut, A. (2012). Bayesian phylogenetics with BEAUti and the BEAST 1.7. *Mol Biol Evol, 29*(8), 1969-1973.

Drury, J., Clavel, J., Manceau, M., & Morlon, H. (2016). Estimating the Effect of Competition on Trait Evolution Using Maximum Likelihood Inference. *Syst Biol, 65*(4), 700-710.

Drury, J. P., Tobias, J. A., Burns, K. J., Mason, N. A., Shultz, A. J., & Morlon, H. (2018). Contrasting impacts of competition on ecological and social trait evolution in songbirds. *PLoS Biol, 16*(1), e2003563.

Felice, R. N., & Goswami, A. (2018). Developmental origins of mosaic evolution in the avian cranium. *Proc Natl Acad Sci U S A, 115*(3), 555-560.

Flenley, J. R. (2011). Why is pollen yellow? And why are there so many species in the tropical rain forest? *Journal of Biogeography, 38*(5), 809-816.

Freeman, B. G. (2015). Competitive Interactions upon Secondary Contact Drive Elevational Divergence in Tropical Birds. *Am Nat, 186*(4), 470-479.

Galtier, N., Blier, P. U., & Nabholz, B. (2009). Inverse relationship between longevity and evolutionary rate of mitochondrial proteins in mammals and birds. *Mitochondrion, 9*(1), 51-57.

Gavrilets, S., & Losos, J. B. (2009). Adaptive radiation: contrasting theory with data. *Science, 323*(5915), 732-737.

Gillman, L. N., Wright, S. D., & Ladle, R. (2014). Species richness and evolutionary speed: the influence of temperature, water and area. *Journal of Biogeography, 41*(1), 39-51.

Grafen, A. (1989). The phylogenetic regression. *Phil. Trans. R. Soc. Lond. B, 326*(1233), 119-157.

Grant, B. R., & Grant, P. R. (2003). What Darwin's Finches Can Teach Us about the Evolutionary Origin and Regulation of Biodiversity. *BioScience, 53*(10), 965-975.

Grant, B. R., & Grant, P. R. (2006). Evolution of Character Displacement in Darwin’s Finches. *Science, 313*(5784), 224-226.

Hackett, S. J., Kimball, R. T., Reddy, S., Bowie, R. C. K., Braun, E. L., Braun, J. B., . . . Yuri, T. (2008). A Phylogenomic Study of Birds Reveals Their Evolutionary History. *Science, 320*(5884), 1763-1768.

Harmon, L. J., Losos, J. B., Jonathan Davies, T., Gillespie, R. G., Gittleman, J. L., Bryan Jennings, W., . . . Mooers, A. O. (2010). Early bursts of body size and shape evolution are rare in comparative data. *Evolution, 64*(8), 2385-2396.

Hijmans, R. J., Cameron, S. E., Parra, J. L., Jones, P. G., & Jarvis, A. (2005). Very high resolution interpolated climate surfaces for global land areas. *International Journal of Climatology, 25*(15), 1965-1978.

Hijmans, R. J., & von Etten, J. (2012). raster: Geographic analysis and modeling with raster data. R package version 2.0-12. http://CRAN.R-project.org/package=raster.

Hughes, M., Gerber, S., & Wills, M. A. (2013). Clades reach highest morphological disparity early in their evolution. *Proc Natl Acad Sci U S A, 110*(34), 13875-13879.

Hulsey, C. D., Roberts, R. J., Loh, Y. H., Rupp, M. F., & Streelman, J. T. (2013). Lake Malawi cichlid evolution along a benthic/limnetic axis. *Ecol Evol, 3*(7), 2262-2272.

Hunter, J. P. (1998). Key innovations and the ecology of macroevolution. *Trends Ecol Evol, 13*(1), 31-36.

Igea, J., Miller, E. F., Papadopulos, A. S. T., & Tanentzap, A. J. (2017). Seed size and its rate of evolution correlate with species diversification across angiosperms. *PLoS Biol, 15*(7), e2002792.

Jetz, W., Thomas, G. H., Joy, J. B., Hartmann, K., & Mooers, A. O. (2012). The global diversity of birds in space and time. *Nature, 491*(7424), 444-448.

Jonsson, K. A., Fabre, A. C., Fritz, S. A., Etienne, R. S., Ricklefs, R. E., Jorgensen, T. B., . . . Irestedt, M. (2012). Ecological and evolutionary determinants for the adaptive radiation of the Madagascan vangas. *Proceedings of the National Academy of Sciences, 109*(17), 6620–6625.

Landis, M. J., & Schraiber, J. G. (2017). Pulsed evolution shaped modern vertebrate body sizes. *Proc Natl Acad Sci U S A, 114*(50), 13224-13229.

Lanfear, R., Ho, S. Y., Love, D., & Bromham, L. (2010a). Mutation rate is linked to diversification in birds. *Proc Natl Acad Sci U S A, 107*(47), 20423-20428.

Lanfear, R., Welch, J. J., & Bromham, L. (2010b). Watching the clock: studying variation in rates of molecular evolution between species. *Trends Ecol Evol, 25*(9), 495-503.

Lawson, A. M., & Weir, J. T. (2014). Latitudinal gradients in climatic-niche evolution accelerate trait evolution at high latitudes. *Ecol Lett, 17*(11), 1427-1436.

Liu, J. Q., Wang, Y. J., Wang, A. L., Hideaki, O., & Abbott, R. J. (2006). Radiation and diversification within the Ligularia-Cremanthodium-Parasenecio complex (Asteraceae) triggered by uplift of the Qinghai-Tibetan Plateau. *Mol Phylogenet Evol, 38*(1), 31-49.

Lloyd, G. T., Wang, S. C., & Brusatte, S. L. (2012). Identifying heterogeneity in rates of morphological evolution: discrete character change in the evolution of lungfish (Sarcopterygii; Dipnoi). *Evolution, 66*(2), 330-348.

Losos, J. B. (2010). Adaptive radiation, ecological opportunity, and evolutionary determinism. American Society of Naturalists E. O. Wilson award address. *Am Nat, 175*(6), 623-639.

Losos, J. B., & Mahler, D. L. (2010). *Evolution since Darwin: the first 150 years. Chapter: Adaptive radiation: the interaction of ecological opportunity, adaptation, and speciation.*: Sunderland (MA): Sinauer.

Losos, J. B., & Ricklefs, R. E. (2009). Adaptation and diversification on islands. *Nature, 457*(7231), 830-836.

Lovette, I. J., Bermingham, E., & Ricklefs, R. E. (2002). Clade-specific morphological diversification and adaptive radiation in Hawaiian songbirds. *Proc Biol Sci, 269*(1486), 37-42.

Lovette, I. J., & Hochachka, W. M. (2006). Simultaneous effects of phylogenetic niche conservatism and competition on avian community structure. *Ecology, 87*(sp7), S14-S28.

Mahler, D. L., Revell, L. J., Glor, R. E., & Losos, J. B. (2010). Ecological opportunity and the rate of morphological evolution in the diversification of Greater Antillean anoles. *Evolution, 64*(9), 2731-2745.

Martin, C. H., & Wainwright, P. C. (2011). Trophic novelty is linked to exceptional rates of morphological diversification in two adaptive radiations of Cyprinodon pupfish. *Evolution, 65*(8), 2197-2212.

Martin, P. R., Montgomerie, R., & Lougheed, S. C. (2010). Rapid sympatry explains greater color pattern divergence in high latitude birds. *Evolution, 64*(2), 336-347.

Martins, E. P., & Hansen, T. F. (1997). Phylogenies and the Comparative Method: A General Approach to Incorporating Phylogenetic Information into the Analysis of Interspecific Data. *Am Nat, 149*(4), 646-667.

Mooers, A. Ø., & Harvey, P. H. (1994). Metabolic rate, generation time, and the rate of molecular evolution in birds. *Molecular phylogenetics and evolution, 3*(4), 344-350.

Orme, D., Freckleton, R. P., Thomas, G. H., Petzoldt, T., Fritz, S., Isaac, N., & Pearse, W. (2013). caper: Comparative Analyses of Phylogenetics and Evolution in R. R package version 0.5.2. http://CRAN.R-project.org/package=caper.

Pagel, M. (1999). Inferring the historical patterns of biological evolution. *Nature, 401*(6756), 877-884.

Pfennig, K. S., & Pfennig, D. W. (2009). Character Displacement: Ecological And Reproductive Responses To A Common Evolutionary Problem. *The Quarterly Review of Biology, 84*(3), 253-276.

Pigot, A. L., & Tobias, J. A. (2013). Species interactions constrain geographic range expansion over evolutionary time. *Ecol Lett, 16*(3), 330-338.

Plummer, M., Best, N., Cowles, K., & vines, K. (2006). CODA: Convergence Diagnosis and Output Analysis for MCMC. *R News, 6*(1), 7-11.

Polly, P. D., Lawing, A. M., Fabre, A. C., & Goswami, A. (2013). Phylogenetic Principal Components Analysis and Geometric Morphometrics. *Italian Journal of Mammology, 24*(1), 33-41.

Price, S. A., Wainwright, P. C., Bellwood, D. R., Kazancioglu, E., Collar, D. C., & Near, T. J. (2010). Functional innovations and morphological diversification in parrotfish. *Evolution, 64*(10), 3057-3068.

Prum, R. O., Berv, J. S., Dornburg, A., Field, D. J., Townsend, J. P., Lemmon, E. M., & Lemmon, A. R. (2015). A comprehensive phylogeny of birds (Aves) using targeted next-generation DNA sequencing. *Nature, 526*(7574), 569-573.

Rabosky, D. L. (2015). No substitute for real data: A cautionary note on the use of phylogenies from birth-death polytomy resolvers for downstream comparative analyses. *Evolution, 69*(12), 3207-3216.

Rabosky, D. L. (2017). Phylogenetic tests for evolutionary innovation: the problematic link between key innovations and exceptional diversification. *Philos Trans R Soc Lond B Biol Sci, 372*(1735).

Rabosky, D. L., & Adams, D. C. (2012). Rates of morphological evolution are correlated with species richness in salamanders. *Evolution, 66*(6), 1807-1818.

Rabosky, D. L., Santini, F., Eastman, J., Smith, S. A., Sidlauskas, B., Chang, J., & Alfaro, M. E. (2013). Rates of speciation and morphological evolution are correlated across the largest vertebrate radiation. *Nat Commun, 4*, 1958.

Reddy, S., Driskell, A., Rabosky, D. L., Hackett, S. J., & Schulenberg, T. S. (2012). Diversification and the adaptive radiation of the vangas of Madagascar. *Proc Biol Sci, 279*(1735), 2062-2071.

Revell, L. J. (2009). Size-correction and principal components for interspecific comparative studies. *Evolution, 63*(12), 3258-3268.

Rhode, K. (1992). Latitudinal gradients in species diversity: the search for the primary cause. *Oikos, 65*(3), 514–527.

Ricklefs, R. E. (2004). Cladogenesis and morphological diversification in passerine birds. *Nature, 430*(6997), 338–341.

Ricklefs, R. E. (2005). Small Clades at the Periphery of Passerine Morphological Space. *Am Nat, 165*(6), 651-659.

Rundle, H. D., & Nosil, P. (2005). Ecological speciation. *Ecology Letters, 8*(3), 336-352.

Schluter, D. (2001). Ecology and the origin of species. *Trends Ecol Evol, 16*(7), 372-380.

Schoener, T. W. (1965). The Evolution of Bill Size Differences Among Sympatric Congeneric Species of Birds. *Evolution, 19*(2), 189-213.

Simpson, G. G. (1953). *The major features of evolution.*: Columbia University Press.

Smith, S. A., & Donoghue, M. J. (2008). Rates of molecular evolution are linked to life history in flowering plants. *Science, 322*(5898), 86-89.

Thomas, G. H., & Freckleton, R. P. (2012). MOTMOT: models of trait macroevolution on trees. *Methods in Ecology and Evolution, 3*(1), 145-151.

Thomas, J. A., Welch, J. J., Lanfear, R., & Bromham, L. (2010). A generation time effect on the rate of molecular evolution in invertebrates. *Mol Biol Evol, 27*(5), 1173-1180.

Thomson, C. E., Gilbert, J. D., & Brooke Mde, L. (2014). Cytochrome b divergence between avian sister species is linked to generation length and body mass. *PLoS One, 9*(2), e85006.

Tobias, J. A., Cornwallis, C. K., Derryberry, E. P., Claramunt, S., Brumfield, R. T., & Seddon, N. (2014). Species coexistence and the dynamics of phenotypic evolution in adaptive radiation. *Nature, 506*(7488), 359-363.

Uyeda, J. C., Caetano, D. S., & Pennell, M. W. (2015). Comparative Analysis of Principal Components Can be Misleading. *Syst Biol, 64*(4), 677-689.

Uyeda, J. C., Hansen, T. F., Arnold, S. J., & Pienaar, J. (2011). The million-year wait for macroevolutionary bursts. *Proc Natl Acad Sci U S A, 108*(38), 15908-15913.

Venditti, C., Meade, A., & Pagel, M. (2011). Multiple routes to mammalian diversity. *Nature, 479*(7373), 393-396.

Vilela, B., Villalobos, F., & Poisot, T. (2015). letsR: a new R package for data handling and analysis in macroecology. *Methods in Ecology and Evolution, 6*(10), 1229-1234.

Voje, K. L., Holen, O. H., Liow, L. H., & Stenseth, N. C. (2015). The role of biotic forces in driving macroevolution: beyond the Red Queen. *Proc Biol Sci, 282*(1808), 20150186.

Weir, J. T., & Mursleen, S. (2013). Diversity-dependent cladogenesis and trait evolution in the adaptive radiation of the auks (aves: alcidae). *Evolution, 67*(2), 403-416.

Wilman, H., Belmaker, J., Simpson, J., de la Rosa, C., Rivadeneira, M. M., & Jetz, W. (2014). EltonTraits 1.0: Species-level foraging attributes of the world's birds and mammals. *Ecological Archives, 95*(7), 2027-2027.

Wright, D. F. (2017). Phenotypic Innovation and Adaptive Constraints in the Evolutionary Radiation of Palaeozoic Crinoids. *Sci Rep, 7*(1), 13745.

Zelditch, M. L., Swiderski, D. L., & Sheets, H. D. (2012). *Geometric Morphometrics for Biologists*. San Diego: Academic Press.

SUPPLEMENTARY MATERIAL

Additional supporting information may be found online in the supporting information tab for this article (doi:10.1111/ele.13131). Supplementary material comprises of tables (ele13131-sup-0002-TableS1-S8.docx) and figures (ele13131-sup-0001-FigS1-S11.pdf).

Table S1. List of alternative runs used in the analyses. Trees were built using: (i) Jetz et al. (2012) and Prum et al. (2015) avian phylogenies, (ii) only species with genetic data (G) or full range of species (F), (iii) maximum clade credibility trees, setting node heights to "common ancestor heights" (CAH) or to heights in the target tree (HTT). We ran both phylogenetic (pPCA) and non-phylogenetic (PCA) principal components analysis on the data, and used a number of PC/pPC axes that covered 95% and 99% of the beak shape variation (#PCs). The models were generally run twice (#Runs), but some trees and datasets were used only once due to time constraints.

Table S2. The percentage of beak shape variation described (phylogenetic) PC axes across alternative phylogenies: (i) using Jetz et al. (2012) and Prum et al. (2015), (ii) using trees built including only species with genetic data (G) or the full range of species (F), (iii) using a maximum clade credibility tree with node heights set to "common ancestor heights" (CAH) or heights in the target tree (HTT). For each run, values adding up to 99% of beak shape variation are shown.

Table S3. Pearson's correlation between tip rates across alternative multivariate BayesTraits runs, using a number of (phylogenetic) PC axes that explain 99% of variation in beak shape. Alternative runs are built (i) using Jetz et al. (2012) and Prum et al. (2015), (ii) using trees built including only species with genetic data (G) or the full range of species (F), (iii) using a maximum clade credibility tree with node heights set to "common ancestor heights" (CAH) or heights in the target tree (HTT). Rate values were logged to ensure a normal distribution. Unless otherwise indicated, traits represent PC axes.

Table S4. Adjusted R-squared values when an interaction between clade names and individual predictors is included in the model. These analyses are run on a tree built using the Jetz et al (2012) phylogeny, including only species with genetic data, and using a maximum clade credibility tree with node heights set to “common ancestor heights”. Traits represent PC axes.

Table S5. Correlates for species-specific rates of evolution. Results across alternative trees built (i) using using Jetz et al. (2012) and Prum et al. (2015), (ii) using trees built including only species with genetic data (G) or the full range of species (F), (iii) using a maximum clade credibility tree with node heights set to “common ancestor heights” (CAH) or heights in the target tree (HTT). We perform PGLS analyses only for the runs in which we used a number of PC/pPCs that covered 99% of variation in beak shape. Given the strong correlations between tip rates across alternative runs (Table S3), we only perform PGLS analyses on a subset of alternative trees and datasets. Unless otherwise indicated, traits represent PC axes.

Table S6. Correlates for clade rates of evolution; results across alternative trees built (i) using using Jetz et al Jetz et al. 2012 and Prum et al Prum et al. 2015, (ii) using trees built including only species with genetic data (G) or the full range of species (F), (iii) using a maximum clade credibility tree with node heights set to “common ancestor heights” (CAH) or heights in the target tree (HTT). We perform PGLS analyses only for the runs in which we used a number of PC/pPCs that covered 99% of variation in beak shape. Given the strong correlations between evolutionary rates across alternative runs (Table S3), we only perform PGLS analyses on a subset of alternative trees and datasets. Unless otherwise indicated, traits represent PC axes.

Table S7. Correlates for clade rates of evolution; d.f. = 6,90; adjusted R-squared = 0.27. A finer division of clades (especially among the Passerines) is used. These analyses are run on a tree built using the Jetz et al (2012) phylogeny, including only

species with genetic data, and using a maximum clade credibility tree with node heights set to “common ancestor heights”. Traits represent PC axes.

Table S8. Correlates for clade rates of evolution; d.f. = 5,34; adjusted R-squared = 0.17. Species richness is excluded as a predictor. These analyses are run on a tree built using the Jetz et al (2012) phylogeny, including only species with genetic data, and using a maximum clade credibility tree with node heights set to “common ancestor heights”. Traits represent PC axes.

Figure S1. Illustration of how clade beak distinctiveness is calculated for target clades (delimitated here by coloured convex hulls) i.e. the Euclidean distance between the centre of the clade and the overall centre of the morphospace. The absolute value of centred PC values is considered; in our analyses we consider the first eight axes of variation when measuring beak clade distinctiveness (i.e. we calculate Euclidean distances in an eightdimensional morphospace).

Figure S2. Reproduced below.

Figure S3. Reproduced below.

Figure S4. Correlates for species-specific rates of evolution; none of the variables correlates significantly with evolutionary rates.

Figure S5. Correlates for species-specific rates of evolution. Each line represents a monophyletic clade of species. Red lines mark slopes for which the confidence interval does not pass 0 .

Figure S6. The relationship between species-specific evolution and (a) mean annual temperature, (b) mean annual UVB levels. Points are coloured by species’ migratory status: residents (red, negative trend) vs full migrants (black).

Figure S7. (a) Reproduced below. (bcd) The relationship between clade rates of evolution and (b) proportion of island species, (c) average range size, and (d) clade age. None of the variables correlates significantly with evolutionary.

Figure S8. Reproduced below.

Figure S9. The relationship between clade rates of evolution and (a) clade age, p = 0.002, (b) clade beak distinctiveness, p <0.001. A finer division of clades (especially among the Passerines) is used.

Figure S10. (a) The relationship between clade rates of evolution and (a) clade species richness, p = 0.014. (b) The relationship between the observed and predicted clade rate of evolution by the full PGLS model (adj. R-sq = 0.27). The dashed line indicates the 1:1 line of predicted versus observed values. A finer division of clades (especially among the Passerines) is used.

Figure S11. Multivariate rates of beak shape evolution for alternative trees built (i) using Jetz et al 2012 and Prum et al 2015, (ii) using trees built including only species with genetic data (G) or the full range of species (F), (iii) using a maximum clade credibility tree with node heights set to “common ancestor heights” (CAH) or heights in the target tree (HTT)

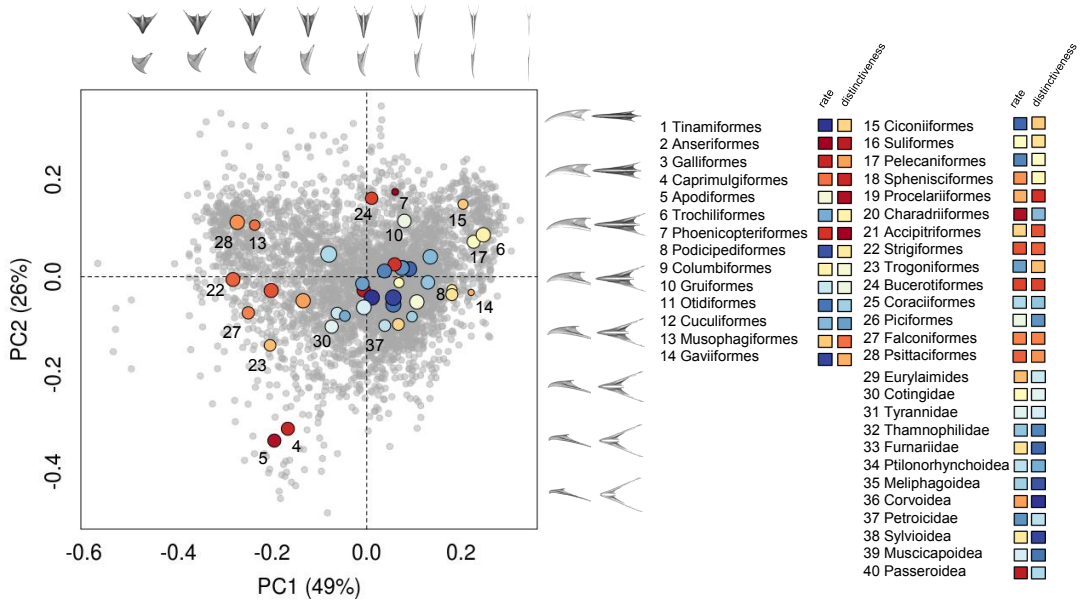

Figure S2a. Avian beak morphospace shown as a pairwise scatter plot of the 1st and 2nd PC axes (the proportion of variance explained by each PC is indicated in brackets). Warps represent the change in beak shape along each axis (top and side views). The centroid of each clade is shown, and the most distinct 10 clades on PC1 and PC2 are numbered on the plot. Centroid points are sized by the species richness of clades, and coloured by clade distinctiveness values across the first eight PC axes. Clade distinctiveness and rate of evolution are also shown in the legend.

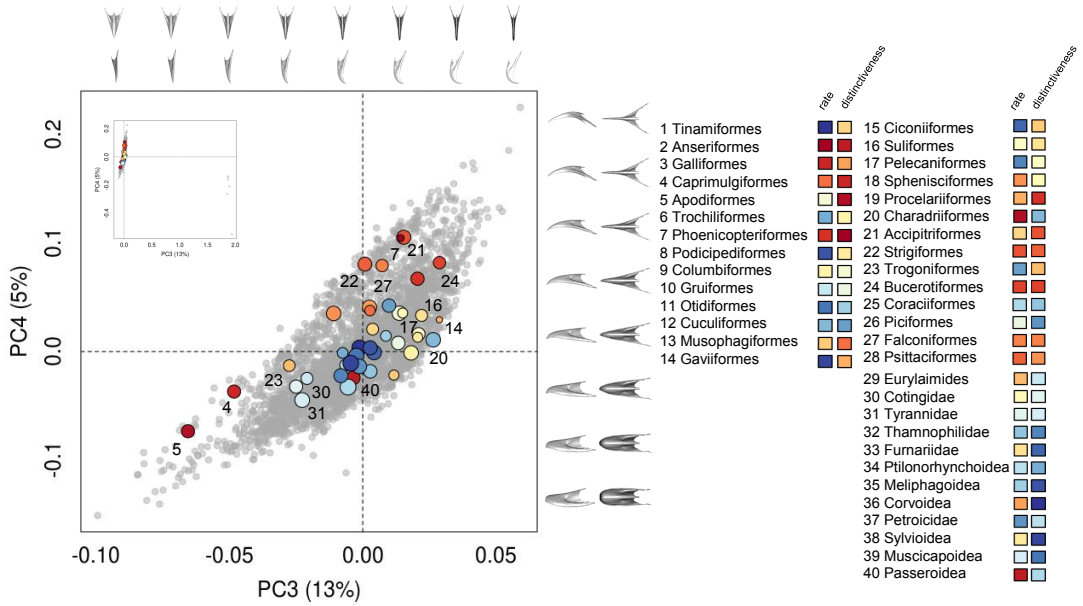

Figure S2b. Avian beak morphospace shown as a pairwise scatter plot of the 3rd and 4th PC axes (the proportion of variance explained by each PC is indicated in brackets). Warps represent the change in beak shape along each axis (top and side views). The centroid of each clade is shown, and the most distinct 10 clades on PC3 and PC4 are numbered on the plot. Centroid points are sized by the species richness of clades, and coloured by clade distinctiveness values across the first eight PC axes. Clade distinctiveness and rate of evolution are also shown in the legend. For a clearer visualisation, outstanding outlier species (i.e. PC3 > 1.5, five *Loxia* species and *Anarhynchus frontalis*) were removed from the plot; full plot given in the top-left corner.

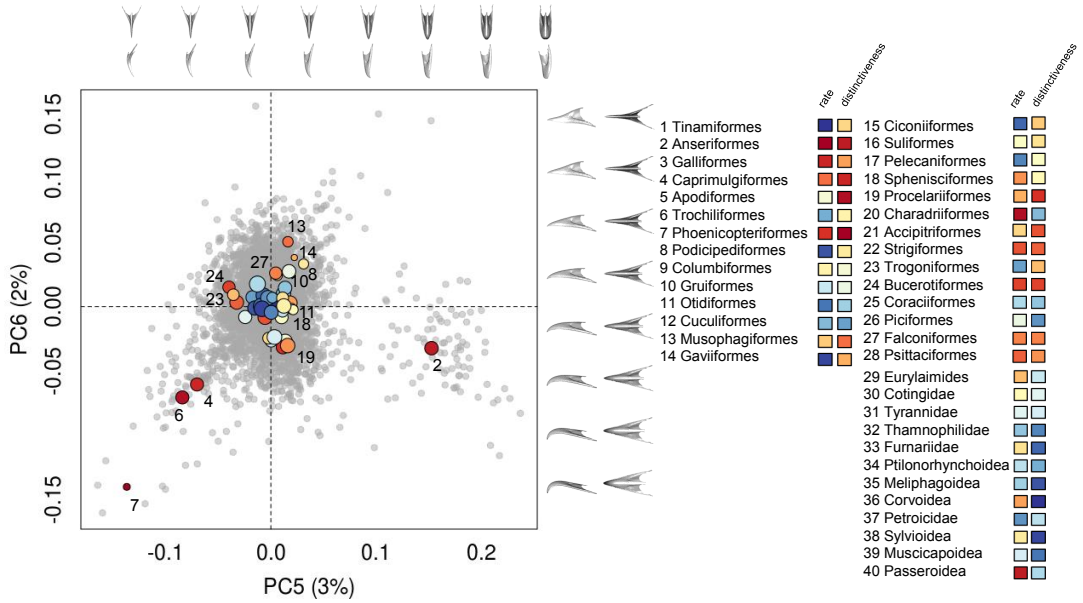

Figure S2c. Avian beak morphospace shown as a pairwise scatter plot of the 1st and 2nd PC axes (the proportion of variance explained by each PC is indicated in brackets). Warps represent the change in beak shape along each axis (top and side views). The centroid of each clade is shown, and the most distinct 10 clades on PC5 and PC6 are numbered on the plot. Centroid points are sized by the species richness of clades, and coloured by clade distinctiveness values across the first eight PC axes. Clade distinctiveness and rate of evolution are also shown in the legend.

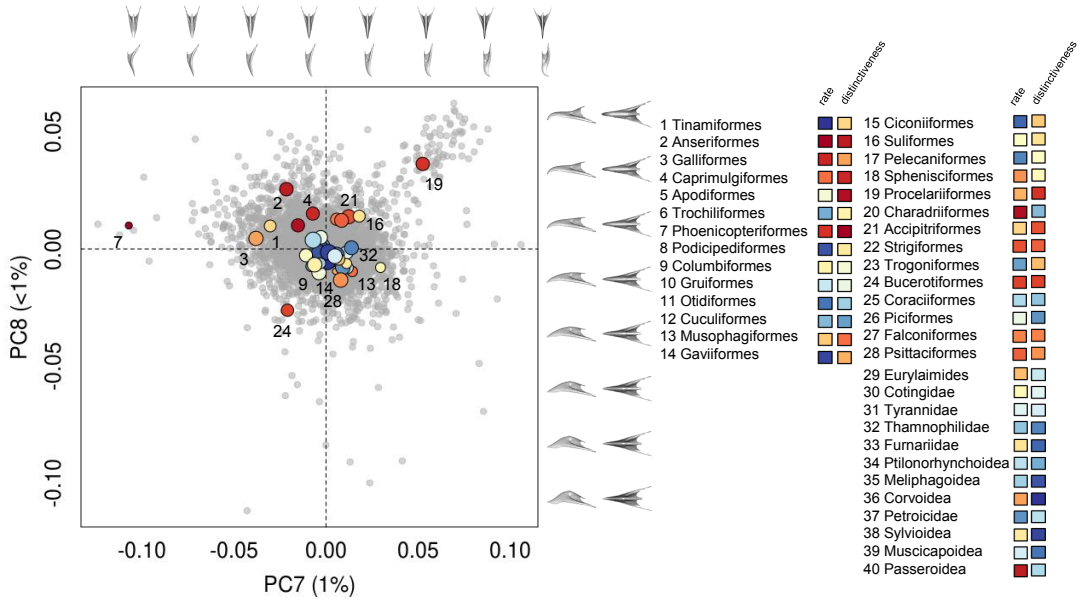

Figure S2d. Avian beak morphospace shown as a pairwise scatter plot of the 1st and 2nd PC axes (the proportion of variance explained by each PC is indicated in brackets). Warps represent the change in beak shape along each axis (top and side views). The centroid of each clade is shown, and the most distinct 10 clades on PC7 and PC8 are numbered on the plot. Centroid points are sized by the species richness of clades, and coloured by clade distinctiveness values across the first eight PC axes. Clade distinctiveness and rate of evolution are also shown in the legend.

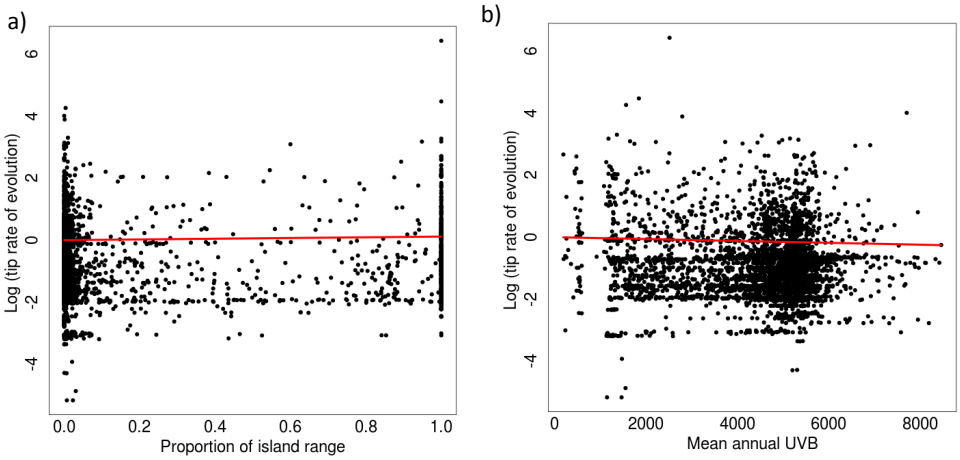

Figure S3. The relationship between species-specific rates of evolution and (a) the proportion of island range, $p = 0.013$, (b) UVB levels, $p = 0.028$.

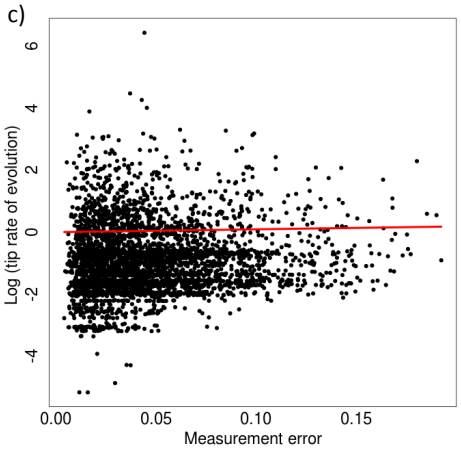

Figure S3. (c) The relationship between species-specific rates of evolution and measurement error (i.e. mean Procrustes distances between users marking each bill), $p = 0.029$.

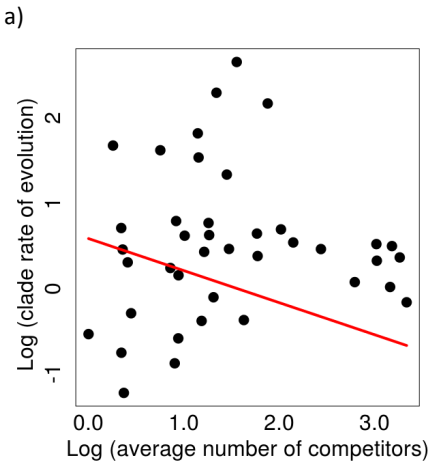

Figure S7. (a) The relationship between clade rates of evolution and average number of competitors for species in each clade, $p = 0.044$.

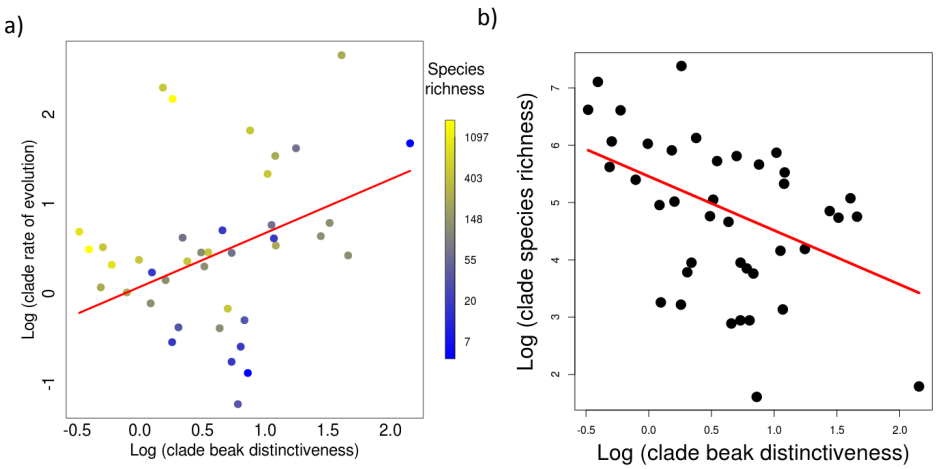

Figure S8. (a) The relationship between clade rate of evolution and clade beak distinctiveness; points are coloured by clade species richness. (b) The relationship between clade species richness and clade beak distinctiveness, $p = 0.01$. There is much variation to this relationship: many clades with unusual beaks have rather intermediate species richness values (e.g. *Anseriformes*, *Accipitriformes*, *Apodiformes*, *Strigiformes*), and some distinctive beak shaped clades are also species rich (e.g. *Psittacidae*).

CHAPTER 4

The signature of competition for shared resources across the avian tree

ABSTRACT

Biotic interactions such as competition have long been considered key factors affecting the evolution of biological diversity. However, the tempo and mode of phenotypic evolution has been mainly approached by using ecologically-neutral trait evolutionary models. Consequently, the role of ecology in driving deep-time macroevolutionary dynamics remains poorly understood. Here, we use methods that model phenotypic evolution with incorporating species interactions, to look for patterns in the distribution of traits consistent with a signal of competition across the evolution of avian ecomorphological traits. We find that while ecologically-neutral models are most frequently supported, ecological models are also preferred in many clades. Further, we find a more frequent signature of competition in the evolution of beak size and shape rather than body mass, and generally, a signal of competition is seen in the divergence of one, rather than multiple axes of morphological specialization. Additionally, the signature of competition is distributed randomly throughout the tree. Lastly, we see a stronger support for ecological models in more recent radiations, suggesting that ecological selection pressures have a stronger impact in compact groups in which species are more similar and likelier to interact. Overall, we find that using models with competition can explain the patterns of phenotypic accumulation better than ecologically-neutral models within an appreciable number of clades, and thus ecological selection on traits can leave a signal into long-term patterns of phenotypic diversification.

INTRODUCTION

A fundamental topic of interest in evolutionary biology is understanding the tempo and mode underlying the accumulation of morphological diversity at macroevolutionary scales (Simpson, 1953). The standard statistical framework for modelling phenotypic differentiation between species while accounting for patterns of phylogenetic relatedness assumes lineages evolve independent from each other. However, ecologically neutral evolution is likely to be unrealistic in many (if not all) cases, and competition for shared resources in particular has been closely linked with patterns of trait diversification. For instance, the absence of competitors offers species access to a multitude of free niches, which can result in bursts of phenotypic diversification as shown for example in iconic island radiations (Grant & Grant, 2006; Losos & Ricklefs, 2009; Lovette et al., 2002). Alternatively, a high density of competitors can speed up trait divergence via character displacement (Dayan & Simberloff, 2005; Pfennig & Pfennig, 2009), or cause convergence in traits involved in competitor recognition (Grether et al., 2009; Tobias et al., 2014). Eventually, the accumulation of many competitors may limit trait evolution if niche spaces are bounded, and even cause the extinction of competitors (e.g. Connell, 1961). But testing the prevalence of competition at macroevolutionary scales has been hindered by the difficulty of incorporating species interactions while modelling trait evolution. Hence, we do not know the importance of competition beyond several recent radiations, and thus whether competition impacts the process of trait evolution across global radiations.

At deep-time scales, competitive interactions have been associated with several patterns and models of trait evolution. Diversity dependent models in particular have been used as a proxy for evidence of species interactions within clades, as the rate of evolution is modelled to change with the number of accumulating lineages (Mahler et al., 2010; Weir & Mursleen, 2013). These models can detect a pattern of

decreased evolutionary rates at high densities of species, which is consistent with a scenario of reduced potential for further evolution in niches saturated by competitors (Harmon et al., 2003 Agrawal et al., 2009; Mahler et al., 2010). Time-dependent models (in which the rate of evolution decreases linearly or exponentially through time, Blomberg et al., 2003), predict a similar outcome in tip-trait distributions, although they do not incorporate a role of species-interactions on evolution explicitly. Conversely, competitive interactions are also associated with fast trait diversification via character displacement, and thus positive diversity-dependence and observations of higher morphological disparity in groups with a higher degree of sympatric congeners are also patterns consistent with strong competitive interactions (Davies et al., 2007; Freeman, 2015).

Recently, significant efforts have been made to further incorporate competitive selection pressures while modelling trait evolution (Nuismer & Harmon, 2015, Drury et al., 2016, Clarke et al., 2017). Novel methods are based on the equation of a random-walk model of evolution (Cavalli-Sforza & Edwards, 1967), to which terms that account for competition are added. The underlying assumption is that similarity in relevant traits (i.e. traits involved in the acquisition of limiting resources) between species enables competition, and so these models look for patterns of increased trait divergence between closely related lineages, as expected if species differentiate to avoid antagonistic competitive interactions. This role of morphological specialization to avoid competition is apparent from observations on localized, short-term radiations (Grant & Grant, 2006; Stuart et al., 2014a). In macroevolutionary models with biotic interactions, species can evolve away from the mean trait value among congeners (Drury et al., 2016), or more subtly, the amount of morphological divergence can be modelled for all pairs of species as a function of pairwise similarity in target traits (Clarke et al., 2017). Further, these methods offer the attractive option to control when and which species are allowed to

interact within clades, either by adding a time-delay after which species can interact (Clarke et al., 2017), or by incorporating spatial coexistence matrices (Drury et al., 2016). By contrasting methods that model trait evolution under the assumptions of competition with ecologically-neutral evolutionary models, we can determine the relative importance of various hypotheses in shaping phenotypic evolution within clades. These methods have already been applied to a few radiations (Clarke et al., 2017; Drury et al., 2018), but we lack a deep-time perspective on how often ecological processes like competition leave a signature in the dynamics of phenotypic accumulation.

Here, we investigate how often we can detect patterns of trait divergence consistent with a signature of competition in the evolution of avian ecomorphological traits. We focus on avian beak shape and size, which are closely related to resource acquisition, as well as body mass. We contrast methods that look for trait-dependent (species evolve to increase morphological differentiation among each other) or diversity-dependent evolution (rates of trait evolution are dependent on the accumulation of species) to ecologically-neutral models of evolution to describe the prevalence of a mode of evolution consistent with species interactions in avian clades. We apply trait evolutionary models in a mixture of well-supported orders and super-families, as well as to more recent radiations within those groups to obtain a comprehensive perspective of the signal of species interactions at various time-scales.

MATERIALS AND METHODS

Morphological data

We used 3D scans of bird beaks to collect beak shape and size measurements for 7,776 avian species. A detailed account of the protocols used to extract this data is given in Cooney et al., 2017. Briefly, we used study skins from the Natural History

Museum in Tring and Manchester Museum, and scanned the beaks using white and blue structured light scanning (*FlexScan3D*, LMI Technologies, Vancouver, Canada). We further extracted information about variation in shape and size between scans using landmark based geometric morphometrics (Zelditch et al., 2012). We chose four key points on the avian beak, which can be easily placed repeatedly in a similar position across specimens: (1) the tip of the beak, (2) the posterior margin of the beak on the dorsal midline, (3) the left, and (4) the right tomial edges. Furthermore, we had 75 semi-landmarks that unite (1) to (2), (3) and (4), forming the dorsal midline, and left and right tomial edges, respectively. The land marking process was performed via the crowdsourcing website http://www.markmybird.org. Both authors and members of the public used this platform to complete the landmarking process. Each 3D image was marked by at least three independent users, and unsuitable landmark efforts (either poor landmarking of individual scans or non-similarity in landmark position between users) were discarded following quality control protocols. Further, suitable landmark configurations were subjected to a generalized Procrustes analysis (to remove the effects of any geometric information unrelated to shape) and alignment (Adams et al., 2017), and we used PCA and phylogenetic PCA (pPCA) analyses (Polly et al., 2013; Revell, 2009) on user-averaged landmarks to extract the main axes of beak shape variation. We performed PCA and pPCA both globally (i.e. including all species), as well as within well-known monophyletic clades of species (see below). Additionally, we used the square root of the sum of squared distances of landmarks from their centroid i.e. centroid size (Zelditch et al., 2012) as a measure of beak size, and extracted species body mass measurements from the EltonTraits database (Wilman et al., 2014).

Phylogenetic data

We split our species into 95 well-supported monophyletic clades, as identified by Jetz et al. (2012). We only considered groups with at least 10 species. We sampled 10,000 random trees from a 10,000 posterior distribution of "full" trees (i.e. trees with all 9,993 avian species) and "genetic" trees (i.e. trees including only species for which genetic data is available) accessed from http://www.birdtree.org (Jetz et al., 2012). We then pruned them to generate tree distributions for species in each clade. We used TreeAnnotator (Drummond et al., 2012) to generate maximum clade credibility trees for all clades, setting branch lengths equal to common ancestor node heights. We then pruned the trees to contain only species for which we have beak shape and size data. We used both "full" and "genetic" trees to ensure that our results are robust to potential phylogenetic error associated with including branches with non-genetic data in the trees. Similarly, we also built a MCC tree for all species we have trait data for, and then collapse species from the same clade to obtain a phylogeny in which tip labels represent clades of interest. Lastly, in each individual clade, we put a time slice half way across the root-tip distance and extracted monophyletic clades with at least 10 members formed after the time slice. These clades (159 in total) represent recent radiations within each parent clade.

Models of trait evolution

We used a suite of ecologically neutral evolutionary models to test how trait diversity accumulates across avian clades: random walk trait divergence (or BM, Cavalli-Sforza & Edwards, 1967), divergence towards a local adaptive optimum (or OU, Butler & King, 2004; Hansen & Martins, 1996), as well as time-dependent models, in which the rate of evolution decreases in time (Blomberg et al., 2003; Harmon et al., 2010). We contrasted the fit of these models with diversity-dependent models, in which the rate of evolution varies linearly (DDlin) or exponential (DDexp) with the number of lineages (Weir & Mursleen, 2013). Both positive (positive r parameter)

and negative (negative r parameter) diversity-dependence can indicate competition, as the accumulation of species can speed up morphological differentiation as species evolve away from competitors (Grant & Grant, 2006; Stuart et al., 2014b) but also cause a slowdown in evolutionary rates as niches fill and ecological opportunity decreases (Mahler et al., 2010). Further, we also considered the recently developed matching-competition model (MC, Drury et al., 2016), in which key traits evolve away from the mean values of clade members. The application of these classes of methods essentially tests for evidence that selection pressures from biotic interactions have influenced the evolution of target traits across clades. We compared the Akaike weights (Burnham & Anderson, 2004) of the matching competition and diversity-dependent models against the weights of ecologically-neutral models, following Drury et al., 2018: relative support for competition = $\max(MC_{wi}, DDlin_{wi}, DDexp_{wi}) / (\max(BM_{wi}, OU_{wi}, TDexp_{wi}, TDlin_{wi}) + \max(MC_{wi}, DDlin_{wi}, DDexp_{wi}))$.

We separately modelled the evolution of body mass, beak size and beak shape. We quantified beak shape variation in two ways. First, we conducted global procrustes alignments of landmarks and extracted the first two PC and pPC axes across all species in our dataset. Second, we conducted within-clade procrustes alignments of landmarks and extracted the first two PC and pPC axes across each of these subsets of species. Across all species, the first two PC axes accounted for a total of 80% (PCA) and 72% (pPCA) variation in beak shape (Figure S1), while across individual clades, variation explained by the first and second PC axes explained between 59 and 99% beak shape variation (Table S1). Additionally, we regressed beak size against body mass using PGLS within individual clades (Grafen, 1989; Martins & Hansen, 1997), and use the residuals as a proxy for beak size relative to body size in evolutionary models. Finally, we analysed the phylogenetic signal for relative support for competition across clades, using the D static (Fritz & Purvis,

2010) and the phylogeny with clades collapsed into branches. The D static generally takes values between 0 (the focal trait is dispersed as expected under a Brownian motion model) and 1 (focal trait is dispersed randomly across the phylogeny). Additionally, D static values outside these ranges can be recovered if the focal trait is extremely clumped (values <0) or overdispersed (values >1). We calculated phylogenetic signal for each trait separately (using as evidence for competition relative support values > 0.5), as well as overall across beak shape (global PC1 and PC2), relative beak size, and body mass (i.e. relative support values > 0.5 in any of the four focal traits is considered as evidence for competition). All analyses were performed using R packages (Morlon et al., 2016; Orne et al., 2013; Pennell et al., 2014). We mainly focus on global PC axes, relative beak size and body mass in the main text, and report the results from the other traits in the supplementary material.

RESULTS

We find that the BM model is the best fitting model (minimum AICc) in 38 (out of 95) clades for global PC1, 25 for global PC2, 22 for relative beak size, and 51 for body mass (Figure 4.1a, Figure S2a). The OU model is also frequently preferred, particularly for global PC2 (38 clades), and relative beak size (50 clades). In comparison, the frequency of time-dependent models is small, but more prevalent in body mass (13 clades in total), compared to beak size (0 clades) and shape (10 and 2 clades for global PC1 and PC2, respectively). Further, values higher than 50% for the relative support for competition are found in 14 clades (out of 95) for global PC1, 30 for global PC2, 23 for relative beak size, and 14 for body mass (Figure 4.2a). Additionally, we see higher values for the relative support for competition in general across clades for beak traits, compared to body mass (Figure 4.1), and thus patterns of beak shape and size evolution are more consistent with a presence of competitive selection pressures compared to body mass divergence. When using “genetic” trees, similar to the analyses on the “full” trees, we only apply evolutionary

models in clades comprising of more than 10 species (total number = 83 clades). Across the “genetic trees”, we find values higher than 50% for the relative support for competition in 11 clades (out of 83) for global PC1, 30 for global PC2, 21 for relative beak size, and 6 for body mass. In terms of percentages, the prevalence of high (>50%) relative support for competition is similar between “full” and “genetic” trees for beak shape and size, however, support for competition is higher in “full” trees for body mass (15% compared to 7%). When diversity-dependent models are the best fit for the data, positive values for the r parameter are largely inferred i.e. an exponential increase in evolutionary rates with increasing number of species (Figure S4ab). We find similar results when we ran the analyses on the “genetic” trees (Figure S4c). We find that clades vary in their relative support for competition (Figure 4.3). We find very high relative support for competition (>95%) in some well-known examples of high morphological specialization, such as hummingbirds (beak shape), or sunbirds and flowerpeckers (beak size relative to body mass). We also find high support for competition in several other clades: leafbirds, fairy-bluebirds, rollers, ground-rollers (global PC1), pheasants, quail, guineafowl and chats, Old World flycatchers (global PC2), falcons, caracaras (relative beak size), antpittas, tits, chickadees and penduline−tits (body mass). A few clades show high relative support for competition in more than one trait, e.g. chats and Old World flycatchers, sandgrouse, manakins, woodpeckers, cuckoo-shirkes, leafbirds and fairy-bluebirds. In general, however, clades tend to show high relative support for competition in one rather than many axes of ecomorphological specialization (Figure 4.3).

We find no evidence for phylogenetic signal in the relative support of competition across deep-time or recent radiations for all the traits considered (Table 4.1, Table S2). Further, we see no phylogenetic signal when considering evidence of competition as high (>0.5) relative support in either beak shape, size or body mass. Our results thus show that variation in relative support for competition is dispersed

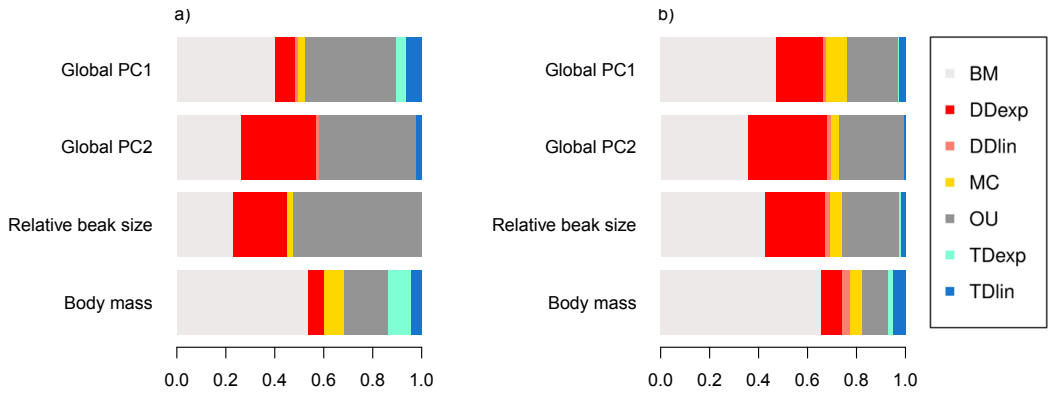

Figure 4.1. Model support (proportion of times each model is chosen as best i.e. smallest AICc values) across clades when modelling the evolution of various ecomorphological traits. The models considered are: Brownian motion (BM), linear (DDlin) and exponential (DDexp) diversity-dependent models, matching competition (MC), Ornstein-Uhlenbeck (OU), linear (TDlin) and exponential (TDexp) time-dependent models. Results across deep-time scales (a) and recent radiations (b).

randomly across the avian tree. Similar results are obtained when running the models on "genetic" trees (Table S1). Further, we see a higher preponderance of diversity-dependent and matching-competition models (and accordingly relative support for competition) in recent compared to deep-time radiations (Figure 4.1, Figure 4.2, Figure S2, Figure S3).

DISCUSSION

Here we investigate the prevalence for a mode of evolution consistent with the presence of competitive selection pressures in shaping the process of evolution for key ecomorphological traits across the bird radiation. Specifically, we look for negative or positive trait diversity-dependence, as well as patterns of increased trait divergence among closely-related, morphologically similar species. We find a signature for species interactions in multiple clades, showing that competition could influence trait evolution beyond a few exceptional radiations and thus contribute to shaping morphological diversity at macroevolutionary scales. The exponential diversity-dependent model is most frequently the best fit of the data among the

models that assume a role of species-interactions on trait evolution. Further, we generally find an increase in rates of ecomorphological evolution with the packing of species (positive r parameters in exponential diversity-dependent models, Figure S4). A better fit of positive exponential diversity-dependent models over the matching competition model has been linked with a signal of both competition and bounded trait evolution occurring simultaneously (Drury et al., 2017), and thus our results also indicate that interactions between lineages could maintain a rapid phenotypic turnover even with the filling of niches (Thompson, 1999). Lastly, our results are not consistent with a scenario of competition limiting the potential for evolution once niches are being filled and ecological opportunity decreases (Weir & Mursleen, 2013).

We found a stronger signal of competition when modelling beak shape and relative size, rather than body mass. These results uphold the tight link between beak attributes and resource acquisition (Foster et al., 2008; Jønsson et al., 2012; Olsen & Gremillet, 2017; Schondube & Martinez del Rio, 2003), and also indicate that if small changes in the beak produce substantial differences in the feeding ecology of species, beak change might represent a parsimonious route towards ecological differentiation (Grant & Grant, 2006; Grant, 1999; Weir & Mursleen, 2013). Conversely, body mass is associated with many aspects of species' ecology and it is influenced by many selection forces, thus we can expect biotic interactions to play a smaller relative contribution to body mass evolution across the bird tree. Further, the allometric link between beak size and body size (here accounted for by using body mass) likely drives the smaller signal of competition we observe when using absolute values of beak size (Weir & Mursleen, 2013).

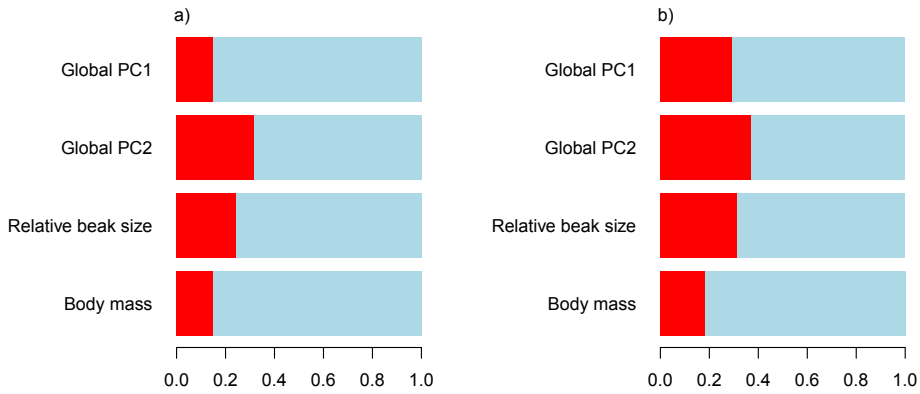

Figure 4.2. Frequency of clades in which the relative support for competition exceeds 50% (red) for various ecomorphological traits. The relative support of competition is based on AICw for process-based models: linear and exponential diversity dependent models, as well as the matching competition model. We consider both deep-time scales (a) and recent radiation (b).

Table 4.1. Phylogenetic signal (D static) for the relative support for competition (a value of 1 is considered for relative support values bigger than 0.5) across various traits. D static values are compared to a Brownian expectation (i.e. evidence for phylogenetic signal) and a random expectation (i.e. no phylogenetic signal). D static values are reported for each trait separately, as well as for analyses scoring relative support across all traits (i.e. a value of 1 is considered for relative support values bigger than 0.5 in at least one of the four focal traits).

Trait	D estimate	Difference from 0 (Brownian expectation)	Difference from 1 (random expectation)	#Clades with support > 0.5 (out of 95)
Global PC1	1.308	0.011	0.762	14
Global PC2	1.011	0.015	0.500	30
Relative beak size	0.923	0.048	0.374	23
Body mass	1.231	0.018	0.704	14
All traits	1.056	0.016	0.556	55

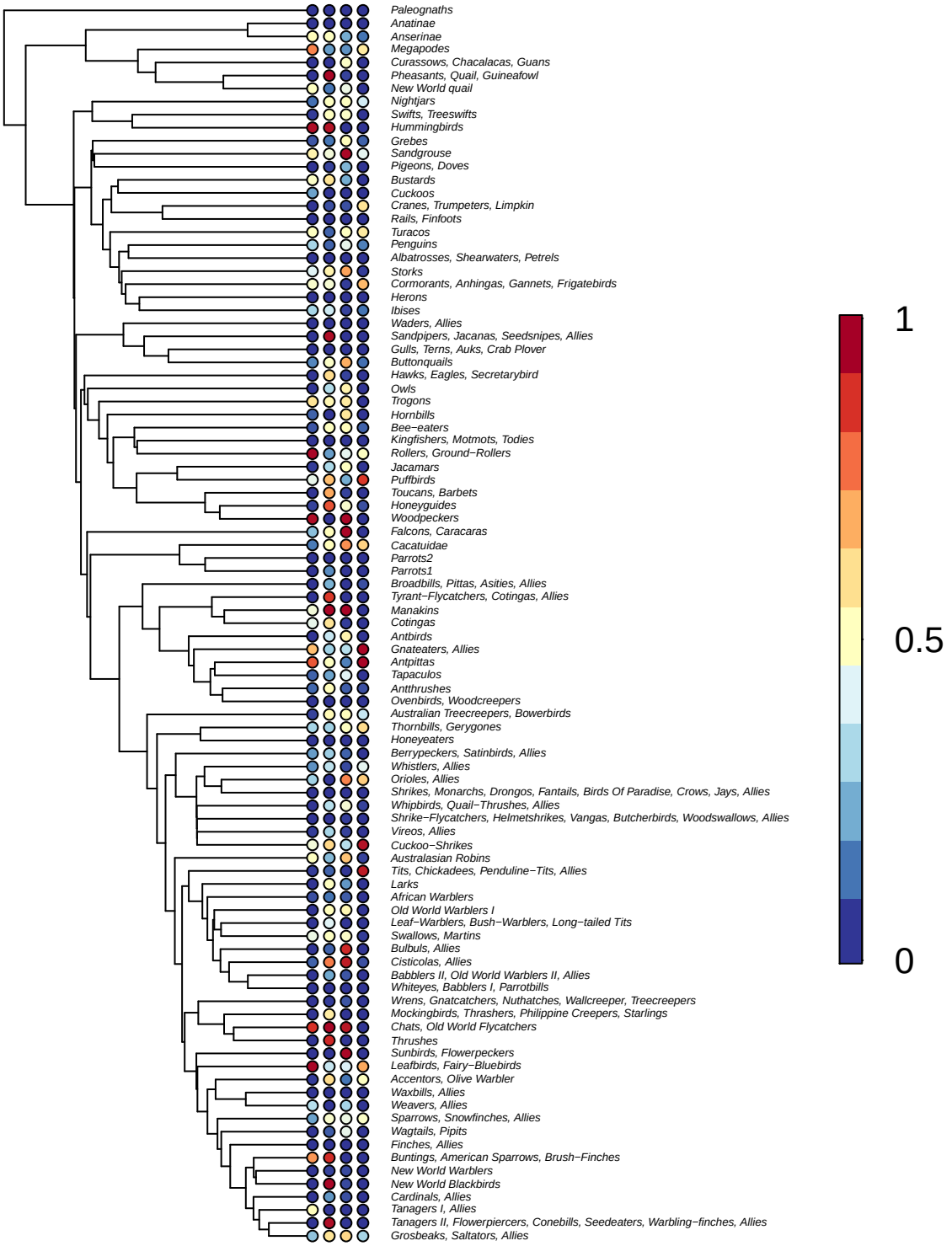

Figure 4.3. Relative support for competition based on AICw of process based models (diversity dependent and the matching competition model) across clades. The following ecomorphological traits are considered: beak shape (global PC1, PC2), relative beak size, and body mass. A list of clade names is provided at the end of the supplementary material.

Both relative beak size and shape are highly integrated in birds, particular with modules of the cranium (Bright et al., 2016; Felice & Goswami, 2018; Kulemeyer et al., 2009). Therefore, we can expect constraints to how labile these traits are in response to selection pressures, but we did not find a substantial difference in how prevalent relative beak size and shape change under competition. Overall, our results show moderate support for a difference in traits in respect to how likely they evolve under selection from competition, but further research is needed to explore and validate candidate mechanisms underlying these trends at a large scale.

Additionally, we found that competitive selection pressures preferably act extensively on one axis of specialization, as generally, we did not see patterns of phenotypic divergence consistent with a strong effect of species-interactions across multiple traits. The target axis of morphological divergence likely depends on which traits are key to acquire the finite shared resources. For example, we detected a signal for competition in beak shape or relative size in several textbook examples of beak specialization such as hummingbirds (Temeles et al., 2009), flowerpiercers (Schondube & Martinez del Rio, 2003), or sunbirds (Lovette et al., 2002). Further, we recovered support for competition in body mass in groups where mass associates with foraging activity, such as diving depth in seabirds (e.g. Cormorants, Anhingas, Gannets, Frigatebirds, Cook et al., 2013). We did, however, also see a handful of clades in which multiple traits evolved consistent with expectations under competitive selection pressures. Most often, we detect a signature for competition across beak shape and relative size e.g. in woodpeckers, a group in which variation in both aspects of beak morphology is closely linked with specialization to foraging substrate (Carrascal et al., 1990; Spring, 1965). Overall, our results indicate that divergence in one trait may be enough to produce differences in the way species acquire various resources, and hence to minimize competition for shared resources. These findings also indicate that a potential signature of competition in the

distribution of extant species' phenotypes can be missed if studies are restricted to single traits.

We found that variation in the relative support for competition is distributed randomly with respect to the avian phylogeny, and hence phylogenetic relatedness cannot predict whether specific groups are prone to competition. These results are in agreement with studies linking the strength of species interactions and stochastic events, such as climatic changes and the associated fluctuations in resource availability (Grant & Grant, 2006; Klanderud, 2005), invasion episodes (Jackson, 2015; Tennessen et al., 2016), and the extinction or conversely, increased abundance of competing clades (Benson et al., 2014). Our findings thus indicate that the distribution of a signature for competitive interactions as a selection force across global radiations is mostly contingent to chance (Thompson, 1999). Short-time scales in particular are subject to high variability in selection pressures, (Benton, 2009; Losos & Ricklefs, 2009), and accordingly, we saw higher levels of relative support in recent compared to deep-time radiations. Moreover, recent radiations generally represent smaller groups of similar species that are likely to interact, as opposed to larger clades, where multiple processes act on trait evolution, and not all lineages will be involved in interactions. However, recent radiations are by definition younger and smaller than deep-time ones. And thus, a pattern of increased trait divergence with the accumulation of lineages or between morphologically similar, closely related species could also be explained by a biased preference for diversity-dependent and the matching competition models in trees with smaller ages and/or species-richness. Further, measurement and phylogenetic error for example can lead to false inference of positive r parameters in diversity-dependent models (Drury et al., 2018). We did not differentiate here between alternative mechanisms underlying the patterns we observe. The analyses on "full" and "genetic" trees gave similar results regarding the prevalence for competition

signal across clades, the lack of phylogenetic signal in relative support for competition, as well as the dominance of positive diversity-dependence. Hence, error due to the incorporation of branches without genetic data in avian trees did not bias our results. We do, however, note higher evidence of a mode of evolution consistent with competition for body mass divergence in “full” compared to “genetic” trees, and therefore, it is possible that our results on competition signal in this trait are overestimated.

Lastly, we acknowledge several caveats to these results. The use of phylogenetic and standard PC axes of variation in univariate trait evolutionary models has been criticised (Uyeda et al., 2015). Specifically, using only the first PC axes can bias model selection criteria towards time-dependent methods. We did not, however, find elevated support for such models in our dataset, and moreover, relative support for competition is high mostly in scenarios of increasing, rather than decreasing, evolutionary rates (as estimated by diversity-dependent models). The development of multivariate methods with competition in the future should limit the concerns associated with using only a subset of the total axes of shape variation (Clarke et al., 2017). Performing model adequacy tests to aid the interpretation of results based on model selection criteria alone (Pennell et al., 2015) would have also alleviated concerns related to biased model preference or overestimation of competition signal due to measurement or phylogenetic error. Trait evolutionary models that incorporate ecological selection pressure are, however, still novel, and therefore they are not yet integrated in current model adequacy frameworks. Additionally, our results likely underestimate the effect of competition, as in the current application of the models, we assume all species in clades are interacting, whereas in reality, many species will not be sympatric nor share the same diets, foraging strategy, diurnal activity patterns etc. Similarly, the development of the MC model that simultaneously accounts both divergence between species as a result of

competition, as well as evolving under constraints will likely increase the detectability of clades where species-interactions impact on trait evolution (Drury et al., 2017).

Here we take a comprehensive approach to evaluate the prevalence of species-interactions across long-term evolutionary scales by looking for patterns consistent with expectations under competitive selection pressures i.e. diversity-dependent and phenotypic evolution mediated by similarity in traits. We find that the signal for competition varies across the avian tree, but methods that assume a role of species-interactions on trait evolution are frequently preferred to ecologically-neutral models in many clades, including some putative examples of competition driven diversification. The prevalence of competitive interactions signature is not predicted by phylogenetic relatedness, and further, the signal of competition is more prevalent in recent groups (where species are more likely to interact) compared to deep-time radiations. Moreover, the signal of species-interactions (when diversity-dependent models fit best) is generally to increase rates of trait divergence with the accumulation of species, as expected under character displacement. Further, we find that a mode of evolution consistent with competition is preferentially detected on one rather than multiple axes of morphological differentiation (more so on beak morphology, rather than body mass), in agreement with the argument that ecological specialization under competition is usually achieved via the most parsimonious route. Taken together, our results suggest that incorporating ecological selection pressures when modelling trait evolution can improve model fit, and hence, ecology can shape patterns of biodiversity accumulation in deep-time. Our results, however, also imply that in large-scale radiations, the signal of competition can be mediated by a mode of evolution under constraints, as well as a reduced potential for meaningful interactions between species (e.g. spatial and foraging niche overlap). Further, as the current trait evolutionary models with

interactions are phenomenological, we cannot also rule out other factors that might produce patterns of trait divergence similar to competitive interactions, not least various types of errors in the data and/or flawed model selection criteria.

REFERENCES

Adams, D. C., Collyer, M. L., Kaliontzopoulou, A., & Sherratt, E. (2017). Geomorph: Software for geometric morphometric analyses. R package version 3.0.5. https://cran.r-project.org/package=geomorph.

Agrawal, A. A., Fishbein, M., Halitschke, R., Hastings, A. P., Rabosky, D. L., & Rasmann, S. (2009). Evidence for adaptive radiation from a phylogenetic study of plant defenses. *Proc Natl Acad Sci U S A, 106*(43), 18067-18072.

Benson, R. B., Frigot, R. A., Goswami, A., Andres, B., & Butler, R. J. (2014). Competition and constraint drove Cope's rule in the evolution of giant flying reptiles. *Nat Commun, 5*, 3567.

Benton, M. J. (2009). The Red Queen and the Court Jester: species diversity and the role of biotic and abiotic factors through time. *Science, 323*(5915), 728-732.

Blomberg, S. P., Garland, T., & Ives, A. R. (2003). Testing for phylogenetic signal in comparative data: behavioral traits are more labile. *Evolution, 57*(4), 717-745.

Bright, J. A., Marugán-Lobón, J., Cobb, S. N., & Rayfield, E. J. (2016). The shapes of bird beaks are highly controlled by nondietary factors. *PNAS, 113*(19), 5352-5357.

Burnham, K. P., & Anderson, D. R. (2004). Multimodel Inference. *Sociological Methods & Research, 33*(2), 261-304.

Butler, M. A., & King, A. A. (2004). Phylogenetic Comparative Analysis: A Modeling Approach for Adaptive Evolution. *American Naturalist, 164*(6), 683-695.

Carrascal, L. M., Moreno, E., & Tellería, J. L. (1990). Ecomorphological relationships in a group of insectivorous birds of temperate forests in winter. *Ecography, 13*(2), 105-111.

Cavalli-Sforza, L. L., & Edwards, A. W. F. (1967). Phylogenetic analysis. Models and estimation procedures. *American Journal of Human Genetics, 19*(3), 233-257.

Clarke, M., Thomas, G. H., & Freckleton, R. P. (2017). Trait Evolution in Adaptive Radiations: Modeling and Measuring Interspecific Competition on Phylogenies. *Am Nat, 189*(2), 121-137.

Connell, J. H. (1961). The Influence of Interspecific Competition and Other Factors on the Distribution of the Barnacle Chthamalus Stellatus. *Ecology, 42*(4), 710-723.

Cook, T. R., Lescroel, A., Cherel, Y., Kato, A., & Bost, C. A. (2013). Can foraging ecology drive the evolution of body size in a diving endotherm? *PLoS One, 8*(2), e56297.

Cooney, C. R., Bright, J. A., Capp, E. J. R., Chira, A. M., Hughes, E. C., Moody, C. J. A., . . . Thomas, G. H. (2017). Mega-evolutionary dynamics of the adaptive radiation of birds. *Nature, 542*(7641), 344-347.

Davies, T. J., Meiri, S., Barraclough, T. G., & Gittleman, J. L. (2007). Species co-existence and character divergence across carnivores. *Ecol Lett, 10*(2), 146-152.

Dayan, T., & Simberloff, D. (2005). Ecological and community-wide character displacement: the next generation. *Ecology Letters, 8*(8), 875-894.

Drummond, A. J., Suchard, M. A., Xie, D., & Rambaut, A. (2012). Bayesian phylogenetics with BEAUti and the BEAST 1.7. *Mol Biol Evol, 29*(8), 1969-1973.

Drury, J., Clavel, J., Manceau, M., & Morlon, H. (2016). Estimating the Effect of Competition on Trait Evolution Using Maximum Likelihood Inference. *Syst Biol, 65*(4), 700-710.

Drury, J. P., Grether, G. F., Garland, T., & Morlon, H. (2017). An Assessment of Phylogenetic Tools for Analyzing the Interplay Between Interspecific Interactions and Phenotypic Evolution. *Syst Biol, 67*(3), 413-427.

Drury, J. P., Tobias, J. A., Burns, K. J., Mason, N. A., Shultz, A. J., & Morlon, H. (2018). Contrasting impacts of competition on ecological and social trait evolution in songbirds. *PLoS Biol, 16*(1), e2003563.

Felice, R. N., & Goswami, A. (2018). Developmental origins of mosaic evolution in the avian cranium. *Proc Natl Acad Sci U S A, 115*(3), 555-560.

Foster, D. J., Podos, J., & Hendry, A. P. (2008). A geometric morphometric appraisal of beak shape in Darwin's finches. *J Evol Biol, 21*(1), 263-275.

Freeman, B. G. (2015). Competitive Interactions upon Secondary Contact Drive Elevational Divergence in Tropical Birds. *Am Nat, 186*(4), 470-479.

Fritz, S. A., & Purvis, A. (2010). Selectivity in mammalian extinction risk and threat types: a new measure of phylogenetic signal strength in binary traits. *Conserv Biol, 24*(4), 1042-1051.

Grafen, A. (1989). The phylogenetic regression. *Philos Trans R Soc Lond B Biol Sci, 326*(1233), 1989.

Grant, B. R., & Grant, P. R. (2006). Evolution of Character Displacement in Darwin's Finches. *Science, 313*(5784), 224-226.

Grant, P. R. (1999). Bill Size, Body Size, and the Ecological Adaptations of Bird Species to Competitive Situations on Islands. *Systematic Zoology, 17*(3), 319-333.

Grether, G. F., Losin, N., Anderson, C. N., & Okamoto, K. (2009). The role of interspecific interference competition in character displacement and the evolution of competitor recognition. *Biol Rev Camb Philos Soc, 84*(4), 617-635.

Hansen, T. F., & Martins, E. P. (1996). Translating between microevolutionary process and macroevolutionary patterns: the correlation structure of interspecific data. *Evolution, 50*(4), 1404-1417.

Harmon, L. J., Losos, J. B., Jonathan Davies, T., Gillespie, R. G., Gittleman, J. L., Bryan Jennings, W., . . . Mooers, A. O. (2010). Early bursts of body size and shape evolution are rare in comparative data. *Evolution, 64*(8), 2385-2396.

Harmon, L. J., Schulte, J. A., Larson, A., & Losos, J. B. (2003). Tempo and Mode of Evolutionary Radiation in Iguanian Lizards. *Science, 301*(5635), 961-964.

Jackson, M. C. (2015). Interactions among multiple invasive animals. *Ecology, 96*(8), 2035-2041.

Jetz, W., Thomas, G. H., Joy, J. B., Hartmann, K., & Mooers, A. O. (2012). The global diversity of birds in space and time. *Nature, 491*(7424), 444-448.

Jønsson, K. A., Fabre, P. H., Fritz, S., Etienne, R. S., Ricklefs, R. E., Jørgensen, T. B., . . . Irestedt, M. (2012). Ecological and evolutionary determinants for the adaptive radiation of the Madagascan vangas. *PNAS, 109*(17), 6620–6625.

Klanderud, K. (2005). Climate change effects on species interactions in an alpine plant community. *Journal of Ecology, 93*(1), 127-137.

Kulemeyer, C., Asbahr, K., Gunz, P., Frahnert, S., & Bairlein, F. (2009). Functional morphology and integration of corvid skulls - a 3D geometric morphometric approach. *Front Zool, 6*(1), 2.

Losos, J. B., & Ricklefs, R. E. (2009). Adaptation and diversification on islands. *Nature, 457*(7231), 830-836.

Lovette, I. J., Bermingham, E., & Ricklefs, R. E. (2002). Clade-specific morphological diversification and adaptive radiation in Hawaiian songbirds. *Proc Biol Sci, 269*(1486), 37-42.

Mahler, D. L., Revell, L. J., Glor, R. E., & Losos, J. B. (2010). Ecological opportunity and the rate of morphological evolution in the diversification of Greater Antillean anoles. *Evolution, 64*(9), 2731-2745.

Martins, E. P., & Hansen, T. F. (1997). Phylogenies and the comparative method: a general approach to incorporating phylogenetic information into the analysis of interspecific data. . *Am Nat, 149*(4), 646–667.

Morlon, H., Lewitus, E., Condamine, F. L., Manceau, M., Clavel, J., & Drury, J. (2016). RPANDA: an R package for macroevolutionary analyses on phylogenetic trees. *Methods in Ecology and Evolution*.

Nuismer, S. L., & Harmon, L. J. (2015). Predicting rates of interspecific interaction from phylogenetic trees. *Ecol Lett, 18*(1), 17-27.

Olsen, A. M., & Gremillet, D. (2017). Feeding ecology is the primary driver of beak shape diversification in waterfowl. *Functional Ecology, 31*(10), 1985-1995.

Orne, D., Freckleton, R. P., Thomas, G. H., Petzoldt, T., Fritz, S., Isaac, N., & Pearse, W. (2013). caper: Comparative Analyses of Phylogenetics and Evolution in R. R package version 0.5.2. http://CRAN.R-project.org/package=caper.

Pennell, M., FitzJohn, R. G., Cornwell, W. K., & Harmon, L. J. (2015). Model Adequacy and the Macroevolution of Angiosperm Functional Traits. *Am Nat, 186*(2), E33-E50.

Pennell, M. W., Eastman, J. M., Slater, G. J., Brown, J. W., Uyeda, J. C., FitzJohn, R. G., . . . Harmon, L. J. (2014). geiger v2.0: an expanded suite of methods for fitting macroevolutionary models to phylogenetic trees. *Bioinformatics, 30*(15), 2216-2218.

Pfennig, K. S., & Pfennig, D. W. (2009). Character Displacement: Ecological And Reproductive Responses To A Common Evolutionary Problem. *The Quarterly Review of Biology, 84*(3), 253-276.

Polly, P. D., Lawing, A. M., Fabre, A. C., & Goswami, A. (2013). Phylogenetic Principal Components Analysis and Geometric Morphometrics. *Italian Journal of Mammology, 24*(1), 33-41.

Revell, L. J. (2009). Size-correction and principal components for interspecific comparative studies. *Evolution, 63*(12), 3258-3268.

Schondube, J. E., & Martinez del Rio, C. (2003). The flowerpiercers' hook: an experimental test of an evolutionary trade-off. *Proc Biol Sci, 270*(1511), 195-198.

Simpson, G. G. (1953). *The major features of evolution.*: Columbia University Press.

Spring, L. W. (1965). Climbing and pecking adaptations in some North American woodpeckers. *The Condor, 67*(6), 457-488.

Stuart, Y. E., Campbell, T. S., Hohenlohe, P. A., Reynolds, R. G., Revell, L. J., & Losos, J. B. (2014a). Rapid evolution of a native species following invasion by a congener. *Science, 346*(6208), 463-436.

Stuart, Y. E., Campbell, T. S., Hohenlohe, P. A., Reynolds, R. G., Revell, L. J., & Losos, J. B. (2014b). Rapid evolution of a native species following invasion by a congener. *Science, 346*(6206), 463-466.

Temeles, E. J., Koulouris, C. R., Sander, S. E., & Kress, W. J. (2009). Effect of flower shape and size on foraging performance and trade-offs in a tropical hummingbird. *Ecology, 90*(5), 1147-1161.

Tennessen, J. B., Parks, S. E., Tennessen, T. P., & Langkilde, T. (2016). Raising a racket: invasive species compete acoustically with native treefrogs. *Animal Behaviour, 114*, 53-61.

Thompson, J. N. (1999). The Evolution of Species Interactions. *Science, 284*(5423), 2116-2118.

Tobias, J. A., Cornwallis, C. K., Derryberry, E. P., Claramunt, S., Brumfield, R. T., & Seddon, N. (2014). Species coexistence and the dynamics of phenotypic evolution in adaptive radiation. *Nature, 506*(7488), 359-363.

Uyeda, J. C., Caetano, D. S., & Pennell, M. W. (2015). Comparative Analysis of Principal Components Can be Misleading. *Syst Biol, 64*(4), 677-689.

Weir, J. T., & Mursleen, S. (2013). Diversity-dependent cladogenesis and trait evolution in the adaptive radiation of the auks (aves: alcidae). *Evolution, 67*(2), 403-416.

Wilman, H., Belmaker, J., Simpson, J., de la Rosa, C., Rivadeneira, M. M., & Jetz, W. (2014). EltonTraits 1.0: Species-level foraging attributes of the world's birds and mammals. *Ecological Archives, 95*(7), 2027-2027.

Zelditch, M. L., Swiderski, D. L., & Sheets, H. D. (2012). *Geometric Morphometrics for Biologists*. San Diego: Academic Press.

SUPPLEMENTARY MATERIAL

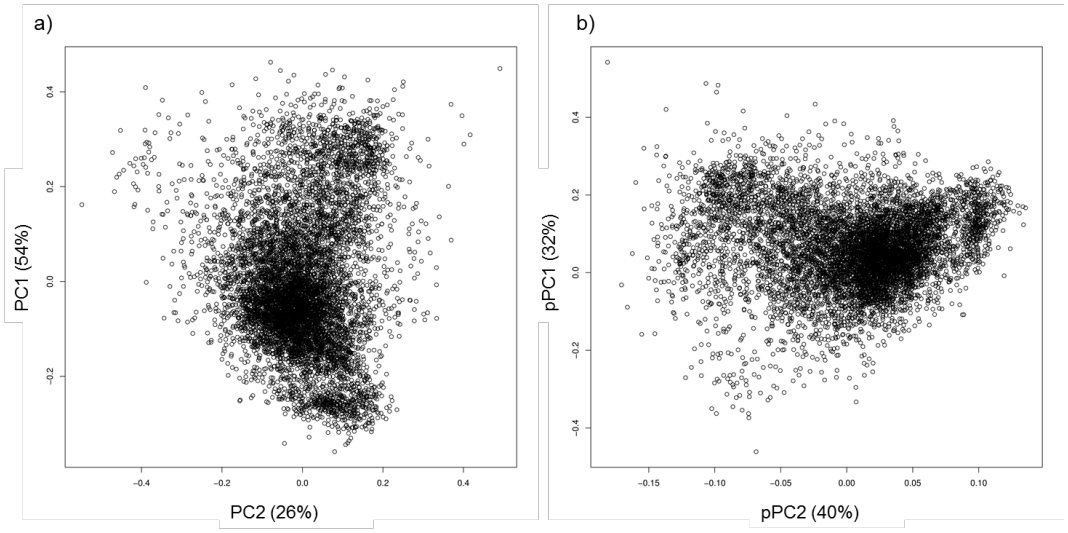

Figure S1. Avian morphospace shown as pairwise scatter plots of standard (a) and phylogenetic (b) PCs 1 and 2. The proportion of variation accounted for by each PC axis is indicated in brackets.

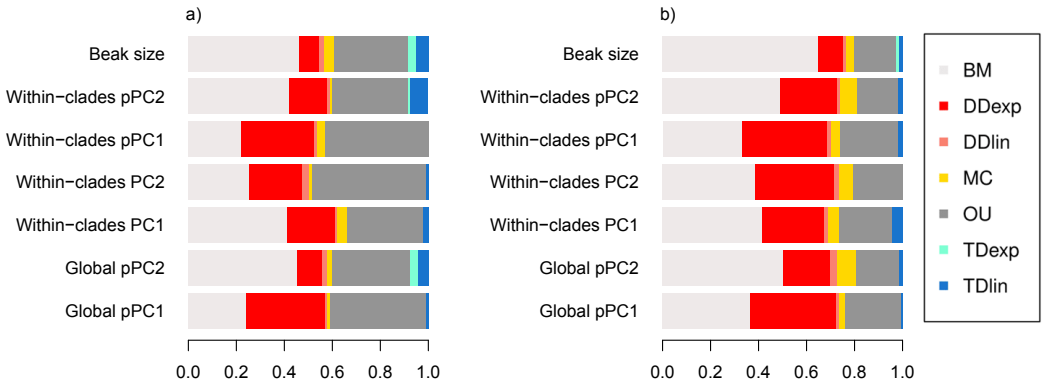

Figure S2. Model support (proportion of times each model is chosen as best i.e. smallest AICc values) across clades when modelling the evolution of various ecomorphological traits. The models considered are: Brownian motion (BM), linear (DDlin) and exponential (DDexp) diversity-dependent models, matching competition (MC), Ornstein-Uhlenbeck (OU), linear (TDlin) and exponential (TDexp) time-dependent models. Results across deep-time (a) and recent scales (b).

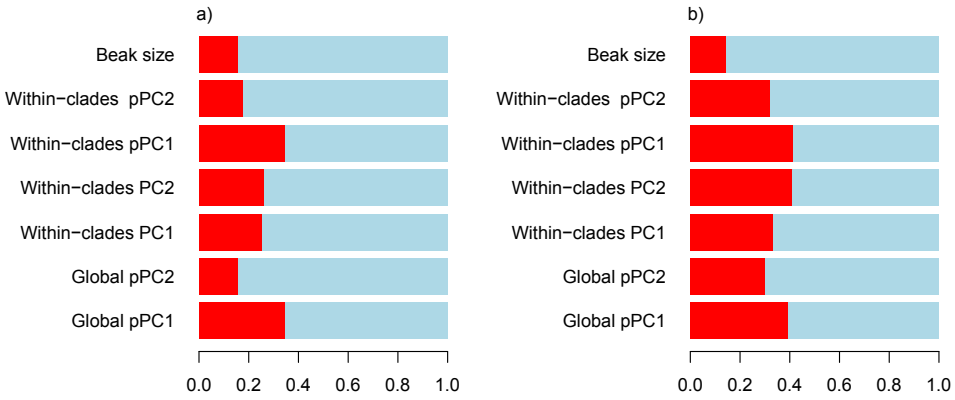

Figure S3. Frequency of clades in which the relative support for competition exceeds 50% (red) for varioecomorphological traits. The relative support of competition is based on AICw for process-based modelslinear and exponential diversity dependent models, as well as the matching competition model. We considered both deep-time (a) and recent (b) time scales.

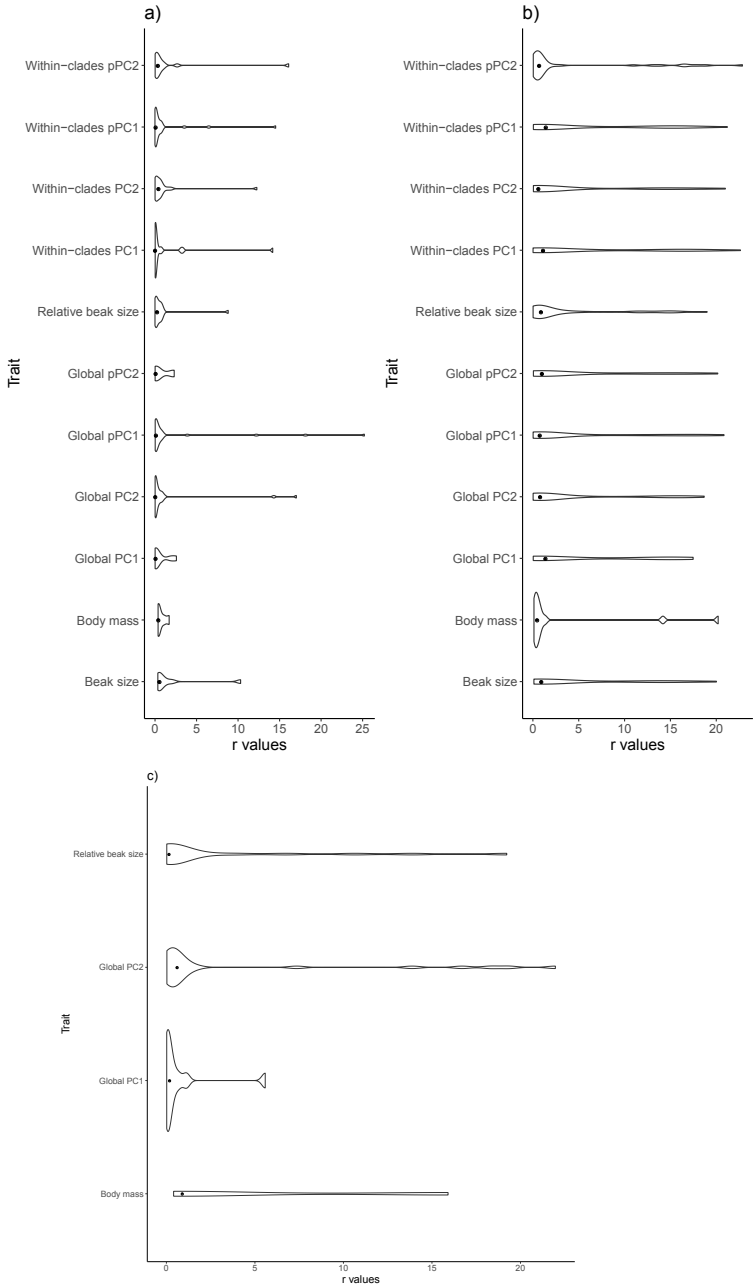

Figure S4. Rate parameter values for exponential diversity-dependent models, applied across deep-time scales (a) and recent radiations (b).

(c) Rate parameter values for exponential diversity-dependent models applied across genetic trees.

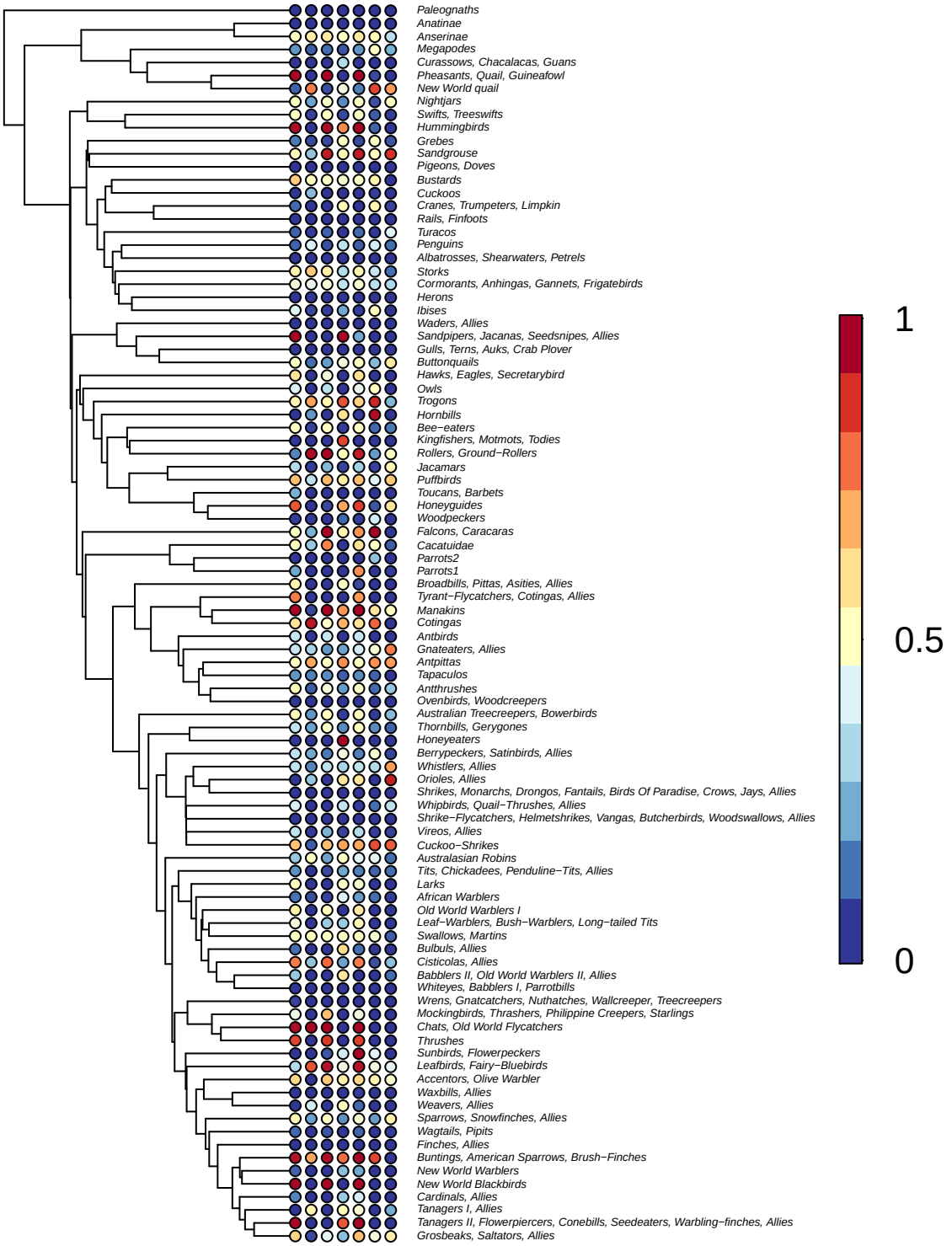

Figure S5. Relative support for competition based on AICw of process based models (diversity dependent and the matching competition model) across clades. The following ecomorphological traits are considered: beak shape (global pPC1, pPC2, within-clades PC1, PC2, pPC1, pPC2), as well as beak size. A list of clade names is provided at the end of the supplementary material.

Table S.1. Phylogenetic signal (D static) for the relative support for competition (a value of 1 is considered for relative support values bigger than 0.5) across various traits. D static values are compared to a Brownian expectation (i.e. evidence for phylogenetic signal) and a random expectation (i.e. no phylogenetic signal). D static values are reported for each trait separately, as well as for analyses scoring relative support across all traits (i.e. a value of 1 is considered for relative support values bigger than 0.5 in at least one of the four focal traits). Results across the "genetic" trees.

Trait	D estimate	Difference from 0 (Brownian expectation)	Difference from 1 (random expectation)	#Clades with support > 0.5 (out of 95)
Global PC1	2.041	0.000	0.987	11
Global PC2	0.845	0.051	0.304	30
Relative beak size	1.190	0.016	0.680	21
Body mass	1.248	0.099	0.647	6

List of clades (top to bottom) in Figure 4.3 and Figure S5.

Paleognaths, Paleognaths; Anserinae; Anatinae; Curassows, Chacalacas, Guans; Megapodes; New World quail; Pheasants, Quail, Guineafowl; Nightjars; Hummingbirds; Swifts, Treeswifts; Grebes; Pigeons, Doves; Sandgrouse; Cuckoos; Bustards; Rails, Finfoots; Cranes, Trumpeters, Limpkin; Turacos; Albatrosses, Shearwaters, Petrels; Penguins; Storks; Cormorants, Anhingas, Gannets, Frigatebirds; Ibises; Herons; Sandpipers, Jacanas, Seedsnipes, Allies; Waders, Allies; Buttonquails; Gulls, Terns, Auks, Crab Plover; Hawks, Eagles, Secretarybird; Owls; Trogons; Hornbills; Bee−eaters; Rollers, Ground−Rollers; Kingfishers, Motmots, Todies; Puffbirds; Jacamars; Toucans, Barbets; Woodpeckers; Honeyguides; Falcons, Caracaras; Parrots1; Parrots2; Cacatuidae; Broadbills, Pittas, Asities, Allies; Tyrant−Flycatchers, Cotingas, Allies; Manakins; Cotingas; Antbirds; Gnateaters, Allies; Antpittas; Tapaculos; Ovenbirds, Woodcreepers; Antthrushes; Australian Treecreepers, Bowerbirds; Honeyeaters; Thornbills, Gerygones; Berrypeckers, Satinbirds, Allies; Whistlers, Allies; Orioles, Allies; Shrikes, Monarchs, Drongos, Fantails, Birds Of Paradise, Crows, Jays, Allies; Shrike−Flycatchers, Helmetshrikes, Vangas, Butcherbirds, Woodswallows, Allies; Whipbirds, Quail−Thrushes, Allies; Vireos, Allies; Cuckoo−Shrikes; Australasian Robins; Tits, Chickadees, Penduline−Tits, Allies; African Warblers; Larks; Old World Warblers I; Leaf−Warblers, Bush−Warblers, Long−tailed Tits; Swallows, Martins; Bulbuls, Allies; Cisticolas, Allies; Whiteyes, Babblers I, Parrotbills; Babblers II, Old World Warblers II, Allies; Wrens, Gnatcatchers, Nuthatches, Wallcreeper, Treecreepers; Mockingbirds, Thrashers, Philippine Creepers, Starlings; Thrushes; Chats, Old World Flycatchers; Sunbirds, Flowerpeckers; Leafbirds, Fairy−Bluebirds; Accentors, Olive Warbler; Weavers, Allies; Waxbills, Allies; Sparrows, Snowfinches, Allies; Wagtails, Pipits; Finches, Allies; New World Warblers; Buntings, American Sparrows, Brush−Finches; New World Blackbirds; Cardinals, Allies; Tanagers I, Allies; Tanagers II, Flowerpiercers, Conebills, Seedeaters, Warbling−finches, Allies; Grosbeaks, Saltators, Allies.

CHAPTER 5

Correlates and consequences of resource competition in avian granivorous assemblages across the globe

ABSTRACT

Interspecific competition for shared resources represents a powerful force of evolution that has driven spectacular phenotypic diversification in several iconic, small-scale radiations. However, we lack evidence on what factors facilitate competition within assemblages, and further, on whether and how competition contributes to global patterns of phenotypic disparity. Here, we address these issues by applying phenomenological models of trait evolution in over 10,000 avian granivorous assemblages across the globe, to investigate patterns of trait divergence consistent with the presence of competitive selection pressures. We first map the signature of competition globally, and further investigate the association between a potential presence of competitive interactions and the evolution of ecomorphological traits (beak shape and size, and body mass). We find that abiotic factors do not correlate strongly with a high prevalence for competition signal, and that hotspots for competition signal are scattered in several areas globally, rather than following an obvious spatial pattern (e.g. latitudinal gradient). Further, we find that higher rates of trait evolution are associated with lower levels of competition signal. These results are consistent with the idea that the role of biotic interactions in driving trait divergence may be limited if rapid trait divergence in allopatry reduces the degree of ecological similarity among species upon secondary contact. Moreover, we find a positive correlation between strong competition signal and morphological disparity within assemblages. Thus, our results show that species

interactions can contribute to increased ecomorphological diversity in assemblages of avian granivores across the globe.

INTRODUCTION

Competition for shared resources represents a powerful selective force that influences species diversity and morphological disparity (Brown & Wilson, 1956; Schluter, 2000; Thompson, 1999; Voje et al., 2015). On Daphe Major island in the Galapagos, competition with *Geospiza magnirostris* drove a decrease in beak size in *G. fortis* populations between consecutive years (Grant & Grant, 2006). Similarly, the invasion and competition with *Anolis sagrei* on several islands in Florida drove an arboreal shift and the evolution of larger toepads in *A. carolinensis* species within 20 generations (Stuart et al., 2014). While these examples represent evidence that competition impacts the morphological differentiation between a few interacting species, it is less clear if and how competition shapes trait evolution in more complex species' assemblages and over broader geographical scales. We might expect particularly strong biotic interactions in environments with a more relaxed abiotic selective pressure (e.g. at lower latitudes, Dobzhansky, 1950), and hence competition may be important in explaining the latitudinal diversity gradient (i.e. the tendency of higher species richness at the equator; Mittelbach et al., 2007; Schemske et al., 2009, but see Rabosky et al., 2018). However, we lack empirical evidence on both the patterns of competition distribution across the globe, and on how competition links with geographical hotspots of morphological diversification. Therefore, the outstanding question of how and when competition for shared resources shapes global patterns of trait evolution and total disparity remains unanswered (Weber et al., 2017; Wiens, 2011).

In order to compete for shared resources species must overlap spatially. For groups speciating in allopatry, the potential for coexistence and thus competition is

dependent on the ability of species to come back to sympatry, and hence, on geographical barriers to secondary contact (e.g. topographical heterogeneity; Jetz et al., 2004), or the dispersal potential of species (Pigot & Tobias, 2014). Within assemblages, competition can be resolved via character displacement, as species evolve away from each other to exploit various resources (Dayan & Simberloff, 2005; Pfennig & Pfennig, 2009). Conversely, competition can also act as a filter to secondary contact when assemblages of species are formed, so that only species that are dissimilar in relevant traits can coexist (or species-sorting; Lovette & Hochachka, 2006; Pigot & Tobias, 2013). Therefore, rapid trait divergence in allopatry could facilitate the resolution of competition prior to secondary sympatry (Drury et al., 2018). Additionally, with more species present, the potential for competitive interactions increases. Therefore, factors that generally enable high levels of coexistence might also link with the prevalence of competition. One such factor is environmental productivity, which provides multiple niches for species to diversify into under selection pressure from competition (Pianka, 1966), reduces the potential of local extinction due to niche saturation (Wright, 1983), and thus promotes high levels of stable coexistence between similar species (Pigot et al., 2016).

The relative importance of biotic interactions as a selective force is also related to the abiotic environment (Dobzhansky, 1950). Specifically, when environmental selection pressures are high (e.g. in cold, highly seasonal or historically climatic-unstable environments), we expect patterns of convergence towards a limited set of adaptive optima or evolution towards generalized phenotypes (MacArthur, 1969; Pianka, 1966). Conversely, benign environments should allow for more flexibility in the way traits evolve, and therefore the potential for specialization and exploitation of various resources under competitive selection pressures is increased (e.g. Barnagaud et al., 2014; Bothwell et al., 2015). These ideas have also led to the

hypothesis that biotic interactions should follow a latitudinal gradient (Schemske et al., 2009). However, investigating the hypothesized links between environmental variables and the prevalence of competitive interactions requires large datasets, and unsurprisingly, empirical evidence on the generality and validity of these trends at a global scale is mostly lacking (Mittelbach et al., 2007; Schemske et al., 2009).

Competitive selective pressures act on the phenotype of species, and hence impact on morphological diversity. If competition is resolved via character displacement, we can expect higher levels of interspecific diversity in ecomorphological traits (or disparity) as species specialize on different resources and foraging techniques (Davies et al., 2007; Freeman, 2015). Conversely, competing species can exclude one another from assemblages, and thus minimize the total variability in phenotypes within assemblages (Connell, 1961; Elton, 1946). Tests for detecting a potential signal for competition include comparing disparity between closely related (sister) species living in sympatry versus allopatry, while controlling for potential confounding factors (e.g. time since divergence, Tobias et al., 2014), or calculating the phylogenetic overdispersion or clustering of species in assemblages (Barnagaud et al., 2014). Further, phenomenological models looking for patterns of trait divergence consistent with competition have been developed (e.g. Drury et al., 2016). These approaches are based on the assumption that similarity in traits used to acquire resources can lead to competitive interactions, and thus a signature of increased phenotypic differences between lineages in a clade or in a sympatric assemblage could be interpreted as a signature of interspecific competition. Therefore, the prevalence of competition is generally inferred indirectly based on the present distribution of species and traits in assemblages, and establishing the causality for the association between competition, trait and species diversity has so far been limited to study systems comprising of a pair or a small number of species (e.g. Grant & Grant, 2006).

Here, we apply a recent phylogenetic comparative method (the matching competition model, Drury et al., 2016) that incorporates the effect of species interactions while modelling phenotypic evolution, to understand the macroevolutionary correlates and consequences of resource competition in assemblages of avian granivores across the globe. We make use of a comprehensive dataset of beak morphology and body size for almost 90% of extant granivorous bird species sampled across over 10,000 grid cell assemblages. We contrast the fit of the matching competition model against alternative trait evolutionary models within grid cells to determine the likelihood that the present distribution of traits in assemblages was generated by processes akin to interspecific competition. We first show the geographical variation and prevalence for a signature of species interactions, and its impact in shaping ecomorphical disparity in avian assemblages at a global scale. We then link the prevalence and strength of competition with environmental variables, as well as with evolutionary rates. We expect a higher signal of competition in highly productive, less seasonal, and topographically homogenous environments (i.e. where the coexistence of many species is favoured). Additionally, we expect a signal of intense species interactions to be associated with rapid trait divergence via character displacement. Lastly, we test for the relationship between the signature of competition and morphological disparity (total variance of phenotypes) within assemblages of species.

MATERIALS AND METHODS

Morphological data

We collected beak shape and size data for granivorous avian species following the protocols described in detail in Cooney et al., 2017. A species was considered granivorous if its diet consists of 50% or more seed material, as recorded in EltonTraits database (Wilman et al., 2014). Study skins were obtained from the Natural History Museum (Tring) and from the Manchester Museum collections. We

took 3D scans of bird beaks using white and blue structured light scanning (*FlexScan3D*, LMI Technologies, Vancouver, Canada), and further processed the scans using landmark based geometric morphometric analysis (Adams et al., 2013). We placed a total of four landmarks (i.e. homologous key points) and 75 semi-landmarks on study surfaces. The landmarks define the tip of the upper beak and the posterior margins of: the midline profile, the left and the right tomial edges. The semi-landmarks join the landmarks to form the dorsal profile, left and right tomial edges. We used a crowdsourcing website (http://www.markmybird.org) to enable the landmarking process. Each beak was marked by at least three independent users (either experts or members of the public). Unsuitable landmarks were discarded following quality control of the data. We used the user-averaged landmark configurations to estimate species' beak size and shape via geometric morphometric analyses (R package Geomorph; Adams et al., 2017). We considered the centroid size (i.e. the square root of the sum of squared distances of a set of landmarks from their centroid; Zelditch et al., 2012) as a proxy for species' beak size. Our species sample includes granivorous species only, and so the chances for dramatic differences in beak shapes between species are reduced. Hence, the issues associated with the fact that very different beak shapes can have the same centroid size were minimized (Zelditch et al., 2012). In order to calculate beak shape, we performed a Generalized Procrustes Analysis on the landmark configurations that removes the effects of size, translational and rotational position (Zelditch et al., 2012), and further, extracted the main axes of shape variation using a PCA analysis. The first PC axis explained 71% of variation across granivorous species, largely showing changes from short, stout beaks to elongated ones (Figure S1). We used PC1 values in standard univariate models of trait evolution to investigate beak shape evolution within assemblages (see below). We used body mass data for each species from the EltonTraits database (Wilman et al., 2014). The data for centroid size and body mass were log-transformed. In total, we

collected data for 759 species, representing almost 90% of extant granivorous species (a complete list of species used in the analyses is given at the end of the supplementary material). The vast majority of these species (545 out of the total 759) belong to seven well-supported monophyletic clades (a mix of families and superfamilies): (i) weavers (*Ploceidae,* select *Passeridae*), (ii) buntings, American sparrows and brush-finches (select *Emberizidae*, select *Thraupidae*), (iii) tanagers, flowerpiercers, conebills, seedeaters and warbling-finches (select *Emberizidae*, select *Thraupidae*), (iv) finches (*Fringillidae*, select *Thraupidae*), (v) pigeons and doves (*Columbidae*), (vi) parrots (*Psittacidae*), and (vii) waxbills (*Viduidae*, *Estrildidae*).

Grid cell species pool

To evaluate the presence or absence of species in each grid cell, we used species' breeding ranges distribution maps (BirdLife International and Handbook of the Birds of the World (2016) Bird species distribution maps of the world. Version 6.0. Available at http://datazone.birdlife.org/species/requestdis). We split the world map into equal-area grid cells with the resolution of 110 km i.e. approximately 1° at the Equator (the coordinates of the map are longitude/latitude relative to the World Geodetic System 1984, or WGS84 datum). For each grid cell, we only recorded the presence of native species that are highly probable or known to occur (as scored in the range maps). We discarded grid cells for which we had trait data for less than 85% of occurring species, as well as grid cells with a species pool smaller than 10 species. The final number of grid cell assemblages was 10,698.

Phylogenetic data

We sampled 10,000 "full" trees (i.e. trees with all 9,993 species, including species for which there is no genetic data) from http://www.birdtree.org (Jetz et al., 2012). We pruned these trees to generate tree distributions for the 759 species in our

dataset, and further used TreeAnnotator (Drummond et al., 2012) to generate a consensus maximum clade credibility tree (setting node heights equal to "common ancestor" node heights). Out of 759 species, 508 represent taxa for which genetic data is available. Finally, we subsetted the consensus tree to build phylogenies for the species pool in each grid cell.

Environmental data

We extracted the following environmental variables for 110km equal-area grid cells: (i) temperature and precipitation seasonality (annual range in temperature and precipitation; Fick & Hijmans, 2017), (ii) NPP (net primary productivity i.e. mean annual energy available to heterotrophs, taken from Pigot et al., 2016), and (iv) elevational range (GTOPO30, USGS 1996, data available from the U.S. Geological Survey). To do this, we used the R package "raster" (Hijmans & van Etten, 2012) to overlap the environmental maps over the maps of 110km equal-area assemblages and extract the average environmental variables for each grid-cell. A more detailed description of data is given at the end of the supplementary material.

Estimating the signal of competition in grid cell assemblages

We used the matching competition model (Drury et al., 2016; Drury et al., 2017; Nuismer & Harmon, 2015, implemented in the R package RPANDA, Morlon et al., 2016) in order to estimate the signal for competition across grid cells. The matching competition method incorporates the effect of species interactions while modelling trait evolution, and can be used to test whether and to what extent the present trait distribution across a phylogeny has been influenced by species interactions. Under the matching competition model, trait divergence between competing lineages is modelled with the simplifying assumption that competitive interactions have similar outcomes across all members in the clade of interest. Each lineage thus evolves away from the mean clade trait value, and the model estimates the repelling force

as the strength of competitive interactions (S parameter, for which more negative values indicate increased competition strength). When the diverging effect of competitive interactions is 0, the model reduces to a random walk (i.e. BM model, Cavalli-Sforza & Edwards, 1967). In order to estimate whether there is evidence that competition between species has influenced the distribution of traits in each grid cell, we fitted the matching competition model alongside a suite of standard trait evolutionary models: Brownian motion (Cavalli-Sforza & Edwards, 1967), Ornstein–Uhlenbeck (Butler & King, 2004; Hansen & Martins, 1996), linear and exponential time-dependent models (Blomberg et al., 2003; Harmon et al., 2010; Weir & Mursleen, 2013), linear and exponential diversity-dependent models (Mahler et al., 2010; Weir & Mursleen, 2013). In each grid cell, we fitted the models to all the species present, and also to subsets of species belonging to the clades described above. We used AIC weights as evidence that competition has influenced the evolution of traits across occupant species (Burnham & Anderson, 2004). Where the matching competition model was the best-fitting model and had a ΔAICc $\geq$ 2 compared to the BM model, we considered the S parameter values as a measure for the strength of species interactions within grid cells. When traits evolve under a BM model, the matching competition model is mostly not favoured by model selection criteria, and moreover, the S parameter values usually take values around 0 (Drury et al., 2016). However, we take the more conservative approach and use the S values only when the matching competition model is sufficiently supported to minimize sources of uncertainty in the analyses.

Estimates of disparity in grid cell assemblages

Disparity within grid cells was estimated as the variance in target traits for species in assemblages. Species rich assemblages are expected to harbour higher morphological disparity. Hence we calculated estimates of standardized effect size of disparity (“sesDisparity”) i.e. how does the observed disparity in each grid cell

compare to the null expectation given that particular species richness (Swenson, 2014). For each species richness value across grid cells, we drew random species from the total seed eater species pool, and calculated disparity as the variance of trait values from the random draws. We repeated the procedure 1,000 times to get a distribution of null disparity values for each species richness value. We then calculated sesDisparity values for each grid cell following the formula: sesDisparity = [obsDisparity – mean(nullDisparity)]/ sd(nullDisparity), where obsDisparity is the variance in traits for species in the focal assemblage, and nullDisparity is the distribution of variances for the equal-richness, randomly drawn assemblages. Positive values indicate that assemblage disparity is greater than expected for that particular species richness, while negative values indicate disparity values lower than expected for the number of species.

Statistical analyses

We tested whether the impact of species interactions on trait evolution across grid cells is correlated with environmental variables and rates of trait evolution. To calculate evolutionary rates, we fitted the BM model to species within assemblages, and extracted the sigma parameter. We also accounted for the number of species in assemblages, as well as for the age of the most recent common ancestor for co-occurring species (as competition could be more prevalent in smaller, more recent radiations; Benton, 2009). We ran two sets of analyses, with the response variable set as (i) the degree of support for the matching competition model (AICw), and (ii) the strength of competition using the S parameter from the matching competition model. We then investigated the effect of competition on sesDisparity values in assemblages, alongside rates of trait evolution (using σ^2 calculated by applying the BM model to species within assemblages), and while accounting for assemblages' species-richness and age of the most recent common ancestor for co-occurring species. We ran these analyses twice. Firstly, competition was measured as a

binary trait (1 if the matching competition model was selected as best in the assemblage and was more than two units away from the AICc values for the BM model). Secondly, we measured competition strength using the S parameter values estimated by the matching competition model.

We used both linear models and simultaneous autoregressive models (SAR) to account for pseudo-replication in the data resultant from the likely similarity in predictors and response variables for neighbouring grid cells (Lagendre, 1993). We applied three SAR types (spatial error, lagged, and mixed), which differ in their assumption on whether the spatial autoregressive process occurs in the error term, response variable, or both in the explanatory and response variables (Kissling & Carl, 2007). To define neighbourhood affiliation for grid cells, we considered lag distances ranging from 50-500 km in 50 km increments, and also two extreme distances of 1,000 and 2,000 km, allowing neighbourhoods to extend largely within, but not across, continents. We used both binary and row standardization neighbourhood structures. The selection for the appropriate combination of SAR type, neighbourhood distance and structure was chosen based on three model selection criteria (Dormann et al., 2007; Kissling & Carl, 2007): (i) minimisation of spatial autocorrelation from the residuals, (ii) highest pseudo-R^2 (calculated as the squared Pearson correlation between observed and predicted values), and (iii) AIC. For analyses within individual clades, we only considered groups for which we had data for more than 50 grid cells (i.e. there were more than 50 assemblages in which there were at least 10 species from that particular clade). Statistical analyses were performed using the SPDEP package in R (Bivand, 2006). We logged values for species richness, rates of trait evolution, and age of the most recent common ancestor for co-occurring species, and squared the values for AICw and elevation ranges. We fitted the spatial autoregressive and linear models separately for beak size, beak shape, and body mass data.

RESULTS

Global distribution of competition signal

The matching competition model provided the best fit to the data (smallest AICc values) in 10% of grid cells for beak shape, 3% for beak size, and 14% for body mass (Figure S2a). When considering all traits together, we saw evidence of competition in 24% of assemblages (i.e. in 24% of assemblages, the matching competition model was the best fitted model in any of the three focal ecological traits). In general, the BM model was dominant in assemblages (79% best fit for beak shape, 75% for beak size, and 70% for body mass, Figure S2a). The matching competition model was the second most frequently favoured model for beak shape and body mass analyses (after the BM model), and the third for beak size analyses (after BM and the Ornstein–Uhlenbeck models). Most S parameter values fell within -0.08 and 0, showing variation in the strength of competition impact across grid cells. Under the current equation behind the matching competition model, rates of trait evolution get higher as species evolve further away from the average group phenotype, and hence high S values are not expected (Drury et al 2016). Hence, we removed outlier S values (one order of magnitude difference) from our spatial analyses (one grid removed for beak shape analyses and five for beak size analyses). When modelling trait evolution within clades, we found that, across all families, the matching competition model was preferred at a frequency of 4% for beak shape, 11% for beak size, and 8% for body mass (Figure S2b). Particular clades, however, showed high prevalence for a best fit from the matching competition model, especially for body mass and beak size e.g. finches, buntings, American sparrows and brush-finches, pigeons and doves, and parrots (Figure S2c).

The global distribution of elevated support for the matching competition model showed localized high support in a few key areas (Figure 5.1): (i) Northern Asia and (particularly northern) Australia for beak shape, (ii) small isolated areas in South America, West-Central Asia, and Indonesia for beak size, and (iii) sub-Saharan Africa, select areas across Central Asia, Arabian Peninsula and Indonesia for body mass. We found no support that these patterns are driven by the presence of particular clades, as there seemed to be no obvious link between the prevalence of competition signal in assemblages, and the presence of specific families (Figure S3). The distribution of S parameter values (i.e. the strength for the impact of species interactions on trait evolution) was also scattered globally (Figure S7), and thus our results do not show an obvious spatial pattern (e.g. latitudinal gradient) for the signal of competition across assemblages (Figure 5.1).

We performed spatial autoregressive and linear regressions for three different ecological traits: beak shape, size, and body mass. Generally, we found that using SAR models minimized spatial autocorrelation and improved model fit (higher pseudo R-squared and lower AIC values) compared to linear models (Tables 1-2, Tables S1-S2). SAR error and mixed type models, with row standardization neighbourhood structure, and neighbouring distances between 150 and 350 km, were generally favoured. Parameter estimates were largely similar for linear and spatial models. However, several correlations were significant only when analysed in a non-spatial framework, confirming that not accounting for spatial autocorrelation can inflate type 1 errors (Lennon, 2000, Dormann, 2007).

Correlates of competition signal in assemblages

The support for the matching competition model (AICw) was negatively correlated with species richness and evolutionary rates of beak shape and body mass evolution (Figure S4a, Table S1). Conversely, when modelling beak size evolution,

we saw a positive relationship between rates and support for competition. Further, the AICw for the matching competition model correlated negatively with the age of the most recent common ancestor of co-occurring species when considering beak size and body mass evolution, but the reverse was true when modelling beak shape. Lastly, we saw higher support for the matching competition model in more productive and less seasonal environments (temperature) when modelling beak size, and also a higher support for the matching competition model in topographically heterogeneous environments in the models of beak size and body mass evolution (Figure S4, Table S1). The effect sizes of the relationship between environmental predictors and support for competition were, however, very small. Overall, although we saw several significant relationships between candidate factors and matching competition model support, the significance of relationships observed was likely driven by the high number of data points (over 10,000 grid cell assemblages of species). When restricting the models to species from the same clade, we also found several significant relationships between our candidate factors and the support for the matching competition model, but there was moderate consensus for the strength and direction of correlations across clades and traits (Table S3). However, in general, the support for the matching competition model correlated negatively with species richness, age of the most recent common ancestor of co-occurring species, and elevational range, and positively with temperature seasonality.

We found a stronger signal of competition (more negative S parameter values) in assemblages with fewer species, lower rates of evolution, and smaller values for the age of the most recent common ancestor of co-occurring species (Table 5.1, Figure 5.2). These results were consistent across all three morphological traits considered. In addition, we found a stronger signal for competition in grid cell with higher levels of temperature seasonality when modelling beak shape.

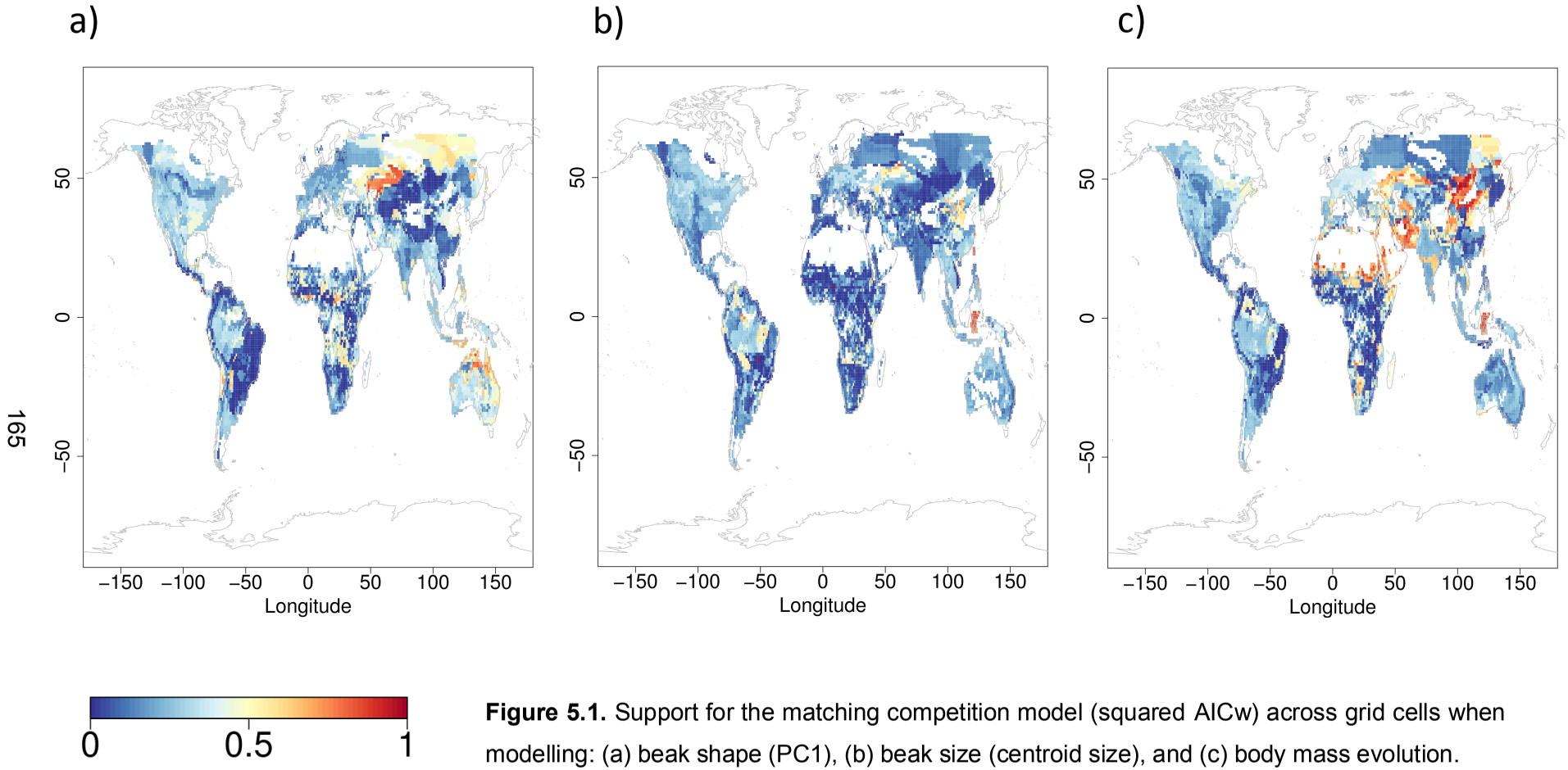

Figure 5.1. Support for the matching competition model (squared AICw) across grid cells when modelling: (a) beak shape (PC1), (b) beak size (centroid size), and (c) body mass evolution.

Also, we saw a stronger signature of competition in less productive, topographically homogenous environments, and with high temperature seasonality in models of beak size evolution (Table 5.1, Figure S5). However, the effect sizes for environmental predictors were very small. The effect of predictors is generally in agreement between multi- and single-predictor SAR models, although some predictors lost significance in the multipredictor model (as also noted in Mittelbach et al., 2007). Further, the support for the matching competition model (AICw) and the strength of competition signal (S values) were not higher in assemblages where the percentage of species with genetic data was lower (Figure S8). We did not test for correlations between candidate factors and S values for individual clades, because, per clade, there were insufficient (<50) grid cells where the matching competition model was chosen as best by model selection criteria.

The relationship between competition signal and morphological disparity in assemblages

The distribution of standardized effect size disparity (sesDisparity) levels within assemblages varied across the globe for beak shape, size, and body mass (Figure 5.3). We found a positive effect of rates of trait evolution and age of the most recent ancestor of co-occurring species on sesDisparity. We also saw higher sesDisparity values in assemblages where the matching competition model was selected as best (and sufficiently distinct from the BM model), and, in agreement, S values were negatively correlated with morphological sesDisparity. Lastly, sesDisparity levels were negatively correlated with species richness in assemblages. These results were consistent across models for the three traits considered (Table 5.2, Table S2, Figure 5.4, Figure S6), and when performing analyses for individual clades within assemblages (Table S4). The rate of evolution, strength of competition signal, and species richness had the same effect in both multi- and single-predictor models. However, when using S values as a predictor, the age of the most recent ancestor

of co-occurring species as not significantly correlated with sesDisparity in single-predictor models (Table 5.2).

DISCUSSION

Here, we investigate the links between a signature of competition and the evolution of ecomorphological traits in granivorous assemblages across the globe. The distribution for the evidence of competition does not follow an obvious spatial pattern (e.g. latitudinal gradient, Figure 5.1), and generally, we do not find strong and consistent links between environmental variables and the strength of competition signal. However, after controlling for assemblage species richness and age of the most recent common ancestor of co-occurring species, we find that the strength of competition in assemblages correlates negatively with trait evolutionary rates, contrary to the prediction of faster trait divergence in ecomorphological traits under competition. We suggest that our results support the hypothesis that fast trait divergence in allopatry reduces the potential for competition upon secondary contact within assemblages (Drury et al., 2018; McEntee et al., 2018; Pigot & Tobias, 2013). Further, despite the negative link between the signature of competitive interactions and rates of evolution, we find that competition signal correlates positively with morphological disparity (total variance) within assemblages, providing support for the hypothesized link between ecological selection pressures and patterns of trait disparity. We found that a BM model of evolution dominated in assemblages, and in comparison, all the other models of evolution fit the data in small proportions (Figure S2). Thus, when analysing each trait individually, we found little evidence for modes of evolution alternative to a random walk in granivorous assemblages. The matching competition model was, however, chosen often compared to other models of evolution apart from the BM model; moreover, it provided the best fit for the data in almost a quarter of assemblages when looking across all traits. Diversity-dependent models too imply

that trait evolution is influenced by the accumulation of species (Weir & Mursleen, 2013), but these were also not chosen in great proportions across assemblages (Figure S2). Here, we considered sympatric species that belong to the same feeding guild, however, species might also partition resources by differentiating in time of feeding, foraging strata etc. (e.g. MacArthur, 1958), and so, we likely underestimated the signal for competition in assemblages. Alternatively, the prevalence of competition as the dominant driver of ecomorphological evolution over a random walk process might not be globally ubiquitous across granivores (Drury et al., 2018), or its effects might only persist over very short time-scales (Benton, 2009). Further, we found that the signature for competition for shared resources in avian granivorous assemblages (AICw of the matching competition model) is scattered in several locations across the globe, which differ depending on the trait of interest (Figure 5.1). As a generality, we found higher signals for competition in Eurasian assemblages (also sub-Saharan Africa for body mass, Northern Australia for beak shape). However, these patterns are likely a consequence of a high presence of avian granivorous assemblages in Eurasia, rather than a difference in the prevalence of competition signal between continents. When we applied evolutionary models to subsets of species (belonging to the same family) within assemblages, we saw high levels of competition signal in particular clades (Figure S2c), indicating that high levels of relatedness in assemblages can link with a strong signature for competition, but the effect is not universal across groups. A pattern of trait divergence consistent with the presence of competition between related taxa was more prevalent in body mass and beak size rather than beak shape (Figure S2c), in agreement with studies showing that size-related traits represent key axes of beak differentiation within clades (Bright et al., 2016). We did not find evidence, however, that the presence of specific families drives the observed spatial distribution of competition signal in assemblages (Figure S3).

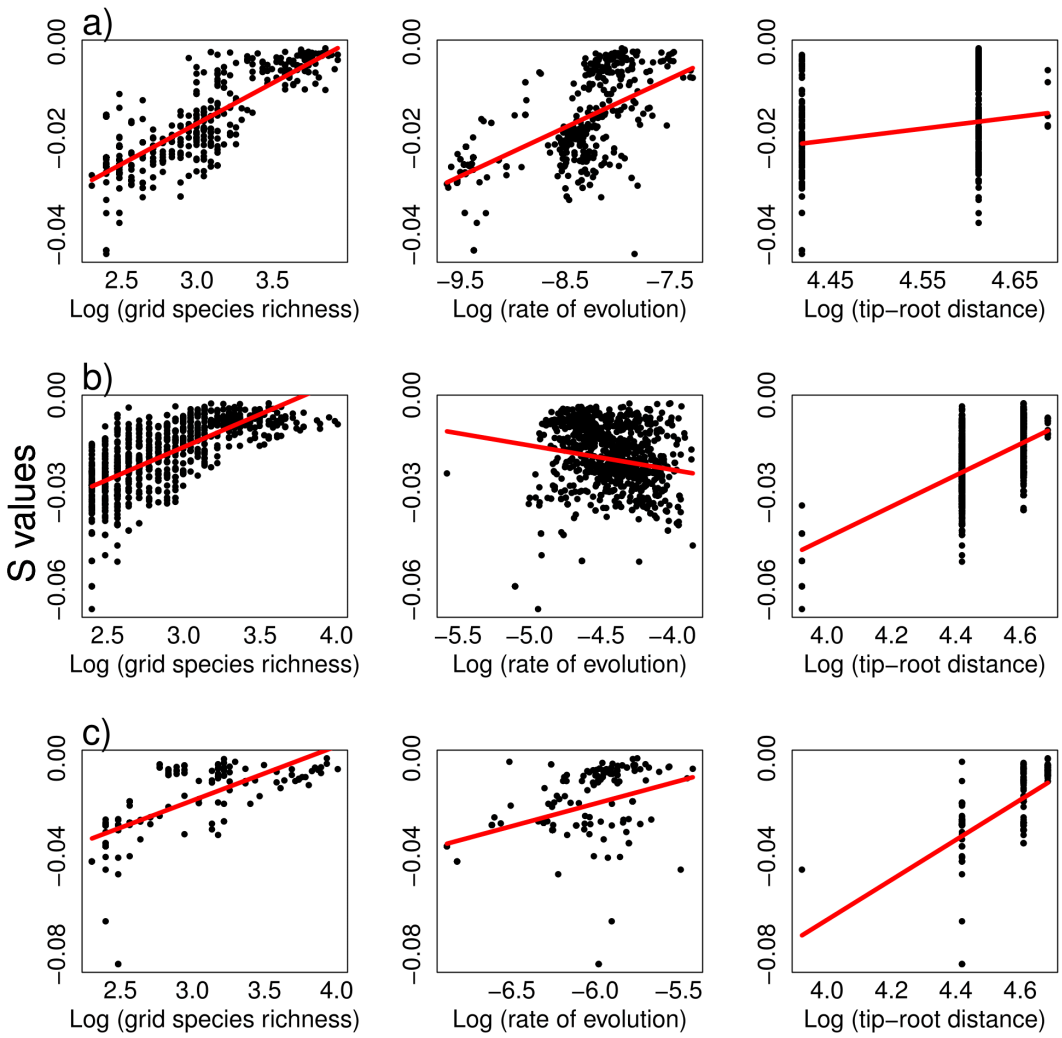

Figure 5.2. Correlations between candidate factors and the strength of competition when modelling (a) beak shape (PC1), (b) body mass, and (c) beak size (centroid size) evolution. S values are considered only in grids where the MC model has smallest AIC values and the AICc difference from the BM model > 2. All relationships are significant in a multipredictor SAR. Lines indicate significant slopes. The age of the most recent common ancestor in assemblages is referred to as “tip-root distance” i.e. the distance from root to tips for species in assemblages.

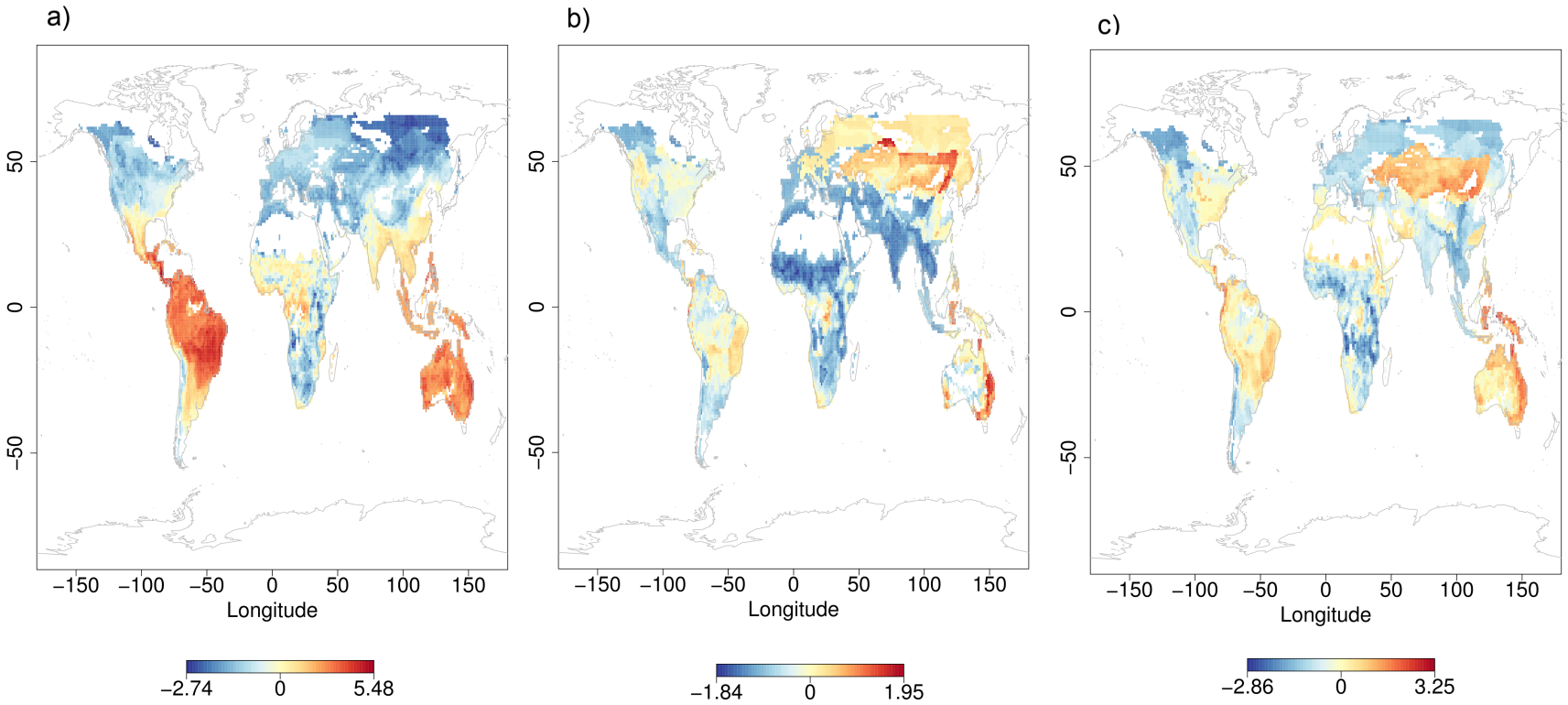

Figure 5.3. Standardized effect size (SES) disparity levels within assemblages (morphological disparity is calculated as the variance in trait values). Traits considered: (a) beak shape (PC1), (b) beak size (centroid size), and (c) body mass evolution.

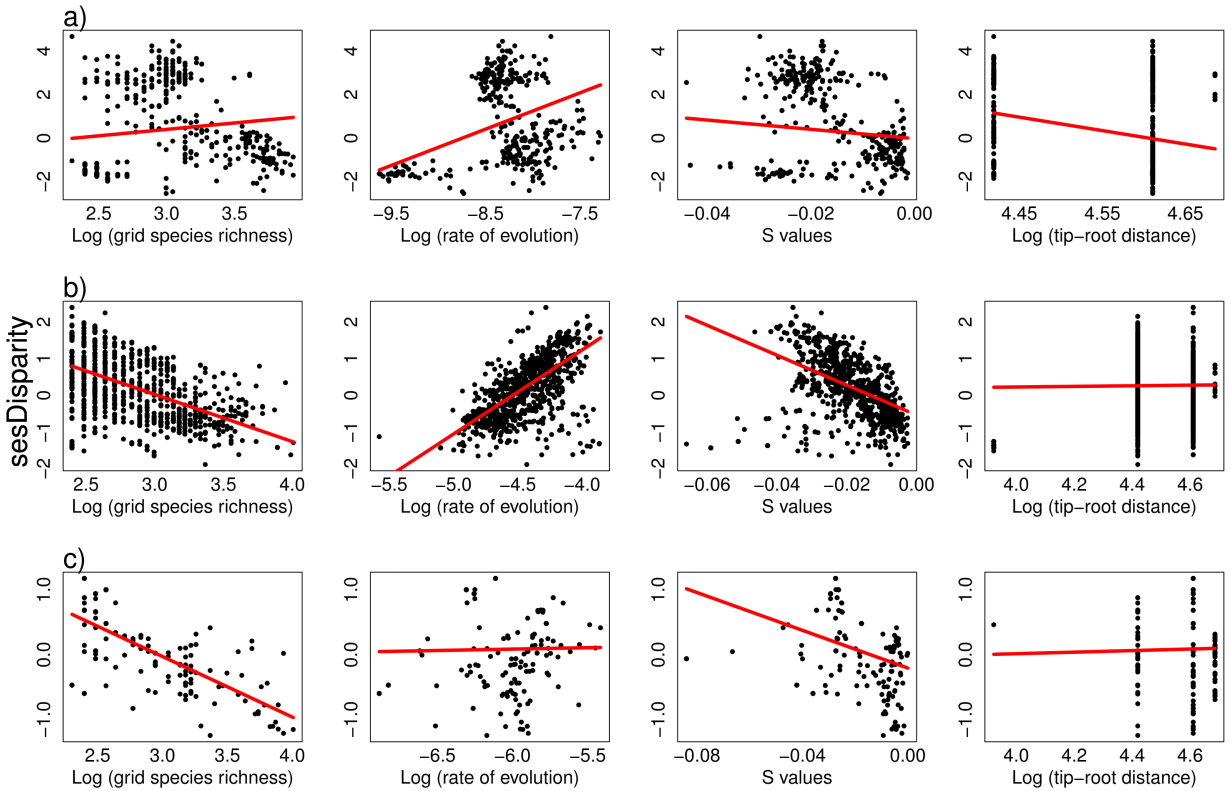

Figure 5.4. Correlations between candidate factors and assemblages' sesDisparity, when considering (a) beak shape (PC1), (b) body mass, and (c) beak size (centroid size) evolution. S values are considered only in grids where the MC model has smallest AIC values and the AICc difference from the BM model > 2. All relationships are significant in a multipredictor SAR. Lines indicate significant slopes. The age of the most recent common ancestor in assemblages is referred to as "tip-root distance" i.e. the distance from root to tips for species in assemblages.

Table 5.1. The relationship between S values (i.e. strength of the signal for competition) and candidate predictors across assemblages. Details on model selection criteria is given in Appendix 1.

Predictor	SAR slope	SAR *p*	OLS slope	OLS *p*
(a) beak shape (PC1)				
Log SR	0.011	**0.000**	0.014	**0.000**
Log BM rate	0.009	**0.000**	0.007	**0.000**
Mean NPP	0.000	0.963	0.000	0.817
Temperature seasonality	0.000	**0.000**	0.000	**0.000**
Precipitation seasonality	0.000	0.269	0.000	0.709
Sqrt (elevation range)	0.000	0.342	0.000	**0.000**
Log (age MRCA)	0.017	**0.000**	0.017	**0.000**
(b) beak size				
Predictor	SAR slope	SAR *p*	OLS slope	OLS *p*
Log SR	0.011	**0.000**	0.019	**0.000**
Log BM rate	0.004	**0.030**	0.002	0.538
Mean NPP	0.000	**0.015**	0.000	0.928
Temperature seasonality	0.000	**0.001**	0.000	0.589
Precipitation seasonality	0.000	0.245	0.000	0.289
Sqrt (elevation range)	0.000	**0.004**	0.000	**0.000**
Log (age MRCA)	0.016	**0.001**	0.049	**0.000**
(c) body mass				
Predictor	SAR slope	SAR *p*	OLS slope	OLS *p*
Log SR	0.011	**0.000**	0.014	**0.000**
Log BM rate	0.005	**0.000**	-0.001	0.284
Mean NPP	0.000	0.548	0.000	**0.000**
Temperature seasonality	0.000	0.633	0.000	**0.000**
Precipitation seasonality	0.000	0.868	0.000	**0.006**
Sqrt (elevation range)	0.000	0.443	0.000	**0.000**
Log (age MRCA)	0.018	**0.000**	0.035	**0.000**

Table 5.2. The relationship between sesDisparity and candidate predictors across assemblages. The slope and p-values (significant in bold) for each predictor are reported. Traits considered: (a) beak shape (PC1). Details on model selection criteria is given in Appendix 1.

Predictor	SAR slope	SAR *p*	OLS slope	OLS *p*
(a) beak shape (PC1)				
Log SR	-0.839	**0.000**	1.040	0.000
Log BM rate	0.415	**0.000**	3.260	0.000
S values	-24.324	**0.000**	-205.926	0.000
Log (age MRCA)	1.203	**0.000**	2.341	0.003
(b) beak size				
Predictor	SAR slope	SAR *p*	OLS slope	OLS *p*
Log SR	-0.447	**0.000**	-1.226	0.000
Log BM rate	0.755	**0.000**	0.538	0.000
S values	-24.121	**0.000**	-2.593	0.486
Log (age MRCA)	1.375	**0.000**	2.269	0.000
(c) body mass				
Predictor	SAR slope	SAR *p*	OLS slope	OLS *p*
Log SR	-0.367	**0.000**	-0.161	0.065
Log BM rate	1.102	**0.000**	0.985	0.000
S values	-15.011	**0.000**	-23.048	0.000
Log (age MRCA)	0.838	**0.000**	1.223	0.000

Furthermore, we found that variation in the signature for competition in assemblages (the AICw for the matching competition model) is hard to predict. The relationships between predictor and response variables were not consistent across the traits considered, and moreover, the effect sizes of these relationships were small. Within families, there was moderate consensus over how the support for the competition model correlated with candidate factors. In general, we found a signature for competition in more seasonal and more homogenous environments, as well as in assemblages with less species and smaller values for the age of the most recent common ancestor of co-occurring species. We further studied variation in the strength of competition signal (S parameter values) in relation to candidate factors. First, we saw a stronger signal of competition for beak size in environments with high temperature seasonality and low productivity. Temperature seasonality also related positively with competition signal for body mass and beak shape in single-predictor models, but the relationship lost significance (or reversed trend for

beak shape) in the multi-predictor model. Therefore, we did not find support for the hypothesis that a signal for biotic interactions is more prevalent in environments with reduced abiotic selection pressures (Dobzhansky, 1950) or with more potential for niche specialization (in line with findings in Gainsbury & Meiri, 2017). Conversely, our results might indicate that faster rates of coming back into sympatry seen at higher latitudes with seasonal and less productive environments facilitate stronger signatures for competition (Martin et al., 2010; Weir & Price, 2011). We also found a lower signal for competition in beak size in topographically heterogenous environments, in agreement with the expectation that geographical barriers to dispersal reduce the potential for secondary contact, and hence the potential for species interactions signatures. The effect sizes of these relationships were, however, very small. Thus overall, although our results bring some support for the ability of environmental variables to determine the prevalence and strength of competition signal, we do not find that abiotic factors have a strong role in predicting global patterns of species-interactions signal.

Secondly, we found that faster trait divergence is negatively associated with the strength of competition signal. Competition can impact negatively on trait evolution if niche space is bounded, and so with the accumulation of species, the available niche space for evolution decreases (Simpson, 1953). However, our results more likely reflect an interaction between the mode of speciation, rates of evolution, and the potential for competitive interactions. Specifically, birds are thought to speciate primarily in allopatry, and generally experience a protracted delay until coming back to sympatry (Phillimore et al., 2008; Pigot & Tobias, 2013). If trait diversification is fast, closely related species will be morphologically (and thus ecologically) dissimilar when their ranges eventually overlap, and subsequent competition and its associated signature of trait character displacement will be minimized. Therefore, our results support the notion that when allopatric speciation is the norm, faster trait

divergence reduces the potential for competition because it increases dissimilarity between species upon secondary contact (Drury et al., 2018). However, interpreting patterns of trait divergence consistent with competitive interactions is difficult. As mentioned, a lot of phenotypic variability in birds assemblages actually accumulates in allopatry rather than sympatry (Phillimore et al., 2008). Hence, alternative processes related to divergence in allopatry followed by community filtering, could also be responsible for the current patterns in phenotypic distribution within assemblages. These hypotheses are difficult to disentangle without determining the history of sympatry-allopatry dynamics in assemblages.

Additionally, we accounted for assemblage species richness and age of the most recent common ancestor for co-occurring species. We saw a stronger signal for competition in smaller assemblages, as well as assemblages with small values for the age of the most recent common ancestor of co-occurring species. We saw similar trends when using the AICw as a response variable in the analyses within individual clades. These results support the idea that a signature for competition is mostly detectable across recent, small scale radiations, but its signal is lost over longer time scales (Losos & Ricklefs, 2009). Moreover, exclusion or extinction of the lesser competitors within assemblages could also create a negative link between the strength of competition and species richness (Connell, 1961; Lovette & Hochachka, 2006). However, several caveats limit the biological interpretation of these results. Uncertainty in S values estimates increases with decreasing species-pool size (Drury et al., 2016), and hence by chance more negative values can appear in species-poor assemblages. Moreover, a high prevalence of short branches throughout the trees can be expected in assemblages with small values for the age of the most recent common ancestor for co-occurring species, which inflates measurement error estimates (Rabosky, 2015). An inflated variance in trait values caused by error could create a false impression of morphological

overdispersion via character displacement, and thus exaggerate the effect of competition in assemblages.

When testing the link between competition signal and levels of morphological disparity in assemblages we found that, as expected, disparity links positively with trait evolutionary rates, and also with the age of the most recent common ancestor for co-occurring species (as, in time, more variance is allowed to accumulate). Further, sesDisparity levels correlated negatively with species richness, potentially indicating that after accounting for the expected increase in disparity with species richness, the accumulation of more species in assemblages is redundant with respect to disparity levels. We found that the presence (binary variable) and strength (S values) of a signature for competition correlated positively with disparity levels, despite the negative association of competition signal with evolutionary rates and the age of the most recent common ancestor of co-occurring species. Therefore, our results show that a link between a competition signature and global levels of disparity can be observed, however, the detectability of such associations is likely moderated by the negative feedback between competition signal and stronger predictors of disparity (like evolutionary rates). We encountered similar patterns in our family-level analyses (Table S4). Further, the observed relationships were consistent across all the traits we consider, expected given that beak shape, beak size and body mass are all ecomorphological traits, predicted to diverge via character displacement under competitive selection pressures (Bothwell et al., 2015; Davies et al., 2007; Grant & Grant, 2006).

Lastly, we acknowledge the limitation of using univariate models, hence for a complex trait like the beak shape for example, we miss the potential impact of competitive selection pressures on biologically important variation unexplained by PC1. Moreover, using only one PC axis of variation can impact on model selection

criteria (Uyeda et al., 2015). Using phylogenetic PCA (Polly et al., 2013; Revell, 2009) has been proposed to reduce this issue, however, recent studies have reported that, when the model used to calculate phylogenetic axes of variation is misspecified, the method suffers from the same biases as standard PCA (Uyeda et al., 2015). An infallible solution to this problem is so far lacking. Also, in our dataset, PC1 represents the transition from stout and wide to elongated beaks, an axis of ecomorphological separation between species generally linked to resource acquisition. Hence the issues associated with PC1 being a biased subset of the whole PC axes distribution should be reduced (Uyeda et al., 2015). We do not find a stronger signal of competition (AICw and S parameter values from the matching competition model) in assemblages with lower percentages of species with genetic data (Figure S8). These results indicate that error caused by uncertainty in phylogenetic relationships between species in assemblages due to lack of genetic data is not likely to cause biased preference for a signal of competition. Nevertheless, we cannot rule out the possibility that the patterns of trait divergence consistent with competition can also be overemphasised as a result of various forms of measurement and phylogenetic error.

Here, we take a comprehensive approach in describing the correlates and consequences of potential signatures of competition for shared resources in avian granivorous assemblages across the globe. We use phenomenological models of trait evolution that look for patterns of trait divergence consistent with the presence of ecological selection pressures to determine the distribution of competition signal in avian assemblages. We find moderate support for the role of abiotic factors in predicting competition signal, and when significant, the prevalence of competition signal is associated with less productive and more seasonal environments (in opposition with the hypothesis of stronger biotic selection pressures at lower latitudes). However, our analyses are restricted to seed-eater assemblages, and the

incorporation of other dietary guilds might reveal different spatial patterns. Furthermore, after accounting for the effect of species richness and the age of the most recent common ancestor of co-occurring species (both negative effects), we see that rates of evolution link negatively with the strength of competition signature. Hence, our findings indicate that species diverging fast in allopatry can minimize competition upon secondary contact. However, the evolutionary dynamics of sympatry and allopatry between interacting lineages is difficult to determine from present-date data, and hence alternative processes related to phenotypic differentiation in allopatry and/or subsequent filtering could also produce similar distribution of present phenotypes. Further, we find that competition signal links with increased morphological disparity in assemblages, and thus our results show that species interactions could contribute to shaping global patterns of morphological disparity. However, the strength of competition as a selection force and our ability to detect its signal is limited by negative feedbacks with the tempo of evolution.

REFERENCES

Adams, D. C., Collyer, M. L., Kaliontzopoulou, A., & Sherratt, E. (2017). Geomorph: Software for geometric morphometric analyses. R package version 3.0.5. https://cran.r-project.org/package=geomorph.

Adams, D. C., Rohlf, F. J., & Slice, D. E. (2013). A field comes of age: geometric morphometrics in the 21st century. *Hystrix, the Italiam Journal of Mammalogy, 24*(1), 7-14.

Barnagaud, J. Y., Daniel Kissling, W., Sandel, B., Eiserhardt, W. L., Sekercioglu, C. H., Enquist, B. J., . . . Svenning, J. C. (2014). Ecological traits influence the phylogenetic structure of bird species co-occurrences worldwide. *Ecol Lett, 17*(7), 811-820.

Benton, M. J. (2009). The Red Queen and the Court Jester: species diversity and the role of biotic and abiotic factors through time. *Science, 323*(5915), 728-732.

Bivand, R. (2006). Implementing Spatial Data Analysis Software Tools in R. *Geographical Analysis, 38*(23-40).

Blomberg, S. P., Garland, T., & Ives, A. R. (2003). Testing for phylogenetic signal in comparative data: behavioral traits are more labile. *Evolution, 57*(4), 717-745.

Bothwell, E., Montgomerie, R., Lougheed, S. C., & Martin, P. R. (2015). Closely related species of birds differ more in body size when their ranges overlap--in warm, but not cool, climates. *Evolution, 69*(7), 1701-1712.

Bright, J. A., Marugán-Lobón, J., Cobb, S. N., & Rayfield, E. J. (2016). The shapes of bird beaks are highly controlled by nondietary factors. *PNAS, 113*(19), 5352-5357.

Brown, W. L., & Wilson, E. O. (1956). Character displacement. *Syst. Zool., 5*(2), 49-64.

Burnham, K. P., & Anderson, D. R. (2004). Multimodel Inference. *Sociological Methods & Research, 33*(2), 261-304.

Butler, M. A., & King, A. A. (2004). Phylogenetic Comparative Analysis: A Modeling Approach for Adaptive Evolution. *American Naturalist, 164*(6), 683-695.

Cavalli-Sforza, L. L., & Edwards, A. W. F. (1967). Phylogenetic analysis. Models and estimation procedures. *American Journal of Human Genetics, 19*(3), 233-257.

Connell, J. H. (1961). The Influence of Interspecific Competition and Other Factors on the Distribution of the Barnacle Chthamalus Stellatus. *Ecology, 42*(4), 710-723.

Cooney, C. R., Bright, J. A., Capp, E. J. R., Chira, A. M., Hughes, E. C., Moody, C. J. A., . . . Thomas, G. H. (2017). Mega-evolutionary dynamics of the adaptive radiation of birds. *Nature, 542*(7641), 344-347.

Davies, T. J., Meiri, S., Barraclough, T. G., & Gittleman, J. L. (2007). Species co-existence and character divergence across carnivores. *Ecol Lett, 10*(2), 146-152.

Dayan, T., & Simberloff, D. (2005). Ecological and community-wide character displacement: the next generation. *Ecology Letters, 8*(8), 875-894.

Dobzhansky, T. (1950). Evolution in the tropics. *Am. Sci., 38*(2), 209-221.

Dormann, C. F. (2007). Effects of incorporating spatial autocorrelation into the analysis of species distribution data. *Global Ecology and Biogeography, 16*(2), 129-138.

Dormann, F. C., M. McPherson, J., B. Araújo, M., Bivand, R., Bolliger, J., Carl, G., . . . Wilson, R. (2007). Methods to account for spatial autocorrelation in the analysis of species distributional data: a review. *Ecography, 30*(5), 609-628.

Drummond, A. J., Suchard, M. A., Xie, D., & Rambaut, A. (2012). Bayesian phylogenetics with BEAUti and the BEAST 1.7. *Mol Biol Evol, 29*(8), 1969-1973.

Drury, J., Clavel, J., Manceau, M., & Morlon, H. (2016). Estimating the Effect of Competition on Trait Evolution Using Maximum Likelihood Inference. *Syst Biol, 65*(4), 700-710.

Drury, J. P., Grether, G. F., Garland, T., & Morlon, H. (2017). An Assessment of Phylogenetic Tools for Analyzing the Interplay Between Interspecific Interactions and Phenotypic Evolution. *Syst Biol, 67*(3), 413-427.

Drury, J. P., Tobias, J. A., Burns, K. J., Mason, N. A., Shultz, A. J., & Morlon, H. (2018). Contrasting impacts of competition on ecological and social trait evolution in songbirds. *PLoS Biol, 16*(1), e2003563.

Elton, C. (1946). Competition and the Structure of Ecological Communities. *Journal of Animal Ecology, 15*(1), 54-68.

Fick, S. E., & Hijmans, R. J. (2017). WorldClim 2: new 1-km spatial resolution climate surfaces for global land areas. *International Journal of Climatology, 37*(12), 4302-4315.

Freeman, B. G. (2015). Competitive Interactions upon Secondary Contact Drive Elevational Divergence in Tropical Birds. *Am Nat, 186*(4), 470-479.

Gainsbury, A., & Meiri, S. (2017). The latitudinal diversity gradient and interspecific competition: no global relationship between lizard dietary niche breadth and species richness. *Global Ecology and Biogeography, 26*(5), 563-572.

Grant, B. R., & Grant, P. R. (2006). Evolution of Character Displacement in Darwin's Finches. *Science, 313*(5784), 224-226.

Hansen, T. F., & Martins, E. P. (1996). Translating between microevolutionary process and macroevolutionary patterns: the correlation structure of interspecific data. *Evolution, 50*(4), 1404-1417.

Harmon, L. J., Losos, J. B., Jonathan Davies, T., Gillespie, R. G., Gittleman, J. L., Bryan Jennings, W., . . . Mooers, A. O. (2010). Early bursts of body size and shape evolution are rare in comparative data. *Evolution, 64*(8), 2385-2396.

Hijmans, R. J., & van Etten, J. (2012). raster: Geographic analysis and modeling with raster data. R package version 2.0-12.

Jetz, W., Rahbek, C., & Colwell, R. K. (2004). The coincidence of rarity and richness and the potential signature of history in centres of endemism. *Ecology Letters, 7*(12), 1180-1191.

Jetz, W., Thomas, G. H., Joy, J. B., Hartmann, K., & Mooers, A. O. (2012). The global diversity of birds in space and time. *Nature, 491*(7424), 444-448.

Kissling, W. D., & Carl, G. (2007). Spatial autocorrelation and the selection of simultaneous autoregressive models. *Global Ecology and Biogeography, 17*(1), 59-71.

Lagendre, P. (1993). Spatial autocorrelation: trouble or new paradigm? *Ecology, 74*, 1659–1673.

Lennon, J. J. (2000). Red-shifts and red herrings in geographical ecology. *Ecography, 23*(1), 101-113.

Losos, J. B., & Ricklefs, R. E. (2009). Adaptation and diversification on islands. *Nature, 457*(7231), 830-836.

Lovette, I. J., & Hochachka, W. M. (2006). Simultaneous effects of phylogenetic niche conservatism and competition on avian community structure. *Ecology, 87*(sp7), S14-S28.

MacArthur, R. H. (1958). Population Ecology of Some Warblers of Northeastern Coniferous Forests. *Ecology, 39*(4), 599-619.

MacArthur, R. H. (1969). Patterns of communities in the tropics. *Biological Journal of the Linnean Society, 1*(1-2), 19-30.

Mahler, D. L., Revell, L. J., Glor, R. E., & Losos, J. B. (2010). Ecological opportunity and the rate of morphological evolution in the diversification of Greater Antillean anoles. *Evolution, 64*(9), 2731-2745.

Martin, P. R., Montgomerie, R., & Lougheed, S. C. (2010). Rapid sympatry explains greater color pattern divergence in high latitude birds. *Evolution, 64*(2), 336-347.

McEntee, J. P., Tobias, J. A., Sheard, C., & Burleigh, J. G. (2018). Tempo and timing of ecological trait divergence in bird speciation. *Nat Ecol Evol, 2*(7), 1120-1127.

Mittelbach, G. G., Schemske, D. W., Cornell, H. V., Allen, A. P., Brown, J. M., Bush, M. B., . . . Turelli, M. (2007). Evolution and the latitudinal diversity gradient: speciation, extinction and biogeography. *Ecol Lett, 10*(4), 315-331.

Morlon, H., Lewitus, E., Condamine, F. L., Manceau, M., Clavel, J., & Drury, J. (2016). RPANDA: an R package for macroevolutionary analyses on phylogenetic trees. *Methods in Ecology and Evolution*.

Nuismer, S. L., & Harmon, L. J. (2015). Predicting rates of interspecific interaction from phylogenetic trees. *Ecol Lett, 18*(1), 17-27.

Pfennig, K. S., & Pfennig, D. W. (2009). Character Displacement: Ecological And Reproductive Responses To A Common Evolutionary Problem. *The Quarterly Review of Biology, 84*(3), 253-276.

Phillimore, A. B., Orme, C. D., Thomas, G. H., Blackburn, T. M., Bennett, P. M., Gaston, K. J., & Owens, I. P. (2008). Sympatric speciation in birds is rare: insights from range data and simulations. *Am Nat, 171*(5), 646-657.

Pianka, E. R. (1966). Latitudinal gradients in species diversity: a review of concepts. *The American Naturalist, 100*(910), 33-46.

Pigot, A. L., & Tobias, J. A. (2013). Species interactions constrain geographic range expansion over evolutionary time. *Ecol Lett, 16*(3), 330-338.

Pigot, A. L., & Tobias, J. A. (2014). Dispersal and the transition to sympatry in vertebrates. *Proceedings of the Royal Society B: Biological Sciences, 282*(1799), 20141929.

Pigot, A. L., Tobias, J. A., & Jetz, W. (2016). Energetic Constraints on Species Coexistence in Birds. *PLoS Biol, 14*(3), e1002407.

Polly, P. D., Lawing, A. M., Fabre, A. C., & Goswami, A. (2013). Phylogenetic Principal Components Analysis and Geometric Morphometrics. *Italian Journal of Mammology, 24*(1), 33-41.

Rabosky, D. L. (2015). No substitute for real data: A cautionary note on the use of phylogenies from birth-death polytomy resolvers for downstream comparative analyses. *Evolution, 69*(12), 3207-3216.

Rabosky, D. L., Chang, J., Title, P. O., Cowman, P. F., Sallan, L., Friedman, M., . . . Alfaro, M. E. (2018). An inverse latitudinal gradient in speciation rate for marine fishes. *Nature, 559*(7714), 392-395.

Revell, L. J. (2009). Size-correction and principal components for interspecific comparative studies. *Evolution, 63*(12), 3258-3268.

Schemske, D. W., Mittelbach, G. G., Cornell, H. V., Sobel, J. M., & Roy, K. (2009). Is There a Latitudinal Gradient in the Importance of Biotic Interactions? *Annual Review of Ecology, Evolution, and Systematics, 40*(1), 245-269.

Schluter, D. (2000). Ecological Character Displacement in Adaptive Radiation. *Am Nat, 156*(S4), S4-S16.

Simpson, G. G. (1953). *The major features of evolution.*: Columbia University Press.

Stuart, Y. E., Campell, T. S., Hohenlohe, P. A., Reynolds, R. G., Revell, L. J., & Losos, J. B. (2014). Rapid evolution of a native species following invasion by a congener. *Science, 346*(6208), 463-466.

Swenson, N. (2014). *Functional and Phylogenetic Ecology in R*. New York: Springer Science & Business Media.

Thompson, J. N. (1999). The Evolution of Species Interactions. *Science, 284*(5423), 2116-2118.

Tobias, J. A., Cornwallis, C. K., Derryberry, E. P., Claramunt, S., Brumfield, R. T., & Seddon, N. (2014). Species coexistence and the dynamics of phenotypic evolution in adaptive radiation. *Nature, 506*(7488), 359-363.

Uyeda, J. C., Caetano, D. S., & Pennell, M. W. (2015). Comparative Analysis of Principal Components Can be Misleading. *Syst Biol, 64*(4), 677-689.

Voje, K. L., Holen, O. H., Liow, L. H., & Stenseth, N. C. (2015). The role of biotic forces in driving macroevolution: beyond the Red Queen. *Proc Biol Sci, 282*(1808), 20150186.

Weber, M. G., Wagner, C. E., Best, R. J., Harmon, L. J., & Matthews, B. (2017). Evolution in a Community Context: On Integrating Ecological Interactions and Macroevolution. *Trends Ecol Evol, 32*(4), 291-304.

Weir, J. T., & Mursleen, S. (2013). Diversity-dependent cladogenesis and trait evolution in the adaptive radiation of the auks (aves: alcidae). *Evolution, 67*(2), 403-416.

Weir, J. T., & Price, T. D. (2011). Limits to speciation inferred from times to secondary sympatry and ages of hybridizing species along a latitudinal gradient. *Am Nat, 177*(4), 462-469.

Wiens, J. J. (2011). The niche, biogeography and species interactions. *Philos Trans R Soc Lond B Biol Sci, 366*(1576), 2336-2350.

Wilman, H., Belmaker, J., Simpson, J., de la Rosa, C., Rivadeneira, M. M., & Jetz, W. (2014). EltonTraits 1.0: Species-level foraging attributes of the world's birds and mammals. *Ecological Archives, 95*(7), 2027-2027.

Wright, D. H. (1983). Species-Energy Theory: An Extension of Species-Area Theory. *Oikos, 41*(3), 496–506.

Zelditch, M. L., Swiderski, D. L., & Sheets, H. D. (2012). *Geometric Morphometrics for Biologists (Second Edition)*. San Diego: Academic Press.

SUPPLEMENTARY MATERIAL

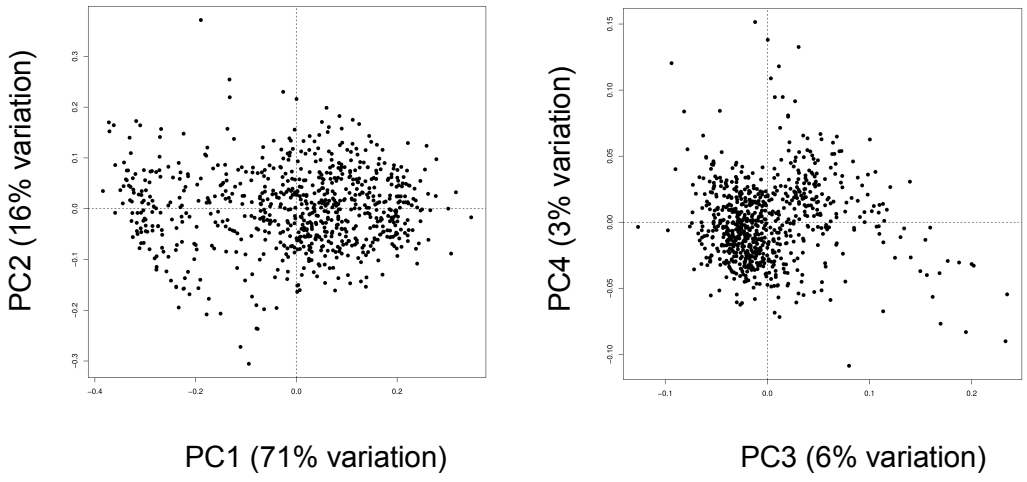

Figure S1. Avian granivorous morphospace shown as pairwise scatter plots of the PCs 1 and 2, and PCs 3 and 4. The proportion of variation accounted for by each PC axis is indicated in brackets.

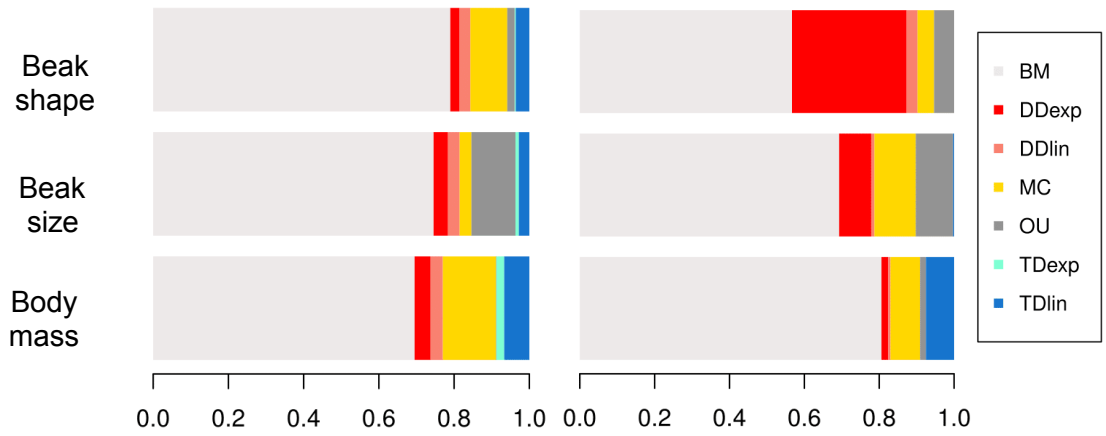

Figure S2. (a) Model support (proportion of times each model is chosen as best i.e. smallest AICc values) across assemblages when modelling beak shape, beak size, and body mass evolution. (b) Model support (proportion of times each model is chosen as best i.e. smallest AICc values) across individual clades within assemblages when modelling beak shape, beak size, and body mass evolution. The models considered are: Brownian motion (BM), linear (DDlin) and exponential (DDexp) diversity-dependent models, matching competition (MC), Ornstein-Uhlenbeck (OU), linear (TDlin) and exponential (TDexp) time-dependent models.

List of clades in figure S2c (next page) (top to bottom): (1) weavers, allies, (2) waxbills, allies, (3) tanagers, flowerpiercers, conebills, seedeaters, warbling-finches, allies, (4) parrots, (5) finches, allies, (6) pigeons, doves, (7) buntings, American sparrows, brush-finches.

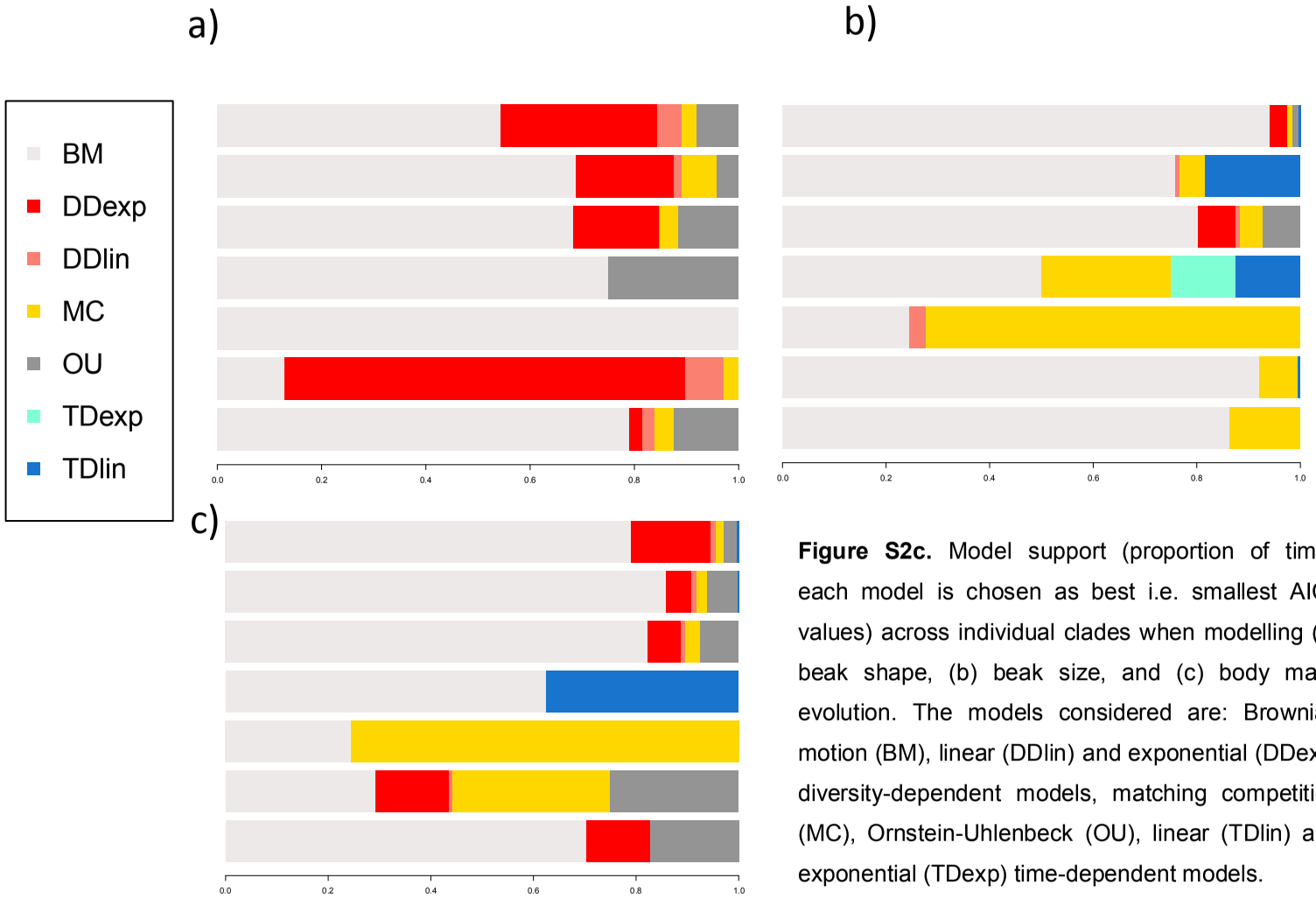

Figure S2c. Model support (proportion of times each model is chosen as best i.e. smallest AICc values) across individual clades when modelling (a) beak shape, (b) beak size, and (c) body mass evolution. The models considered are: Brownian motion (BM), linear (DDlin) and exponential (DDexp) diversity-dependent models, matching competition (MC), Ornstein-Uhlenbeck (OU), linear (TDlin) and exponential (TDexp) time-dependent models.

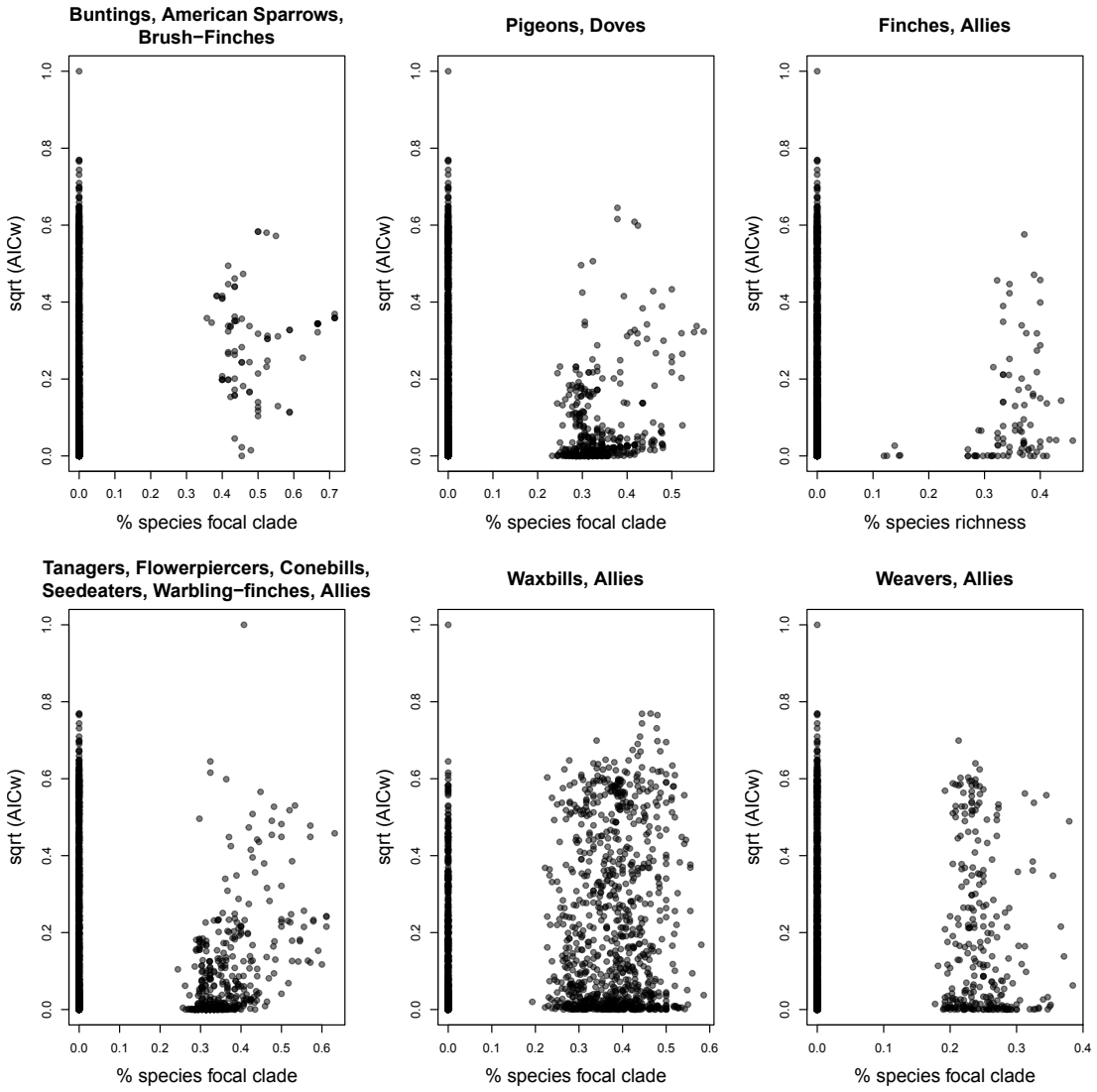

Figure S3a. Relationship between the support for the MC model (on beak shape) and the proportion of species in particular clades within assemblages.

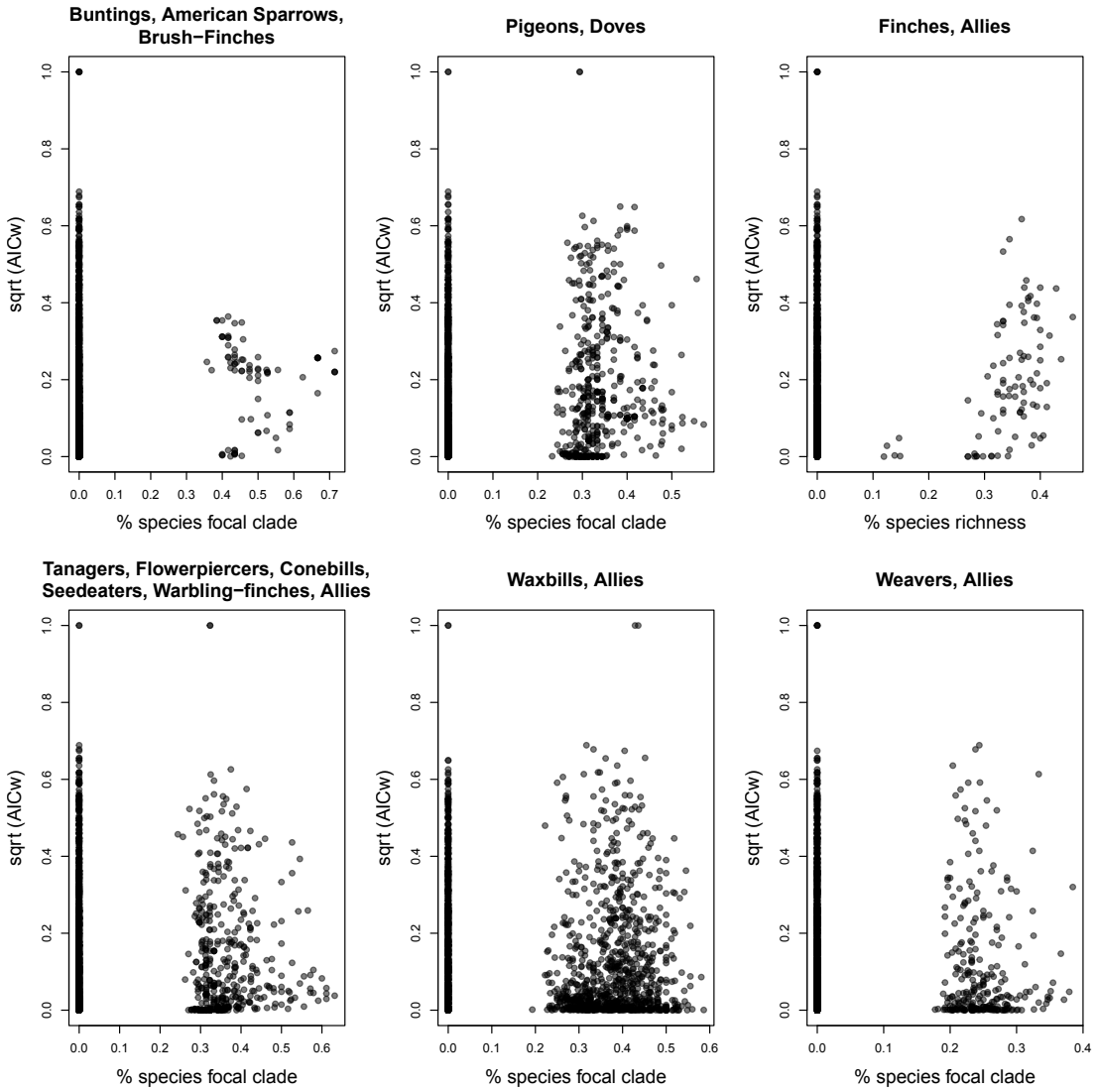

Figure S3b. Relationship between the support for the MC model (on beak size) and the proportion of species in particular clades within assemblages.

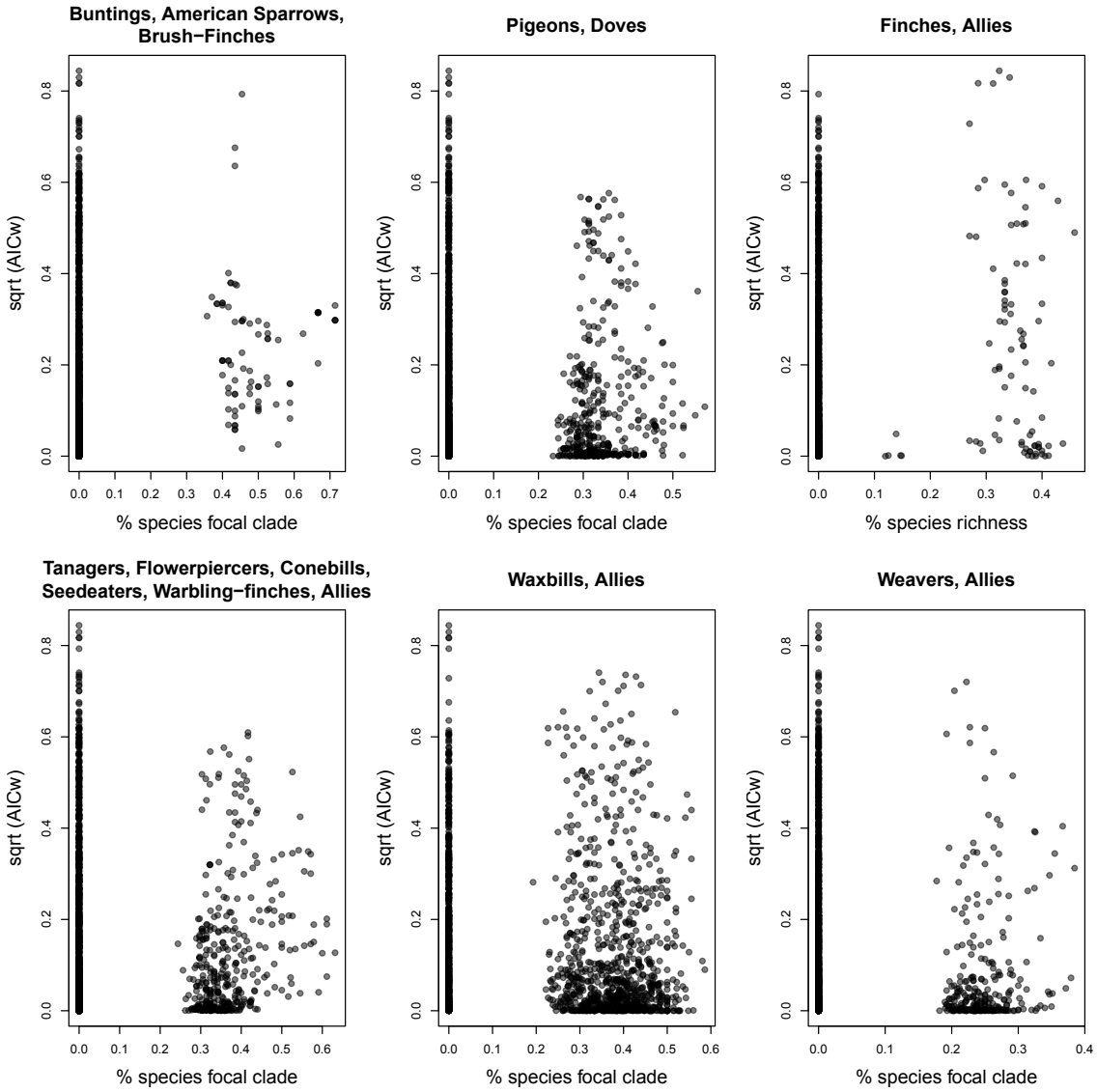

Figure S3c. Relationship between the support for the MC model (on body mass) and the proportion of species in particular clades within assemblages.

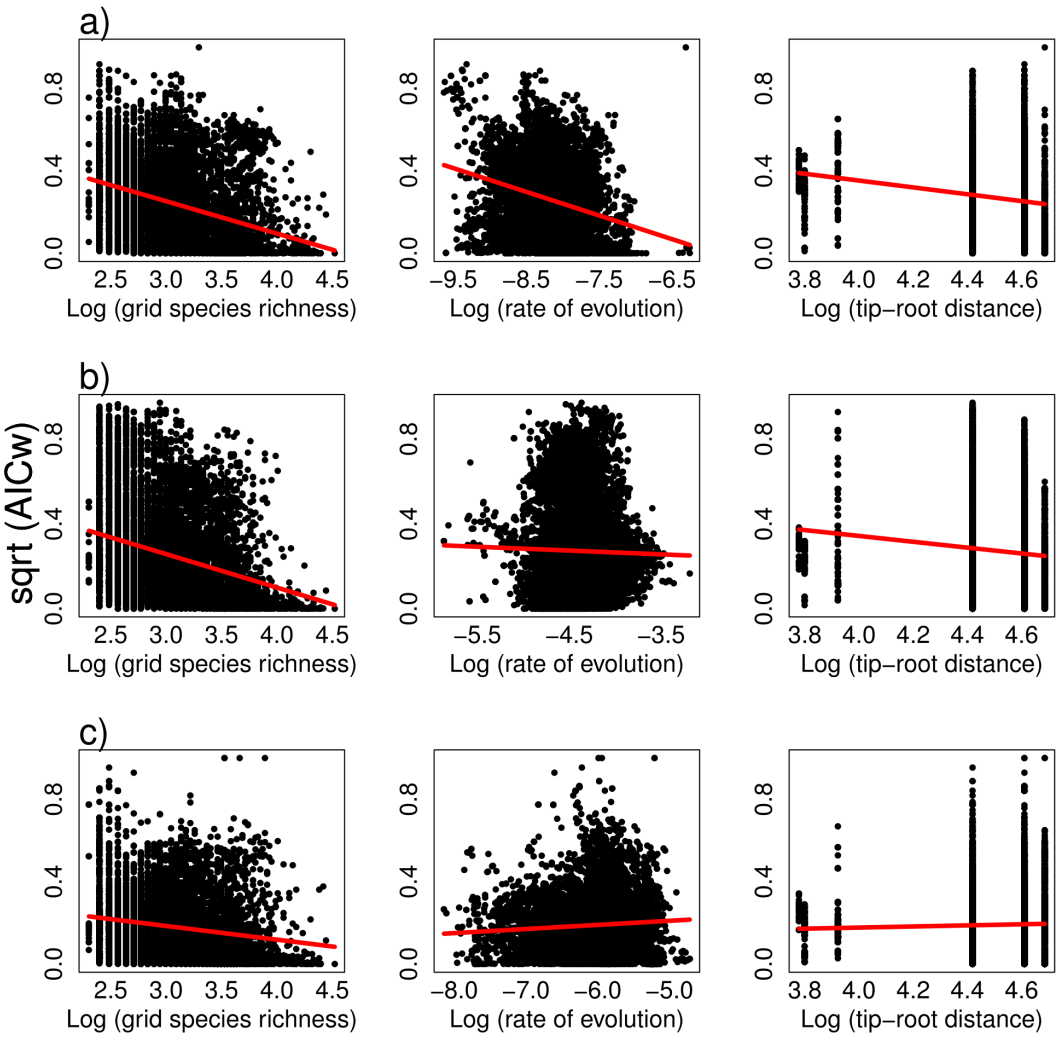

Figure S4a. Correlations between candidate factors and the support for competition (MC AICw) when modelling (a) beak shape (PC1), (b) body mass, and (c) beak size (centroid size) evolution. Lines indicate significant slopes. The age of the most recent common ancestor in assemblages is referred to as "tip-root distance" i.e. the distance from root to tips for species in assemblages.

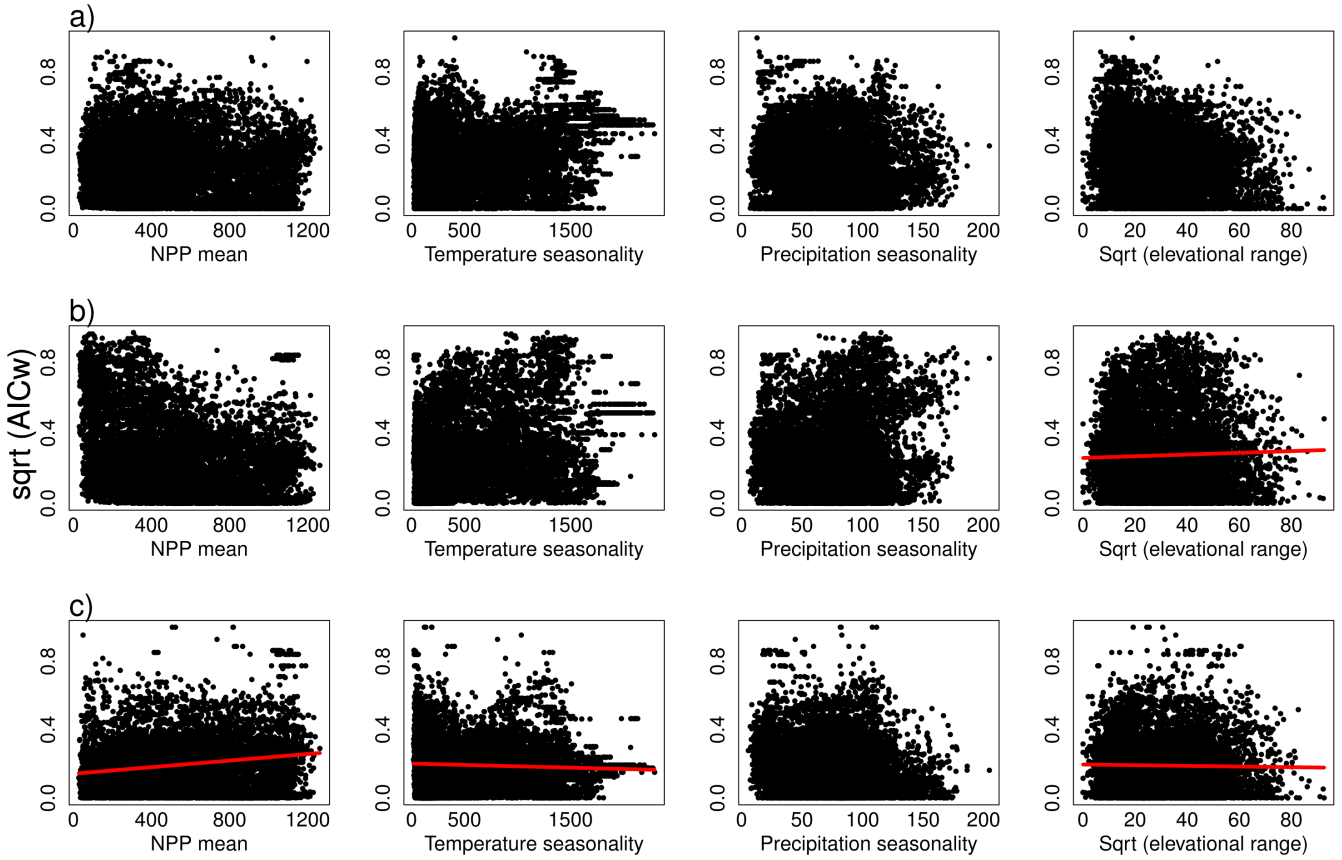

Figure S4b. Correlations between environmental factors and the support for competition (MC AICw) when modelling (a) beak shape (PC1), (b) body mass, and (c) beak size (centroid size) evolution. Where drawn, relationships are significant in a multipredictor SAR. Lines indicate significant slopes. The age of the most recent common ancestor in assemblages is referred to as “tip-root distance” i.e. the distance from root to tips for species in assemblages.

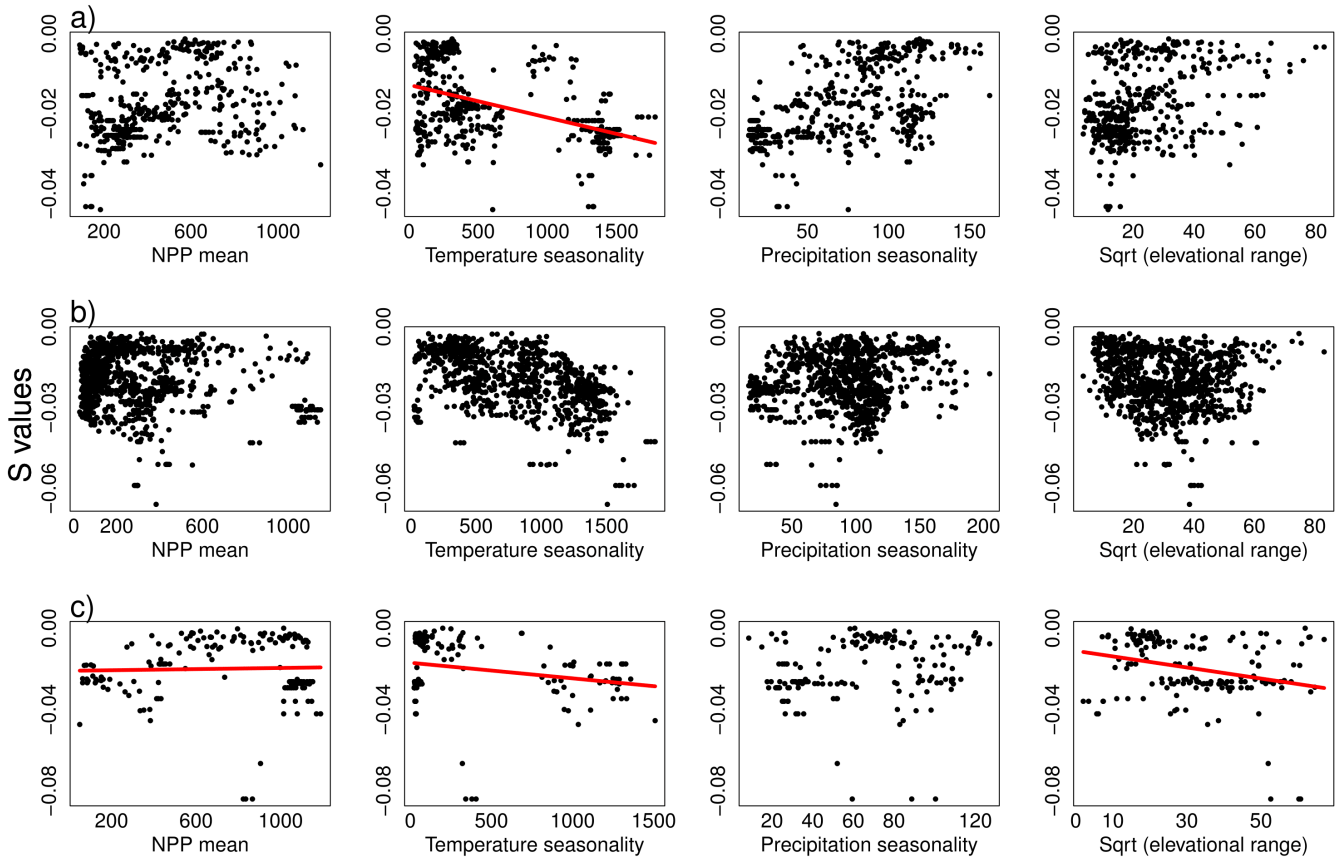

Figure S5. Correlations between environmental factors and the strength of competition when modelling (a) beak shape (PC1), (b) body mass, and (c) beak size (centroid size) evolution. S values are considered only in grids where the MC model has smallest AIC values and the AICc difference from the BM model > 2. Where drawn, relationships are significant in a multipredictor SAR. Lines indicate significant slopes. The age of the most recent common ancestor in assemblages is referred to as “tip-root distance” i.e. the distance from root to tips for species in assemblages.

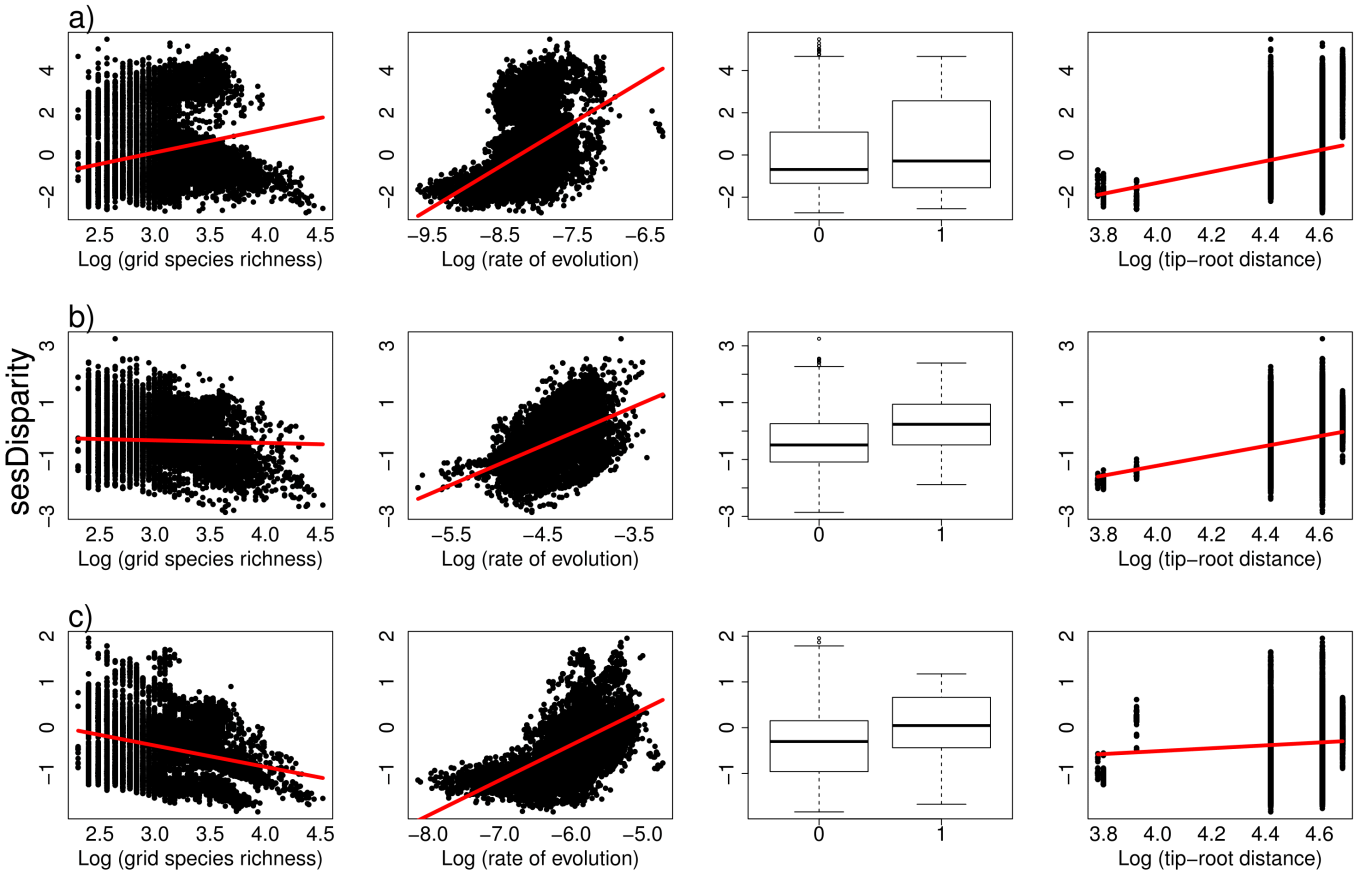

Figure S6. Correlations between candidate factors and community sesDisparity, when considering (a) beak shape (PC1), (b) body mass, and (c) beak size (centroid size) evolution. Smaller AIC values for the MC model and an AICc difference from the BM model > 2 are considered as evidence for biotic interactions in assemblages. All relationships are significant in a multipredictor SAR. Lines indicate significant slopes. The age of the most recent common ancestor in assemblages is referred to as “tip-root distance” i.e. the distance from root to tips for species in assemblages.

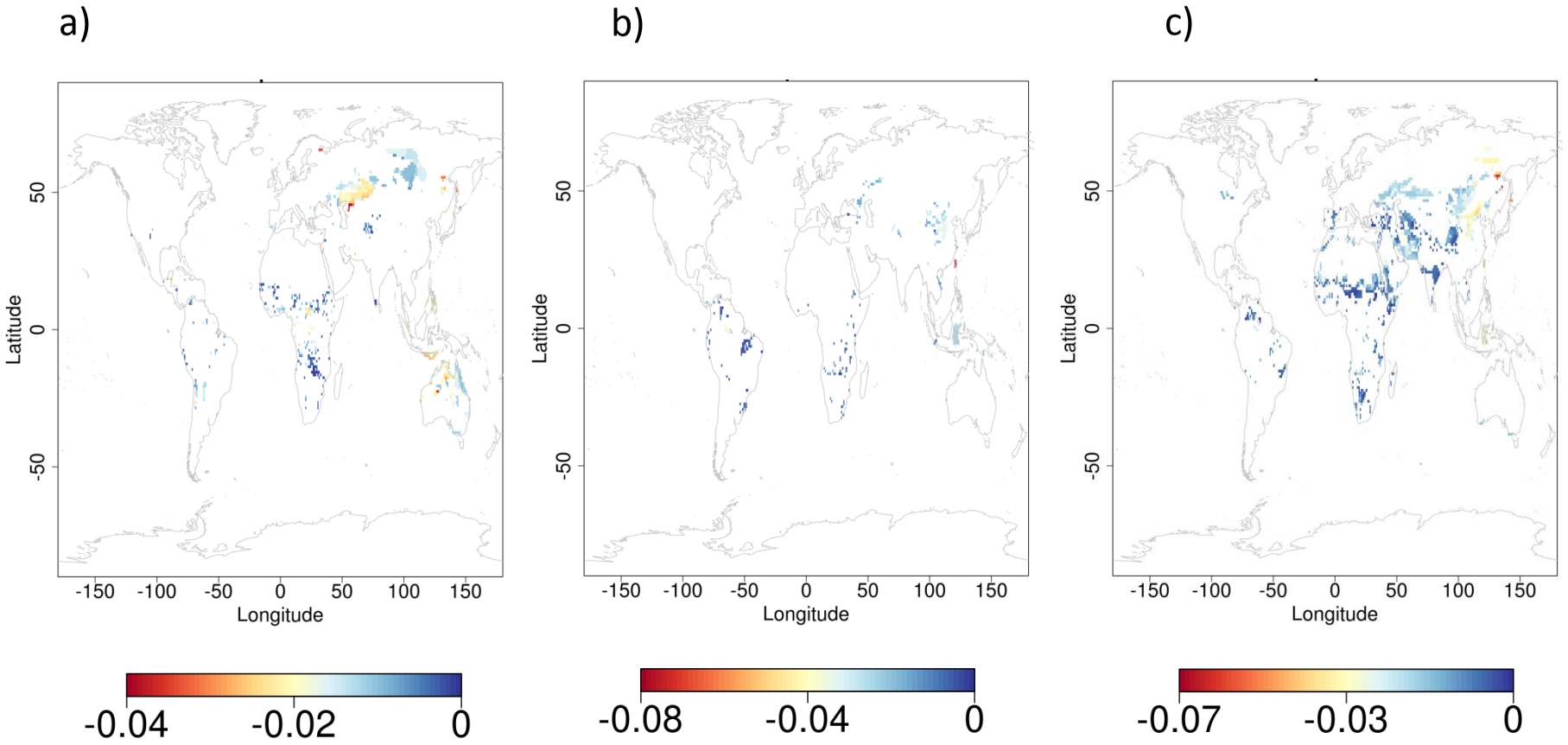

Figure S7. S values from the MC model within grid cells, considered only in grids where the MC model has smallest AIC values. Traits considered: (a) beak shape (PC1), (b) beak size (centroid size), and (c) body mass evolution. Outlier values (more than an order of magnitude difference) were removed from the analyses (one outlier removed for beak shape, and five outliers removed for beak size).

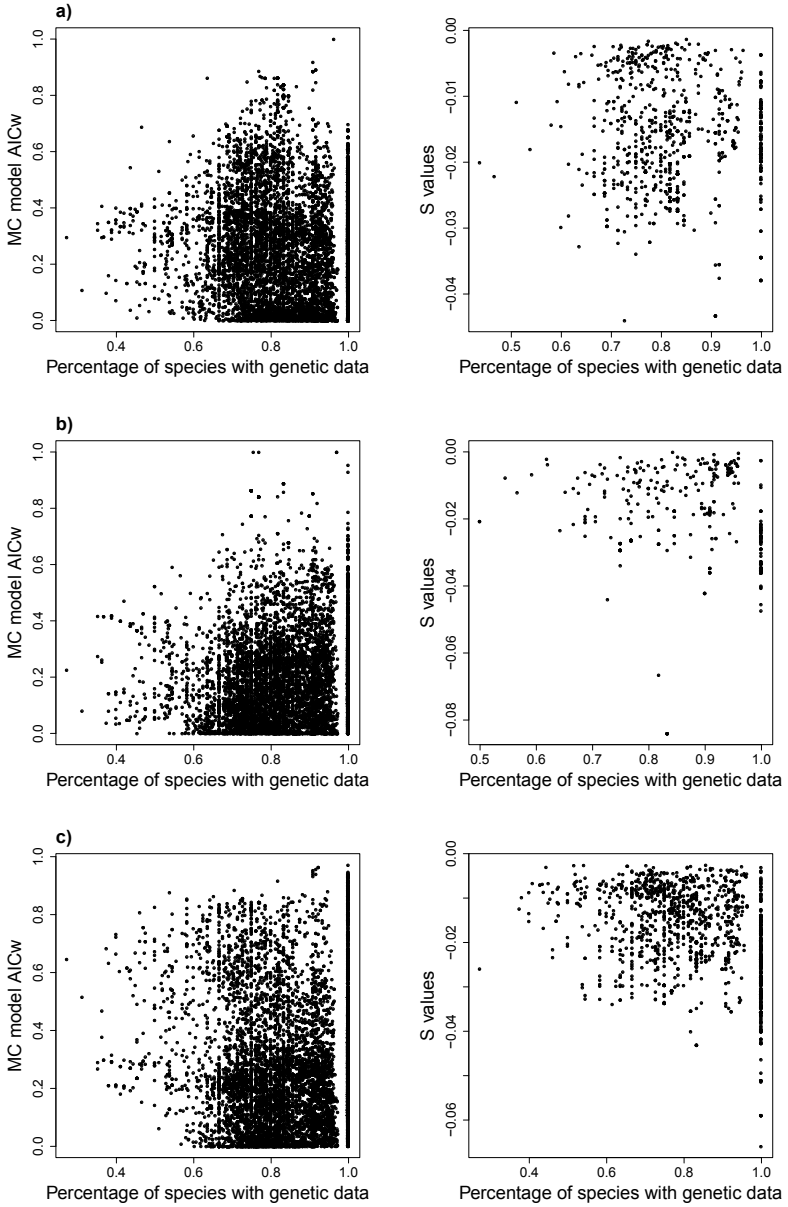

Figure S8. Relationship between the support (sqrt AICw of the matching competition model) and strength (S parameter values) of competition signal and the percentage of species with genetic data in assemblages. Relationships for (a) beak shape (PC1), (b) beak size, and (c) body mass.

Appendix 1.

Table 5.1. The relationship between S values (i.e. strength of the signal for competition) and candidate predictors across assemblages. The slope and p-values (significant in bold) for each predictor are reported. Traits considered: (a) beak shape (PC1). A SAR error type model with row standardization neighbourhood structure and a lag distance of 250km is selected as best among SAR models. SAR pseudo R-sq = 0.91, AIC = -4105, minRSA = 1.72. OLS adj. R-sq = 0.78, AIC = -3774, minRSA = 3.91. (b) beak size (centroid size). A SAR mixed type model with row standardization neighbourhood structure and a lag distance of 200km is selected as best among SAR models. SAR pseudo R-sq = 0.94, AIC = -1303, minRSA = 2.60. OLS adj. R-sq = 0.63, AIC = -1074, minRSA = 3.98. (c) body mass. A SAR error type model with row standardization neighbourhood structure and a lag distance of 150km is selected as best among SAR models. SAR pseudo R-sq = 0.86, AIC = -8382, minRSA = 1.02. OLS adj. R-sq = 0.73, AIC = -7858, minRSA = 3.15. Results from single-predictor models are also given below.

Predictor	SAR single slope	SAR single *p*	OLS single slope	OLS single *p*
(a) beak shape (PC1)				
Log SR	0.014	**0.000**	0.017	**0.000**
Log BM rate	0.010	**0.000**	0.010	**0.000**
Mean NPP	0.000	0.306	0.000	**0.000**
Temperature seasonality	0.000	**0.000**	0.000	**0.000**
Precipitation seasonality	0.000	**0.005**	0.000	**0.000**
Sqrt (elevation range)	0.000	**0.029**	0.000	**0.000**
Log (age MRCA)	0.025	**0.000**	0.024	**0.000**
(b) beak size				
Predictor	SAR single slope	SAR single *p*	OLS single slope	OLS single *p*
Log SR	0.015	**0.000**	0.022	**0.000**
Log BM rate	0.006	0.061	0.018	**0.000**
Mean NPP	0.000	**0.000**	0.000	0.681
Temperature seasonality	0.000	**0.000**	0.000	**0.002**
Precipitation seasonality	0.000	0.314	0.000	**0.022**
Sqrt (elevation range)	0.000	0.904	0.000	**0.000**
Log (age MRCA)	0.045	**0.000**	0.082	**0.000**
(c) body mass				
Predictor	SAR single slope	SAR single *p*	OLS single slope	OLS single *p*
Log SR	0.014	**0.000**	0.020	**0.000**
Log BM rate	0.002	**0.011**	-0.008	**0.000**
Mean NPP	0.000	0.066	0.000	**0.000**
Temperature seasonality	0.000	**0.000**	0.000	**0.000**
Precipitation seasonality	0.000	0.051	0.000	**0.000**
Sqrt (elevation range)	0.000	**0.000**	0.000	**0.000**
Log (age MRCA)	0.033	**0.000**	0.048	**0.000**

Table 5.2. The relationship between sesDisparity and candidate predictors across assemblages. The slope and p-values (significant in bold) for each predictor are reported. Traits considered: (a) beak shape (PC1). A SAR mixed type model with row standardization neighbourhood structure and a lag distance of 450km is selected as best among SAR models. SAR pseudo R-sq = 0.95, AIC = 638, minRSA = 0.92. OLS adj. R-sq = 0.56, AIC = 1598, minRSA = 8.84. (b) beak size (centroid size). A SAR mixed type model with row standardization neighbourhood structure and a lag distance of 300km is selected as best among SAR models. SAR pseudo R-sq = 0.9, AIC = 22.48, minRSA = 2.48. OLS adj. R-sq = 0.55, AIC = 222, minRSA = 10.53. (c) body mass. A SAR error type model with row standardization neighbourhood structure and a lag distance of 350km is selected as best among SAR models. SAR pseudo R-sq = 0.87, AIC = 569, minRSA = 1.07. OLS adj. R-sq = 0.24, AIC = 2131, minRSA = 8.83. Results from single-predictor models are also given below.

Predictor	SAR single slope	SAR single *p*	OLS single slope	OLS single *p*
(a) beak shape (PC1)				
Log SR	-1.004	**0.000**	0.591	0.004
Log BM rate	0.037	0.417	1.668	0.000
S values	-29.601	**0.000**	-21.324	0.035
Log (age MRCA)	-0.378	0.115	-6.182	0.000
(b) beak size				
Predictor	SAR single slope	SAR single *p*	OLS single slope	OLS single *p*
Log SR	-0.706	**0.000**	-0.940	0.000
Log BM rate	0.493	**0.002**	0.073	0.683
S values	-23.817	**0.000**	-12.741	0.000
Log (age MRCA)	0.012	0.953	0.577	0.224
(c) body mass				
Predictor	SAR single slope	SAR single *p*	OLS single slope	OLS single *p*
Log SR	-0.518	**0.000**	-0.682	0.000
Log BM rate	1.113	**0.000**	1.272	0.000
S values	-13.459	**0.000**	-22.889	0.000
Log (age MRCA)	0.306	0.074	0.091	0.649

Table S1. The relationship between support for competition (i.e. AICw of MC model) and candidate predictors across assemblages. The slope and p-values (significant in bold) for each predictor are reported. Traits considered: (a) beak shape (PC1). A SAR error type model with row standardization neighbourhood structure and a lag distance of 200km is selected as best among SAR models. SAR pseudo R-sq = 0.69, AIC = -16649, minRSA = 0.76. OLS adj. R-sq = 0.17, AIC = -8158, minRSA = 3.6.84. (b) beak size (centroid size). A SAR error type model with row standardization neighbourhood structure and a lag distance of 200km is selected as best among SAR models. SAR pseudo R-sq = 0.62, AIC = -19160, minRSA = 0.67. OLS adj. R-sq = 0.10, AIC = -11996, minRSA = 5.63. (c) body mass. A SAR mixed type model with row standardization neighbourhood structure and a lag distance of 200km is selected as best among SAR models. SAR pseudo R-sq = 0.70, AIC = -14155, minRSA = 0.73. OLS adj. R-sq = 0.18, AIC = -5439, minRSA = 7.21.

Predictor	SAR slope	SAR *p*	OLS slope	OLS *p*
(a) beak shape (PC1)				
Log SR	-0.124	**0.000**	-0.110	**0.000**
Log BM rate	-0.055	**0.000**	-0.087	**0.000**
Mean NPP	0.000	0.245	0.000	0.907
Temperature seasonality	0.000	0.831	0.000	**0.000**
Precipitation seasonality	0.000	0.312	0.000	**0.030**
Sqrt (elevation range)	0.000	0.233	-0.002	**0.000**
Log (age MRCA)	-0.039	**0.020**	-0.083	**0.000**
(b) beak size				
Predictor	SAR slope	SAR *p*	OLS slope	OLS *p*
Log SR	-0.112	**0.000**	-0.108	**0.000**
Log BM rate	0.040	**0.000**	0.022	**0.000**
Mean NPP	0.000	**0.013**	0.000	**0.000**
Temperature seasonality	0.000	**0.000**	0.000	**0.000**
Precipitation seasonality	0.000	0.998	0.000	0.470
Sqrt (elevation range)	0.000	**0.003**	0.000	**0.000**
Log (age MRCA)	0.041	**0.005**	0.042	**0.000**
(c) body mass				
Predictor	SAR slope	SAR *p*	OLS slope	OLS *p*
Log SR	-0.178	**0.000**	-0.211	**0.000**
Log BM rate	-0.036	**0.000**	-0.005	0.447
Mean NPP	0.000	0.748	0.000	**0.000**
Temperature seasonality	0.000	0.998	0.000	**0.000**
Precipitation seasonality	0.000	0.160	0.001	**0.000**
Sqrt (elevation range)	0.000	**0.034**	0.001	**0.000**
Log (age MRCA)	0.083	**0.000**	0.031	**0.005**

Table S2. The relationship between sesDisparity and candidate predictors across assemblages. The slope and p-values (significant in bold) for each predictor are reported. Traits considered: (a) beak shape (PC1). A SAR error type model with row standardization neighbourhood structure and a lag distance of 150km is selected as best among SAR models. SAR pseudo R-sq = 0.98, AIC = 5332, minRSA = 0.54. OLS adj. R-sq = 0.31, AIC = 38977, minRSA = 13.93. (b) beak size (centroid size). A SAR error type model with row standardization neighbourhood structure and a lag distance of 150km is selected as best among SAR models. SAR pseudo R-sq = 0.94, AIC = -5353.88, minRSA = 0.94. OLS adj. R-sq = 0.52, AIC = 13547, minRSA = 12.17. (c) body mass. A SAR mixed type model with row standardization neighbourhood structure and a lag distance of 150km is selected as best among SAR models. SAR pseudo R-sq = 0.93, AIC = 2880, minRSA = 0.80. OLS adj. R-sq = 0.35, AIC = 23952, minRSA = 11.58.

Predictor	SAR slope	SAR *p*	OLS slope	OLS *p*
(a) beak shape (PC1)				
Log SR	-0.645	**0.000**	-0.087	**0.036**
Log BM rate	0.406	**0.000**	2.050	**0.000**
Competition 0/1	0.038	**0.026**	0.956	**0.000**
Log (age MRCA)	0.231	**0.000**	1.756	**0.000**
(b) beak size				
Predictor	SAR slope	SAR *p*	OLS slope	OLS *p*
Log SR	-0.481	**0.000**	-0.544	**0.000**
Log BM rate	0.735	**0.000**	0.765	**0.000**
Competition 0/1	0.095	**0.000**	0.458	**0.000**
Log (age MRCA)	0.478	**0.000**	0.710	**0.000**
(c) body mass				
Predictor	SAR slope	SAR *p*	OLS slope	OLS *p*
Log SR	-0.423	**0.000**	-0.292	**0.000**
Log BM rate	0.878	**0.000**	1.243	**0.000**
Competition 0/1	0.126	**0.000**	0.733	**0.000**
Log (age MRCA)	0.988	**0.000**	1.494	**0.000**

Table S3. The relationship between support for competition (i.e. AICw of MC model) and candidate predictors across assemblages. The slope and p-values (significant in bold) for each predictor are reported. Traits considered: (a) beak shape (PC1), (b) beak size (centroid size), and (c) body mass. Relationships are done separately for each family in the community. NA values appear for predictors with extremely low to no variability in values.

(a) Beak shape (PC1)

Buntings, American sparrows, Brush finches				
Predictor	SAR slope	SAR *p*	OLS slope	OLS *p*
Log SR	0.087	0.762	0.173	0.636
Log BM rate	-0.072	0.457	0.081	0.296
Mean NPP	0.000	0.711	0.000	**0.035**
Temperature seasonality	-0.103	0.425	0.000	**0.022**
Precipitation seasonality	-0.001	**0.049**	0.002	**0.042**
Sqrt (elevation range)	-0.005	**0.003**	-0.003	**0.024**
Log (age MRCA)	-1.011	**0.017**	-1.078	**0.003**
Predictor	SAR slope	SAR *p*	OLS slope	OLS *p*
Doves, Pigeons				
Log SR	-0.184	**0.034**	-0.092	0.444
Log BM rate	0.063	**0.013**	0.053	0.118
Mean NPP	0.000	0.666	0.000	0.101
Temperature seasonality	0.025	0.342	0.000	0.445
Precipitation seasonality	0.001	0.396	-0.001	0.236
Sqrt (elevation range)	-0.002	**0.025**	-0.002	**0.005**
Log (age MRCA)	NA	NA	NA	NA
Finches, allies				
Predictor	SAR slope	SAR *p*	OLS slope	OLS *p*
Log SR	-0.191	**0.001**	-0.253	**0.000**
Log BM rate	-0.104	**0.000**	-0.136	**0.000**
Mean NPP	0.000	**0.002**	0.000	**0.013**
Temperature seasonality	0.091	**0.005**	0.000	0.221
Precipitation seasonality	0.000	0.571	0.000	0.851
Sqrt (elevation range)	0.002	**0.001**	0.002	**0.000**
Log (age MRCA)	-0.297	**0.000**	-0.146	**0.023**
Tanagers, Flowerpiercers, Conebills, Seedeaters, Warbling finches, allies				
Predictor	SAR slope	SAR *p*	OLS slope	OLS *p*
Log SR	-0.047	0.184	0.024	0.525
Log BM rate	0.002	0.881	-0.032	**0.011**
Mean NPP	0.000	**0.001**	0.000	**0.000**
Temperature seasonality	0.005	0.804	0.000	0.186
Precipitation seasonality	0.001	**0.006**	0.000	0.297
Sqrt (elevation range)	0.001	0.115	0.002	**0.000**
Log (age MRCA)	-0.372	**0.000**	-0.363	**0.000**
Waxbills, allies				
Predictor	SAR slope	SAR *p*	OLS slope	OLS *p*
Log SR	-0.126	**0.000**	-0.146	**0.000**
Log BM rate	-0.075	**0.000**	-0.112	**0.000**
Mean NPP	0.000	0.927	0.000	0.568
Temperature seasonality	-0.010	0.642	0.000	0.906
Precipitation seasonality	0.001	**0.007**	0.002	**0.000**
Sqrt (elevation range)	0.003	**0.000**	0.004	**0.000**
Log (age MRCA)	-0.427	**0.005**	-0.008	0.935

Weavers, allies				
Predictor	SAR slope	SAR *p*	OLS slope	OLS *p*
Log SR	-0.166	**0.003**	-0.191	**0.000**
Log BM rate	0.041	0.121	0.044	**0.044**
Mean NPP	0.000	**0.009**	0.000	**0.001**
Temperature seasonality	0.000	0.994	0.000	0.246
Precipitation seasonality	0.000	0.805	0.000	0.827
Sqrt (elevation range)	-0.001	0.391	-0.001	0.167
Log (age MRCA)	0.065	0.458	0.191	**0.022**

(b) Beak size (centroid size)

Buntings, American sparrows, Brush finches				
Predictor	SAR slope	SAR *p*	OLS slope	OLS *p*
Log SR	-0.242	**0.042**	-0.511	**0.008**
Log BM rate	0.121	**0.012**	0.142	**0.002**
Mean NPP	0.000	0.239	0.000	**0.024**
Temperature seasonality	-0.080	0.054	0.000	**0.032**
Precipitation seasonality	-0.001	0.073	-0.001	**0.029**
Sqrt (elevation range)	-0.003	**0.000**	-0.002	**0.003**
Log (age MRCA)	0.514	**0.011**	1.609	**0.000**
Predictor	SAR slope	SAR *p*	OLS slope	OLS *p*
Doves, Pigeons				
Log SR	-0.166	0.343	-0.263	**0.019**
Log BM rate	0.143	**0.000**	0.194	**0.000**
Mean NPP	0.000	0.055	0.000	**0.000**
Temperature seasonality	-0.005	0.925	0.000	**0.000**
Precipitation seasonality	-0.002	0.051	-0.003	**0.000**
Sqrt (elevation range)	-0.001	0.567	0.000	0.900
Log (age MRCA)	-0.023	0.953	NA	NA
Finches, allies				
Predictor	SAR slope	SAR *p*	OLS slope	OLS *p*
Log SR	0.233	0.174	0.319	**0.057**
Log BM rate	0.041	0.636	-0.187	**0.009**
Mean NPP	0.000	**0.041**	0.000	0.589
Temperature seasonality	-0.045	0.665	-0.001	**0.009**
Precipitation seasonality	0.001	0.462	0.001	0.262
Sqrt (elevation range)	-0.001	0.366	-0.006	**0.001**
Log (age MRCA)	0.741	**0.002**	1.043	**0.000**
Tanagers, Flowerpiercers, Conebills, Seedeaters, Warbling finches, allies				
Predictor	SAR slope	SAR *p*	OLS slope	OLS *p*
Log SR	-0.091	0.077	-0.100	**0.047**
Log BM rate	-0.037	0.067	-0.046	**0.002**
Mean NPP	0.000	0.504	0.000	**0.038**
Temperature seasonality	-0.063	0.090	0.000	**0.000**
Precipitation seasonality	0.002	**0.000**	-0.002	**0.000**
Sqrt (elevation range)	0.001	0.528	0.000	0.419
Log (age MRCA)	-0.153	**0.028**	-0.146	0.081
Waxbills, allies				
Predictor	SAR slope	SAR *p*	OLS slope	OLS *p*
Log SR	0.009	0.746	-0.071	**0.000**
Log BM rate	-0.041	**0.008**	-0.017	0.141
Mean NPP	0.000	0.348	0.000	**0.000**
Temperature seasonality	-0.006	0.808	0.000	**0.000**

Precipitation seasonality	0.000	0.401	0.002	**0.000**
Sqrt (elevation range)	0.000	0.643	0.002	**0.000**
Log (age MRCA)	-0.240	0.077	-0.078	0.311
Weavers, allies				
Predictor	SAR slope	SAR *p*	OLS slope	OLS *p*
Log SR	-0.074	0.082	-0.059	0.130
Log BM rate	0.042	0.106	0.034	0.116
Mean NPP	0.000	0.819	0.000	0.610
Temperature seasonality	-0.015	0.547	0.000	0.157
Precipitation seasonality	-0.001	0.177	0.000	0.411
Sqrt (elevation range)	-0.002	**0.008**	-0.002	**0.000**
Log (age MRCA)	-0.146	**0.024**	-0.197	**0.002**

(c) Body mass

Buntings, American sparrows, Brush finches				
Predictor	SAR slope	SAR *p*	OLS slope	OLS *p*
Log SR	0.318	0.147	0.216	0.675
Log BM rate	-0.343	**0.000**	0.202	**0.014**
Mean NPP	0.000	0.054	-0.002	**0.000**
Temperature seasonality	-0.076	0.550	0.000	0.720
Precipitation seasonality	-0.002	**0.005**	0.000	0.861
Sqrt (elevation range)	-0.001	0.577	0.001	0.639
Log (age MRCA)	0.370	0.336	0.482	0.339
Predictor	SAR slope	SAR *p*	OLS slope	OLS *p*
Doves, Pigeons				
Log SR	-0.334	**0.000**	-0.457	**0.000**
Log BM rate	0.052	0.206	0.243	**0.000**
Mean NPP	0.000	0.945	0.000	**0.000**
Temperature seasonality	0.047	**0.005**	0.001	**0.000**
Precipitation seasonality	0.000	0.545	0.000	0.951
Sqrt (elevation range)	-0.002	**0.003**	-0.003	**0.000**
Log (age MRCA)	NA	NA	NA	NA
Finches, allies				
Predictor	SAR slope	SAR *p*	OLS slope	OLS *p*
Log SR	0.922	**0.000**	0.647	**0.001**
Log BM rate	-0.352	0.096	-0.296	**0.024**
Mean NPP	-0.001	**0.004**	0.000	0.053
Temperature seasonality	-0.185	0.277	0.000	0.530
Precipitation seasonality	-0.001	0.526	-0.003	0.050
Sqrt (elevation range)	-0.003	0.137	-0.003	0.166
Log (age MRCA)	0.914	0.082	0.742	**0.001**
Tanagers, Flowerpiercers, Conebills, Seedeaters, Warbling finches, allies				
Predictor	SAR slope	SAR *p*	OLS slope	OLS *p*
Log SR	-0.168	**0.001**	-0.219	**0.000**
Log BM rate	-0.019	0.511	-0.071	**0.001**
Mean NPP	0.000	**0.027**	0.000	**0.037**
Temperature seasonality	0.048	0.153	-0.001	**0.000**
Precipitation seasonality	0.001	**0.028**	0.000	0.476
Sqrt (elevation range)	0.000	0.731	0.001	**0.014**
Log (age MRCA)	-0.167	**0.017**	-0.234	**0.011**
Waxbills, allies				
Predictor	SAR slope	SAR *p*	OLS slope	OLS *p*
Log SR	-0.096	**0.007**	-0.157	**0.000**
Log BM rate	0.033	0.261	0.047	**0.027**

Mean NPP	0.000	**0.037**	0.000	0.276
Temperature seasonality	-0.012	0.803	0.001	**0.000**
Precipitation seasonality	0.001	0.207	0.001	**0.000**
Sqrt (elevation range)	0.001	0.528	0.003	**0.000**
Log (age MRCA)	0.005	0.929	0.067	0.521
Weavers, allies				
Predictor	SAR slope	SAR *p*	OLS slope	OLS *p*
Log SR	-0.111	**0.005**	-0.009	0.794
Log BM rate	0.106	**0.000**	0.025	0.110
Mean NPP	0.000	0.112	0.000	0.069
Temperature seasonality	0.060	0.086	0.000	0.313
Precipitation seasonality	0.000	0.488	0.000	0.220
Sqrt (elevation range)	-0.002	**0.002**	-0.001	**0.025**
Log (age MRCA)	-0.061	0.236	-0.209	**0.000**

Table S4. The relationship between sesDisparity and candidate predictors across assemblages. Multipredictor SAR and OLS models are considered, and the slope and p-values (significant in bold) for each predictor are reported. Traits considered: (a) beak shape (PC1), (b) beak size (centroid size), and (c) body mass. Relationships are done separately for each family in the community. NA values appear for predictors with extremely low to no variability in values.

(a) Beak shape

Buntings, American sparrows, Brush finches				
Predictor	SAR slope	SAR *p*	OLS slope	OLS *p*
Log SR	-0.315	0.351	-0.126	0.932
Log BM rate	1.448	**0.000**	2.091	**0.000**
Competition 0/1	1.975	**0.001**	NA	NA
Log (age MRCA)	NA	NA	2.390	0.079
Doves, Pigeons				
Predictor	SAR slope	SAR *p*	OLS slope	OLS *p*
Log SR	-0.321	0.056	2.092	**0.000**
Log BM rate	0.104	**0.046**	0.065	0.496
Competition 0/1	0.111	0.169	0.122	0.377
Log (age MRCA)	0.913	**0.000**	NA	NA
Finches, allies				
Predictor	SAR slope	SAR *p*	OLS slope	OLS *p*
Log SR	-0.888	**0.000**	-0.888	**0.001**
Log BM rate	1.340	**0.000**	2.111	**0.000**
Competition 0/1	1.651	**0.000**	NA	NA
Log (age MRCA)	0.776	**0.005**	1.960	**0.000**
Tanagers, Flowerpiercers, Conebills, Seedeaters, Warbling finches, allies				
Predictor	SAR slope	SAR *p*	OLS slope	OLS *p*
Log SR	0.468	**0.002**	1.268	**0.000**
Log BM rate	0.844	**0.000**	0.416	**0.000**
Competition 0/1	0.305	0.184	0.319	0.439
Log (age MRCA)	0.134	0.513	0.594	0.188
Waxbills, allies				
Predictor	SAR slope	SAR *p*	OLS slope	OLS *p*
Log SR	-0.518	**0.000**	-0.528	**0.000**
Log BM rate	0.304	**0.000**	0.351	**0.000**
Competition 0/1	0.053	0.497	0.133	0.246

Log (age MRCA)	2.877	**0.000**	2.345	**0.000**

Weavers, allies				
Predictor	SAR slope	SAR *p*	OLS slope	OLS *p*
Log SR	0.473	**0.018**	1.637	**0.000**
Log BM rate	0.631	**0.000**	0.683	**0.000**
Competition 0/1	0.177	0.386	0.324	0.297
Log (age MRCA)	-0.705	**0.013**	-3.466	**0.000**

(b) Beak size (centroid size)

Buntings, American sparrows, Brush finches				
Predictor	SAR slope	SAR *p*	OLS slope	OLS *p*
Log SR	-0.325	0.555	-1.359	0.164
Log BM rate	2.733	**0.000**	1.996	**0.000**
Competition 0/1	6.483	**0.000**	NA	NA
Log (age MRCA)	-2.402	**0.037**	11.295	**0.000**
Doves, Pigeons				
Predictor	SAR slope	SAR *p*	OLS slope	OLS *p*
Log SR	-0.204	**0.001**	0.289	0.056
Log BM rate	0.322	**0.000**	0.417	**0.000**
Competition 0/1	-0.042	**0.003**	-0.189	**0.000**
Log (age MRCA)	NA	NA	NA	NA
Finches, allies				
Predictor	SAR slope	SAR *p*	OLS slope	OLS *p*
Log SR	-0.886	**0.000**	-0.813	**0.000**
Log BM rate	1.179	**0.000**	1.296	**0.000**
Competition 0/1	0.017	0.599	-0.057	0.188
Log (age MRCA)	1.222	**0.000**	1.797	**0.000**
Tanagers, Flowerpiercers, Conebills, Seedeaters, Warbling finches, allies				
Predictor	SAR slope	SAR *p*	OLS slope	OLS *p*
Log SR	-0.134	0.310	0.209	0.334
Log BM rate	1.430	**0.000**	1.514	**0.000**
Competition 0/1	-0.009	0.930	-0.425	0.072
Log (age MRCA)	0.259	0.157	-0.268	0.521
Waxbills, allies				
Predictor	SAR slope	SAR *p*	OLS slope	OLS *p*
Log SR	-0.268	**0.000**	-0.420	**0.000**
Log BM rate	2.292	**0.000**	2.815	**0.000**
Competition 0/1	0.009	0.938	0.009	0.963
Log (age MRCA)	-0.381	0.488	-1.505	**0.000**

Weavers, allies				
Predictor	SAR slope	SAR *p*	OLS slope	OLS *p*
Log SR	-0.087	0.587	0.268	0.119
Log BM rate	1.069	**0.000**	1.850	**0.000**
Competition 0/1	-0.436	**0.020**	-0.381	0.326
Log (age MRCA)	0.683	**0.005**	1.885	**0.000**

(c) Body mass

Buntings, American sparrows, Brush finches				
Predictor	SAR slope	SAR *p*	OLS slope	OLS *p*
Log SR	-0.431	0.391	-1.277	0.102
Log BM rate	2.028	**0.000**	2.252	**0.000**
Competition 0/1	-0.036	0.605	-0.220	**0.032**
Log (age MRCA)	0.922	0.229	5.472	**0.000**
Doves, Pigeons				
Predictor	SAR slope	SAR *p*	OLS slope	OLS *p*
Log SR	0.298	**0.000**	0.728	**0.000**
Log BM rate	1.291	**0.000**	1.555	**0.000**
Competition 0/1	0.291	**0.007**	0.469	**0.007**
Log (age MRCA)	-0.005	0.967	NA	NA
Finches, allies				
Predictor	SAR slope	SAR *p*	OLS slope	OLS *p*
Log SR	-0.655	**0.000**	-0.408	**0.031**
Log BM rate	1.526	**0.000**	1.402	**0.000**
Competition 0/1	0.046	0.195	-0.022	0.650
Log (age MRCA)	3.288	**0.000**	1.442	**0.000**
Tanagers, Flowerpiercers, Conebills, Seedeaters, Warbling finches, allies				
Predictor	SAR slope	SAR *p*	OLS slope	OLS *p*
Log SR	-0.453	**0.000**	0.060	0.607
Log BM rate	0.599	**0.000**	0.805	**0.000**
Competition 0/1	0.074	0.381	0.023	0.869
Log (age MRCA)	0.026	0.801	0.005	0.982
Waxbills, allies				
Predictor	SAR slope	SAR *p*	OLS slope	OLS *p*
Log SR	0.506	**0.000**	0.276	**0.001**
Log BM rate	2.129	**0.000**	2.587	**0.000**
Competition 0/1	0.081	0.345	0.348	**0.021**
Log (age MRCA)	1.948	**0.000**	-0.831	0.051

Weavers, allies				
Predictor	SAR slope	SAR *p*	OLS slope	OLS *p*
Log SR	-0.231	0.252	-0.472	**0.016**
Log BM rate	1.687	**0.000**	2.596	**0.000**
Competition 0/1	-3.063	**0.000**	-3.908	**0.000**
Log (age MRCA)	1.827	**0.000**	2.478	**0.000**

List of granivorous species used in the analyses:

Taoniscus_nanus, Crypturellus_parvirostris, Crypturellus_obsoletus, Odontophorus_hyperythrus, Odontophorus_strophium, Colinus_cristatus, Colinus_nigrogularis, Colinus_leucopogon, Colinus_virginianus, Callipepla_californica, Philortyx_fasciatus, Tympanuchus_cupido, Syrmaticus_soemmerringii, Perdix_hodgsoniae, Lophophorus_sclateri, Tragopan_caboti, Perdicula_argoondah, Perdicula_asiatica, Francolinus_nobilis, Francolinus_castaneicollis, Coturnix_delegorguei, Coturnix_coromandelica, Coturnix_coturnix, Coturnix_pectoralis, Dendrocygna_guttata, Aix_sponsa, Netta_erythrophthalma, Aythya_innotata, Turnix_castanotus, Turnix_tanki, Turnix_suscitator, Turnix_pyrrhothorax, Turnix_olivii, Turnix_nigricollis, Turnix_velox, Ortyxelos_meiffrenii, Neophema_petrophila, Neophema_splendida, Neophema_elegans, Neophema_chrysostoma, Neopsephotus_bourkii, Cyclopsitta_gulielmitertii, Melopsittacus_undulatus, Psittacella_madaraszi, Psittacella_picta, Psittacella_modesta, Platycercus_venustus, Psephotus_chrysopterygius, Psephotus_varius, Psephotus_dissimilis, Purpureicephalus_spurius, Pezoporus_wallicus, Pezoporus_occidentalis, Agapornis_pullarius, Agapornis_taranta, Agapornis_canus, Agapornis_roseicollis, Agapornis_nigrigenis, Agapornis_personatus, Agapornis_fischeri, Polytelis_alexandrae, Polytelis_swainsonii, Alisterus_chloropterus, Geoffroyus_simplex, Psittinus_cyanurus, Psittacula_derbiana, Psittacula_longicauda, Tanygnathus_lucionensis, Poicephalus_crassus, Poicephalus_rufiventris, Psittacus_erithacus, Forpus_cyanopygius, Forpus_xanthopterygius, Forpus_coelestis, Forpus_modestus, Diopsittaca_nobilis, Leptosittaca_branickii, Primolius_maracana, Primolius_auricollis, Ara_ambiguus, Ara_severus, Ara_rubrogenys, Aratinga_auricapillus, Aratinga_wagleri, Aratinga_mitrata, Aratinga_acuticaudata, Aratinga_canicularis, Pyrrhura_hoffmanni, Pyrrhura_cruentata, Rhynchopsitta_terrisi, Rhynchopsitta_pachyrhyncha, Pionites_leucogaster, Brotogeris_versicolurus, Ognorhynchus_icterotis, Hapalopsittaca_amazonina, Pyrilia_barrabandi, Pyrilia_caica, Pionus_maximiliani, Pionus_senilis, Alipiopsitta_xanthops, Amazona_ventralis, Amazona_albifrons, Amazona_finschi, Amazona_dufresniana, Amazona_aestiva, Bolborhynchus_orbygnesius, Bolborhynchus_ferrugineifrons, Touit_stictopterus, Nymphicus_hollandicus, Cacatua_roseicapilla, Cacatua_sulphurea, Cacatua_pastinator, Cacatua_haematuropygia, Cacatua_tenuirostris, Cacatua_leadbeateri, Calyptorhynchus_lathami, Calyptorhynchus_latirostris,

Calyptorhynchus_funereus, Calyptorhynchus_banksii, Calyptorhynchus_baudinii, Asthenes_huancavelicae, Asthenes_arequipae, Asthenes_dorbignyi, Geositta_punensis, Geositta_antarctica, Grallaria_przewalskii, Amytornis_striatus, Amytornis_goyderi, Amytornis_housei, Amytornis_barbatus, Dasyornis_longirostris, Pyrrholaemus_brunneus, Aphelocephala_leucopsis, Psophodes_cristatus, Dendrocitta_occipitalis, Cyanocorax_mystacalis, Nucifraga_columbiana, Nucifraga_caryocatactes, Iole_indica, Babax_lanceolatus, Garrulax_austeni, Gypsophila_crispifrons, Pnoepyga_albiventer, Pnoepyga_formosana, Paradoxornis_gularis, Paradoxornis_flavirostris, Paradoxornis_margaritae, Ammomanes_phoenicura, Ammomanes_deserti, Ammomanes_cinctura, Eremopterix_australis, Eremopterix_leucotis, Eremopterix_griseus, Eremopterix_signatus, Eremopterix_leucopareia, Eremopterix_nigriceps, Eremopterix_verticalis, Ammomanes_grayi, Mirafra_williamsi, Mirafra_passerina, Mirafra_africanoides, Mirafra_rufa, Mirafra_assamica, Mirafra_cheniana, Mirafra_hova, Mirafra_microptera, Mirafra_erythrocephala, Mirafra_cordofanica, Mirafra_cantillans, Mirafra_affinis, Mirafra_erythroptera, Melanocorypha_yeltoniensis, Melanocorypha_leucoptera, Melanocorypha_mongolica, Melanocorypha_bimaculata, Chersophilus_duponti, Galerida_malabarica, Galerida_modesta, Galerida_magnirostris, Galerida_deva, Alauda_gulgula, Pseudalaemon_fremantlii, Spizocorys_fringillaris, Spizocorys_conirostris, Spizocorys_personata, Spizocorys_sclateri, Eremalauda_starki, Eremalauda_dunni, Calandrella_acutirostris, Calandrella_cinerea, Eremophila_alpestris, Eremophila_bilopha, Onychognathus_fulgidus, Brachypteryx_stellata, Sitta_neumayer, Sitta_krueperi, Sitta_canadensis, Sitta_whiteheadi, Sitta_villosa, Sitta_carolinensis, Prunella_modularis, Prunella_rubeculoides, Pseudonigrita_arnaudi, Pseudonigrita_cabanisi, Euplectes_afer, Euplectes_diadematus, Euplectes_hordeaceus, Euplectes_nigroventris, Euplectes_orix, Euplectes_franciscanus, Euplectes_gierowii, Euplectes_jacksoni, Euplectes_psammocromius, Euplectes_progne, Euplectes_axillaris, Euplectes_albonotatus, Euplectes_macroura, Euplectes_capensis, Euplectes_aureus, Foudia_madagascariensis, Quelea_cardinalis, Quelea_quelea, Quelea_erythrops, Ploceus_aurantius, Ploceus_luteolus, Ploceus_subaureus, Ploceus_pelzelni, Ploceus_melanocephalus, Ploceus_taeniopterus, Ploceus_superciliosus, Ploceus_olivaceiceps, Ploceus_spekei, Ploceus_megarhynchus, Ploceus_castanops, Ploceus_reichardi, Ploceus_katangae, Ploceus_sakalava, Ploceus_bojeri, Ploceus_badius,

Ploceus_rubiginosus, Ploceus_jacksoni, Ploceus_subpersonatus, Ploceus_dichrocephalus, Ploceus_philippinus, Ploceus_manyar, Ploceus_bertrandi, Ploceus_hypoxanthus, Ploceus_castaneiceps, Ploceus_galbula, Ploceus_spekeoides, Ploceus_benghalensis, Bubalornis_niger, Sporopipes_frontalis, Sporopipes_squamifrons, Dinemellia_dinemelli, Brachycope_anomala, Plocepasser_superciliosus, Plocepasser_rufoscapulatus, Plocepasser_mahali, Plocepasser_donaldsoni, Amadina_erythrocephala, Amadina_fasciata, Euschistospiza_dybowskii, Euschistospiza_cinereovinacea, Hypargos_margaritatus, Hypargos_niveoguttatus, Pytilia_melba, Pytilia_afra, Pytilia_phoenicoptera, Pytilia_hypogrammica, Pytilia_lineata, Clytospiza_monteiri, Lagonosticta_rhodopareia, Lagonosticta_virata, Lagonosticta_larvata, Lagonosticta_senegala, Lagonosticta_rufopicta, Lagonosticta_nitidula, Uraeginthus_cyanocephalus, Uraeginthus_bengalus, Uraeginthus_angolensis, Uraeginthus_ianthinogaster, Spermophaga_poliogenys, Spermophaga_ruficapilla, Pyrenestes_minor, Pyrenestes_ostrinus, Pyrenestes_sanguineus, Mandingoa_nitidula, Cryptospiza_jacksoni, Cryptospiza_reichenovii, Cryptospiza_salvadorii, Cryptospiza_shelleyi, Estrilda_thomensis, Estrilda_charmosyna, Estrilda_melpoda, Estrilda_paludicola, Estrilda_troglodytes, Estrilda_rufibarba, Estrilda_nonnula, Estrilda_astrild, Nesocharis_capistrata, Estrilda_erythronotos, Estrilda_caerulescens, Estrilda_perreini, Nesocharis_shelleyi, Nesocharis_ansorgei, Estrilda_quartinia, Estrilda_melanotis, Estrilda_poliopareia, Heteromunia_pectoralis, Ortygospiza_locustella, Erythrura_prasina, Erythrura_hyperythra, Erythrura_viridifacies, Erythrura_tricolor, Erythrura_trichroa, Erythrura_coloria, Erythrura_gouldiae, Padda_oryzivora, Padda_fuscata, Lonchura_monticola, Lonchura_fringilloides, Lonchura_ferruginosa, Lonchura_tristissima, Lonchura_fuscans, Lonchura_griseicapilla, Lonchura_leucogastra, Lonchura_leucogastroides, Lonchura_striata, Lonchura_kelaarti, Lonchura_pallida, Lonchura_maja, Lonchura_atricapilla, Lonchura_malacca, Lonchura_nevermanni, Lonchura_castaneothorax, Lonchura_quinticolor, Lonchura_punctulata, Lonchura_spectabilis, Lonchura_nana, Lonchura_molucca, Lonchura_caniceps, Lonchura_malabarica, Lonchura_cantans, Lonchura_flaviprymna, Lonchura_grandis, Stagonopleura_bella, Stagonopleura_guttata, Stagonopleura_oculata, Taeniopygia_guttata, Taeniopygia_bichenovii, Oreostruthus_fuliginosus, Emblema_pictum, Poephila_personata, Poephila_cincta, Poephila_acuticauda, Neochmia_ruficauda, Neochmia_modesta, Neochmia_temporalis, Neochmia_phaeton, Amandava_amandava, Amandava_subflava, Amandava_formosa, Vidua_orientalis,

Vidua_interjecta, Vidua_obtusa, Vidua_paradisaea, Vidua_macroura, Vidua_hypocherina, Vidua_togoensis, Vidua_codringtoni, Vidua_funerea, Vidua_regia, Vidua_raricola, Vidua_chalybeata, Vidua_purpurascens, Vidua_nigeriae, Vidua_wilsoni, Vidua_camerunensis, Vidua_fischeri, Anomalospiza_imberbis, Anthus_bogotensis, Mycerobas_affinis, Eophona_migratoria, Eophona_personata, Pyrrhula_erythrocephala, Carpodacus_edwardsii, Carpodacus_rubicilloides, Carpodacus_vinaceus, Carpodacus_rodochroa, Carpodacus_pulcherrimus, Carpodacus_roseus, Carpodacus_trifasciatus, Carpodacus_roborowskii, Carpodacus_eos, Carpodacus_rodopeplus, Carpodacus_rubescens, Leucosticte_australis, Leucosticte_atrata, Leucosticte_brandti, Leucosticte_nemoricola, Neospiza_concolor, Eremopsaltria_mongolicus, Loxia_scotica, Loxia_pytyopsittacus, Carduelis_atriceps, Linurgus_olivaceus, Carduelis_johannis, Serinus_buchanani, Serinus_tristriatus, Serinus_pusillus, Serinus_rothschildi, Serinus_menachensis, Serinus_alario, Serinus_flavivertex, Serinus_canicollis, Serinus_thibetanus, Serinus_serinus, Serinus_xanthopygius, Serinus_reichardi, Serinus_xantholaemus, Serinus_sulphuratus, Serinus_syriacus, Serinus_melanochrous, Serinus_donaldsoni, Serinus_koliensis, Serinus_burtoni, Serinus_mozambicus, Serinus_dorsostriatus, Serinus_citrinipectus, Serinus_nigriceps, Serinus_frontalis, Serinus_atrogularis, Serinus_leucopygius, Serinus_hypostictus, Serinus_citrinelloides, Serinus_capistratus, Carduelis_cannabina, Carduelis_dominicensis, Carduelis_tristis, Carduelis_lawrencei, Carduelis_yemenensis, Carduelis_pinus, Carduelis_monguilloti, Carduelis_atrata, Carduelis_xanthogastra, Carduelis_cucullata, Carduelis_yarrellii, Carduelis_siemiradzkii, Carduelis_barbata, Carduelis_uropygialis, Carduelis_spinescens, Carduelis_notata, Carduelis_chloris, Carduelis_ambigua, Carduelis_spinoides, Carduelis_sinica, Calamospiza_melanocorys, Chondestes_grammacus, Spizella_arborea, Zonotrichia_capensis, Zonotrichia_albicollis, Zonotrichia_querula, Zonotrichia_leucophrys, Zonotrichia_atricapilla, Junco_hyemalis, Aimophila_ruficeps, Pipilo_crissalis, Pipilo_fuscus, Pooecetes_gramineus, Ammodramus_nelsoni, Ammodramus_leconteii, Melospiza_lincolnii, Ammodramus_bairdii, Spizella_atrogularis, Spizella_wortheni, Spizella_breweri, Spizella_pusilla, Spizella_passerina, Spizella_pallida, Amphispiza_bilineata, Aimophila_carpalis, Ammodramus_humeralis, Ammodramus_aurifrons, Emberiza_impetuani, Emberiza_tahapisi, Emberiza_striolata, Emberiza_cabanisi, Emberiza_flaviventris, Miliaria_calandra, Emberiza_caesia, Emberiza_buchanani,

Emberiza_cirlus, Emberiza_citrinella, Emberiza_leucocephalos, Emberiza_stewarti, Emberiza_godlewskii, Emberiza_cia, Emberiza_cioides, Emberiza_jankowskii, Emberiza_bruniceps, Emberiza_melanocephala, Melophus_lathami, Emberiza_yessoensis, Emberiza_pallasi, Emberiza_schoeniclus, Emberiza_rustica, Emberiza_poliopleura, Emberiza_aureola, Emberiza_sulphurata, Emberiza_affinis, Emberiza_fucata, Emberiza_pusilla, Emberiza_cineracea, Emberiza_variabilis, Emberiza_tristrami, Emberiza_chrysophrys, Emberiza_elegans, Agelaius_assimilis, Agelaius_phoeniceus, Agelaius_humeralis, Molothrus_rufoaxillaris, Molothrus_ater, Quiscalus_nicaraguensis, Quiscalus_niger, Agelasticus_cyanopus, Agelasticus_thilius, Chrysomus_icterocephalus, Chrysomus_ruficapillus, Sturnella_loyca, Sturnella_neglecta, Spiza_americana, Passerina_amoena, Passerina_rositae, Passerina_ciris, Passerina_leclancherii, Passerina_cyanea, Rhodothraupis_celaeno, Cardinalis_sinuatus, Tiaris_obscurus, Tiaris_fuliginosus, Tiaris_canorus, Tiaris_bicolor, Tiaris_olivaceus, Buthraupis_eximia, Diuca_diuca, Diuca_speculifera, Gubernatrix_cristata, Phrygilus_alaudinus, Phrygilus_fruticeti, Phrygilus_punensis, Coryphospingus_pileatus, Coryphospingus_cucullatus, Conirostrum_sitticolor, Phrygilus_dorsalis, Phrygilus_erythronotus, Haplospiza_rustica, Haplospiza_unicolor, Phrygilus_plebejus, Phrygilus_unicolor, Catamenia_inornata, Catamenia_homochroa, Catamenia_analis, Melanodera_melanodera, Melanodera_xanthogramma, Phrygilus_gayi, Phrygilus_patagonicus, Phrygilus_atriceps, Sicalis_citrina, Sicalis_raimondii, Sicalis_columbiana, Sicalis_uropygialis, Sicalis_flaveola, Sicalis_luteola, Sicalis_auriventris, Sicalis_luteocephala, Sicalis_lebruni, Sicalis_taczanowskii, Sicalis_lutea, Sicalis_olivascens, Oryzoborus_funereus, Oryzoborus_angolensis, Oryzoborus_nuttingi, Oryzoborus_crassirostris, Oryzoborus_maximiliani, Sporophila_americana, Sporophila_corvina, Sporophila_intermedia, Sporophila_murallae, Sporophila_simplex, Sporophila_leucoptera, Sporophila_luctuosa, Sporophila_peruviana, Sporophila_caerulescens, Sporophila_nigricollis, Sporophila_torqueola, Sporophila_schistacea, Sporophila_lineola, Sporophila_collaris, Sporophila_bouvronides, Sporophila_albogularis, Sporophila_plumbea, Sporophila_frontalis, Sporophila_cinnamomea, Sporophila_nigrorufa, Sporophila_palustris, Sporophila_ruficollis, Sporophila_bouvreuil, Sporophila_hypoxantha, Sporophila_minuta, Sporophila_telasco, Sporophila_castaneiventris, Calcarius_mccownii, Calcarius_lapponicus, Calcarius_pictus, Calcarius_ornatus, Petronia_dentata, Passer_griseus, Passer_rufocinctus, Passer_melanurus, Passer_motitensis, Passer_ammodendri, Passer_cordofanicus,

Passer_hispaniolensis, Passer_domesticus, Passer_montanus, Passer_suahelicus, Passer_flaveolus, Passer_luteus, Passer_eminibey, Passer_simplex, Passer_shelleyi, Passer_moabiticus, Passer_gongonensis, Passer_pyrrhonotus, Passer_swainsonii, Passer_castanopterus, Passer_rutilans, Passer_euchlorus, Montifringilla_taczanowskii, Montifringilla_adamsi, Montifringilla_nivalis, Montifringilla_theresae, Montifringilla_ruficollis, Montifringilla_davidiana, Montifringilla_blanfordi, Petronia_brachydactyla, Aethopyga_christinae, Urocynchramus_pylzowi, Celeus_torquatus, Veniliornis_mixtus, Melanerpes_formicivorus, Porphyrio_flavirostris, Coturnicops_notatus, Coturnicops_exquisitus, Amaurornis_akool, Rougetius_rougetii, Sarothrura_boehmi, Sarothrura_lugens, Sarothrura_insularis, Grus_virgo, Columbina_cruziana, Columbina_picui, Columbina_minuta, Columbina_talpacoti, Columbina_passerina, Columbina_inca, Columbina_squammata, Uropelia_campestris, Claravis_mondetoura, Claravis_pretiosa, Claravis_godefrida, Geophaps_scripta, Geophaps_smithii, Geophaps_plumifera, Petrophassa_rufipennis, Petrophassa_albipennis, Phaps_histrionica, Phaps_chalcoptera, Phaps_elegans, Ocyphaps_lophotes, Geopelia_striata, Geopelia_maugeus, Geopelia_placida, Geopelia_cuneata, Gallicolumba_tristigmata, Phapitreron_amethystinus, Phapitreron_brunneiceps, Turtur_tympanistria, Turtur_afer, Turtur_chalcospilos, Turtur_abyssinicus, Turtur_brehmeri, Oena_capensis, Chalcophaps_stephani, Trugon_terrestris, Caloenas_nicobarica, Goura_cristata, Otidiphaps_nobilis, Leptotila_battyi, Leptotila_cassini, Leptotila_plumbeiceps, Leptotila_rufaxilla, Leptotila_pallida, Leptotila_jamaicensis, Leptotila_verreauxi, Zenaida_auriculata, Zenaida_macroura, Zenaida_asiatica, Zenaida_meloda, Geotrygon_caniceps, Geotrygon_violacea, Geotrygon_linearis, Geotrygon_albifacies, Geotrygon_frenata, Geotrygon_saphirina, Geotrygon_montana, Starnoenas_cyanocephala, Geotrygon_goldmani, Macropygia_nigrirostris, Macropygia_ruficeps, Macropygia_phasianella, Macropygia_amboinensis, Reinwardtoena_reinwardtsi, Nesoenas_picturata, Stigmatopelia_senegalensis, Stigmatopelia_chinensis, Streptopelia_tranquebarica, Streptopelia_hypopyrrha, Streptopelia_turtur, Streptopelia_bitorquata, Streptopelia_roseogrisea, Streptopelia_decipiens, Columba_eversmanni, Columba_livia, Columba_rupestris, Columba_leuconota, Columba_guinea, Columba_oliviae, Columba_albitorques, Patagioenas_fasciata, Patagioenas_plumbea, Patagioenas_maculosa, Pterocles_exustus, Pterocles_bicinctus, Pterocles_quadricinctus, Pterocles_namaqua, Pterocles_burchelli, Pterocles_coronatus, Pterocles_senegallus, Pterocles_alchata, Pterocles_decoratus, Pterocles_lichtensteinii, Pterocles_indicus,

Pterocles_orientalis, Pterocles_personatus, Pterocles_gutturalis, Syrrhaptes_tibetanus, Syrrhaptes_paradoxus.

Environmental data description:

Variable	Description
Temperature seasonality	Annual range in temperature - standard deviation *100
Precipitation seasonality	Annual range in precipitation - coefficient of variation
Net primary productivity	Mean annual energy available to heterotrophs gCM^{-2}, 30′ resolution, reflected and square-root-transformed
Elevational range	range in elevation with 30′ resolution, square-root-transformed

CHAPTER 6

General discussion

GENERAL DISCUSSION

In this thesis I investigate patterns and correlates for ecomorphological diversification across the global radiation of birds. In chapters 2 and 3, I focused on the tempo of evolution. Specifically, I investigated the ability of single-process trait evolutionary models to describe the temporal patterns of evolution in the face of rate heterogeneity using both simulated and empirical datasets. Secondly, I used variable-rates models of evolution to describe the patterns of beak shape rate variation across over 5,000 bird species, and further, to test for multiple candidate drivers for the tempo of evolution at both recent and deep-time scales. In chapters 4 and 5, I focused more broadly on the mode of evolution, with specific focus on the potential impact of ecological selection pressures on the evolution of ecomorphological traits. I first investigated whether patterns of trait divergence consistent with the presence of competitive selection pressures are prevalent across the bird radiation (using beak shape, beak size and body mass data for over 8,000 bird species). Further, I mapped the geographical variation in the strength of competition signal in over 10,000 avian granivorous assemblages distributed globally, and investigated the association between competition signal and the process of ecomorphological differentiation (rate and total disparity) in assemblages. In the next section, I will discuss the main findings of this work, with focus on how my results provide insights into our understanding of the tempo and mode of phenotypic accumulation at macroevolutionary scales.

How accurately do single-process models describe the process of evolution in the face of heterogeneity in rates of trait change?

In chapter 2, I first showed that variation in the tempo of body mass evolution is prevalent across both small (20-30 species) and larger (100+ species) bird clades. At these phylogenetic scales, however, single-process models of evolution are typically applied. Therefore, I applied both rate-static and rate-variable trait evolutionary models on simulated and empirical datasets, and further used absolute adequacy tests to describe the extent to which the conclusions we draw from trait evolutionary models are misled by the presence of rate heterogeneity. I showed that rate-static models commonly mislabel temporal variation in rates, and thus can lead to spurious inferences about the process of trait evolution. For example, if one lineage within a clade shows rapid evolution, a rate-static model estimates general high rates of evolution for all clade members, which can further be erroneously interpreted as evidence for a clade wide radiation (as exemplified in mammals also by Venditti et al., 2011 vs Cooper & Purvis, 2010 or Slater et al., 2010). Further, my results add to the argument that absolute and relative fit are not necessarily linked (e.g. Kaliontzopoulou & Adams, 2016; Pennell et al., 2015), and testing for absolute model adequacy can correct systematic biases in the process of model selection criteria in the presence of rate heterogeneity. For example, rapid morphological differentiation at the tips of the phylogeny consistently results in a high preference for a single stationary peak model, which represents a clear shift in interpretation from isolated radiations within a clade to constrained evolution across the whole group. Variable-rates models are also not infallible, and for example early-burst processes are easily missed. However, absolute adequacy tests can pick-up that misspecification of the temporal pattern of evolution, and thus correct the conclusion that rate accelerations and decelerations are uncommon (an issue also recognized in Slater & Pennell, 2014).

More broadly, the results of chapter 2 show that efforts to add complexity in evolutionary models are rewarding, especially when accounting for a common feature of evolution, such as rate heterogeneity. Through-out my analyses, I found that variable-rate models are robust and describe the data well, which highlights the potential for accurate conclusions on the process of trait evolution in clades up to hundreds of species when more flexible approaches are used. Further, the extension of these models to other common comparative analyses, such as correlation between traits (Mazel et al., 2016) or between rates of disparification and diversification (e.g. Rabosky et al., 2013) is a useful direction to a better understanding of macroevolutionary morphological differentiation. The findings also highlight the importance of co-utilizing relative and absolute fit when modelling trait evolution and thus argue for developing adequacy tools further in the future, for example, by extending the existing absolute fit framework to other models of trait evolution (diversity-dependent models, Weir & Mursleen, 2013, jump models, Landis & Schraiber, 2017 etc.).

What predicts rates of phenotypic macroevolution?

In chapter 2, I found a high prevalence of variation in the speed at which body mass evolves within avian clades. In chapter 3, I explored the potential for rate heterogeneity more broadly across the bird radiation, and I found frequent episodes of rapid evolution in beak shape across both recent (i.e. species level) and deep-time (clade level) scales. I further showed that species-specific rates of evolution are not impacted by factors associated with the overall genetic variability in populations, or mutation and fixation rates (e.g. life history traits, the climatic environment, or range sizes, Gillman et al., 2014; Lanfear et al., 2014; Thomas et al., 2010; Thomson et al., 2014). Although I found localized effects for some factors related to species' ecologies (e.g. evidence of rapid evolution in some island-dwelling clades), the ecological predictors in the analyses also failed to explain

significant amounts of variation in evolutionary rates. More broadly, these results imply that the underlining mechanisms behind patterns of morphological differentiation between species are complex and their effects are inconsistent. Consequently, heterogeneity in rates of evolution between species across global radiations is hard to predict.

In contrast to species-level trends, deep-time patterns of rate heterogeneity are more tightly and consistently linked with a few key ecological processes. Specifically, I found rapid rates of evolution in clades evolving at the periphery of the morphospace, as well as in species-rich clades. Further, I found that species richness and morphological distinctiveness are negatively correlated (in agreement with Ricklefs, 2005), and so overall, my results highlight two distinct routes to rapid trait evolution. First, the evolution of "odd", specialised beaks frees species from competitors by enabling them to tap into new ecological resources, similar to Simpsonian ideas that "jumps" in the phenotypic space allow species to invade new adaptive zones with increased ecological opportunity and thus potential for rapid interspecific differentiation (Simpson, 1953, Hunter, 1998; Losos, 2010; Losos & Mahler, 2010; Rabosky, 2017). Alternatively, species with average-typed beaks evolving in species-rich clades likely access a limited number of ecological niches. Finding high rates of evolution in such groups suggests a potential role of biotic interactions in creating dynamic adaptive landscapes that facilitate a fast turnover of phenotypic traits via ecological character displacement (Schluter, 2001; Thompson, 1999).

How frequent do we find patterns of trait divergence consistent with the presence of ecological selection pressures at macroevolutionary scales?

In chapter 4, I surveyed the signal of species-interactions across the bird radiation, and so I took a first step in exploring whether biotic interactions could be a potential

mechanism behind macroevolutionary trends such as the positive link between species richness and trait evolutionary rates revealed in chapter 3. To do this, I applied models with species interactions i.e. trait-dependent methods, in which phenotypic evolution is influenced by similarity in trait values (Drury et al., 2016) as well as diversity-dependent methods, in which phenotypic evolution is influenced by the accumulation of species (Weir & Mursleen, 2013) in 95 avian clades (over 8,000 species in total). I showed that a mode of evolution consistent with the presence of biotic interactions is not ubiquitous, but also not uncommon at macroevolutionary scales, and I found support for competition signal in 15% up to 30% of bird groups (depending on the trait of interest). Also, I found stronger signals of competition in recent radiations, adding to the argument that the effect and detectability of species-interactions signals at broad scales are mediated by conditions such as the requisite of species to share similar foraging niches or to overlap extensively to allow meaningful interactions (Arthur, 1982; Grant, 1972). Overall, these results imply a middle ground between hypotheses arguing that competition is one of the core drivers of global phenotypic diversity (Darwin, 1859; Thompson, 1999; Van Valen, 1973) and ideas that argue for a small to null importance of biotic interactions in deep-time compared to other selection pressures (e.g. abiotic, Benton, 2009). However, we acknowledge that the patterns of trait divergence we see could also arise from processes alternative to ecological selection pressures (not the least the presence of measurement and/or phylogenetic error in the data).

Further, in clades with high support for competition signal, the models showed increased rates of evolution with high densities of species, in agreement with my previous results of high rates of beak shape evolution in species-rich clades (chapter 3), and with the observations across recent time scales that competition accelerates morphological differentiation as species partition the trait space (Grant & Grant, 2006; Stuart et al., 2014). However, my results also show a preference for

diversity-dependent models over trait-dependent methods, a trend that has been interpreted as a signature of character displacement occurring simultaneously with bounded evolution (Drury et al., 2018). Hence these results imply that, while competition can leave a signal at macroevolutionary scales, the impact on deep-time phenotypic accumulation might be mediated by factors such as evolution under constraints (Drury et al., 2018). Additionally, I found that competitive selective pressures do not leave a signal in the mode of evolution across random, multiple traits. Rather, the most parsimonious route to ecological specialization (i.e. change in a single key trait linked to resource acquisition, Grant, 1999; Weir & Mursleen, 2013) is most often selected for. Therefore, we expect species interactions to impact global patterns of biodiversity to a lesser extent than factors driving extensive diversification across multiple traits simultaneously.

What is the geographical distribution of competition signature across the globe, and how does it associate with the process of trait evolution in assemblages of species?

In chapter 5, I applied models of trait evolution with competition in assemblages of granivorous birds in order to map the geographical variation in patterns of trait divergence consistent with the presence of competitive interactions globally. I further linked the signature for competition with the process of phenotypic evolution (rate and disparity). Focusing on sympatric assemblages of species sharing the same dietary guild should increase the potential for meaningful interactions in target species pools (Grant, 1972). Therefore, the concerns about not detecting a signal of competition when looking across entire avian clades (chapter 4) should be to some extent alleviated. I showed that, across granivorous birds, a mode of evolution consistent with competition for ecomorphological traits does not follow an obvious spatial pattern (e.g. latitudinal gradient, Dobzhansky, 1950). Rather, areas of high support for competition are scattered in a few areas around the globe. Moreover, I

found moderate to little support for environmental predictors of the strength of biotic interactions signal. Hence overall, my results suggest a low predictability for the global distribution of evolution consistent with competition. These findings are also in agreement with the idea that strong biotic interactions are triggered by unpredictable events (e.g. irregular resource shortage episodes or increases in number of competitors, e.g. Grant & Grant, 2006), and thus represent an unpredictable, dynamic selective force, potentially capable of creating rapidly changing adaptive landscapes (Thompson, 1999).

I showed that the prevalence and strength of a signature of species-interactions associate negatively with trait evolutionary rates, implying that most often the resolution of competition in granivorous birds happens prior to secondary contact (similar to other studies in birds, Drury et al., 2018; McEntee et al., 2018). Specifically, when phenotypic evolution is rapid, by the time diverging species come back to sympatry they will be ecologically sufficiently distinct and competition will be reduced or annulled. This interpretation is also supported by the fact that avian species speciate predominantly in allopatry (Phillimore et al., 2008), and further the role of trait dissimilarity to enable secondary contact has been shown (Pigot & Tobias, 2013). More broadly, these results imply that the predicted trend of rapid character displacement under competition (as exemplified by iconic radiations such as Darwin's finches, Grant & Grant, 2006) can be difficult to detect at global scales. Moreover, the potential for secondary contact when speciation is allopatric can create a pattern of negative association between rates of evolution and competition. Because the evolutionary history of allopatric-symaptric dynamics between interacting species is difficult to determine, we are also cautious of the fact that divergence in allopatry can be extensive in birds, and hence the patterns of trait divergence we detect could result mainly from phenotypic differentiation in allopatry, rather than when species co-occur. Nonetheless, we found that competition signal is

associated with higher levels of disparity in assemblages, and thus, despite the constraints on the potential for strong competitive selection pressures in sympatry, the resolution of competition seems to leave a signal of increased phenotypic biodiversity globally.

IMPLICATIONS

In this thesis I focused on the accumulation of diversity in ecomorphological traits across birds. I show that the dynamics between two key components of biodiversity - rates of trait diversification and species richness, can be influenced by ecological opportunities and constraints of the eco-morphospace. Specifically, invading peripheral niches enables subsequent rapid trait evolution, but the confined nature of specialized phenotypes limits diversity in terms of number of species (similar to Ricklefs, 2005). Conversely, central areas of the morphospace accommodate high density of species and also facilitate rapid evolutionary rates. The analyses in chapter 4 also reveal a signal of positive diversity-dependence in beak shape, size, and body mass in many avian clades. The positive coupling between the speed of trait evolution and total number of species does not bring support to the hypothesis that a reduction in niche availability with increased diversity necessarily drives a deceleration in trait evolutionary rates (e.g. Gavrilets & Losos, 2009, Mahler et al., 2010 but see Claramunt et al., 2012). A pattern of high rates of evolution with high density of species can be, however, attributed to interspecific competition, which represents a dynamic selection pressure that could regularly drive rapid phenotypic differentiation between species (Schluter, 2001; Thompson, 1999). More broadly, these findings imply that competition could maintain rapid rates of phenotypic turnover between species even with limited availability of ecological niches. However, it has been suggested that competition contributes little to patterns of morphological diversification in deep-time (Benton, 2009). Conversely, my results suggest that, although not ubiquitous, a mode of evolution consistent with

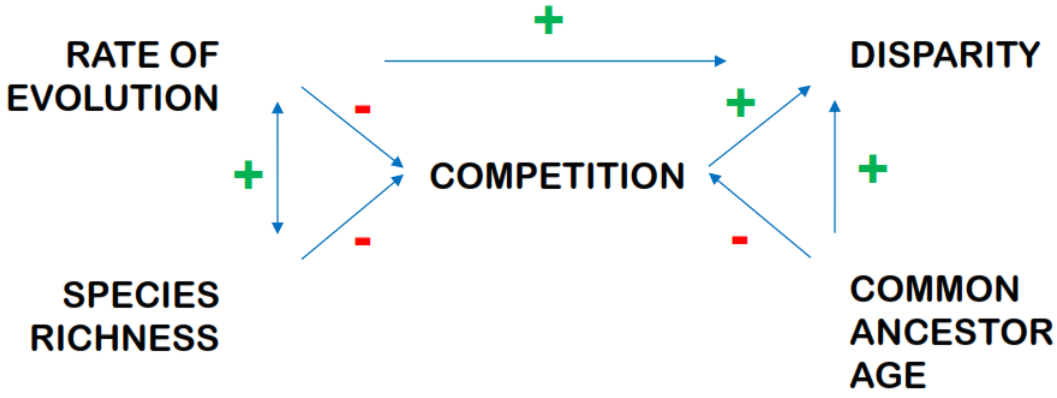

Figure 6.1. Overview of relationships between competition signal, rates of evolution, disparity, species richness, and age of most recent common ancestor of focal species (based largely on results in chapter 5). A signature of competition appears negatively correlated with rates of evolution, as well as species richness in assemblages, however these relationship likely indicate the resolution of competition in allopatry, as well as issues related to sample size. With increasingly old assemblages, the signal of competition is also likely to decay. Competition signal is also coincident with increased disparity in assemblages, despite the negative links with evolutionary rates, number of species, and ancestor age of species – factors that impact positively on disparity.

competition is not uncommon across avian clades, and therefore, biotic interactions could influence the dynamics of trait evolution at macroevolutionary scales.

If a high density of species facilitates higher rates of trait evolution via rapid character displacement, we expect to see a positive relationship between the strength of species interactions signal, trait evolutionary rates, and also phenotypic disparity i.e. we expect competition to be a driver of increased biodiversity. Such a relationship has been shown already in a few iconic sympatric recent radiations (Grant & Grant, 2006; Stuart et al., 2014). Conversely, I found that high levels of competition signal are associated with slow evolutionary rates in granivores assemblages (Figure 6.1 is an overall representation of how competition signal, rates and total disparity are inter-linked). I interpreted this trend as a by-product of the resolution of competition prior to secondary contact in birds, and so my results cannot infer on how competition signal links with the rate of morphological

differentiation when lineages evolve in sympatry through-out their evolutionary history. Further, extensive trait differentiation in allopatry, also followed by filtering could also contribute to the distribution of present-day trait values across lineages. Overall, my findings are in agreement with a positive association between species richness and trait evolutionary rates due to competition within clades. Within assemblages of species, however, the findings imply that the resolution of competition in allopatry could leave an unintuitive pattern of negative association between rapid morphological differentiation and competition signal. Nonetheless, I found that strong competition signal coincides with increased disparity in assemblages, in agreement with the predictions that lineages differentiate extensively under competition, and thus competitive selection pressures can shape biodiversity in terms of morphological disparity across the globe.

LIMITATIONS AND FURTHER WORK

Several caveats of the work presented here are discussed in detail in each data chapter. I will, however, reiterate some key points that relate more generally to findings through-out the thesis. First, in chapter 2, I highlight the potential improvements in the interpretation of trait evolutionary models when absolute fit is taken into account. However, an absolute adequacy framework is not readily available for models of evolution with competition. In my analyses, co-utilizing absolute and relative fit would reduce the concerns about overinflated best fit for exponential positive diversity-dependent models in the presence of measurement error (Drury et al., 2018), but also inform when relative support for competition is underestimated, e.g. if falsely inflated inter-tip variability increases preference for single stationary peak methods (as shown in chapter 2). Further, the development of multivariate models of evolution with competition (e.g. Clarke et al., 2017) could provide a better approximation on how competition acts on complex traits, e.g. if the resolution of competition implies changes on multiple PC axes of variation in beak

shape. The same logic could be extended to including multiple traits into models, however, given that my results imply that species interactions impacts preferentially on a single axis of morphological variation, modelling multiple distinct traits in multivariate models is probably of less interest.

Additionally, several developments would extend the findings from chapters 4 and 5. First, in the current implementation of models in chapter 4, I assume that all species in a clade interact through-out their evolutionary history. However, this assumption is likely often false, particularly in birds where allopatric speciation is dominant (Phillimore et al., 2008), and even more so when rates to secondary contact are slow (e.g. in *Furnariidae*, Pigot & Tobias, 2014). The potential for interaction (and thus competition) between species also requires overlap in method of resource acquisition, as well as a shortage of shared resources (Arthur, 1982; Grant, 1972). My results thus likely underestimate the signal of biotic interactions within clades, and would benefit from restricting the pool of potential interacting lineages by incorporating data on foraging strata, dietary guild (e.g. from Wilman et al., 2014), and range overlap. The latter is, however, difficult to achieve because of the issues related to ancestral range reconstruction, though cruder estimates could be obtained by restricting interactions between lineages that reside in the same broad ecoregion (e.g. Drury et al., 2018). These concerns are illustrated by examples of clades where I find a lack of support for competition when applying models to the whole clade, but moderate to strong support within sympatric assemblages (e.g. Finches). Similar improvements could also be implemented in chapter 5 (e.g. include information on the percentage of overall range overlap between species co-occurring in grid cells). Further, an obvious expansion to this chapter would be to increase the phylogenetic breadth of the analyses by incorporating phenotypic data across other dietary guilds.

Lastly, the findings of this thesis point out to some additional questions to be answered. For example, the debate over the relationship between the process of morphological and species diversification is ongoing (Adams et al., 2009; Burbrink et al., 2012; Rabosky & Adams, 2012; Rabosky et al., 2013). In chapter 3, I found high rates of evolution in species-rich clades, but I did not further explore the underlying mechanism or causality of this relationship. Further, I do not differentiate between biological and statistical (type 1 or type 2 errors) explanations behind several trends I find in the thesis, including the negative relationship between age and evolutionary rates (chapter 3), the negative relationship between competition signal and species richness in sympatric assemblages (chapter 5), or the trend of increased strength of competition signal at more recent time-scales (chapters 4 and 5). While these relationships deserve further attention, in this thesis I mostly focused on richness and age as cofounding factors (e.g. as variables accounting for sample size). Additionally, through-out this thesis, I highlight several avian groups with striking rapid evolutionary rates (e.g. flamigos, ducks, shore birds) or extremely high signal for species interactions (e.g. tits, chickadees and penduline−tits, sandgrouse, antpittas). Given the macroevolutionary scale of my work, I do not focus on these individual clades further, but these analyses highlight potentially interesting study-systems beyond the few well-known adaptive radiations for understanding more fine details on the tempo and mode of evolution.

GENERAL CONCLUSION

In this thesis, I took a comprehensive approach to investigate the evolution of ecomorphological traits across the bird radiation with the aim of understanding the patterns, correlates and consequences for the tempo and mode of trait evolution at macroevolutionary scales. I found evidence for extensive rate heterogeneity when modelling body mass and beak shape evolution across birds, supporting the hypothesis that variation in the tempo of phenotypic evolution is widespread

(Rabosky et al., 2013; Simpson, 1953; Venditti et al., 2011). Further, I found that while the tempo of evolution at recent phylogenetic scales can be hard to predict, variation in clade rates of evolution is tightly linked with the potential for ecological opportunity as well as the process of niche filling. I also explored the predictability of evolutionary modes, and I found that a mode of evolution consistent with competition seems contingent on chance at both large-scale phylogenetic scales, and in sympatric assemblages of species across the globe. Additionally, I explored the consequences of ecological processes on the accumulation of ecomorphological diversity. I found that an increase in ecological opportunity associated with invasion of unoccupied, peripheral areas of the morphospace can drive subsequent rapid evolutionary rates, but it also causes reduced biodiversity in terms of species richness. Rapid morphological differentiation is also associated with species-rich, central areas of the morphospace, implying that species-interactions could potentially maintain a rapid turnover in phenotypes despite the reduced availability for ecological niches in species-rich clades. However, I found a negative link between evolutionary rates and competition strength in assemblages around the globe. This trend is likely caused by high levels of allopatric speciation and trait-dependent filtering for secondary contact in birds, and generally, these results imply that unexpected apparent relationships between signatures of biotic interactions in trait divergence and rates of evolution can emerge at broad scales. Furthermore, I found that a signal for species-interactions coincided with increased morphological disparity within assemblages, supporting the hypothesis that ecological selection pressures can act as generators of biodiversity. Taken together, the results of this thesis highlight how the potential for ecological opportunities, the process of niche filling, and the resolution of competition concurrently shape the accumulation of morphological biodiversity at broad temporal and spatial scales, and thus shed light on some underlying mechanisms of present-day diversity of life.

REFERENCES

Adams, D. C., Berns, C. M., Kozak, K. H., & Wiens, J. J. (2009). Are rates of species diversification correlated with rates of morphological evolution? *Proc Biol Sci, 276*(1668), 2729-2738.

Arthur, W. (1982). The Evolutionary Consequences of Interspecific Competition. *12*, 127-187.

Benton, M. J. (2009). The Red Queen and the Court Jester: species diversity and the role of biotic and abiotic factors through time. *Science, 323*(5915), 728-732.

Burbrink, F. T., Chen, X., Myers, E. A., Brandley, M. C., & Pyron, R. A. (2012). Evidence for determinism in species diversification and contingency in phenotypic evolution during adaptive radiation. *Proc Biol Sci, 279*(1748), 4817-4826.

Claramunt, S., Derryberry, E. P., Brumfield, R. T., & Remsen, J. V., Jr. (2012). Ecological opportunity and diversification in a continental radiation of birds: climbing adaptations and cladogenesis in the Furnariidae. *Am Nat, 179*(5), 649-666.

Clarke, M., Thomas, G. H., & Freckleton, R. P. (2017). Trait Evolution in Adaptive Radiations: Modeling and Measuring Interspecific Competition on Phylogenies. *Am Nat, 189*(2), 121-137.

Cooper, N., & Purvis, A. (2010). Body size evolution in mammals: complexity in tempo and mode. *Am Nat, 175*(6), 727-738.

Darwin, C. (1859). *On the origin of species*. London UK: John Murray.

Dobzhansky, T. (1950). Evolution in the tropics. *Am. Sci., 38*(2), 209-221.

Drury, J., Clavel, J., Manceau, M., & Morlon, H. (2016). Estimating the Effect of Competition on Trait Evolution Using Maximum Likelihood Inference. *Syst Biol, 65*(4), 700-710.

Drury, J. P., Tobias, J. A., Burns, K. J., Mason, N. A., Shultz, A. J., & Morlon, H. (2018). Contrasting impacts of competition on ecological and social trait evolution in songbirds. *PLoS Biol, 16*(1), e2003563.

Gavrilets, S., & Losos, J. B. (2009). Adaptive radiation: contrasting theory with data. *Science, 323*(5915), 732-737.

Gillman, L. N., Wright, S. D., & Ladle, R. (2014). Species richness and evolutionary speed: the influence of temperature, water and area. *Journal of Biogeography, 41*(1), 39-51.

Grant, B. R., & Grant, P. R. (2006). Evolution of Character Displacement in Darwin's Finches. *Science, 313*(5784), 224-226.

Grant, P. R. (1972). Convergent and divergent character displacement. *Biological Journal of Linnean Society, 4*(1), 39-68.

Grant, P. R. (1999). Bill Size, Body Size, and the Ecological Adaptations of Bird Species to Competitive Situations on Islands. *Systematic Zoology, 17*(3), 319-333.

Hunter, J. P. (1998). Key innovations and the ecology of macroevolution. *Trends Ecol. Evol., 13*(1), 31-36.

Kaliontzopoulou, A., & Adams, D. C. (2016). Phylogenies, the Comparative Method, and the Conflation of Tempo and Mode. *Syst Biol, 65*(1), 1-15.

Landis, M. J., & Schraiber, J. G. (2017). Pulsed evolution shaped modern vertebrate body sizes. *PNAS, 114*(50), 13224-13229.

Lanfear, R., Kokko, H., & Eyre-Walker, A. (2014). Population size and the rate of evolution. *Trends Ecol Evol, 29*(1), 33-41.

Losos, J. B. (2010). Adaptive radiation, ecological opportunity, and evolutionary determinism. American Society of Naturalists E. O. Wilson award address. *Am Nat, 175*(6), 623-639.

Losos, J. B., & Mahler, D. L. (2010). *Evolution since Darwin: the first 150 years. Chapter: Adaptive radiation: the interaction of ecological opportunity, adaptation, and speciation.*: Sunderland (MA): Sinauer.

Mahler, D. L., Revell, L. J., Glor, R. E., & Losos, J. B. (2010). Ecological opportunity and the rate of morphological evolution in the diversification of Greater Antillean anoles. *Evolution, 64*(9), 2731-2745.

Mazel, F., Davies, T. J., Georges, D., Lavergne, S., Thuiller, W., & Peres-Neto, P. R. (2016). Improving phylogenetic regression under complex evolutionary models. *Ecology, 97*(2), 286-293.

McEntee, J. P., Tobias, J. A., Sheard, C., & Burleigh, J. G. (2018). Tempo and timing of ecological trait divergence in bird speciation. *Nat Ecol Evol, 2*(7), 1120-1127.

Pennell, M., FitzJohn, R. G., Cornwell, W. K., & Harmon, L. J. (2015). Model Adequacy and the Macroevolution of Angiosperm Functional Traits. *Am Nat, 186*(2), E33-E50.

Phillimore, A. B., Orme, C. D., Thomas, G. H., Blackburn, T. M., Bennett, P. M., Gaston, K. J., & Owens, I. P. (2008). Sympatric speciation in birds is rare: insights from range data and simulations. *Am Nat, 171*(5), 646-657.

Pigot, A. L., & Tobias, J. A. (2013). Species interactions constrain geographic range expansion over evolutionary time. *Ecol Lett, 16*(3), 330-338.

Pigot, A. L., & Tobias, J. A. (2014). Dispersal and the transition to sympatry in vertebrates. *Proceedings of the Royal Society B: Biological Sciences, 282*(1799), 20141929.

Rabosky, D. L. (2017). Phylogenetic tests for evolutionary innovation: the problematic link between key innovations and exceptional diversification. *Philos Trans R Soc Lond B Biol Sci, 372*(1735), 20160417.

Rabosky, D. L., & Adams, D. C. (2012). Rates of morphological evolution are correlated with species richness in salamanders. *Evolution, 66*(6), 1807-1818.

Rabosky, D. L., Santini, F., Eastman, J., Smith, S. A., Sidlauskas, B., Chang, J., & Alfaro, M. E. (2013). Rates of speciation and morphological evolution are correlated across the largest vertebrate radiation. *Nat Commun, 4*, 1958.

Ricklefs, R. E. (2005). Small Clades at the Periphery of Passerine Morphological Space. *Am Nat, 165*(651-659).

Schluter, D. (2001). Ecology and the origin of species. *Trends Ecol Evol, 16*(7), 372-380.

Simpson, G. G. (1953). *The major features of evolution.*: Columbia University Press.

Slater, G. J., & Pennell, M. W. (2014). Robust regression and posterior predictive simulation increase power to detect early bursts of trait evolution. *Syst Biol, 63*(3), 293-308.

Slater, G. J., Price, S. A., Santini, F., & Alfaro, M. E. (2010). Diversity versus disparity and the radiation of modern cetaceans. *Proc Biol Sci, 277*(1697), 3097-3104.

Stuart, Y. E., Campbell, T. S., Hohenlohe, P. A., Reynolds, R. G., Revell, L. J., & Losos, J. B. (2014). Rapid evolution of a native species following invasion by a congener. *Science, 346*(6206), 463-466.

Thomas, J. A., Welch, J. J., Lanfear, R., & Bromham, L. (2010). A generation time effect on the rate of molecular evolution in invertebrates. *Mol Biol Evol, 27*(5), 1173-1180.

Thompson, J. N. (1999). The Evolution of Species Interactions. *Science, 284*(5423), 2116-2118.

Thomson, C. E., Gilbert, J. D., & Brooke Mde, L. (2014). Cytochrome b divergence between avian sister species is linked to generation length and body mass. *PLoS One, 9*(2), e85006.

Van Valen, L. (1973). A new evolutionary law. *Evol Theory, 1*, 1-30.

Venditti, C., Meade, A., & Pagel, M. (2011). Multiple routes to mammalian diversity. *Nature, 479*(7373), 393-396.

Weir, J. T., & Mursleen, S. (2013). Diversity-dependent cladogenesis and trait evolution in the adaptive radiation of the auks (aves: alcidae). *Evolution, 67*(2), 403-416.

Wilman, H., Belmaker, J., Simpson, J., de la Rosa, C., Rivadeneira, M. M., & Jetz, W. (2014). EltonTraits 1.0: Species-level foraging attributes of the world's birds and mammals. *Ecological Archives, 95*(7), 2027-2027.